Technische Universität München
TUM School of Engineering and Design

Decision support with health monitoring for deteriorating engineering systems

Antonios Kamariotis

Vollständiger Abdruck der von der TUM School of Engineering and Design zur Erlangung eines

Doktors der Ingenieurwissenschaften (Dr.-Ing.)

genehmigten Dissertation.

Vorsitz: Prof. Dr.-Ing. habil. Fabian Duddeck

Prüfer*innen der Dissertation:

1. Prof. Dr. sc. techn. Daniel Straub
2. Assoc. Prof. Dr. Eleni Chatzi
3. Prof. Keith Worden

Die Dissertation wurde am 22.06.2023 bei der Technischen Universität München eingereicht und durch die TUM School of Engineering and Design am 18.10.2023 angenommen.

Contents

Abstract

Deterioration processes of various forms can adversely affect the intended performance of engineering components and systems. Life-cycle management of deteriorating components/systems is a laborious task, which is associated with multiple sources of uncertainty. In this context, various actions are typically performed, such as inspections and maintenance, which may generally come at a large cost. In an effort to facilitate and enhance maintenance planning, continuous information can be harnessed via the adoption of online health monitoring systems. The synergy between monitoring and model-driven or data-driven prognostic approaches enables online data-informed predictions of the future condition of the deteriorating component/system. Decision policies for planning maintenance operate on the basis of these predictions. The resulting framework is referred to as predictive maintenance (PdM) planning. This thesis investigates PdM planning within two different contexts, aiming to address distinct challenges that two connected scientific disciplines face.

1. An optimal Operation & Maintenance (O&M) decision making process can be facilitated by Structural Health Monitoring (SHM) systems. To date, SHM systems are not extensively applied on real-world, safety-critical structures and infrastructure systems. Actionable use cases illustrating how SHM can provide optimal decision support for such systems are essential to a more widespread adoption. Bayesian decision analysis provides the necessary theoretical basis for rigorously quantifying *a-priori* the effect of SHM systems on expected life-cycle costs in terms of the Value of Information (VoI) metric or the more specialized Value of SHM (VoSHM) metric. This thesis proposes a framework for the quantification of the VoSHM, which is suited for application to a wide range of vibration-based SHM use cases. Several original contributions introduce the framework, discuss the underlying modeling assumptions, and investigate various computational aspects related to stochastic sequential decision problems, Bayesian filtering, and time-variant structural reliability analysis. The framework can be viewed as a decision support tool with which one can *a-priori* assess the potential economic benefit associated with installing a vibration-based SHM system on a deteriorating engineering system in a specific decision context.

2. In various engineering disciplines, e.g., in mechanical engineering, systems exist that are typically non-unique. For such systems, the application of online health monitoring is ever-increasing. Continuous monitoring data from run-to-failure experiments of nominally identical deteriorating components/systems are often available. The discipline of Prognostic Health Management (PHM) has significantly benefited from such datasets, in that a multitude of prognostic solutions have been developed that employ data-driven methods. These aim at predicting the Remaining Useful Life (RUL) of deteriorating components/systems based on online input sensor data, rather than at an explicit focus on the subsequent PdM planning effort. In this context, this thesis contributes by proposing a metric for assessing and optimizing data-driven prognostic algorithms based on their impact on downstream PdM decisions within a given decision setting. New light is shed on the role of PdM policies in this context. PdM policies that are suggested in the literature are investigated and some alternatives/improvements are proposed. The availability of run-to-failure monitoring data further allows for evaluating PdM policies directly on a subset thereof. This relaxes the need for defining a stochastic deterioration model *a-priori*.

Zusammenfassung

Verschiedene Formen von Abnutzungs- und Alterungsprozessen können die Leistung technischer Komponenten und Systeme beeinträchtigen. Das Lebenszyklusmanagement solcher Komponenten und Systeme ist eine anspruchsvolle Aufgabe, die mit zahlreichen Unsicherheitsfaktoren verbunden ist. In diesem Zusammenhang werden in der Regel verschiedene Maßnahmen wie zum Beispiel Inspektionen und Wartungen durchgeführt, welche häufig mit hohen Kosten verbunden sind. Der Einsatz sogenannter Online-Zustandsmonitoringsysteme ermöglicht eine kontinuierliche Messung von System- bzw. Komponentenzuständen. Diese Information kann eingesetzt werden um die Planung von Wartungs- und Inspektionsmaßnahmen effizienter zu gestalten. Die Synergie zwischen Monitoring und modell- oder datengesteuerten Prognoseansätzen ermöglicht datengestützte Online-Vorhersagen über den zukünftigen Zustand der Komponenten/Systeme. Auf Basis solcher Vorhersagen können Entscheidungsstrategien für die Planung von Wartungs- und Instandhaltungsmaßnahmen formuliert werden. Dies wird als *Predictive Maintenance* (PdM) Planung bezeichnet. In der vorliegenden Arbeit wird die Behandlung der PdM-Planung in zwei verschiedenen wissenschaftlichen Disziplinen untersucht, in denen es jeweils unterschiedliche Herausforderungen zu bewältigen gilt.

1. Eine optimale Entscheidungsstrategie für Betrieb und Instandhaltung kann durch *Structural Health Monitoring* (SHM) Systeme erleichtert werden. Bislang werden SHM-Systeme nicht in großem Umfang auf reale, sicherheitskritische Strukturen und Infrastruktursysteme angewendet. Anwendungsfälle, die zeigen, wie SHM eine optimale Entscheidungsunterstützung für solche Systeme bieten kann, sind für eine breitere Akzeptanz der Methodik unerlässlich. Die Bayes'sche Entscheidungsanalyse bietet die notwendige theoretische Grundlage, um die Auswirkungen von SHM-Systemen auf die zu erwartenden Lebenszykluskosten im Sinne der *Value of Information* (VoI) Metrik oder der spezielleren *Value of SHM* (VoSHM) Metrik *a-priori* zu quantifizieren. In dieser Arbeit wird ein Rahmen für die Quantifizierung des VoSHM vorgeschlagen, der sich für die Anwendung auf eine große Auswahl von vibrationsbasierten SHM-Anwendungsfällen eignet. In mehreren Erstpublikationen werden der konzeptionelle Rahmen definiert, die diesem zugrunde liegenden Modellierungsannahmen diskutiert und verschiedene rechnerische Aspekte im Zusammenhang mit stochastischen sequentiellen Entscheidungsproblemen, Bayes'scher Filterung und zeitvarianter Zuverlässigkeitsanalyse besprochen und untersucht. Der konzeptionelle Rahmen kann als ein Werkzeug zur Untersützung von Entscheidungen betrachtet werden, mit dem man *a-priori* den potenziellen wirtschaftlichen Nutzen bewerten kann, der mit der Installation eines vibrationsbasierten SHM-Systems an einem abnutzenden und alternden technischen System in einem bestimmten Entscheidungskontext verbunden ist.

2. In diversen Ingenieursdisziplinen liegt der Fokus auf der Vorhersage des Versagensverhaltens einer Vielzahl identischer Systeme. Für solche nicht einzigartigen Systeme existieren oft kontinuierliche Monitoring-Daten aus sogenannten *Run-to-Failure*-Experimenten. Diese Daten werden zunehmend zur Formulierung von Online-Zustandsmonitoring-Strategien herangezogen. Die Disziplin des Prognostic Health Managements (PHM) hat von solchen Datensätzen erheblich profitiert, da eine Vielzahl von Prognoselösungen entwickelt wurde, die datengesteuerte Methoden verwenden. Diese zielen auf die Vorhersage des *Remaining Useful Life* (RUL) der Komponenten/Systeme auf der Grundlage von Online-Eingangs-Sensordaten ab, anstatt sich explizit auf die anschließende PdM-Planung zu konzentrieren. In diesem Zusammenhang leistet die vorliegende Arbeit einen Beitrag, indem sie eine Metrik zur Bewertung und Optimierung von datengesteuerten Prognosealgorithmen auf der Grundlage ihrer Auswirkungen auf nachgelagerte PdM-Entscheidungen inner-

halb eines bestimmten Entscheidungsrahmens vorschlägt. Die Rolle der PdM-Strategie wird in diesem Zusammenhang neu beleuchtet. Die in der Literatur vorgeschlagenen PdM-Strategien werden untersucht und einige Alternativen/Verbesserungen werden vorgeschlagen. Die Verfügbarkeit von *Run-to-Failure*-Monitoring-Daten ermöglicht es außerdem, einen Teil des Datensatzes zu Validierungszwecken zurückzuhalten, anhand dessen die Performance verschiedener PdM-Maßnahmen gemessen werden kann. Dadurch entfällt die Notwendigkeit, ein stochastisches Alterungs- bzw. Abnutzungsmodell *a-priori* zu definieren.

Acknowledgements

Over the course of the past four years, I have had the great pleasure of doing my PhD in the Engineering Risk Analysis group in Munich, while working in close collaboration with the Structural Mechanics and Monitoring group of ETH Zurich.

I would like to express my sincere gratitude to Daniel and Eleni for their unwavering positivity, friendly demeanor, and the consistent support throughout the past four years. The numerous insightful discussions, both pertaining to research and various aspects of academic life, have been truly invaluable. The work in this thesis would not have been possible without Daniel's indispensable weekly supervision and constant creative input. Eleni, my second supervisor, has consistently made herself available whenever her insightful guidance and expertise were needed. I hope that both of them found this collaboration to be as enjoyable as I did.

I consider myself fortunate to have been part of an exceptional group of people at the ERA group. I want to thank them for keeping me good company throughout the years. Max E., thank you for being a good friend, and for providing detailed comments on this thesis. Iason, thank you for imparting so much knowledge to the group, and for our fruitful collaboration. Elizabeth, thank you for always keeping our lunch breaks interesting. I would also like to thank: Ji-Eun, Sebastian, Felipe, Max T., Hugo, Amelie, Mara and Marco.

I am thankful to Konstantinos Tatsis from the SMM group for generously sharing code and technical expertise, and for the fruitful collaboration we had on the final paper of this thesis.

Denise, thank you for being by my side since the beginning of my PhD. I am grateful for your support and patience throughout the past four years. Your presence in my life has brought a much-needed balance, and I cannot thank you enough for that.

Lastly, I would like to express my heartfelt gratitude to my parents and siblings for their unconditional love, and their steadfast support and encouragement in every single one of my plans and endeavors.

Munich, May 2023.

List of publications

Antonios Kamariotis is the first author of the following published or submitted journal articles:

- A. Kamariotis, E. Chatzi, and D. Straub. "Value of information from vibration-based structural health monitoring extracted via Bayesian model updating". In: *Mechanical Systems and Signal Processing* 166, 108465 (2022). https://doi.org/10.1016/j.ymssp.2021.108465.
- A. Kamariotis, E. Chatzi, and D. Straub. "A framework for quantifying the value of vibration-based structural health monitoring". In: *Mechanical Systems and Signal Processing* 184, 109708 (2023). https://doi.org/10.1016/j.ymssp.2022.109708.
- A. Kamariotis, L. Sardi, I. Papaioannou, E. Chatzi, and D. Straub. "On off-line and on-line Bayesian filtering for uncertainty quantification of structural deterioration". In: *Data-Centric Engineering* 4, e17 (2023). https://doi.org/10.1017/dce.2023.13.
- A. Kamariotis, K. Tatsis, E. Chatzi, K. Goebel, and D. Straub. "A metric for assessing and optimizing data-driven prognostic algorithms for predictive maintenance". In: *Reliability Engineering & System Safety* 242, 109723 (2024). https://doi.org/10.1016/j.ress.2023.109723.

Antonios Kamariotis is the first author of the following published conference articles:

- A. Kamariotis, E. Chatzi, and D. Straub. (2022). "Quantifying the value of vibration-based structural health monitoring considering environmental variability". In: *Structural Health Monitoring 2021. Proceedings of the 13th International Workshop on Structural Health Monitoring (IWSHM).* https://doi.org/10.12783/shm2021/36356.
- A. Kamariotis, E. Chatzi, and D. Straub. (2022). "The effect of the likelihood function on the value of SHM extracted via sequential Bayesian updating". In: *Proceedings of ICOSSAR 2021-2022, 13th International Conference on Structural Safety & Reliability.*
- A. Kamariotis, L. Sardi, I. Papaioannou, E. Chatzi, and D. Straub. (2022) "A comparative assessment of online and offline Bayesian estimation of deterioration model parameters". In: *Model Validation and Uncertainty Quantification, Volume 3: Proceedings of the 40th IMAC, A Conference and Exposition on Structural Dynamics 2022.* pp. 17-20. https://doi.org/10.1007/978-3-031-04090-0_2.
- A. Kamariotis, E. Chatzi, and D. Straub. (2021) "Value of Information from SHM via estimating deterioration jump processes with particle filtering". In: *Engineering Mechanics Institute Conference and Probabilistic Mechanics & Reliability Conference (EMI/PMC 2021).*
- A. Kamariotis, D. Straub, and E. Chatzi. (2020) "Optimal maintenance decisions supported by SHM: A benchmark study". In: *Life-Cycle Civil Engineering: Innovation, Theory and Practice. Proceedings of the 7th International Symposium on Life-Cycle Civil Engineering. IALCCE 2020.* https://doi.org/10.1201/9780429343292-88

Part I

Synopsis

Chapter 1

Introduction

1.1 Motivation & context

In science and engineering, problems that require making decisions under uncertainty [99] are omnipresent. For tackling such problems, scientists and engineers often either rely on available information, or seek to gather new information, which can support their decisions. Management of deteriorating engineering systems throughout their life-cycle forms a problem of decision making under uncertainty. This is an elaborate task, which involves a sequence of decisions on logistics, maintenance, repair or replacement actions that need to be assumed within a dynamic setting, under uncertainties that are intrinsic to the problem at hand. This decision making task is often executed in high-risk environments. Engineers and operators that are charged with this task are typically aided by information related to the condition of the system that is obtained from data-gathering actions, such as inspections or monitoring. This information can reduce the uncertainty and, thus, enable enhanced decision making for operation and maintenance planning. However, there is always a cost associated with extraction of more or richer information.

Advances in sensor and information technology have laid the groundwork for a paradigm shift with regard to how information is collected and processed. Specifically, these advances have rendered the continuous monitoring of a deteriorating engineering system's health a viable option. In particular for safety-critical civil, aerospace and mechanical structures and infrastructure systems, Structural Health Monitoring (SHM) has been established as the enabling technology for continuous, long-term monitoring [47]. SHM can be defined as a continuous, automated, online process for damage assessment, whose ultimate purpose is to provide cradle-to-grave system state awareness [48]. The specific tasks with which an SHM system is charged have been divided into a hierarchy of levels in [158, 198]. The first three levels progress from damage detection to localization and quantification. The last level in this hierarchy is damage prognosis, which defines the task of predicting the remaining useful life (RUL) and safety of the system through simulation and past monitoring data [49]. In the damage prognosis task lies the connection between the disciplines of SHM and that of Prognostics and Health Management (PHM) [95, 209]. PHM primarily aims to deliver predictions of the RUL of a deteriorating system by utilizing monitoring data ("prognostics"), with the end goal of supporting decisions related to maintenance planning ("health management"). The PHM discipline centers on the provision of support for decision making and more generally targets application to a broad

range of engineering systems, notably mechanical, aerospace, industrial, energy and transportation engineering systems [105, 54, 74, 103]. One key difference between the two distinct disciplines is that SHM targets application to unique systems (e.g., a bridge structure), whereas PHM typically targets non-unique components/systems that belong to a homogeneous population of components/systems of the same type (e.g., rolling bearings). Regardless of their application scope, the union between online health monitoring and model-driven or data-driven prognostic approaches forms the basis for maintenance planning supported by prognostic predictions. The resulting framework is referred to as predictive maintenance [54, 67].

Through the definition of its fourth hierarchical level, it is implied that the eventual goal of SHM is to provide decision support for life-cycle management of deteriorating systems. It might therefore appear counter-intuitive that, until recently, not much research work focused on the role of SHM for decision support [175, 184, 78, 88]. This, among other factors, has contributed to the fact that adoption of SHM systems on real-world safety-critical structures and infrastructure systems falls short of the mark, despite the maturity and successful developments in the SHM field [25]. There are multiple challenges in making efficient use of acquired monitoring data for decision making. Damage must typically be inferred from indirect and/or incomplete measurements, such as natural frequencies in vibration-based SHM [48]. An intricacy stems from the fact that engineering systems are not only subjected to a number of damaging processes and events, but also to confounding processes, such as environmental and operational variability [142, 34, 170, 11], the effect of which might obscure damage. Different processes act on different time scales and therefore inspection and maintenance actions have a different degree of urgency. Safety-critical structures and infrastructure systems are associated with high reliability and prohibitive failure consequences. This leads to a scarcity of real monitoring data corresponding to the whole spectrum of damaged states, which impairs the prognostic capabilities of many SHM techniques that rely on such data. Finally, target engineering systems for SHM deployment are typically unique, it is therefore not straightforward how damage state information from a single system can be transferred across a population of systems [20], which would enable a more classical approach to statistical decision making. In order to move towards a more widespread adoption of SHM, actionable use cases are needed. They should demonstrate how SHM systems can provide optimal decision support in different contexts, thus generating economic value.

Industrial engineering is likely the domain in which adoption of health monitoring, powered by PHM frameworks, has recorded the most success to date [103, 105, 31, 209]. For several non-unique engineering components and systems, real-world datasets containing monitoring data from run-to-failure experiments have been made readily available for training and validation [127]. This constitutes a key difference compared to SHM of unique safety-critical structures and infrastructure systems, where such datasets are oftentimes nearly impossible to obtain in practice, and are instead predominantly generated via physics simulations [61]. The availability of the above-mentioned datasets has created a data-rich environment, from which the PHM community has greatly benefited.

Model-driven, and more recently data-driven prognostic solutions trained on available run-to-failure monitoring data, lie at the core of PHM for engineering components/systems. These furnish – inherently uncertain – on-line predictions of the remaining useful life of the deteriorating component/system. There is a vast amount of recent literature on the development of data-driven prognostic algorithms [105, 82]. However, less work has focused on the subsequent planning effort [130, 54]. One fundamental question for the use of PHM in practice relates to the selection of the most suited prognostic method and decision policy for optimally supporting decision making. Thus,

ideally, the development, optimization and assessment of prognostic algorithms should be driven by explicitly taking into account the nature of decisions that their outcome aims to support.

1.2 Scope of work

Several fronts need to be pushed further for reaching a synergy between health monitoring and decision making. This thesis adopts a decision-oriented approach to addressing some of the above-mentioned challenges that obstruct or complicate the real-world application of SHM and PHM.

One primary goal of this thesis is to deliver virtual use cases, elaborating on the decision support capabilities of vibration-based SHM systems [48, 36]. To this end, the Bayesian decision analysis framework is employed [149]. This framework allows for a rigorous quantification of the Value of Information (VoI) from vibration-based SHM [175, 184, 89]. A VoI analysis quantifies the expected improvement in decision making on the basis of exploitation of monitoring information for reducing the uncertainty in the problem. A more specialized metric, the Value of SHM (VoSHM) [8, 88], which also emerges from Bayesian decision analysis, is adopted in place of the VoI in parts of this work. The VoSHM is quantified as the difference in expected improvement in decision making between two different strategies for optimizing inspection and maintenance plans: one based solely on intermittent visual inspections, which represents the current state-of-the-art for many systems, and the other based on SHM in combination with inspections.

A VoI analysis and a VoSHM analysis are associated with large modeling and computational challenges [175, 6]. In this thesis, we strive to avoid the overly simplifying modeling assumptions that are followed as a rule in the recent literature concerning the quantification of the VoI from SHM. A more sophisticated modeling calls for efficient computational algorithms, which are essential to a computationally viable VoI/VoSHM analysis. Heuristics, which are simple and intuitive parametrized decision rules [112, 17], yield a pragmatic approach for solving stochastic sequential decision problems. Efficient methods for performing a time-variant reliability analysis [120, 181] are discussed and implemented throughout this work. With respect to the Bayesian analysis task, which forms a computationally expensive element of a VoI/VoSHM analysis, in this thesis we employ on-line Bayesian filtering algorithms [163, 92], which are selected and adapted following a rigorous comparative assessment. The VoI and VoSHM analysis frameworks presented herein are decision support tools for providing the answer to whether SHM can generate economic value when used within certain decision contexts. This thesis delivers a novel VoI/VoSHM analysis framework, which is shown to be flexibly applied to different use cases, ranging from near-real time diagnostics to predictive maintenance planning in cases of slowly evolving deterioration processes.

In the PHM literature, various metrics have been introduced for assessing and comparing the performance of prognostic techniques [164, 128, 73, 105, 141]. They investigate from different angles the predictive capabilities of prognostic algorithms. No metric has been designed to explicitly incorporate in its evaluation the predictive maintenance (PdM) decisions that are to be informed by the outcome of a prognostic algorithm. Instead, some metrics only implicitly take into account the subsequent PdM planning task, e.g., by penalizing more late predictions compared to early ones [164]. Decision-oriented performance metrics could have a large utility in supporting researchers, who are at the forefront of prognostic algorithmic development, PHM practitioners, as well as decision-makers

and operators. Availability of such metrics could also set the stage for a paradigm shift with regard to optimizing the training process of prognostic algorithms (e.g., hyperparameter tuning) from a prediction-based approach to a decision-based one. In this context, this thesis proposes a metric for assessing and optimizing prognostic algorithms based on PdM decisions. The definition of this metric is fairly general. However, it is defined in conjunction with a specific decision setting and a corresponding PdM policy, which dictates the maintenance actions based on input RUL predictions obtained from the prognostics [39, 130].

Throughout this work, we attempt to highlight the value of integrating decision making in the scientific and practical development process of SHM and PHM towards transitioning these disciplines from research to a more widespread adoption in practice.

1.3 Thesis organization and contributions

This dissertation is split into two parts. Part I (Chapters 1 to 3) does not contain original research contributions, but instead provides the overarching scientific context. The current Chapter 1 constitutes an introduction to the motivation, context and scope of the work conducted in this thesis. Chapter 2 progressively introduces the theoretical, methodological and computational foundations of this work. Chapter 3 summarizes the contributions of this thesis and provides an outlook for future work.

Part II (Chapters 4 to 7) consists of the four original publications on which this dissertation is based. Each publication is incorporated as a separate chapter, as follows:

- Publication 1 (original publication [89]; Chapter 4) focuses on the quantification of the Value of Information (VoI) from vibration-based SHM by adapting the Bayesian decision analysis framework. Bayesian model updating [168] forms a fundamental element of the presented VoI analysis framework.
- Publication 2 (original publication [88]; Chapter 5) forms an extension of the work of publication 1. Specifically, a framework is developed for quantifying the expected gains that continuous vibration-based SHM-aided maintenance planning can provide when compared against intermittent inspection-based maintenance planning; the Value of SHM (VoSHM) metric is introduced for formally computing this benefit.
- Publication 3 (original publication [90]; Chapter 6) rigorously investigates and adapts selected sampling-based Bayesian filtering algorithms for pure recursive estimation of time-invariant model parameters. The presented algorithms are challenged with the task of properly quantifying the full posterior uncertainty of time-invariant deterioration model parameters. Bayesian filtering constitutes an important element of the VoSHM framework of publication 2.
- Publication 4 (original publication [91]; Chapter 7) deviates from the model-driven setting of the former publications, and instead focuses on data-driven predictive maintenance of non-unique engineering systems, for which monitoring data from several run-to-failure experiments are available. Specifically, this work proposes a decision-oriented metric for evaluating and optimizing data-driven RUL prediction algorithms.

Chapter 2

Decision Support with Health Monitoring

2.1 Maintenance planning - a problem of decision making under uncertainty

Various real-world engineering tasks involve decisions on logistic, inspection, maintenance, repair or replacement actions throughout a system's life-cycle. Several engineering systems operate in high-risk environments, hence such decisions often need to be made in view of the estimated risk associated with various potential threats (e.g., deterioration, extreme events). Maintenance actions typically come at a large cost. Thus, a main goal is to determine an optimized action plan that leads to an optimal balance between the cost of these actions and the estimated risk. A maintenance plan needs to determine the type of action as well as the time for performing this action. In this thesis, the term *maintenance planning* is used to generally refer to the task of planning logistic, inspection, maintenance, repair or replacement actions over the life-cycle of a component/system. Uncertainty characterizing the state of the system, the effect of maintenance actions on the system, and the information provided by data-gathering actions, such as inspections or monitoring, is ubiquitous in maintenance planning problems. Therefore, maintenance planning forms a *decision making under uncertainty* problem.

2.1.1 Predictive maintenance

Within a high-level classification, maintenance strategies can be classified into two main categories [67], namely 1) *corrective maintenance* and 2) *preventive maintenance*. Following the former, maintenance actions are performed upon failure of the component/system (e.g., replace a rolling bearing in a machine when it fails). On the contrary, a preventive maintenance strategy aims to inform maintenance actions before any failure occurrence. For certain components/systems, corrective maintenance is acceptable (e.g., to change the light bulb when it fails). However, for components/systems associated with high failure consequences, corrective maintenance is clearly a poor strategy, and development of effective preventive maintenance strategies is imperative.

Preventive maintenance strategies can be distinguished into three different types, namely 1) *periodi-*

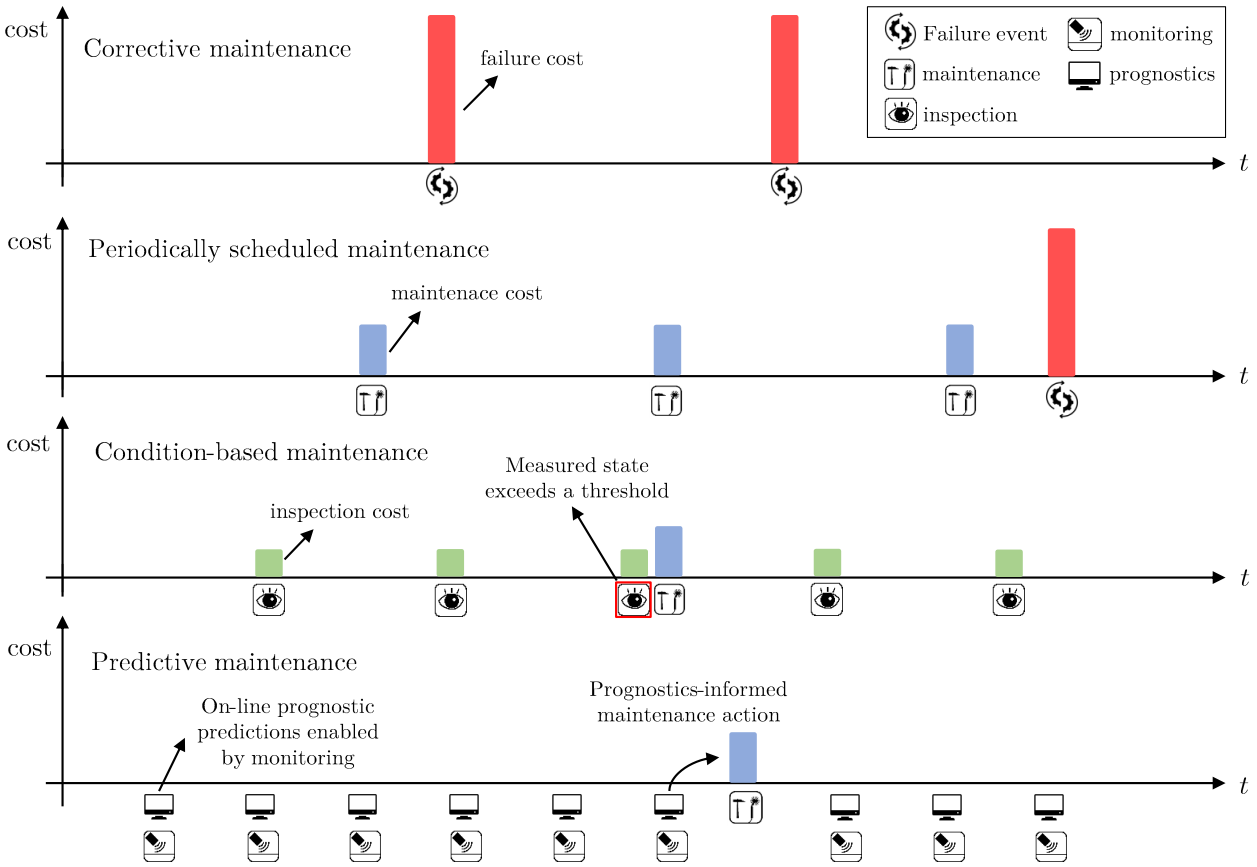

Figure 2.1: Illustration of the different types of maintenance strategies, the performed actions and the associated costs, for a safety-critical asset. It is herein assumed that predictive maintenance relies on on-line monitoring information and prognostic models. The cost of monitoring and the cost of prognostics are not included in the figure.

cally scheduled maintenance [12, 2], 2) *condition-based maintenance* [70, 81, 186, 3] and 3) *predictive maintenance* [31, 53, 130]. Periodically scheduled maintenance is performed at predefined points in time, which are fixed based on a regular time interval (e.g., replace a rolling bearing in a machine every 2 years). Naturally, it is possible to miss failure events that occur between these regular intervals. Condition-based maintenance (CBM) relies on data obtained from regular inspections and/or monitoring, whereby maintenance is performed at the exact moment when the measured current state, or a function thereof (e.g., some estimate of structural performance conditional on the measured current state), reaches or exceeds an unacceptable threshold (e.g., replace a component when the measured crack length exceeds 2mm). Predictive maintenance (PdM) instead employs data from continuous monitoring and/or inspections to update model-driven (see Section 2.1.4) or create data-driven prognostic models (see Section 2.2). These models are employed to perform predictions of different decision-relevant quantities, such as the time to failure or the probability of failure of the component/system. Thereby, maintenance is decided based on the prognostic model output (e.g., perform a repair action on the pier of a bridge structure when the predicted probability of failure of the structure within the next year exceeds an unacceptable threshold). In literature, the distinction between CBM and PdM may often be unclear, with the terms used interchangeably [58]. Fig. 2.1 provides a high-level illustration of the different types of maintenance strategies and the resulting costs, in particular for a system associated with high failure consequences. This thesis

focuses on predictive maintenance, which is the linchpin of all presented contributions, in which predictive maintenance is investigated in diverse decision contexts.

2.1.2 Cost-based criteria for predictive maintenance planning

In any decision making under uncertainty problem, such as the predictive maintenance planning problem, the goal is to find the optimal actions (or sequence of actions) that maximize the expected utility. In decision theory, *utility* provides the formal mathematical term that assesses the optimality of different decision alternatives [111, 173]. A *utility function* is a mathematical function that assigns a real number, the utility, to each possible outcome of a decision problem. The form of this mathematical function is defined by the decision maker, and is supposed to reflect the decision maker's preferences. For most engineering applications, the utility function is typically replaced by a *cost function* [57]. Cost can be equated to the negative utility.

The different predictive maintenance (PdM) policies investigated in this thesis are evaluated with respect to the expected value of some cost-based criterion. The cost-based criteria that are most often used in engineering applications are 1) the *expected total life-cycle cost* [57] and 2) the *long-run expected total cost per unit time* (or the *long-run expected maintenance cost per unit time*) [190, 39]. This section introduces these criteria and aims to provide suggestions for the choice of the appropriate one in function of certain application characteristics.

In decision analysis, every action has an associated cost. These are reflected in the initial definition of a cost model by the analyst, which strongly influences the results of the decision analysis. For instance, performing an inspection induces a cost $\widetilde{c}_{\text{insp}}$, a failure event induces a cost $\widetilde{c}_{\text{f}}$, etc. Different cost components synthesize the total life-cycle cost [57]. For maintenance planning in safety-critical components/systems (e.g., bridge structures or nuclear facilities), which are associated with high failure consequences (e.g., loss of life), the total life-cycle cost C_{tot} is typically taken as the sum of the total cost of inspections C_{I}, the total maintenance/repair/replacement costs C_{M}, and the risk of failure (the expected cost of failures) R_{F} over the life-cycle of a component/system:

$$C_{\text{tot}} = C_{\text{I}} + C_{\text{M}} + R_{\text{F}}. \tag{2.1}$$

For maintenance planning in non-safety-critical components/systems (e.g., a rolling bearing in machinery), the risk term may often be omitted from the total cost summation. Note that Eq. (2.1) ignores other costs that are present, such as the initial cost of construction or the decommissioning cost at the end of the structure's lifetime. This is because these costs are typically not affected by the maintenance strategy that is applied.

Calculating C_{I} and C_{M} throughout the life-cycle entails recording the time and the type of all actions performed (see Section 2.1.5.2). The risk of failure R_{F} is quantified via the solution of a time-variant reliability problem (see Sections 2.1.5.2 and 2.1.8).

The expected total life-cycle cost, $\mathbb{E}[C_{\text{tot}}]$, is an appropriate cost-based criterion for problems with a bounded time horizon, which is equal to the intended lifetime of a structural component/system (e.g., a bridge structure with an intended lifetime of 100 years). This criterion is employed in Sections 4.5 and 5.3 of this thesis.

In maintenance planning problems, replacement actions are commonly assumed to be perfect, bringing the component/system back to its original condition. In *renewal theory* [187, 155, 148], this is called the *renewal assumption*. A perfect replacement action defines a *renewal event*. A renewal event at time t leads to the end of one life-cycle of the component. Thereupon, a new life-cycle of the component initiates, and the component starts deteriorating anew. The stochastic deterioration process initiating after a renewal event at time t is a probabilistic replica of the process starting at time 0 [187]. The time interval between two successive replacements defines a renewal cycle. Renewal cycles are assumed to be independent of each other. Under these assumptions, the (non-discounted) long-run expected cost per unit time over an infinite time horizon, C_∞, is typically employed as the cost-based criterion for maintenance planning [190, 39]:

$$C_\infty = \lim_{t\to\infty} \frac{C_{\text{tot}}(t)}{t}. \tag{2.2}$$

According to the renewal-reward theorem [187], computation of C_∞ in Eq. (2.2) corresponds to evaluating the ratio:

$$C_\infty = \frac{\mathbb{E}[C_{\text{tot}}]}{\mathbb{E}[T_{\text{lc}}]}, \tag{2.3}$$

where $\mathbb{E}[C_{\text{tot}}]$ is the expected total cost induced during one life-cycle and $\mathbb{E}[T_{\text{lc}}]$ is the expected length of one life-cycle. This criterion is employed in Section 7.2.1 of this thesis.

The above renewal theory-based formulation is grounded on the assumption of an infinite time horizon, which is not realistic for most engineering components/systems [136]. Renewal theory-based formulations for finite time horizon have also been proposed [102, 136].

Discounting is an important concept that is implemented in life-cycle costing, especially when investment decisions are explored [57, 56]. It defines the process of converting a value received in the future into an equivalent value received now, thus accounting for the influence of time on the value of money. The costs at time t are typically multiplied with a *discounting function* $\gamma(t)$. A representative discounting function is:

$$\gamma(t) = \frac{1}{(1+r)^t}, \tag{2.4}$$

where r is the annually compounded discount rate, typically chosen in the range of 2-5%. Discounting may frequently be applied in decision problems with a finite or infinite time horizon [190, 56].

2.1.3 Optimization of predictive maintenance planning

In maintenance planning for engineering components/systems, decisions materialize in multiple diverse settings. Exemplary decision settings include, among others:

- Find the optimal time to perform a single replacement action that might be required over the bounded life-cycle of a component/system (see Section 4.5).
- Optimize the time(s) to perform inspection actions, and optimize decision on replacement action based on the inspection/monitoring information (see Section 5.3).

- Find the optimal time for a logistic action (e.g., order a spare component for replacement), and the optimal time for a replacement action (see Section 7.2.4).
- Choose the optimal inspection strategy, i.e., when to inspect, what to inspect for, how to inspect, where to inspect [112, 17].
- Decide *a-priori* (i.e., before actual installation) whether or not to install an SHM system on a target structure (see Chapters 4 and 5).

The life-cycle T_{lc} of a component/system is generally discretized in n_T time steps at which decisions on single or multiple actions can be made under sequential data [121, 8, 169, 124]. The full sequence of decisions on actions over the entire life-cycle must be considered in order to assess their impact on the life-cycle costs [18]. At all points in time, there is uncertainty characterizing the state of the system, the effect of maintenance actions on the system and the information provided by data-gathering actions, e.g., inspections and monitoring. This yields a *stochastic sequential decision problem* [99], the solution to which can be cumbersome and calls for large computational efforts [124, 112, 174, 138, 8].

In the predictive maintenance planning problems addressed in this thesis, the goal is to find the optimal sequence of actions $\boldsymbol{a} = \{a_1, \dots, a_{n_T}\}$ to perform at different points in time over the system's life-cycle, which minimize the expected total life-cycle cost, or the long-run expected cost per unit time (see Section 2.1.2). Without loss of generality, the formulations presented in this section use the expected total life-cycle cost as the cost-based criterion for PdM optimization. A solution to the following optimization problem is targeted:

$$\boldsymbol{a}_{\text{opt}} = \arg\min_{\boldsymbol{a}} \mathbb{E}[C_{\text{tot}}(\boldsymbol{a})]. \tag{2.5}$$

Let us consider a simple hypothetical decision setting, where one has to decide at each time step $t_k,\ k = 1, \dots, n_T$ throughout a component's life-cycle whether to repair (R) the component or do nothing (DN), in view of continuous monitoring information (i.e., monitoring data are available at each t_k). The set of possible actions at time t_k is $a_{\text{rep},k} = \{\text{R, DN}\}$. The sequence of actions throughout the life-cycle is $\boldsymbol{a} = \{a_{\text{rep},1}, \dots, a_{\text{rep},k}\}$. Monitoring data obtained at each time step affect the repair decision. In turn, repair decisions affect the state of the component, and consequently also the decisions at future points in time. This simple example aims to demonstrate the complex nature of stochastic sequential decision problems.

Numerous frameworks and algorithms have been applied for the solution of stochastic sequential decision problems in the context of maintenance planning, including Markov decision processes (MDPs) [72, 151, 138, 99], partially observable Markov decision processes (POMDPs) [99, 138, 121, 165, 8, 124, 9, 169], and (deep) reinforcement learning (RL) [6, 7, 153, 75, 104]. The framework that is employed in this thesis for the solution to this problem entails the proposal of a set of decision *heuristics* [112, 17, 18]. These are simple and intuitive parametrized decision rules that dictate the action(s) to take at any time step, based on all the available information up to that point in time. The aim is that developed heuristics should be comprehensible for engineers and operators. Nowadays, algorithmic explainability and interpretability is a crucial topic [24, 157]. A significant advantage associated with the heuristics-based framework for solving stochastic sequential decision problems compared to other black-box frameworks lies in its ability to provide interpretable solutions to the decision problem. However, as will be discussed shortly, heuristics provide only approximate solutions to the decision problem, and the optimality thereof cannot be guaranteed. The desideratum is that heuristics should lead to solutions that are reasonably close to the optimum.

2.1.3.1 Heuristics-based optimization of predictive maintenance plans

To present the heuristics-based framework, the concepts of policies and strategies need to be introduced first [83]. Essentially, a *policy* π is a set of rules that specify the actions to take at time t based on all the information that is already available up to t, that is, past inspection and/or monitoring data, as well as performed actions. For instance, a policy could provide the answer to the following question: "Given sensor data up to time t, and given that no replacement has been previously performed, should the component be replaced at t?" {yes,no}. The set of policies for all time steps of the decision problem time horizon define a *strategy* S. A *stationary* strategy consists of policies that remain the same at all times [83, 99]. Development of non-stationary strategies is only sensible in decision problems with a bounded finite time horizon. All adopted strategies in this thesis are stationary. A generic stationary policy for predictive maintenance planning is thus referred to as the *PdM policy* in the remainder of this thesis.

Heuristics are functional forms of the policies. They are decision rules that are typically formulated as functions of a set of heuristic parameters, contained within a vector $\boldsymbol{w}$, that may be used to parametrize a stationary strategy, as well as of inspection/monitoring data. Essentially, heuristics take as input all the information available up to a point in time and dictate the type and time of actions to perform. For instance, a heuristic for condition-based maintenance with vibration-based structural health monitoring could be: "Repair the structure immediately at the point in time when the identified first eigenfrequency f_1 presents a decrease of $p\%$ compared to its value in the initial undamaged state". In this example, the heuristic is a function h of the single heuristic parameter p and of the data, which in this case is the identified first eigenfrequency f_1, i.e., $h(p, f_1)$. Examples of heuristics for predictive maintenance include: "Repair the structure at t if the predicted failure rate at time $t+1$, conditional on all data from time 0 to t, exceeds a heuristic threshold h_{thres}" or "Replace the component when the estimated remaining useful life is smaller than a threshold value t_{thres}".

With parametrized heuristics, the predictive maintenance planning optimization is no longer performed in the space of actions $\boldsymbol{a}$. Instead, the optimization is performed in two layers. To begin with, a set of meaningful and actionable heuristics need to be defined. Engineering knowledge and domain expertise can be incorporated in this task. Thus, the first optimization layer involves the choice of the best heuristics among a devised set. Thereafter, if the heuristics are parametrized, the optimal policy can be approximated by applying the chosen heuristics with optimal heuristic parameter values. The latter emerge from the solution to the following optimization problem:

$$\boldsymbol{w}_{\text{opt}} = \arg\min_{\boldsymbol{w}} \mathbb{E}[C_{\text{tot}}(\boldsymbol{w})]. \tag{2.6}$$

It should be noted that the expression in Eq. (2.6) does not address both the optimization layers mentioned above, but rather only focuses on the second layer. It directly assumes that parametrized heuristics have been defined, and only addresses the optimization of the heuristic parameters. Eq. (2.6) reflects what is done in most numerical investigations in this thesis, where depending upon the problem at hand, heuristics are predefined based on engineering understanding, and no formal optimization is performed in the space of heuristics, but rather in the space of the parameters of the chosen heuristics.

Comparing Eqs. (2.5) and (2.6), it becomes clear that, with parametrized heuristics, the space of solutions to the decision problem is drastically reduced from the action space to the heuristic parameter

space. Heuristics thus provide simpler, viable solutions to stochastic sequential decision problems[1], as they seek to eliminate the sequential nature of the decision optimization problem. This, however, requires the sensible definition of heuristics in the first place, as well as their parametrization, and eventually comes at the expense of not finding the globally optimal solution. Still, in the context of maintenance planning, heuristics have been found to provide reasonable solutions [131, 18]. Furthermore, adaptive heuristic-based maintenance planning strategies have been developed and shown to provide improved solutions to stochastic sequential decision problems [17].

It should be noted that heuristics can and typically do involve models of large complexity. For instance, a heuristic that dictates that a repair action should be performed when the predicted failure rate of a component at a future time exceeds a heuristic threshold requires the solution to a time-variant reliability problem [181, 120], which is a complex task (see Section 2.1.8). Such heuristics are used in this thesis. A heuristic could also involve the solution to a complex optimization problem (e.g., see Section 7.2.3.3), or could even emerge from POMDP or deep RL solutions.

The heuristic parameter optimization problem defined in Eq. (2.6) belongs to the class of stochastic optimization problems, which deal with noisy objective functions. Such problems are omnipresent in science and engineering, and the development of stochastic optimization methods has attracted a significant amount of research [96, 144]. In the numerical investigations in this thesis, the heuristic parameter space for the optimization of Eq. (2.6) is small, and an approximate solution is found through an exhaustive search among a large discrete set of values of the heuristic parameters. This process does not address the stochastic nature of the objective function.

2.1.4 Model-based predictive maintenance planning

The model-based predictive maintenance (PdM) framework that will be introduced in this section constitutes the classical approach to PdM planning. It requires the *a-priori* definition of a stochastic deterioration model describing the evolution of deterioration over time, and its performance greatly depends on the adopted model. Section 2.1.4.1 first discusses different types of stochastic deterioration models, followed by Section 2.1.4.2, which addresses the model-based evaluation of a PdM policy.

2.1.4.1 Stochastic deterioration modeling

One can distinguish two main classes of structural deterioration, namely (1) gradual deterioration and (2) shock deterioration [159, 84]. Deterioration modeling is a rather complex task, with multiple sources of uncertainty influencing the deterioration process [43, 160]. This thesis is concerned with stochastic deterioration models that consider the state of deterioration as a continuous random variable, while discrete state deterioration models are not addressed. For reference to the latter type see, e.g., [160, Chapter 6].

[1] In the context of this thesis, heuristics are mainly introduced for the solution to a preposterior decision analysis (see Section 2.1.5), which yields a stochastic sequential decision problem, and thus poses significant computational challenges.

With respect to the form of the mathematical equation describing the deterioration process, deterioration models can be classified into two categories, *empirical models* or *physics-based models*.

1. *Empirical deterioration models* assume a specific, typically simple, mathematical form for the equation describing the deterioration process, and do not (necessarily) rely on physics. Appropriate choice of the model form and fitting of the model parameters is typically conditional on the existence of experimental data. As described in [43], despite their simplicity, empirical models are still flexible enough to model different kinds of deterioration mechanisms. [43] further argues that, even though certain deterioration mechanisms might be captured by more precise physics-based modeling, the benefit of employing physics-based models instead of simple empirical models for time-dependent reliability purposes is not clear. The following is an example of an empirical model that is commonly employed for modeling the exponential growth of battery deterioration [68]:

$$D(t) = C \exp(-\lambda t), \tag{2.7}$$

where $\boldsymbol{\theta} = [C, \lambda]$ is the vector of model parameters, and $D(t)$ is the level of battery capacity deterioration at time t for given $\boldsymbol{\theta}$. Development and application of empirical deterioration models can be found in multiple literature sources [44, 125, 147, 118, 56, 43, 68, 140]. Empirical deterioration models are adopted in numerical investigations in Sections 4.6.2, 5.4.2 and 6.3.2 of this thesis.

2. *Physics-based deterioration models* typically involve the use of mathematical equations and physical laws to simulate the effect of different deterioration processes on structural, mechanical, electronics components/systems, etc. Uncertain parameters appear in the equations of physics-based models. For certain types of deterioration processes, well-established physics-based models exist that form the state-of-the-art. For example, the Paris-Erdogan law describing the evolution of fatigue crack growth is one of the most commonly employed physics-based deterioration models [139, 38] (see Eq. (6.7) in Section 6.3.1). Corrosion is another deterioration process which is amenable to more detailed physics-based modeling [119]. There is potentially vast utility in developing physics-based deterioration models [117]. However, in practice, establishing such models poses a significant challenge. Structural deterioration processes are highly complex, highly uncertain and strongly interacting with other processes, such as environmental variability. Even once a model is developed, validating it is a notoriously difficult task. Furthermore, such models typically contain a relatively large number of uncertain parameters, the estimation of which requires availability of a large amount of experimental data, which are typically not available.

With respect to the way in which randomness is introduced in the mathematical equation describing the deterioration process, empirical and physics-based deterioration models can be classified into *random variable models* and *stochastic process models* [56].

1. *Random variable deterioration models* describe the temporal evolution of deterioration as a function of time and one or more unknown time-invariant parameters, modeled as random variables (RVs). For example, with reference to Eq. (2.7), variables C, λ are typically modeled as RVs that follow a certain probability distribution. With this type of models, all the uncertainty characterizing the deterioration process is contained within a vector $\boldsymbol{\theta} \in \mathbb{R}^d$, with

d being the total number of RVs. For fixed values of the RVs in $\boldsymbol{\theta}$, the temporal evolution of deterioration is completely fixed. Therefore, as noted in [56, 190], RV models are more "static" compared to other types of models, such as the stochastic process models that are introduced in the next paragraph, as they cannot properly describe the temporal variability of the process.

2. *Stochastic process deterioration models* describe the temporal evolution of deterioration as a stochastic process, which is a collection of random variables that evolve over time according to a fixed set of rules [192]. Empirical and physics-based models can be combined with stochastic processes, e.g., via modeling one or more of the uncertain parameters in the mathematical equation as a stochastic process of time [13], or via the inclusion of additive Gaussian or multiplicative lognormal stochastic process noise terms in the equation [179, 32]. Structural deterioration processes are often modeled via continuous-time Markov processes [190]. The most common stochastic process models of this type include the Wiener process [208] for modeling non-monotonously increasing deterioration processes, the Gamma process [190] for modeling strictly monotonic and gradual deterioration processes, and the compound Poisson process [190, 160] for modeling shock deterioration processes (the compound Poisson process is employed in Section 5.4.2).

2.1.4.2 Model-based evaluation of a predictive maintenance policy

Section 2.1.2 introduced the expected total life-cycle cost, $\mathbb{E}[C_{\text{tot}}]$, and the long-run expected cost per unit time, $C_\infty = \frac{\mathbb{E}[C_{\text{tot}}]}{\mathbb{E}[T_{\text{lc}}]}$, on the basis of which a PdM policy is evaluated. Both quantities require the estimation of expected values. Similar to Section 2.1.3, without loss of generality, the presentations in the current section concentrate only on the evaluation of the expected total life-cycle cost, $\mathbb{E}[C_{\text{tot}}]$.

Thus far, it has not been discussed with respect to which uncertain quantity this expectation is taken. The model-based PdM framework is conditional on the a-priori availability of a stochastic deterioration model. A random vector $\boldsymbol{X}$ is defined, which contains time-invariant uncertain deterioration model(s) parameters $\boldsymbol{\theta}$, time-variant uncertain deterioration state(s), as well as uncertain loads acting on the engineering component/system. Some random variables in $\boldsymbol{X}$ may therefore be functions of time. The total cost C_{tot} now becomes a function of the random vector $\boldsymbol{X}$ and the set of actions $\boldsymbol{a}$, i.e., $C_{\text{tot}}(\boldsymbol{X}, \boldsymbol{a})$. Respectively, with heuristics, the total cost is denoted by $C_{\text{tot}}(\boldsymbol{X}, \boldsymbol{w})$. In this case, the expectation in $\mathbb{E}[C_{\text{tot}}]$ is taken with respect to $\boldsymbol{X}$. Monte Carlo (MC) simulation-based methods are typically employed for evaluating this expectation (e.g., see Section 2.1.5.1). The performance of the model-based PdM framework entirely depends on the prior knowledge on $\boldsymbol{X}$. This prior knowledge is typically embedded within the definition of a joint prior probability density function (PDF) $f_{\boldsymbol{X}}(\boldsymbol{x})$ for the random vector $\boldsymbol{X}$. The terms prior knowledge and prior PDF set the stage for introducing the Bayesian decision analysis framework [149, 15].

2.1.5 Bayesian decision analysis and value of information

Bayesian decision analysis is a model-based mathematical framework for the solution to decision making under uncertainty problems, in which data of some sort becomes available and can be used to reduce the uncertainty in the problem [149, 15]. It is based on the Bayesian interpretation

of probability theory [62]. This section discusses Bayesian decision analysis within the context of model-based predictive maintenance planning, which is introduced in Section 2.1.4.2.

Prior decision analysis

An initial assumption needs to be made for the probabilistic model of the uncertain quantities of the problem at hand, which in the context of model-based predictive maintenance planning refers to the random vector $\boldsymbol{X}$ that is introduced in Section 2.1.4.2. The *a-priori* assumption for the probabilistic model of $\boldsymbol{X}$ reflects the subjective degree of belief of the analyst, based on all available prior information and engineering expertise. For some types of deterioration (e.g., fatigue, corrosion), prior knowledge on certain parameters in $\boldsymbol{X}$ is typically available. The *a-priori* assigned joint PDF $f_{\boldsymbol{X}}(\boldsymbol{x})$ is called the *prior* distribution.

A *prior decision analysis* seeks to find the optimal set of actions over the life-cycle $\boldsymbol{a}_{\text{opt}}$ by solving the following minimization problem:

$$\boldsymbol{a}_{\text{opt}} = \arg\min_{\boldsymbol{a}} \mathbb{E}_{\boldsymbol{X}}[C_{\text{tot}}(\boldsymbol{X}, \boldsymbol{a})], \tag{2.8}$$

where $\mathbb{E}_{\boldsymbol{X}}$ is the expectation with respect to the prior PDF $f_{\boldsymbol{X}}(\boldsymbol{x})$.

Posterior decision analysis

When data $\boldsymbol{z}$ of some sort becomes available, e.g., via visual inspections, non-destructive evaluations (NDEs), or structural health monitoring (SHM) systems, it can be used to update the distribution of $\boldsymbol{X}$. This is done via *Bayesian analysis*, which is introduced in Section 2.1.6. The distribution of $\boldsymbol{X}$ given $\boldsymbol{z}$, denoted by $f_{\boldsymbol{X}|\boldsymbol{z}}(\boldsymbol{x}|\boldsymbol{z})$, is called the *posterior* distribution. Once the posterior distribution is obtained, a *posterior decision analysis* can be performed, which yields the set of actions that are optimal conditional on the observed data:

$$\boldsymbol{a}_{\text{opt}|\boldsymbol{z}} = \arg\min_{\boldsymbol{a}} \mathbb{E}_{\boldsymbol{X}|\boldsymbol{z}}[C_{\text{tot}}(\boldsymbol{X}, \boldsymbol{a})]. \tag{2.9}$$

Data provides information that reduces the uncertainty in $\boldsymbol{X}$. This uncertainty reduction, which is reflected in the shift from a prior to a posterior distribution, is expected to lead to enhanced decision making compared to the prior case. Note that the expectation in Eq. (2.9) is taken with respect to the posterior distribution $f_{\boldsymbol{X}|\boldsymbol{z}}(\boldsymbol{x}|\boldsymbol{z})$. The task of obtaining this distribution often relies on Monte Carlo simulation-based methods, which significantly increases the computational burden associated with a posterior decision analysis.

The focus of this thesis is on PdM planning for components/systems that are continuously monitored by SHM systems. Long-term monitoring leads to a sequence of noisy measurements $\boldsymbol{z}_{1:n} = \{z_1, \dots z_n\}$ obtained sequentially at different points in time $\{t_1, \dots, t_n\}$, of the decision making problem. Therefore, in this thesis, $\boldsymbol{z}$ in most cases denotes the sequence of data $\boldsymbol{z}_{1:n}$. At t_1 only the monitoring outcome z_1 is available for the decision a_1, whereas the set $\boldsymbol{z}_{1:2}$ is available for the decision a_2 at t_2, etc. The sequential nature of the monitoring data calls for a *sequential Bayesian analysis*, with the goal of sequentially updating the distribution of $\boldsymbol{X}$ conditional on the sequence of

measurements $\boldsymbol{z}_{1:n}$. Sequential Bayesian analysis is introduced in Section 2.1.7.1. In such cases, the optimization of the decisions on actions must also be performed sequentially, following the sequence of data $\boldsymbol{z}_{1:n}$. As discussed in Section 2.1.3, this sequential decision optimization calls for large computational efforts. A simpler solution to this problem is enabled by the use of heuristics, through which the decisions at each time step are readily identified.

Preposterior decision analysis

Data $\boldsymbol{z}$ of some sort only becomes available in the operational phase upon performing data-gathering actions. For instance, monitoring data becomes available only after the actual installation and operation of an SHM system, or visual inspection data only becomes available after performing an inspection campaign. Nonetheless, one is often interested in investigating the potential economic benefit that is associated with gathering data $\boldsymbol{z}$ for reducing the uncertainty in the problem, prior to performing inspections, NDEs, or installing and operating SHM systems. Such investigations can be performed within the framework of a *preposterior decision analysis*.

A preposterior decision analysis requires a dedicated model of the data-gathering technique that is investigated [2]. Such a model is required for generating probabilistic predictions of the data $\boldsymbol{Z}$ that one expects to extract in practice with this technique, for sampled realizations of the random vector $\boldsymbol{X}$. Upper case $\boldsymbol{Z}$ denotes the random vector containing the yet unknown monitoring information, while a realization of $\boldsymbol{Z}$ is denoted by lower case $\boldsymbol{z}$. A preposterior analysis therefore relies on simulated data. Generating $\boldsymbol{Z}|\boldsymbol{X}$, i.e., realizations of $\boldsymbol{Z}$ conditional on $\boldsymbol{X}$, is performed with the aid of a probabilistic model that describes the quality of the data provided by the data-gathering technique. This probabilistic model is typically a *likelihood function*, e.g., a probability of detection (POD) or a receiver operating characteristic (ROC) curve [59, 126, 19]. Alternatively, this data generation may be facilitated by use of a *digital twin* [89, 150, 93, 201, 183, 199, 191, 189, 188], as discussed in the following paragraph.

Fig. 2.2 schematically represents how an SHM system could provide decision support in a practical setting when implemented on a bridge system. The figure separates between two distinct domains, namely the physical domain, which consists of the actual structure being in operation and monitored by the deployed SHM system, and the digital domain, which involves a finite element model that aims to represent the real physical system as closely as possible. The connection between the two domains may be established via a *model updating* process on the basis of the information obtained from the SHM system (see Section 2.1.6). This is often referred to as the process of establishing a digital twin. A preposterior decision analysis is performed before the actual installation of an SHM system, and aims to represent the life-cycle deterioration and management process in a simulated environment. This is illustrated in Fig. 2.3, which replaces the left-hand-side physical domain of Fig. 2.2 with a digital domain, which simulates the life-cycle operation of the structure and the associated SHM data by use of the digital twin. In this manner, the digital domain represented in the left-hand-side of Fig. 2.3 synthetically generates realizations of $\boldsymbol{Z}|\boldsymbol{X}$. This process is implemented in the numerical investigations of Sections 4.6.3 and 5.6.1 in this thesis.

The expected total life-cycle cost in a preposterior decision analysis is quantified by solving the expectation with respect to both $\boldsymbol{X}$ and $\boldsymbol{Z}$, i.e., $\mathbb{E}_{\boldsymbol{X},\boldsymbol{Z}}[C_{\text{tot}}(\boldsymbol{X}, \boldsymbol{a}_{\text{opt}|\boldsymbol{Z}})]$. Hence, for different real-

[2] This is also required in a posterior decision analysis in the definition of a likelihood function.

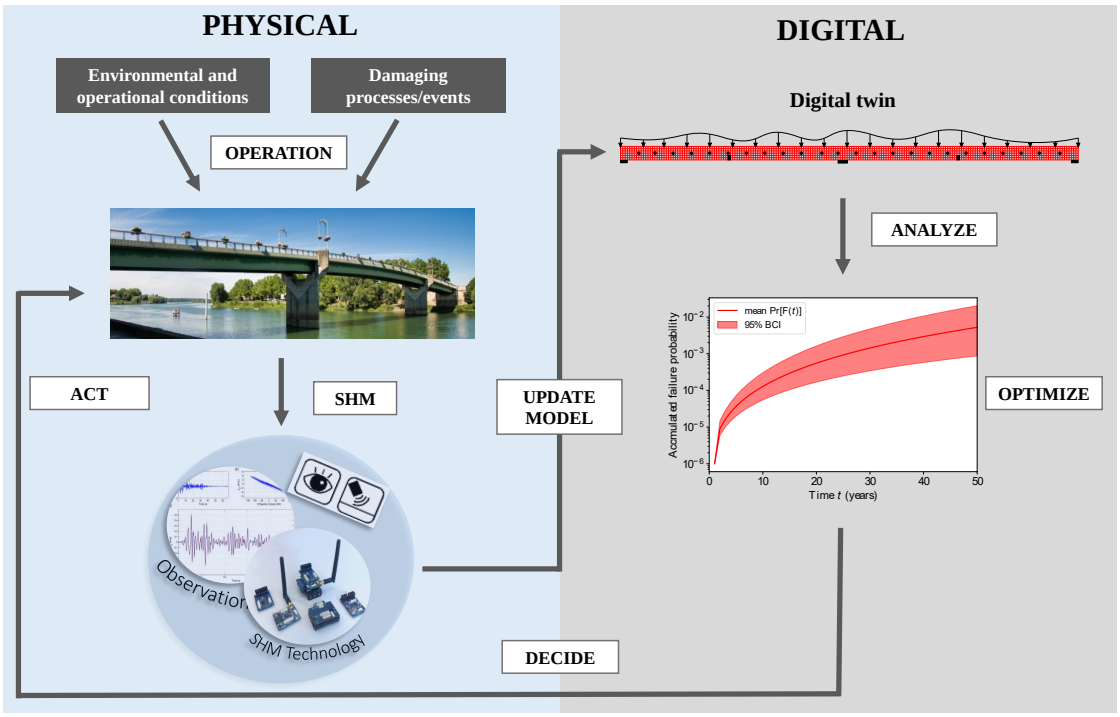

Figure 2.2: High-level representation of the manner in which SHM can provide decision support when implemented on a bridge system.

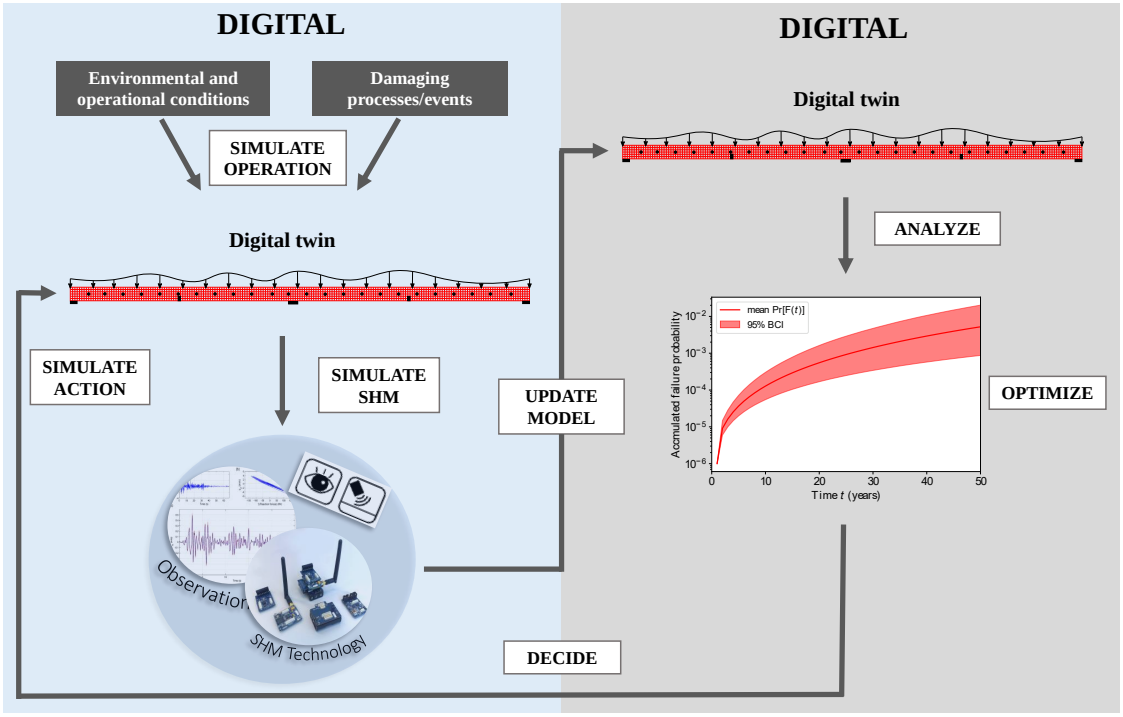

Figure 2.3: Digital-twin-enabled preposterior decision analysis, whose goal is to investigate in a simulated environment whether installing an SHM system on a bridge structure is cost-beneficial.

izations of $\boldsymbol{Z}$, the optimal actions as a function of $\boldsymbol{Z}$, i.e., $\boldsymbol{a}_{\text{opt}|\boldsymbol{Z}}$, need to be found. This requires the solution to multiple posterior decision analysis problems (i.e., multiple solutions to the problem of Eq. (2.9)). This renders the computation of the expected total life-cycle cost in a preposterior analysis cumbersome and expensive. Heuristics can significantly simplify this computation.

Parametrized heuristics reduce the burden of having to find $\boldsymbol{a}_{\text{opt}|\boldsymbol{Z}}$ for multiple sampled realizations of $\boldsymbol{Z}$. Instead, the optimal actions are approximated by the heuristic as a function of the heuristic parameters and $\boldsymbol{Z}$. Optimizing heuristics in a preposterior decision analysis boils down to solving the following optimization problem:

$$\boldsymbol{w}_{\text{opt}}^{\text{prepost}} = \arg\min_{\boldsymbol{w}} \mathbb{E}_{\boldsymbol{X},\boldsymbol{Z}}[C_{\text{tot}}(\boldsymbol{X}, \boldsymbol{Z}, \boldsymbol{w})]. \tag{2.10}$$

The problem can be further simplified by replacing the optimization of the heuristic parameters in Eq. (2.10) by a choice based on expert assessment. For instance, an expert might assign a value of 10^{-5} as the heuristic threshold on the probability of failure that triggers an inspection, without further optimizing it (e.g., see Section 5.6.3.4). This resembles real practical settings, where optimization is rarely performed.

The classical preposterior decision analysis [149] can further include an additional optimization layer, e.g., it is often employed for optimizing inspections and/or SHM systems. Examples include the optimization of inspection schedules or the design of monitoring systems [177, 18] (e.g., see Section 4.6.6.3).

Value of Information

Solving both a prior and a preposterior decision analysis enables the quantification of the Value of Information (VoI). This is done by taking the difference in expected total life-cycle costs between the prior and the preposterior case:

$$VoI = \mathbb{E}_{\boldsymbol{X}}[C_{\text{tot}}(\boldsymbol{X}, \boldsymbol{a}_{\text{opt}})] - \mathbb{E}_{\boldsymbol{X},\boldsymbol{Z}}[C_{\text{tot}}(\boldsymbol{X}, \boldsymbol{a}_{\text{opt}|\boldsymbol{Z}})]. \tag{2.11}$$

With parametrized heuristics, the equation for the VoI is written as:

$$VoI = \mathbb{E}_{\boldsymbol{X}}[C_{\text{tot}}(\boldsymbol{X}, \boldsymbol{w}_{\text{opt}}^{\text{pr}})] - \mathbb{E}_{\boldsymbol{X},\boldsymbol{Z}}[C_{\text{tot}}(\boldsymbol{X}, \boldsymbol{Z}, \boldsymbol{w}_{\text{opt}}^{\text{prepost}})]. \tag{2.12}$$

The outcome of a VoI analysis depends on the assumed prior probabilistic model for $\boldsymbol{X}$, as well as on the assumed conditional probabilistic model $\boldsymbol{Z}|\boldsymbol{X}$ of the data. A full VoI analysis is typically associated with large modeling and computational challenges, as graphically summarized in Fig. 4.1.

The VoI provides a formal Bayesian decision theory-based metric for quantifying *a-priori* the effect of data-gathering techniques on life-cycle costs. It can be utilized as a tool to support decisions on whether or not to invest in a specific data-gathering technique for obtaining information that reduces the uncertainty in the system. The VoI can alternately be used as a metric for choosing what to observe with a fixed data-gathering technique (e.g., which component in a system should be inspected), for optimal allocation of resources, or for providing a ranking among various candidate data-gathering techniques.

Computation of the VoI does not include the total life-cycle cost of the data-gathering process itself (e.g., cost of installation, maintenance or repair of an SHM system). Hence for decision making,

one should subtract the cost associated with implementing a specific data-gathering technique from the VoI. The resulting quantity is the net VoI. Investing in a data-gathering technique is worthwhile only when its VoI is larger than its cost, i.e., only when the net VoI is positive.

Under the premise of finding the optimal solutions to the prior and the preposterior decision analysis, the VoI cannot be negative. However, in many practical situations this may not hold true [195, 146].

VoI analysis has found application in many different domains, e.g., in environmental health risk assessment [202], medical decision making [1], informatics [101], ecology [21], among others. The next paragraph focuses on reviewing works related to the VoI within different contexts related to civil, infrastructure and mechanical engineering systems.

The VoI has been used in the context of planning inspections and maintenance for deteriorating structural systems in [176, 37, 193, 109, 213, 100, 212]. Multiple papers have appeared within the last decade that investigate quantification of the value of the information provided by SHM systems to support single or sequential decisions throughout the structural life-cycle [145, 106, 89, 133, 132, 110, 26, 185, 184, 79, 175, 65, 66, 206, 205, 98, 194, 211, 195, 94, 80, 129, 204]. Few authors have investigated the VoI within the context of partially observable Markov decision processes (POMDPs) [8, 169, 121, 171]. The VoI has further been used as a heuristic metric for optimizing decisions on future inspections in the context of sequential decision making problems [76, 77, 50]. Optimal sensor placement is another important area of application of the VoI, wherein it acts as the objective function for the optimization problem [22, 23, 71, 114, 115, 113, 42]. Efficient techniques for evaluation of the VoI have also been investigated [174, 203, 180].

Value of (Partial) Perfect Information

A VoI analysis typically requires detailed domain-specific modeling and entails large computational challenges, which might often be difficult to justify in real-world projects. A quantity which can be computed with much less effort, and which provides an upper limit to the VoI, is the so-called value of perfect information (VoPI) [149, 173]. This relates to the hypothetical scenario of a perfect data-gathering process that provides full deterministic knowledge of the random vector $\boldsymbol{X}$. The VoPI quantifies the maximum value that information from any data-gathering technique can bring in supporting decisions within a certain decision setting, i.e., it provides a first estimate on the maximum investment that should be made. Thus, it is always sensible to perform a VoPI analysis prior to a VoI analysis, as the former may provide results that might render the latter redundant (e.g., if one finds that the VoPI for a certain decision setting is anyway too small).

The VoPI assumes elimination of all the uncertainty in vector $\boldsymbol{X}$, which however is never practically feasible. Uncertainties are classified into two categories, aleatory and epistemic [97, 46]. Aleatory uncertainty is due to inherent randomness related to a physical process (e.g., the annual extreme wind load acting on the structure), and is irreducible. Epistemic uncertainty is due to incomplete knowledge, and is considered reducible, e.g., by gathering additional data. Thus, only the epistemic uncertainty in $\boldsymbol{X}$ can be reduced. The value of partial perfect information (VPPI) is a metric that is similar to the VoPI, with the difference that it corresponds to the hypothetical scenario where only the epistemic uncertainty in $\boldsymbol{X}$ is completely eliminated by a data-gathering process. The VPPI metric assumes a smaller value than the VoPI, however it provides a practicable upper limit to the

VoI. In Section 4.5.5, the VPPI metric is introduced in the context of vibration-based structural health monitoring of a bridge structure, and is numerically investigated in Section 4.6.6.

Value of structural health monitoring

The VoI metric compares the resulting expected total life-cycle cost computed with a prior decision analysis, where neither inspection nor monitoring data are assumed available, with the one resulting from a preposterior decision analysis, where data from a specific data-gathering process are assumed available. However, following the maintenance planning dictated by a prior decision analysis throughout the whole life-cycle is unreasonable when managing engineering components/systems, especially in the case of safety-critical systems. For such systems, some data-gathering scheme is always implemented, with information collected at different points in time throughout the life-cycle. Therefore, the more appropriate question to answer when managing such systems is which data-gathering technique is most beneficial to invest in. For instance, a relevant question that a bridge operator may try to address is: "Should I manage the bridge based on data obtained from visual inspections or is it worth investing in installing and operating an SHM system?". Such questions can be answered through the solution to two (or more) preposterior decision analysis problems.

Let the quantity of interest be the difference in expected total life-cycle costs between two considered cases: 1) perform predictive maintenance planning based on data from intermittent visual inspections and/or NDEs and 2) perform predictive maintenance planning based on continuous long-term data from an SHM system and additional visual inspection data. The data obtained from intermittent visual inspections and/or NDEs is denoted by $\boldsymbol{Z}_{\text{insp}}$, whereas the data obtained from an SHM system is denoted by $\boldsymbol{Z}_{\text{SHM}}$. In this setting, a metric called the value of structural health monitoring (VoSHM) is introduced:

$$VoSHM = \mathbb{E}_{\boldsymbol{X},\boldsymbol{Z}_{\text{insp}}}[C_{\text{tot}}(\boldsymbol{X}, \boldsymbol{a}_{\text{opt}|\boldsymbol{Z}_{\text{insp}}})] - \mathbb{E}_{\boldsymbol{X},\boldsymbol{Z}_{\text{SHM}},\boldsymbol{Z}_{\text{insp}}}[C_{\text{tot}}(\boldsymbol{X}, \boldsymbol{a}_{\text{opt}|\boldsymbol{Z}_{\text{SHM}},\boldsymbol{Z}_{\text{insp}}})]. \tag{2.13}$$

With parametrized heuristics, the expression for the VoSHM metric becomes:

$$VoSHM = \mathbb{E}_{\boldsymbol{X},\boldsymbol{Z}_{\text{insp}}}[C_{\text{tot}}(\boldsymbol{X}, \boldsymbol{Z}_{\text{insp}}, \boldsymbol{w}^{\text{prepost}}_{\text{opt,insp}})] - \mathbb{E}_{\boldsymbol{X},\boldsymbol{Z}_{\text{SHM}},\boldsymbol{Z}_{\text{insp}}}[C_{\text{tot}}(\boldsymbol{X}, \boldsymbol{Z}_{\text{SHM}}, \boldsymbol{Z}_{\text{insp}}, \boldsymbol{w}^{\text{prepost}}_{\text{opt,SHM}})]. \tag{2.14}$$

This metric has been recently introduced in [8, 88]. It is numerically investigated in Section 5.6 of this thesis.

2.1.5.1 Monte Carlo simulation for evaluating the value of information

Quantifying the VoI, or a more specialized metric such as the VoSHM, requires evaluating expected values. In this section, a Monte Carlo simulation (MCS) approach [156] is presented for the heuristics-based evaluation of the VoI, based on [89, 180]. Initially, Eq. (2.12) is rearranged as:

$$\begin{aligned} VoI &= \mathbb{E}_{\boldsymbol{X}}[C_{\text{tot}}(\boldsymbol{X}, \boldsymbol{w}^{\text{pr}}_{\text{opt}})] - \mathbb{E}_{\boldsymbol{X},\boldsymbol{Z}}[C_{\text{tot}}(\boldsymbol{X}, \boldsymbol{Z}, \boldsymbol{w}^{\text{prepost}}_{\text{opt}})] \\ &= \mathbb{E}_{\boldsymbol{X}}\left\{C_{\text{tot}}(\boldsymbol{X}, \boldsymbol{w}^{\text{pr}}_{\text{opt}}) - \mathbb{E}_{\boldsymbol{Z}|\boldsymbol{X}}[C_{\text{tot}}(\boldsymbol{X}, \boldsymbol{Z}, \boldsymbol{w}^{\text{prepost}}_{\text{opt}})]\right\}. \end{aligned} \tag{2.15}$$

The VoI in Eq. (2.15) can be approximated with MCS:

$$VoI \approx \frac{1}{n_{\text{MCS}}} \sum_{i=1}^{n_{\text{MCS}}} \left\{ \frac{1}{n_{\text{z}}} \sum_{j=1}^{n_{\text{z}}} \left[C_{\text{tot}}(\boldsymbol{x}^{(i)}, \boldsymbol{w}_{\text{opt}}^{\text{pr}}) - C_{\text{tot}}(\boldsymbol{x}^{(i)}, \boldsymbol{z}^{(i,j)}, \boldsymbol{w}_{\text{opt}}^{\text{prepost}}) \right] \right\}, \tag{2.16}$$

where $\boldsymbol{x}^{(i)}$ are sampled realizations of $\boldsymbol{X}$ drawn from the probability distribution $f_{\boldsymbol{X}}(\boldsymbol{x})$, and $\boldsymbol{z}^{(i,j)}$ are samples drawn from the probabilistic model $f_{\boldsymbol{Z}|\boldsymbol{X}}(\cdot|\boldsymbol{x}^{(i)})$. Typically, $n_{\text{z}} = 1$, i.e, for each sample $\boldsymbol{x}^{(i)}$, a single conditional sample of the data $\boldsymbol{z}^{(i)}$ is generated. With $n_{\text{z}} = 1$, the MCS approximation of the VoI simplifies to:

$$VoI \approx \frac{1}{n_{\text{MCS}}} \sum_{i=1}^{n_{\text{MCS}}} \left\{ C_{\text{tot}}(\boldsymbol{x}^{(i)}, \boldsymbol{w}_{\text{opt}}^{\text{pr}}) - C_{\text{tot}}(\boldsymbol{x}^{(i)}, \boldsymbol{z}^{(i)}, \boldsymbol{w}_{\text{opt}}^{\text{prepost}}) \right\}. \tag{2.17}$$

In cases when the risk of failure is included in the total life-cycle cost calculation, the variance of $C_{\text{tot}}(\boldsymbol{X}, \boldsymbol{w}_{\text{opt}}^{\text{pr}})$ and $C_{\text{tot}}(\boldsymbol{X}, \boldsymbol{Z}, \boldsymbol{w}_{\text{opt}}^{\text{prepost}})$ is typically rather large [180]. This is because the risk of failure is obtained as the product of the cost of a failure event (usually a rather large value for safety-critical components/systems) and the probability of failure (often a rather small value, especially for safety critical components/systems). Therefore, also the MCS estimate of the VoI in Eq. (2.17) is subject to fairly large uncertainty, even when evaluated with a relatively large n_{s}.

[180] presents a conditional Monte Carlo-based variance reduction technique [156] for estimating the VoI. This algorithm can be very effective for reliability applications wherein the probability of failure can be efficiently evaluated conditional on a subset of $\boldsymbol{X}$, as discussed in Section 2.1.8.2. This approach is employed in the VoI and VoSHM analyses in Chapters 4 and 5 in this thesis.

2.1.5.2 Cost breakdown

This section aims to break down the computation of the total cost $C_{\text{tot}}(\boldsymbol{x}^{(i)}, \boldsymbol{z}^{(i)}, \boldsymbol{w}_{\text{opt}}^{\text{prepost}})$ of Eq. (2.17). It is computed via the following summation:

$$C_{\text{tot}}(\boldsymbol{x}^{(i)}, \boldsymbol{z}^{(i)}, \boldsymbol{w}_{\text{opt}}^{\text{prepost}}) = C_{\text{I}}(\boldsymbol{x}^{(i)}, \boldsymbol{z}^{(i)}, \boldsymbol{w}_{\text{opt}}^{\text{prepost}}) + C_{\text{M}}(\boldsymbol{x}^{(i)}, \boldsymbol{z}^{(i)}, \boldsymbol{w}_{\text{opt}}^{\text{prepost}}) + R_{\text{F}}(\boldsymbol{x}^{(i)}, \boldsymbol{z}^{(i)}, \boldsymbol{w}_{\text{opt}}^{\text{prepost}}) \tag{2.18}$$

Following any PdM policy, different inspection and repair actions will be performed throughout the life-cycle of a component/system. Calculating the total cost of inspection and maintenance actions simply requires recording the times of performed inspections in a vector $\boldsymbol{t}_{\text{insp}}^{(i)}$ and the times of performed maintenance actions in a vector $\boldsymbol{t}_{\text{maint}}^{(i)}$. The total discounted cost of inspections is then computed as:

$$C_{\text{I}}(\boldsymbol{x}^{(i)}, \boldsymbol{z}^{(i)}, \boldsymbol{w}_{\text{opt}}^{\text{prepost}}) = \sum_{j=1}^{n_{\text{insp}}} \gamma\left(t_{\text{insp}}^{(j)}\right) \widetilde{c}_{\text{insp}}, \tag{2.19}$$

and the total discounted cost of maintenance:

$$C_{\text{M}}(\boldsymbol{x}^{(i)}, \boldsymbol{z}^{(i)}, \boldsymbol{w}_{\text{opt}}^{\text{prepost}}) = \sum_{j=1}^{n_{\text{maint}}} \gamma\left(t_{\text{maint}}^{(j)}\right) \widetilde{c}_{\text{maint}}, \tag{2.20}$$

where $\widetilde{c}_{\text{insp}}$ and $\widetilde{c}_{\text{maint}}$ are the costs of an individual inspection and maintenance/repair/replacement action respectively, and $\gamma(t)$ is the discounting function defined in Eq. (2.4).

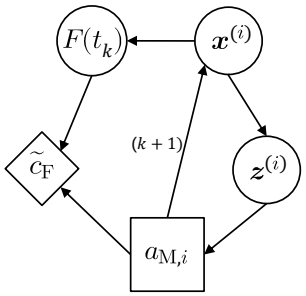

Figure 2.4: Influence diagram corresponding to the estimation of the risk of failure R_{F}.

The risk of failure over the bounded lifetime T is computed as:

$$R_{\mathrm{F}}(\boldsymbol{x}^{(i)}, \boldsymbol{z}^{(i)}, \boldsymbol{w}_{\mathrm{opt}}^{\mathrm{prepost}}) = \sum_{j=1}^{T} \gamma(t_j) \widetilde{c}_{\mathrm{F}} \left\{ \Pr[F(t_j)|\boldsymbol{x}^{(i)}] - \Pr[F(t_{j-1})|\boldsymbol{x}^{(i)}] \right\}, \tag{2.21}$$

where $\widetilde{c}_{\mathrm{F}}$ is the cost of a failure event, and $\Pr[F(t_j)|\boldsymbol{x}^{(i)}]$ is the probability of failure of the structure up to time t_j, conditional on a sampled value $\boldsymbol{x}^{(i)}$ of the random vector $\boldsymbol{X}$. As presented shortly in Section 2.1.8.2, under certain assumptions, this conditional probability of failure can be computed efficiently. Note that $\boldsymbol{z}^{(i)}$ does not appear on the right-hand side of Eq. (2.21). This is because for fixed $\boldsymbol{x}^{(i)}$, the data $\boldsymbol{z}^{(i)}$ influence the risk of failure only through the maintenance/repair/replacement action $a_{\mathrm{M},i}$ as demonstrated in the influence diagram (ID) of Fig. 2.4. IDs are decision-oriented extensions of Bayesian networks (BNs). An BN is a probabilistic graphical model for representing conditional variable dependencies in a directed acyclic graph [83]. An ID adds square decision and oval utility nodes to the BN to model decision making under uncertainty [83].

2.1.6 Bayesian analysis

Bayesian analysis is the essential probabilistic component underlying the Bayesian decision analysis framework. It is a statistical inference method that utilizes Bayes' theorem to update prior belief/knowledge on uncertain quantities based on observed data [62]. Prior belief/knowledge is incorporated in the subjective definition of a probabilistic model, the so-called *prior distribution*. When data of some sort becomes available, the prior probability distribution is updated using Bayes' theorem. The updated distribution is called the *posterior distribution*, which incorporates both the prior belief/knowledge and the data.

The uncertain quantities that one aims to infer are random variables contained in a vector $\boldsymbol{X} \in \mathbb{R}^d$. A realization of $\boldsymbol{X}$ is denoted by the lower case $\boldsymbol{x}$. $\boldsymbol{Z}$ denotes noisy data that can generally be direct (observe $\mathbf{X}$) or indirect (observe $f(\boldsymbol{X})$ where $f(\cdot)$ is some arbitrary function) and complete (observe all the elements of $\boldsymbol{X}$) or incomplete (observe a proper subset of $\boldsymbol{X}$) observations of $\boldsymbol{X}$. A realization of the noisy data is denoted by $\boldsymbol{z}$. The updating of the prior belief about $\boldsymbol{X}$ based on data $\boldsymbol{z}$ is reflected in the posterior distribution, which takes the form of the conditional PDF $f_{\boldsymbol{X}|\boldsymbol{Z}}(\boldsymbol{x}|\boldsymbol{z})$ that is found via application of Bayes' rule:

$$f_{\boldsymbol{X}|\boldsymbol{Z}}(\boldsymbol{x}|\boldsymbol{z}) = \frac{L(\boldsymbol{x};\boldsymbol{z}) f_{\boldsymbol{X}}(\boldsymbol{x})}{f_{\boldsymbol{Z}}(\boldsymbol{z})}. \tag{2.22}$$

$f_{\boldsymbol{X}}(\boldsymbol{x})$ is the prior PDF of the random variables contained in $\boldsymbol{X}$. The likelihood function $L(\boldsymbol{x};\boldsymbol{z}) := f_{\boldsymbol{Z}|\boldsymbol{X}}(\boldsymbol{z}|\boldsymbol{x})$ provides the link between the data and the uncertain quantities that we aim to infer. The value that the likelihood function assumes for a given $\boldsymbol{x}$ corresponds to how likely $\boldsymbol{x}$ is to have generated the observed data $\boldsymbol{z}$. The denominator in Eq. (2.22) is called the *model evidence* (also known as the *marginal likelihood*), and is found by solving the following integral:

$$f_{\boldsymbol{Z}}(\boldsymbol{z}) = \int L(\boldsymbol{x};\boldsymbol{z}) f_{\boldsymbol{X}}(\boldsymbol{x}) \mathrm{d}\boldsymbol{x}. \tag{2.23}$$

The model evidence represents the probability of observing the data, marginalized over all possible values of the uncertain parameters, and provides a measure of how well a particular model (likelihood and prior) explains the data. It is frequently used in Bayesian model selection [62], which refers to the task of comparing different models, and selecting the one that entails the largest model evidence.

Getting an exact closed-form solution for the posterior distribution is rarely the case (e.g., when using conjugate priors [62]). In the general case, to compute the posterior distribution, one typically needs to resort to approximation techniques, numerical integration or sampling-based methods [62]. Among others, common solution approaches include Laplace approximations [62], Markov chain Monte Carlo (MCMC) methods [63], importance sampling [156] and variational Bayesian inference [55] techniques.

Following the computation of the full posterior distribution, the expected value of an arbitrary function $g(\boldsymbol{X})$ (e.g., the total life-cycle cost $C_{\mathrm{tot}}(\boldsymbol{X})$) can be computed over the posterior distribution:

$$\mathbb{E}[g(\boldsymbol{X})|\boldsymbol{z}] = \int g(\boldsymbol{x}) f_{\boldsymbol{X}|\boldsymbol{Z}}(\boldsymbol{x}|\boldsymbol{z}) \mathrm{d}\boldsymbol{x}. \tag{2.24}$$

Summary statistics for the posterior distribution can also be derived. The most relevant ones for the remainder of this thesis are the posterior mean (PM) estimate $\boldsymbol{x}_{\mathrm{PM}} = \int \boldsymbol{x}\ f_{\boldsymbol{X}|\boldsymbol{Z}}(\boldsymbol{x}|\boldsymbol{z})\mathrm{d}\boldsymbol{x}$, the maximum a posteriori (MAP) estimate $\boldsymbol{x}_{\mathrm{MAP}} = \arg\max_{\boldsymbol{x}} f_{\boldsymbol{X}|\boldsymbol{Z}}(\boldsymbol{x} \mid \boldsymbol{z})$, and credible intervals (CIs) [152].

2.1.7 Bayesian analysis of monitored deterioration processes

This thesis is concerned with cases in which $\boldsymbol{X}$ contains uncertain quantities related to a deterioration process affecting a component/system, as discussed in Section 2.1.4.1.

In the case of random variable deterioration models, $\boldsymbol{X}$ only consists of the time-invariant uncertain parameters, which completely describe the uncertainty in the deterioration model. These are contained in the vector $\boldsymbol{\theta}$. E.g., considering Eq. (2.7), $\boldsymbol{X} = \boldsymbol{\theta} = [C, \lambda]$. The task of inferring $\boldsymbol{\theta}$ based on observed data $\boldsymbol{z}$, i.e., the task of obtaining the posterior distribution $f_{\boldsymbol{\Theta}|\boldsymbol{Z}}(\boldsymbol{\theta}|\boldsymbol{z})$, is referred to as *Bayesian parameter estimation*. Particularly of interest for this thesis is the case when indirect noisy observations $\boldsymbol{z}$ are implicitly connected to the deterioration through the output of a computational model $\mathcal{G}$, which is parametrized by $\boldsymbol{\theta}$; the task of inferring $\boldsymbol{\theta}$ in this context is referred to as *Bayesian model updating* [168, 14]. In this case, the likelihood function is typically formulated by assuming a probabilistic model for the discrepancy $\boldsymbol{\eta} = \boldsymbol{z} - \mathcal{G}(\boldsymbol{\theta}) \sim f_{\boldsymbol{H}}(\boldsymbol{\eta})$ between the noisy data $\boldsymbol{z}$ and the computational model-predicted output $\mathcal{G}(\boldsymbol{\theta})$. Bayesian model updating is employed in the context of vibration-based SHM in Section 4.3 of this thesis.

Long-term continuous monitoring of deterioration processes, which forms the main focus of this thesis, delivers a set of noisy data $\boldsymbol{z}_{1:n} = \{z_1, \dots z_n\}$ in a sequential manner at different points in time $\{t_1, \dots t_n\}$ throughout the life-cycle of a component/system. This allows for updating the knowledge about $\boldsymbol{X}$ at any fixed time step t_N using the sequence of data $\boldsymbol{z}_{1:N}$. In this case, Bayesian analysis is performed via Bayes' rule as:

$$f_{\boldsymbol{X}|\boldsymbol{Z}}(\boldsymbol{x}|\boldsymbol{z}_{1:N}) = \frac{L(\boldsymbol{x}; \boldsymbol{z}_{1:N}) f_{\boldsymbol{X}}(\boldsymbol{x})}{f_{\boldsymbol{Z}}(\boldsymbol{z}_{1:N})}. \tag{2.25}$$

With the assumption of independence for the data in $\boldsymbol{z}_{1:N}$ given $\boldsymbol{x}$, the likelihood function can be expressed as the product of the individual likelihoods as:

$$L(\boldsymbol{x}; \boldsymbol{z}_{1:N}) = \prod_{n=1}^{N} L(\boldsymbol{x}; z_n). \tag{2.26}$$

Use of Eq. (2.25) corresponds to the *off-line framework* for performing Bayesian analysis in settings in which the data arrives in a sequential manner [92, 90]. The off-line framework is often referred to as *batch estimation* in the literature [163]. With the off-line framework, updating the knowledge on $\boldsymbol{X}$ in view of new data in the sequence $\boldsymbol{z}_{1:n}$ requires solving the problem in Eq. (2.25) anew every time. Thus, when inference of the sequence of posterior distributions $\{f_{\boldsymbol{X}|\boldsymbol{Z}}(\boldsymbol{x}|\boldsymbol{z}_{1:n})\}_{n\geq 1}$ is of interest, as is typically the case in PdM planning problems, which this thesis addresses, the off-line framework can quickly become inefficient and computationally prohibitive. For the latter task, the *on-line framework* is typically employed, which entails performing *recursive Bayesian analysis* with a set of algorithms called *Bayesian filters* to sequentially update the distribution of $\boldsymbol{X}$ [163]. The on-line Bayesian framework is particularly suited for the case when the temporal evolution of a monitored deterioration process is modeled as a Markovian stochastic process and is subject to stochastic process noise.

2.1.7.1 Bayesian filtering for deterioration state estimation

For a comprehensive, rigorous review on Bayesian filtering, the interested reader is referred to [163].

A Markovian discrete-time state-space model of the monitored deterioration process must be defined, rendering the problem suitable for application of Bayesian filters. This is given in a general form as:

$$\begin{aligned} \boldsymbol{x}_k &= d_k(\boldsymbol{x}_{k-1}) + \boldsymbol{\omega}_{k-1} \\ \boldsymbol{z}_k &= h_k(\boldsymbol{x}_k) + \boldsymbol{\eta}_k, \end{aligned} \tag{2.27}$$

for $k = 1, \dots T$, where:

- $\boldsymbol{x}_k \in \mathbb{R}^n$ is the deterioration state(s) of the system at time step k,
- $\boldsymbol{z}_k \in \mathbb{R}^m$ is the noisy measurement(s) at time step k,
- $d_k(\cdot)$ is the dynamic process equation describing the evolution of deterioration,
- $h_k(\cdot)$ is the measurement equation,
- $\boldsymbol{\omega}_k$ is a process noise vector (often assumed in an additive Gaussian form),
- $\boldsymbol{\eta}_k$ is a measurement noise vector (often assumed in an additive Gaussian form).

The model is assumed to be *Markovian*. This means that, given $\boldsymbol{x}_{k-1}$, the state $\boldsymbol{x}_k$ is assumed independent of anything that has happened before the time step $k-1$. Naturally, this is an assumption, which might not always be realistic when modeling deterioration processes. Yet, state-space augmentation can be applied to render any deterioration model Markovian. The second assumption attached to the Markovian property is that, given the current state $\boldsymbol{x}_k$, the current measurement $\boldsymbol{z}_k$ is conditionally independent of previous measurements and states.

Both $d_k(\cdot)$ and $h_k(\cdot)$ can be linear or nonlinear equations. The process and measurement noise vectors $\boldsymbol{\omega}_k, \boldsymbol{\eta}_k$ are introduced in Eq. (2.27) as additive Gaussian terms; however this modeling choice is not strictly required. For instance, multiplicative lognormal terms may be introduced instead (see Eq. (6.3)) [32]. In terms of probability densities, the state-space model of Eq. (2.27) provides the transition density $f(\boldsymbol{x}_k|\boldsymbol{x}_{k-1})$ through the process equation, and the likelihood function $f(\boldsymbol{z}_k|\boldsymbol{x}_k)$ through the measurement equation.

The goal of Bayesian filtering is to compute the distribution of the state $\boldsymbol{x}_k$ at time step k given the sequence of data $\boldsymbol{z}_{1:k}$, i.e., the distribution $f(\boldsymbol{x}_k|\boldsymbol{z}_{1:k})$. This is known as the *filtering distribution*, which can be determined recursively following a two-step process, starting from the prior distribution $f(\boldsymbol{x}_0)$:

- Step 1: Prediction. The predictive distribution of the state $\boldsymbol{x}_k$ at time step k is computed according to the Chapman-Kolmogorov equation [154]:

$$f(\boldsymbol{x}_k|\boldsymbol{z}_{1:k-1}) = \int f(\boldsymbol{x}_k|\boldsymbol{x}_{k-1}) f(\boldsymbol{x}_{k-1}|\boldsymbol{z}_{1:k-1}) \mathrm{d}\boldsymbol{x}_{k-1}. \tag{2.28}$$

- Step 2: Update. Given the new measurement $\boldsymbol{z}_k$ at time step k, the filtering distribution of the state $\boldsymbol{x}_k$ is computed using Bayes' rule:

$$f(\boldsymbol{x}_k|\boldsymbol{z}_{1:k}) = \frac{f(\boldsymbol{z}_k|\boldsymbol{x}_k) f(\boldsymbol{x}_k|\boldsymbol{z}_{1:k-1})}{f(\boldsymbol{z}_k|\boldsymbol{z}_{1:k-1})}. \tag{2.29}$$

This two-step process employs the posterior distribution $f(\boldsymbol{x}_{k-1}|\boldsymbol{z}_{1:k-1})$ computed at the previous time step $k-1$ as the prior distribution for the prediction step at time step k. The term $f(\boldsymbol{z}_k|\boldsymbol{z}_{1:k-1})$ in the denominator of Eq. (2.29) is the model evidence in the recursive Bayesian setting. It can be interpreted as the probability of observing $\boldsymbol{z}_k$ given the prior distribution $f(\boldsymbol{x}_k|\boldsymbol{z}_{1:k-1})$.

When the dynamic process equation and the measurement equation are linear Gaussian, the closed-form solution to the Bayesian filtering equations is provided by the classical Kalman filter (KF) [87]. Deterioration models are commonly nonlinear models and contain non-Gaussian random variables, therefore use of the classical Kalman filter is not appropriate. Nonlinear variants of the KF exist, such as the extended Kalman filter (EKF) and the unscented Kalman filter (UKF). For a detailed discussion of these, the reader is referred to [163, Chapter 5]. For nonlinear and non-Gaussian problems, one typically needs to resort to sampling-based methods, such as the particle filter (PF) [40, 41] or the ensemble Kalman filter (EnKF) [45].

An example of a state-space model for fatigue deterioration

Fatigue crack growth under increasing stress cycles follows the first-order differential Eq. (2.30), known as Paris-Erdogan law [38, 179]:

$$\frac{da\,(n)}{dn} = C\left[\Delta S\sqrt{\pi a\,(n)}\right]^{m}, \tag{2.30}$$

where a is the crack length, n is the number of stress cycles, ΔS is the stress range per cycle when assuming constant stress amplitudes, C and m represent empirical model parameters. This model contains three time-invariant model parameters in $\boldsymbol{\theta} = [C, m, \Delta S]$. The goal is to cast this model into a Markovian discrete-time state-space representation. Solving the first-order differential Eq. (2.30) leads to a recursive dynamic process equation for the crack length state at time step k as:

$$a_k = \left[\left(1-\frac{m}{2}\right)C\Delta S^m \pi^{m/2}\Delta n + a_{k-1}^{(1-m/2)}\right]^{(1-m/2)^{-1}}, \quad k = 1,\ldots,T, \tag{2.31}$$

where Δn is the number of stress cycles during one time step. A process noise may additionally be included in the dynamic process equation to describe additional uncertainty, such as model uncertainty, or uncertainty related to the effect of other processes, such as environmental variability, on the deterioration process. For the illustration in this section, an additive zero-mean Gaussian noise term ω_k is included:

$$a_k = \left[\left(1-\frac{m}{2}\right)C\Delta S^m \pi^{m/2}\Delta n + a_{k-1}^{(1-m/2)}\right]^{(1-m/2)^{-1}} + \omega_k. \tag{2.32}$$

An underlying assumption is that the process noise ω_k is constant within each time interval, while the process noises of different time intervals are independent from each other.

Assuming that the measurements are direct noisy observations of the crack length a_k, and including an additive zero-mean Gaussian noise term η_k, the observation equation is:

$$z_k = a_k + \eta_k. \tag{2.33}$$

The measurements at different time steps are also assumed to be independent from each other. This measurement equation corresponds to the following likelihood function:

$$L(a_k; z_k) = f(z_k|a_k) = \frac{1}{\sigma\sqrt{2\pi}}\exp\left(-\frac{1}{2}\left(\frac{z_k - a_k}{\sigma}\right)^2\right). \tag{2.34}$$

The resulting Markovian discrete-time state-space model can be expressed in the form of Eq. (2.27):

$$\begin{aligned} a_k &= d_k(a_{k-1}) + \omega_{k-1} \\ z_k &= h_k(a_k) + \eta_k. \end{aligned} \tag{2.35}$$

In this formulation, it is assumed that the time-invariant parameters in $\boldsymbol{\theta}$ are known deterministic quantities. Thus, the recursive Bayesian analysis task relates to the sequential updating of the deterioration state a_k; this task is referred to as *state estimation* [163].

Structural deterioration processes are often modeled as Wiener processes, Gamma processes or Poisson processes [190]. This modeling choice allows for a Markovian discrete-time state-space representation of deterioration, which in turn allows for the application of Bayesian filtering [166, 208].

2.1.7.2 Bayesian filtering for joint deterioration state-parameter estimation

The description in Section 2.1.7.1 assumes that the time-invariant parameters $\boldsymbol{\theta}$ of the deterioration model are known quantities. However, this is usually not the case. In the case of structural deterioration processes, $\boldsymbol{\theta}$ contains uncertain model parameters that also need to be estimated along with the estimate of the state; this task is referred to as *joint state-parameter estimation*. An approach for the solution to this problem entails augmenting the state space. In this case, the Markovian discrete-time state-space representation can be written as:

$$\begin{aligned} \boldsymbol{\theta}_k &= \boldsymbol{\theta}_{k-1} \\ \boldsymbol{x}_k &= d_k(\boldsymbol{x}_{k-1}, \boldsymbol{\theta}_{k-1}) + \boldsymbol{\omega}_{k-1} \\ \boldsymbol{z}_k &= h_k(\boldsymbol{x}_k, \boldsymbol{\theta}_k) + \boldsymbol{\eta}_k, \end{aligned} \tag{2.36}$$

where the artificial dynamic process equation for $\boldsymbol{\theta}$ simply reflects that the time-invariant parameters are constant. State space augmentation involves redefining the state as $\tilde{\boldsymbol{x}}_k = (\boldsymbol{x}_k, \boldsymbol{\theta}_k)$. With the augmented state-space, the Markovian discrete-time state-space model can be expressed in the general form of Eq. (2.27):

$$\begin{aligned} \tilde{\boldsymbol{x}}_k &= d_k(\tilde{\boldsymbol{x}}_{k-1}) + \tilde{\boldsymbol{\omega}}_{k-1} \\ \boldsymbol{z}_k &= h_k(\tilde{\boldsymbol{x}}_k) + \boldsymbol{\eta}_k, \end{aligned} \tag{2.37}$$

and the joint state-parameter estimation task is cast into a state estimation task (Section 2.1.7.1). This approach is employed in Section 5.4.2.1 of this thesis, where Bayesian filtering is employed for joint state-parameter estimation of a combined gradual and shock deterioration process, which is continuously monitored by a vibration-based SHM system.

There are several issues associated with the state-augmentation approach. The fact that the time-invariant parameters are not subject to any process noise causes solutions based on the Kalman filter to diverge, and gives rise to sample impoverishment issues in sampling-based Bayesian filters (see Fig. 6.1), such as the particle filter [163]. The Bayesian filtering community has proposed various methods for resolving these issues, e.g., [122, 172, 64, 5, 29, 27].

2.1.7.3 Bayesian filtering for deterioration parameter estimation

In the case of random variable deterioration models, all the uncertainty about the deterioration process is contained in the vector of time-invariant deterioration model parameters $\boldsymbol{\theta}$. Bayesian filtering can also be applied for pure recursive Bayesian estimation of time-invariant parameters, for which the noise in the dynamic process equation is formally zero. To this end, the Bayesian parameter estimation problem is cast into a Markovian discrete-time state-space representation:

$$\begin{aligned} \boldsymbol{\theta}_k &= \boldsymbol{\theta}_{k-1} \\ \boldsymbol{z}_k &= h_k(\boldsymbol{\theta}_k) + \boldsymbol{\eta}_k. \end{aligned} \tag{2.38}$$

The fact that the artificial dynamic process equation for the time-invariant parameters is not subject to any process noise only amplifies the issues of divergence of KF solutions and sample impoverishment of sampling-based filters mentioned above [30, 123]. The contribution in Chapter 6 of this thesis focuses on the sample impoverishment issue encountered when using particle filters in the context of Bayesian parameter estimation, and investigates methods for alleviating it.

2.1.8 Reliability analysis of deteriorating systems

Structural reliability analysis [38, 120] forms an integral part of model-based predictive maintenance planning for deteriorating components/systems. Specifically, it forms the basis for estimating the risk of failure. As discussed in Section 2.1.2, the risk of failure enters the total life-cycle cost summation, which is the cost-based criterion used for PdM planning in safety-critical components/systems. Such systems are typically unique (e.g., a bridge structure) and are associated with high reliability, i.e., they are not supposed to fail, as failure is associated with adverse consequences. Thus, a structural reliability analysis is indispensable for computing the probability of component/system failure, which, multiplied with the cost of failure, delivers an estimate of the risk of failure (e.g., see Eq. (2.21)). The outcome of a structural reliability analysis also forms the basis for devised heuristics that are employed for the solution to stochastic sequential decision problems for PdM planning [112, 17, 88], e.g., see Section 5.3.1. The current section focuses on time-variant reliability analysis of deteriorating systems; for a comprehensive description of this task, the reader is referred to [120, 181].

2.1.8.1 Time-variant reliability analysis

This thesis focuses on cases when failure of the component/system may occur due to the adverse effects of deterioration. Therefore, assessing the reliability requires stochastic models of the deterioration process(es) acting on the component/system. As the deterioration process evolves over time, estimating the time-varying reliability of a deteriorating component/system requires a time-variant reliability analysis [120].

In general, a limit state function $g(\boldsymbol{X}, t)$ can be introduced that models the component/system, where $\boldsymbol{X}$ is the vector of input random variables. In its simplest form, a failure event of a component/system at time t can be expressed in terms of its capacity $R(t)$ and demand $S(t)$. Both $R(t)$ and $S(t)$ are random variables, and $\boldsymbol{X} = [R(t), S(t)]$ [3]. The capacity $R(t)$ decreases over time due to the effects of deterioration, and can only increase after a maintenance/repair/replacement action is performed on the component/system. A failure event is defined at time t when the demand $S(t)$ exceeds the capacity $R(t)$, hence the limit state function at time t is defined as $g(\boldsymbol{X}, t) = R(t) - S(t)$. The *time to failure* T_F is an important random variable that expresses the elapsed time from the beginning of the operation of the component/system to the occurrence of the first failure event:

$$T_F = \arg\min_t g(\boldsymbol{X}, t) \leq 0. \tag{2.39}$$

For systems associated with high reliability, the focus is typically not on direct estimation of T_F, as such systems are not supposed to fail throughout their intended lifetime, but rather on estimating the *accumulated probability of a failure event* $F(t)$ up to time t. This is connected to T_F via the cumulative distribution function (CDF) of T_F:

$$\Pr[F(t)] = \Pr(T_F \leq t) = F_{T_F}(t). \tag{2.40}$$

The probability density function (PDF) of T_F is denoted by $f_{T_F}(t)$. The *hazard function* $h(t)$ is defined as:

$$h(t) = \frac{f_{T_F}(t)}{1 - F_{T_F}(t)}, \tag{2.41}$$

[3] Please note that the vector $\boldsymbol{X}$ defined here is different to the vector $\boldsymbol{X}$ used in previous sections of this thesis.

and it expresses the failure rate of the structure conditional on the fact that it has survived up to time t. Imposing thresholds on the hazard function is a commonly used heuristic for informing inspections and repairs (see Section 5.3.1).

Time is discretized in intervals $k = 1, \dots T$, where the k-th interval corresponds to $t \in (t_{k-1}, t_k]$. The choice of the discretization scheme is problem-dependent. For bridge structures, e.g., a choice of yearly intervals may be reasonable. The *interval failure event* F_k^* is defined as the event of failure in the interval $(t_{k-1}, t_k]$ ignoring previous failures [181]. In the discretized setting, the event of a failure up to time t_k is denoted by F_k, and can be approximated by the union of the interval failure events as:

$$F_k = F_1^* \cup F_2^* \cup ...F_k^*. \tag{2.42}$$

The accumulated probability of a failure event up to time t_k can correspondingly be computed as:

$$\Pr(F_k) = \Pr(F_1^* \cup F_2^* \cup ...F_k^*). \tag{2.43}$$

2.1.8.2 Structures with independent capacity and demand

Chapters 4 and 5 of this thesis address a common class of structural problems, wherein the random vector $\boldsymbol{X}$ can be decomposed into two separate sub-vectors $\boldsymbol{X}_R$ and $\boldsymbol{X}_S$, containing uncertain quantities related to the capacity and the demand, respectively. Naturally, this is an assumption that may often not be justified. The simplest case emerges when the demand can be described by a scalar random variable $S(t)$ (e.g., maximum yearly wind load). The capacity can then be written as a function of the vector $\boldsymbol{X}_R$, i.e., $R(\boldsymbol{X}_R, t)$, resulting in the limit state function $g(\boldsymbol{X}, t) = R(\boldsymbol{X}_R, t) - S(t)$.

In simplified cases when the demand within an interval can be described by a scalar random variable $S_{\max,k} = \max_{t \in (t_{k-1}, t_k]} S(t)$, the computation of $\Pr(F_k^*)$ can be approximated as:

$$\Pr(F_k^*) \approx \Pr[R(\boldsymbol{X}_R, t_k) \leq S_{\max,k}], \tag{2.44}$$

which requires solving a time-invariant reliability analysis. Thus, the time-variant reliability problem can be replaced by a series of time-invariant reliability problems [181].

An efficient solution of the time-variant reliability analysis problem is facilitated in cases when a deterministic function $R(\boldsymbol{x}_R, t_k)$ can be constructed. $R(\boldsymbol{x}_R, t_k)$ is a function that determines the reduced capacity for a fixed realization of $\boldsymbol{x}_R$, i.e., a realization of the uncertain quantities related to the capacity, and for a given time t_k. The *conditional interval probability of failure* can then be computed as:

$$\Pr(F_k^* | \boldsymbol{X}_R = \boldsymbol{x}_R) = \Pr(S_{\max} > R(\boldsymbol{x}_R, t_k)) = 1 - F_{S_{\max}}(R(\boldsymbol{x}_R, t_k)), \tag{2.45}$$

where $S_{\max}$ is the random variable denoting the maximum load in the k-th time interval, and $F_{S_{\max}}$ denotes its CDF. For instance, $S_{\max}$ may follow a Gumbel distribution modeling the maximum annual load.

The *conditional accumulated probability of a failure event* up to time t_k can be computed via the probabilities of the conditional interval failure events as:

$$\Pr(F_k|\boldsymbol{X}_R = \boldsymbol{x}_R) = 1 - \prod_{m=1}^{k} \left[1 - \Pr(F_m^* \mid \boldsymbol{X}_R = \boldsymbol{x}_R)\right]. \tag{2.46}$$

The unconditional accumulated probability of a failure event up to time t_k is then computed by use of the *total probability theorem*:

$$\Pr(F_k) = \int \Pr(F_k|\boldsymbol{X}_R = \boldsymbol{x}_R) f_{\boldsymbol{X}_R}(\boldsymbol{x}_R) \mathrm{d}\boldsymbol{x}_R \tag{2.47}$$

The hazard function at time t_k can be computed as:

$$h_k = \frac{\Pr(F_k) - \Pr(F_{k-1})}{1 - \Pr(F_{k-1})} \tag{2.48}$$

As outlined in Section 2.1.6, data from continuous monitoring and/or inspections can be used to update the knowledge on the random vector $\boldsymbol{X}_R$. Upon updating the knowledge on $\boldsymbol{X}_R$ via Bayesian analysis, the time-variant reliability estimates may also be updated, in a process referred to as *reliability updating* [178]. For instance, the filtering distribution $f(\boldsymbol{x}_R|\boldsymbol{z}_{1:k})$ can replace the prior distribution $f_{\boldsymbol{X}_R}(\boldsymbol{x}_R)$ in Eq. (2.47). This leads to the filtered estimate of the accumulated probability of a failure event up to time t_k, conditional on the whole sequence of monitoring data $\boldsymbol{z}_{1:k}$:

$$\Pr(F_k|\boldsymbol{z}_{1:k}) = \int \Pr(F_k|\boldsymbol{X}_R = \boldsymbol{x}_R) f(\boldsymbol{x}_R|\boldsymbol{z}_{1:k}) \mathrm{d}\boldsymbol{x}_R. \tag{2.49}$$

As an alternative, e.g., an l-step-ahead prediction for the accumulated probability of a failure event up to time t_{k+l} may be obtained:

$$\Pr(F_{k+l}|\boldsymbol{z}_{1:k}) = \int \Pr(F_{k+l}|\boldsymbol{X}_R = \boldsymbol{x}_R) f(\boldsymbol{x}_R|\boldsymbol{z}_{1:k}) \mathrm{d}\boldsymbol{x}_R. \tag{2.50}$$

More generally, the accumulated probability of a failure event $\Pr[F(t)|\boldsymbol{z}_{1:k}]$ up to any point in time $t \geq t_k$, conditional on the data $\boldsymbol{z}_{1:k}$, can be computed. This leads to an approximation of the full time-dependent function, which corresponds to the CDF $F_{T_F|\boldsymbol{z}_{1:k}}(t)$ of the conditional distribution of the time to failure T_F given all the information up to t_k.

It should be noted that, although in this section Eq. (2.50) is introduced in particular for the case of structures with independent capacity and demand, the time-dependent function $\Pr[F(t)|\boldsymbol{z}_{1:k}]$, respectively the CDF $F_{T_F|\boldsymbol{z}_{1:k}}(t)$, can typically be computed within the context of any given problem in which the system performance can be described in relation to a limit state function.

Preposterior decision analysis and VoI/VoSHM analyses require solving multiple time-variant reliability and reliability updating problems. To render VoI/VoSHM analyses computationally viable, simplified modeling choices for the time-variant reliability analysis problem may be adopted, in conjunction with efficient methods for its solution [175, 88].

As discussed in Section 2.1.5.1, in cases of structural systems associated with high reliability, the basic Monte Carlo estimate of the VoI is inefficient. [180] presents a conditional Monte Carlo-based approach that can increase the computational efficiency and reduce the variance of a VoI analysis for systems with independent capacity and demand, wherein $\boldsymbol{X}$ can be split into $\boldsymbol{X}_R$ and $\boldsymbol{X}_S$. It is based on the premise that an efficient evaluation of $\Pr(F_k|\boldsymbol{X}_R = \boldsymbol{x}_R)$ is possible. This approach is employed in the VoI and VoSHM analyses in Chapters 4 and 5 in this thesis.

2.1.9 Model-based remaining useful life estimation of deteriorating systems

In various engineering disciplines, systems often consist of non-unique components, which fail and are replaced upon failure, or are timely replaced before failure. On-line monitoring strategies from deployed sensors are common for such systems. In such context, the main effort focuses on estimating the *remaining useful life* (RUL) of a component/system utilizing monitoring data. RUL estimation is a primary goal of the discipline of Prognostics and Health Management (PHM) [95]. This section provides a concise description of *model-based prognostics*, which aim to deliver RUL predictions on the basis of an available deterioration model and on-line health monitoring data. In this section we further draw a connection between the tasks of estimating the time-variant reliability (Section 2.1.8.1), which falls within the scope of the structural reliability analysis community, and estimating the RUL of a component/system, which is the main focus of the PHM community. The two tasks appear to be disconnected in most of the literature.

The RUL at a given point in time t is defined as:

$$RUL = T_F - t, \tag{2.51}$$

where T_F is the time to failure. The RUL corresponds to the remaining time until a component/system becomes dysfunctional or fails. The RUL is not strictly expressed in time units, but may instead be expressed in, e.g., load cycles to failure.

In the context of an on-line health monitoring strategy, prognostics define the process of estimating the RUL at each time step t_k on the basis of all available monitoring data up to t_k. The estimated distribution of the uncertain time to failure is updated conditional on the sequence of monitoring data $\boldsymbol{z}_{1:k}$. The CDF of this conditional distribution is denoted by $F_{T_F|\boldsymbol{z}_{1:k}}(t)$. Let $T_{F,k}$ be the random variable that corresponds to this distribution. The following equation summarizes the RUL estimation task in a discrete setting:

$$RUL_k = T_{F,k} - t_k. \tag{2.52}$$

The estimated RUL at t_k conditional on $\boldsymbol{z}_{1:k}$, denoted by RUL_k, is therefore a random variable. The following equation connects the PDFs of RUL_k and $T_{F,k}$:

$$f_{T_{F,k}}(t) = f_{RUL_k}(t - t_k), \tag{2.53}$$

with the PDF $f_{T_{F,k}}(t)$ being bounded from below at t_k. The same equation connects the CDFs of RUL_k and $T_{F,k}$.

At this point, it should be noted that the CDF of the conditional distribution of the time to failure $F_{T_F|\boldsymbol{z}_{1:k}}(t)$ has already been introduced in the context of time-variant reliability analysis in the end of Section 2.1.8. Here lies the connection between the tasks of RUL estimation and time-variant reliability analysis. Specifically, based on Eq. (2.53), it becomes clear that the CDF of RUL_k can be derived from the CDF of $F_{T_F|\boldsymbol{z}_{1:k}}(t)$, which can typically be obtained from a time-variant reliability analysis [28].

Model-based prognostics are established upon availability of a model that describes the evolution of an uncertain deterioration process and allows for making uncertain predictions of the the deterioration state in future points in time (see Section 2.1.4.1). Failure, or exceedance of the RUL,

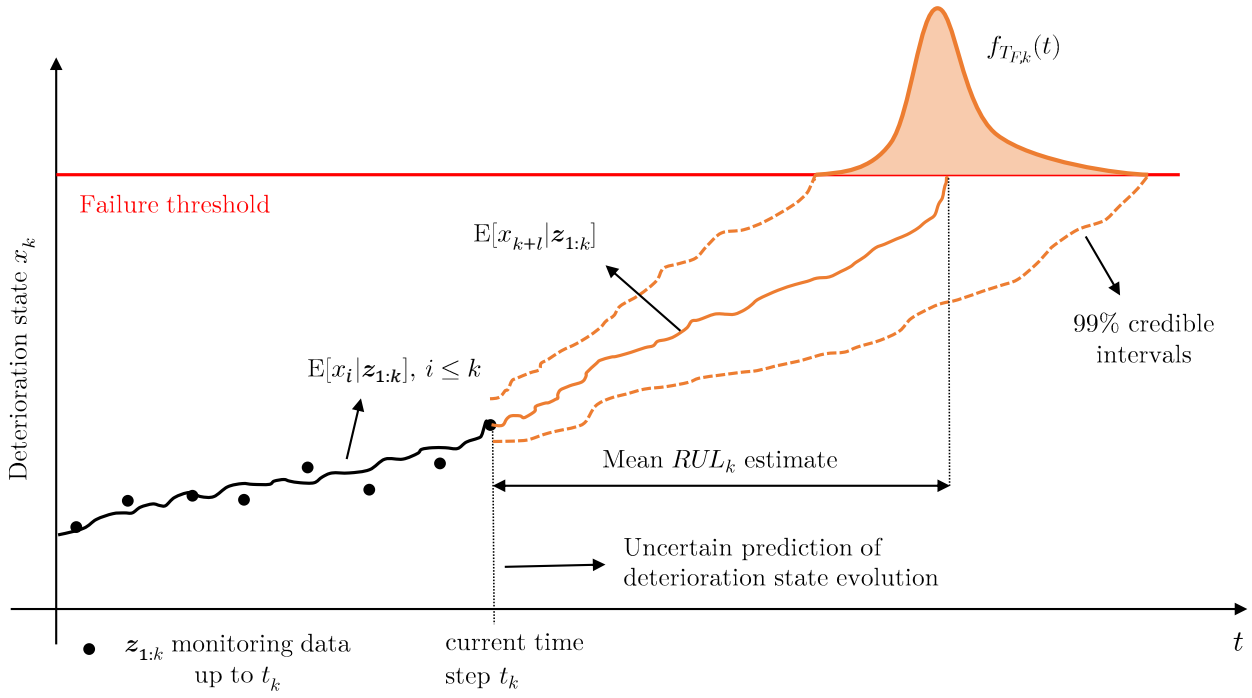

Figure 2.5: Representation of the model-based prognostics process. The black circles correspond to monitoring measurements z_k of the deterioration state x_k, obtained sequentially at different points in time. The black full line plots the mean smoothed estimates $\mathbb{E}[x_i|\boldsymbol{z}_{1:k}], i \leq k$ of the deterioration state. The orange full line corresponds to the mean of the predictive distribution $\mathbb{E}[x_{k+l}|\boldsymbol{z}_{1:k}]$ of the deterioration state. The orange dashed lines represent the 99% credible intervals of the predictive distribution of the deterioration state. The red vertical line defines the critical failure threshold. The PDF $f_{T_{F,k}}(t)$ of the conditional distribution of the estimated time to failure is also plotted.

occurs at the point in time when the deterioration state exceeds some critical threshold, which defines transition to the failure domain. The graph in Fig. 2.5 illustrates the model-based prognostics process. Naturally, multiple sources of uncertainty enter this process, owing among other factors, to inherent uncertainties of the degradation process, noisy monitoring data, operational/environmental conditions, modeling errors, prediction method uncertainty [162]. Model-based prognostics typically rely on Bayesian filtering algorithms (see Section 2.1.7) for obtaining posterior estimates such as $\mathbb{E}[x_k|\boldsymbol{z}_{1:k}]$ and $\mathbb{E}[x_{k+l}|\boldsymbol{z}_{1:k}]$ [210, 86], which are shown in Fig. 2.5.

RUL estimation forms the basis for subsequent RUL-driven decision making for predictive maintenance. PdM policies that receive as input RUL estimates and determine maintenance actions throughout the life-cycle of components are followed as a rule in the literature state of the art [39, 196, 200, 35]. Such PdM policies are investigated in the contribution found in Chapter 7 in this thesis, with the difference that therein the prognostics process is performed in a data-driven fashion. The data-driven PdM planning framework, enabled by data-driven prognostics and monitoring datasets from run-to-failure experiments, is introduced in the following Section 2.2.

2.2 Data-driven predictive maintenance planning

To date, SHM system deployments are available on a rather limited number of real-world, safety-critical engineering systems, with most SHM deployments predominantly serving research purposes [33, 4]. An increasing trend of such deployments for real-world practical tasks is, however, observed. In an attempt to make monitoring data publicly available, the SHM research community has delivered various datasets from real-world monitoring of safety-critical civil and infrastructure engineering systems [143, 52, 116, 197, 51, 134]. As such systems are typically associated with high reliability, even in the presence of SHM, such datasets rarely contain, if at all, monitoring data corresponding to damaged states. This poses a significant challenge to the application of data-driven pattern recognition methods [48]. For monitoring data corresponding to damaged states, the SHM community heavily relies on synthetic generation based on simulations [61]. Various numerical benchmark structural models have been introduced for simulation-based performance evaluation of model-driven and data-driven SHM techniques [85, 182, 197].

An additional intricacy associated with monitoring of safety-critical civil and infrastructure engineering systems arises from the fact that such systems are typically unique. Thus, even if availability of monitoring data from damaged states allows for extracting useful insights related to a specific monitored structure, the transfer of these insights to other structures is not straightforward. Researchers from the SHM community have recently introduced the population-based SHM framework [20, 69, 60], which aims to tackle this transferability issue, primarily based on transfer learning principles [135].

The above discussion points to the fact that, for safety-critical civil and infrastructure engineering systems, it is mostly not clear hitherto how acquired monitoring data can pave the way for the establishment of a data-driven predictive maintenance (PdM) planning framework. Instead, the state of the art in PdM planning for such systems heavily relies on the model-based framework, which is introduced in Section 2.1.4.

For certain non-unique engineering components/systems (e.g., in industrial engineering), monitoring data from several run-to-failure experiments are available. Such datasets typically contain multivariate time series sensor data obtained from physical or simulated run-to-failure experiments on deteriorating components/systems. This means that data that cover the whole spectrum of damaged states up to failure are available. For instance, such datasets exist for bearings, batteries, turbofan engines, CFRP composites, capacitors or milling machines. Several of these datasets are made publicly available by the NASA Prognostics Center of Excellence [127]. There is a vast amount of recent literature on the development of prognostic solutions, which rely on such data to employ data-driven methods, such as artificial intelligence (AI) approaches enabled by machine learning (ML) predictive tools [105, 167, 82]. One of the biggest advantages of data-driven approaches compared to model-driven ones is that the former are exempted from the task of *a-priori* defining a physics-based or empirical model to describe the deterioration pattern. Instead, data-driven methods aim to learn this pattern based on the training data.

One significant advantage associated with such non-unique components/systems relates to the fact that individual components/systems can be considered as part of a population of nominally identical components/systems. This constitutes a key difference compared to other systems, such as civil and infrastructure engineering systems, where such an assumption is strictly invalid.

The availability of monitoring run-to-failure datasets and data-driven prognostic approaches has paved the way for establishment of the *data-driven PdM* paradigm [53, 130, 207, 104]. Within this paradigm, evaluation of the available run-to-failure monitoring data not only forms part of the prognostic algorithm training process, but can be further extended to a data-driven estimation of the expected cost-based criterion, on the basis of which PdM policies are evaluated. This is discussed in Section 2.2.2.

2.2.1 Data-driven prognostic modeling

This section provides a concise description of data-driven prognostic modeling, subsequently focusing on the task of data-driven estimation of the RUL of engineering components/systems.

From a purely data-driven point of view, prognostic models are trained based on available training data to perform either regression or classification tasks [16, 126], as graphically depicted in Fig. 2.6. Regardless of the pursued task, data-driven prognostic models can generally be considered as functions that map a set of input quantities $\boldsymbol{z} \in \mathbb{R}^{n_z}$, which represent the available monitoring measurements of system response, to a set of output quantities of interest $\boldsymbol{y} \in \mathbb{R}^{n_y}$, such that $\mathcal{F} : \boldsymbol{z} \rightarrow \boldsymbol{y}$. This mapping can be expressed by the following mathematical model:

$$\boldsymbol{y} = \mathcal{F}_{\mathbf{H}}\left(\boldsymbol{z}, \boldsymbol{p}\right), \tag{2.54}$$

where $\boldsymbol{p}$ denotes a set of model-specific parameters, which can be estimated from the training data and are used to properly configure the structure of the underlying model, and $\boldsymbol{H}$ is the vector of model hyperparameters. The latter are external to the model and their values control the learning process. When using regression models for prognosis, as shown in Fig. 2.6a, the output is predicted as a continuous variable. On the other hand, the output is slightly different in the case of classification modeling. Concretely, prognostic classifiers predict the class in which the output belongs. This requires an additional preprocessing step of labeling the training data such that they belong in certain classes of interest. For instance, Fig. 2.6b shows the output of a binary classifier, which differentiates between two classes of deterioration, one corresponding to a safe domain (green dots), and one corresponding to an unsafe domain (red dots).

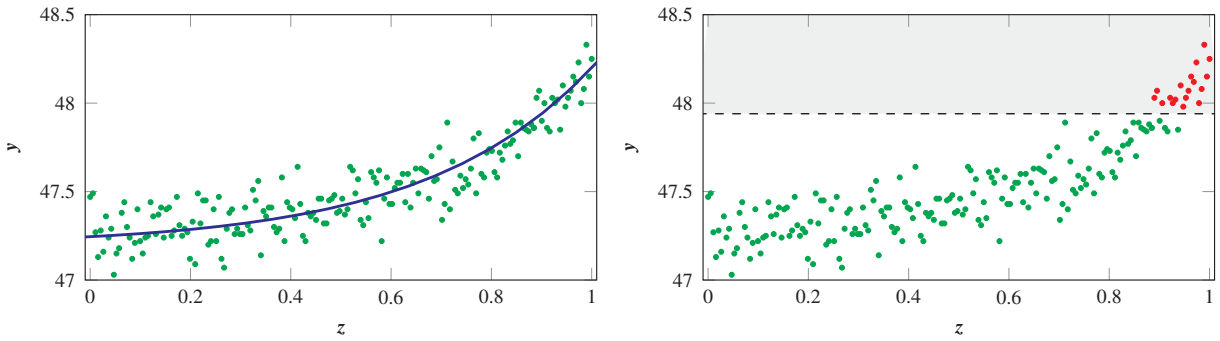

(a) Regression (b) Classification

Figure 2.6: Representation of the output from data-driven prognostic models performing regression or classification tasks.

In either case, the training of data-driven models aims at minimizing an error metric using an

available set of input and output data points, denoted by $\boldsymbol{Z}_N = [\boldsymbol{z}_1, \boldsymbol{z}_2, \ldots, \boldsymbol{z}_N]$ and $\boldsymbol{Y}_N = [\boldsymbol{y}_1, \boldsymbol{y}_2, \ldots, \boldsymbol{y}_N]$, respectively. This metric, which is dependent on the parameters $\boldsymbol{p}$ and is herein denoted by $Q_{\boldsymbol{p},i}$ for each pair of input-output data $(\boldsymbol{z}_i, \boldsymbol{y}_i)$ for $i = 1, 2, \ldots, N$, is selected according to the type of the model and is described for each data point as follows:

$$Q_{\boldsymbol{p},i}\big(\boldsymbol{y}_i, \mathcal{F}_{\mathbf{H}}\left(\boldsymbol{z}_i, \boldsymbol{p}\right)\big) = \begin{cases} \big(\boldsymbol{y}_i - \mathcal{F}_{\mathbf{H}}\big(\boldsymbol{z}_i, \boldsymbol{p}\big)\big)^2 & \text{Regression,} \\ \mathcal{L}_{0/1}\left(\boldsymbol{y}_i, \mathcal{F}_{\mathbf{H}}\big(\boldsymbol{z}_i, \boldsymbol{p}\big)\right) & \text{Classification,} \end{cases} \tag{2.55}$$

where $\mathcal{L}_{0/1}$ denotes the 0-1 loss function. Different possibilities exist in terms of the cost function to be minimized, as a function of the error metrics defined in Eq. (2.55). These include the Mean Squared Error (MSE) and the Mean Absolute Error (MAE) for regression, or the binary cross entropy and the categorical cross entropy loss for classification [126].

In contrast to the model parameters $\boldsymbol{p}$, whose values are calculated at the training phase, the selection of hyperparameters $\boldsymbol{H}$ for each type of model is often carried out through an optimization step that minimizes some function $G(Q_{\boldsymbol{p},i})$ of the error metric $Q_{\boldsymbol{p},i}$, when evaluated on a set of test or validation data points. This process is concisely defined as:

$$\boldsymbol{H}^* = \arg\min_{\mathbf{H}} G\left(Q_{\boldsymbol{p}}\right), \tag{2.56}$$

where $\boldsymbol{H}^*$ denotes the optimal hyperparameter configuration that corresponds to the minimum prediction error. The error function to be minimized at this step follows the same logic as the one involved in the training process, with the difference that the evaluation in Eq. (2.56) is based on data points that are not seen during the training process. Please note that cross-validation is another approach for determining $\boldsymbol{H}^*$ [126], which is a process performed at the training phase.

2.2.1.1 Data-driven remaining useful life estimation of deteriorating systems

In the context of PHM, data-driven prognostic algorithms are frequently trained on the basis of available datasets containing sensor information from run-to-failure experiments of deteriorating components/systems. These trained algorithms aim to provide on-line estimates of the RUL in view of on-line monitoring data. Thus, the prognostic output $\boldsymbol{y}$ is typically either directly the RUL, or some health indicator based on which the RUL is inferred. Data-driven prognostic algorithms are predominantly black-box models, which do not rely on any prior knowledge related to the physical nature of the deterioration mechanism. Instead, the black box model is designed to learn the deterioration pattern explicitly from input monitoring data. This process is inherently different from the model-driven RUL estimation process, which relies on the *a-priori* definition of a stochastic deterioration model, as discussed in Section 2.1.9.

Data-driven prognostic algorithms rely on a series of operations, concisely summarized below:

- Acquisition of monitoring data through deployed sensors.
- Preprocessing — this step notably entails data normalization, denoising, or labeling.
- Feature selection — the goal in this step is to extract important damage-sensitive features from the – often high-dimensional – monitoring data, in a process relying on domain knowledge and signal processing or machine learning techniques.

Naturally, the performance of data-driven prognostic algorithms heavily depends on the quantity and quality of the available training data.

The RUL estimation process is subject to various sources of uncertainty, such as model uncertainty, measurement uncertainty, unknown future loading conditions [161, 82]. It is thus imperative to incorporate uncertainty in the prognostic output $\boldsymbol{y}$ obtained from data-driven models, especially when this output forms the basis for the subsequent PdM planning task [54]. However, with several data-driven prognostic algorithms, such as deep learning algorithms on which the recent literature heavily relies [107, 108], the uncertainty quantification task, as well as downstream tasks such as uncertainty propagation, is not as straightforward (if at all) as with model-driven approaches [53].

The contribution in Chapter 7 of this thesis concentrates on this topic. In particular, it investigates data-driven prognostic models, whose classification or regression prognostic output is directly used as input to PdM policies for determining maintenance actions. The PdM policies by definition rely on the availability of probabilistic output from prognostics. Certain policies rely on selected probabilities, e.g., the probability of the output $\boldsymbol{y}$ reaching a limit point $\bar{\boldsymbol{y}}$, while others rely on the full probability density of the uncertain output $\boldsymbol{y}$. As previously discussed in Section 2.1.9, RUL-based PdM policies have been proposed in the literature, e.g., [39, 196, 130, 200, 35]. Some of these policies are investigated in some detail in Chapter 7, which further proposes some alternatives/improvements.

2.2.2 Data-driven evaluation of a predictive maintenance policy

Section 2.1.4.2 discussed the evaluation of a PdM policy for the case when a stochastic deterioration model is available. This evaluation is typically performed with Monte Carlo simulation (MCS), whereby multiple "what-if" life-cycle realizations of the deterioration process are sampled from the available deterioration model, in conjunction with the corresponding synthetically generated monitoring measurements. A purely data-driven scheme instead does not employ a stochastic deterioration model, or a model for generating monitoring measurements. Hence a MCS-based evaluation of a PdM policy is not possible. However, the available run-to-failure monitoring datasets can straightforwardly be considered as joint true realizations of the deterioration process and the corresponding monitoring data. Therefore, in a data-driven scheme, any PdM policy can be evaluated based on a subset of the available run-to-failure dataset, as explained in the next paragraph.

Let us assume that the long-run expected maintenance cost per unit time is the quantity of interest for evaluating a PdM policy, as is often the case for non-safety-critical components/systems. The expected values in Eq. (2.3) can be evaluated based on a subset of the available run-to-failure monitoring dataset. Concretely, the dataset is split into a training and an evaluation subset, with the former used for the training of a data-driven prognostic algorithm, as described in the previous Section 2.2.1, and the latter used for the evaluation of a PdM policy. Specifically, a PdM policy is applied on n_{eval} independent components of the evaluation dataset, and the cost of the informed maintenance action(s), as well as the length of each component life-cycle, are evaluated. The data-driven evaluation of the PdM policy is then performed as:

$$\frac{\mathbb{E}[C_{\text{M}}]}{\mathbb{E}[T_{\text{lc}}]} \approx \frac{\sum_{i=1}^{n_{\text{eval}}} C_{\text{M}}^{(i)}}{\sum_{i=1}^{n_{\text{eval}}} T_{\text{lc}}^{(i)}}, \tag{2.57}$$

where $C_{\text{M}}^{(i)}$ and $T_{\text{lc}}^{(i)}$ are the cost of maintenance and the length of the first life-cycle of the i-

th component of the evaluation dataset, respectively. Naturally, the quality of the estimator of Eq. (2.57) depends on the number n_{eval} of available datasets in the evaluation subset. If this number is small, the estimator in Eq. (2.57) is subject to rather large variability. This is investigated in detail in Chapter 7 of this thesis.

Investigations of this end-to-end data-driven PdM framework [130], i.e., from data-driven RUL prognostics to data-driven evaluation of a PdM policy, are found in the contribution in Chapter 7 of this thesis.

Chapter 3

Summary & Outlook

3.1 Summary

In Chapter 4, we adapt the Bayesian decision analysis framework for quantifying the value of information (VoI) from structural health monitoring (SHM). Specifically, we investigate the quantification of the VoI yielded via adoption of long-term vibration-based SHM for supporting decisions. An influence diagram is introduced, which concisely summarizes the modeling efforts required for a full VoI from SHM analysis and reflects the associated computational challenges. Drawing from this influence diagram, and avoiding common overly simplified assumptions, this contribution presents – for the first time in literature – a VoI analysis on the full SHM chain, from sensor data acquisition and processing via operational modal analysis schemes, to Bayesian model updating for estimating parameters of structural deterioration models. A time-variant structural reliability analysis forms the basis for estimating the risk of failure throughout the life-cycle on account of gradual deterioration processes. The investigated decision setting relates to predictive maintenance (PdM) planning of repair actions. The PdM plan is optimized via the adoption of heuristic decision rules. A numerical benchmark structural model of a bridge system serves as the basis for numerical investigations, which showcase that the presented VoI from SHM analysis can quantitatively assess the optimality of an SHM system in certain decision contexts.

In Chapter 5, we focus on quantifying the potential economic benefit that vibration-based structural health monitoring (SHM) can generate by enhancing maintenance planning, compared against the currently dominant approach, which is based on information from intermittent inspections. To this end, a formal metric deriving from Bayesian decision analysis is introduced, namely the Value of SHM (VoSHM) metric. The VoSHM is quantified by the difference in expected total life-cycle costs with and without the SHM. This contribution presents a rigorous, comprehensive VoSHM analysis framework, which is shown to be applicable to a wide range of vibration-based SHM use cases across different time scales. We present in detail the various computational aspects of a – computationally intensive – VoSHM analysis, and we concurrently introduce efficient methods for performing the computations. These include heuristics for the solution to stochastic sequential decision problems and Bayesian filtering for joint deterioration state-parameter estimation. In contrast to Chapter 4 and to most of the literature, where just individual decisions are considered, the framework of Chapter 5 includes the full sequence of inspection and maintenance decisions throughout the structural

life-cycle. Various decision settings are numerically investigated with the aid of a numerical benchmark model of a bridge system, which range from predictive maintenance planning in the light of gradual deterioration processes and environmental variability, to near-real time decision support following extreme event occurrences. Results motivate the large potential economic benefit associated with investing in SHM systems to support maintenance planning in specific decision settings.

Chapter 6 focuses on the use of sampling-based Bayesian filtering algorithms in the context of deterioration model parameter estimation, which is an indispensable task in predictive maintenance planning. On-line (recursive) estimation of time-invariant parameters poses a computational challenge for on-line sampling-based Bayesian filters, which are confronted with sample degeneracy and impoverishment issues. These issues hinder the use of on-line Bayesian filters in problems where quantification of the full posterior parameter uncertainty is of interest, creating the need for tailored solutions. Off-line (batch) algorithms are – in principle – better suited for the uncertainty quantification task, yet they are computationally prohibitive in sequential settings. In Chapter 6, we present in full algorithmic detail adapted on-line and off-line (batch) Bayesian filters. These are the on-line particle filter with Gaussian mixture resampling (PFGM), the on-line iterated batch importance sampling filter (IBIS), which performs off-line Markov chain Monte Carlo (MCMC) move steps, and the off-line MCMC-based sequential Monte Carlo (SMC) filter. A comparative assessment is performed with the aid of two numerical examples of different nature and complexity. The accuracy of posterior estimates and the computational cost form the criteria for this assessment. Several conclusions are drawn, most notably that the presented on-line PFGM filter proves competitive with off-line, computationally expensive filters.

Finally, in Chapter 7, we propose a novel decision-oriented metric for assessing data-driven prognostic algorithms. The novelty of the proposed metric compared to other metrics from the literature is that it assesses algorithms on the basis of downstream predictive maintenance (PdM) decisions that are to be triggered by their outcome, i.e., the predictions of the remaining useful life (RUL). It is thus defined in conjunction with a specific decision setting and a corresponding PdM policy, which dictates the maintenance actions based on input RUL predictions. The work in Chapter 7 focuses specifically on two common decision settings pertinent to industrial assets, for which we employ and improve some relevant PdM policies of varying complexity from the literature. The metric further serves as the basis for a decision-oriented optimization of data-driven prognostic algorithms. The availability of run-to-failure monitoring datasets is essential to a data-driven evaluation of the metric, freeing the analyst altogether from the need of *a-priori* defining a stochastic model describing the deterioration process. A limited amount of such data, however, may pose a bottleneck for this evaluation, as it leads to an estimate with non-negligible variability. We rigorously investigate the metric with the aid of two numerical examples, one theoretical virtual case study and one benchmark case study related to degrading turbofan engines. These provide valuable insights on the proposed decision-oriented performance assessment and optimization of prognostic algorithms.

3.2 Outlook

The VoI/VoSHM analysis presented in this thesis constitutes a rigorous framework for *a-priori* quantifying the expected economic gains associated with the adoption of SHM on deteriorating systems. There are few additional aspects that future work may incorporate into the presented

framework towards enhancing its degree of realism. In a real SHM setting, the Bayesian model updating process is subject to an unknown model error, which often constitutes the most significant source of uncertainty in the process. Model errors are not considered in this work. Such errors can be incorporated in the framework, e.g., by deliberately introducing a model discrepancy. This entails utilizing different models for the tasks of generating the monitoring data and performing the Bayesian updating. A hierarchical Bayesian model updating approach [14] can then be employed in the framework, which has been shown to appropriately account for model errors. Moreover, SHM systems are themselves subject to deterioration, which may inhibit their uninterrupted functionality. This is an issue that could potentially lead to a non-negligible reduction of the VoI/VoSHM. In this context, probabilistic models describing the SHM system performance deterioration as well as associated maintenance actions may additionally be incorporated in the framework. Furthermore, the costs assigned to different actions and events are in principle uncertain variables. The values of these costs significantly affect the VoI/VoSHM analysis results. Thus, the rigorous, and ideally standardized, definition of cost models is an important area of future research in the direction of more precisely quantifying the VoI/VoSHM.

Utilization of the VoSHM framework for optimizing monitoring systems seems straightforward. For instance, the VoSHM metric can serve as the decision-theoretic objective function for sensor placement optimization studies. For this problem, information-theoretic objective functions are typically adopted [137].

In this work, we employ heuristic decision policies, which rely on time-variant reliability or remaining useful life estimates, for predictive maintenance planning. The heuristics-based approach allows for interpretable, yet sub-optimal, solutions to the stochastic sequential decision problem. One can certainly not overlook the unprecedented potential that deep reinforcement learning (RL) offers for finding optimal solutions to such problems. Casting the predictive maintenance planning problem into a deep RL problem is certainly a promising research direction, with existing studies already revealing its large potential [6, 104].

This thesis discusses various limitations of purely model-based and data-driven prognostic approaches for supporting predictive maintenance planning tasks, and demonstrates that the development of hybrid frameworks [10] is a promising avenue towards reaching an optimal synergy between these two approaches. As motivated by the proposal of a novel decision-oriented metric in Chapter 7 of this dissertation, to bring the most added value, the development and implementation of any novel hybrid prognostic framework ideally has to be targeted towards its role in decision support.

The scarcity of real-world run-to-failure monitoring datasets poses a major bottleneck to the development of purely data-driven prognostic approaches and to the application of the data-driven predictive maintenance paradigm. To alleviate this issue, the scientific community and practitioners must work closely together towards fostering a data-sharing approach. An open-data approach can generally prove vastly beneficial to future scientific and practical developments in the fields of SHM and PHM. The Prognostics Data Repository [127] is an excellent example of such an approach.

Finally, in the experience of the author, researchers may often have different perspectives depending on whether they come from the SHM community, the PHM community, or the risk/reliability analysis and decision-making community. This thesis endeavors to bring some of these perspectives together. It is the author's belief that similar collaborative efforts are key to reaching a reliable synergy between health monitoring and decision making.

References

[1] A. E. Ades, G. Lu, and K. Claxton. "Expected Value of Sample Information Calculations in Medical Decision Modeling". In: *Medical Decision Making* 24.2 (2004). PMID: 15090106, pp. 207–227.

[2] R. Ahmad and S. Kamaruddin. "An overview of time-based and condition-based maintenance in industrial application". In: *Computers & Industrial Engineering* 63.1 (2012), pp. 135–149.

[3] S. Alaswad and Y. Xiang. "A review on condition-based maintenance optimization models for stochastically deteriorating system". In: *Reliability Engineering & System Safety* 157 (2017), pp. 54–63.

[4] D. Anastasopoulos, G. De Roeck, and E. P. Reynders. "One-year operational modal analysis of a steel bridge from high-resolution macrostrain monitoring: Influence of temperature vs. retrofitting". In: *Mechanical Systems and Signal Processing* 161 (2021), p. 107951.

[5] C. Andrieu, A. Doucet, and R. Holenstein. "Particle Markov chain Monte Carlo methods". In: *Journal of the Royal Statistical Society: Series B (Statistical Methodology)* 72.3 (2010), pp. 269–342.

[6] C. P. Andriotis and K. G. Papakonstantinou. "Managing engineering systems with large state and action spaces through deep reinforcement learning". In: *Reliability Engineering & System Safety* 191 (2019), p. 106483.

[7] C. P. Andriotis, K. G. Papakonstantinou, and E. N. Chatzi. "Deep reinforcement learning driven inspection and maintenance planning under incomplete information and constraints". In: *Reliability Engineering & System Safety* 212 (2021), p. 107551.

[8] C. P. Andriotis, K. G. Papakonstantinou, and E. N. Chatzi. "Value of structural health information in partially observable stochastic environments". In: *Structural Safety* 93 (2021), p. 102072.

[9] G. Arcieri, C. Hoelzl, O. Schwery, D. Straub, K. G. Papakonstantinou, and E. Chatzi. "Bridging POMDPs and Bayesian decision making for robust maintenance planning under model uncertainty: An application to railway systems". In: *Reliability Engineering & System Safety* 239 (2023), p. 109496.

[10] M. Arias Chao, C. Kulkarni, K. Goebel, and O. Fink. "Fusing physics-based and deep learning models for prognostics". In: *Reliability Engineering & System Safety* 217 (2022), p. 107961.

[11] L. D. Avendaño-Valencia, E. N. Chatzi, K. Y. Koo, and J. M. W. Brownjohn. "Gaussian Process Time-Series Models for Structures under Operational Variability". In: *Frontiers in Built Environment* 3 (2017).

[12] R. Barlow and L. Hunter. "Optimum Preventive Maintenance Policies". In: *Operations Research* 8.1 (1960), pp. 90–100.

[13] A. T. Beck and R. E. Melchers. "Overload failure of structural components under random crack propagation and loading – a random process approach". In: *Structural Safety* 26.4 (2004), pp. 471–488.

[14] I. Behmanesh, B. Moaveni, G. Lombaert, and C. Papadimitriou. "Hierarchical Bayesian model updating for structural identification". In: *Mechanical Systems and Signal Processing* 64-65 (2015), pp. 360–376.

[15] J. Benjamin and C. Cornell. *Probability, Statistics, and Decision for Civil Engineers*. Dover Books on Engineering. Dover Publications, 1970.

[16] C. M. Bishop. *Pattern recognition and machine learning*. New York: Springer, 2006.

[17] E. Bismut and D. Straub. "Optimal Adaptive Inspection and Maintenance Planning for Deteriorating Structural Systems". In: *Reliability Engineering and System Safety* 215 (2021), p. 107891.

[18] E. Bismut. *Optimal heuristic strategies for risk- and reliability-based inspection and maintenance planning*. PhD thesis, Technische Universität München, Germany, 2022.

[19] E. Bismut and D. Straub. "A unifying review of NDE models towards optimal decision support". In: *Structural Safety* 97 (2022), p. 102213.

[20] L. Bull, P. Gardner, J. Gosliga, T. Rogers, N. Dervilis, E. Cross, E. Papatheou, A. Maguire, C. Campos, and K. Worden. "Foundations of population-based SHM, Part I: Homogeneous populations and forms". In: *Mechanical Systems and Signal Processing* 148 (2021), p. 107141.

[21] S. Canessa, G. Guillera-Arroita, J. J. Lahoz-Monfort, D. M. Southwell, D. P. Armstrong, I. Chadès, R. C. Lacy, and S. J. Converse. "When do we need more data? A primer on calculating the value of information for applied ecologists". In: *Methods in Ecology and Evolution* 6.10 (2015), pp. 1219–1228.

[22] S. Cantero-Chinchilla, J. Chiachío, M. Chiachío, D. Chronopoulos, and A. Jones. "Optimal sensor configuration for ultrasonic guided-wave inspection based on value of information". In: *Mechanical Systems and Signal Processing* 135 (2020), p. 106377.

[23] S. Cantero-Chinchilla, C. Papadimitriou, J. Chiachío, M. Chiachío, P. Koumoutsakos, A. T. Fabro, and D. Chronopoulos. "Robust optimal sensor configuration using the value of information". In: *Structural Control and Health Monitoring* 29.12 (2022), e3143.

[24] D. Castelvecchi. "Can we open the black box of AI?" In: *Nature* 538 (2016), pp. 20–23.

[25] P. Cawley. "Structural health monitoring: Closing the gap between research and industrial deployment". In: *Structural Health Monitoring* 17(5) (2018), pp. 1225–1244.

[26] M. Chadha, Z. Hu, and M. D. Todd. "An alternative quantification of the value of information in structural health monitoring". In: *Structural Health Monitoring* 21.1 (2022), pp. 138–164.

[27] E. Chatzi and A. Smyth. "Particle filter scheme with mutation for the estimation of time-invariant parameters in structural health monitoring applications". In: *Structural Control and Health Monitoring* 20 (2013), pp. 1081–1095.

[28] J. Chiachío, M. Chiachío, S. Sankararaman, A. Saxena, and K. Goebel. "Condition-based prediction of time-dependent reliability in composites". In: *Reliability Engineering & System Safety* 142 (2015), pp. 134–147.

[29] N. Chopin, P. E. Jacob, and O. Papaspiliopoulos. "SMC2: an efficient algorithm for sequential analysis of state space models". In: *Journal of the Royal Statistical Society: Series B (Statistical Methodology)* 75.3 (2013), pp. 397–426.

[30] N. Chopin. "A Sequential Particle Filter Method for Static Models". In: *Biometrika* 89(3) (Aug. 2002), pp. 539–552.

[31] M. Compare, P. Baraldi, and E. Zio. "Challenges to IoT-Enabled Predictive Maintenance for Industry 4.0". In: *IEEE Internet of Things Journal* 7.5 (2020), pp. 4585–4597.

[32] M. Corbetta, C. Sbarufatti, M. Giglio, and M. D. Todd. "Optimization of nonlinear, non-Gaussian Bayesian filtering for diagnosis and prognosis of monotonic degradation processes". In: *Mechanical Systems and Signal Processing* 104 (2018), pp. 305–322.

[33] E. Cross, K. Koo, J. Brownjohn, and K. Worden. "Long-term monitoring and data analysis of the Tamar Bridge". In: *Mechanical Systems and Signal Processing* 35.1 (2013), pp. 16–34.

[34] E. J. Cross and K. Worden. "Cointegration and why it works for SHM". In: *J. Phys.: Conf. Ser.* 382 (2012).

[35] I. de Pater, A. Reijns, and M. Mitici. "Alarm-based predictive maintenance scheduling for aircraft engines with imperfect Remaining Useful Life prognostics". In: *Reliability Engineering & System Safety* 221 (2022), p. 108341.

[36] A. Deraemaeker, E. Reynders, G. De Roeck, and J. Kullaa. "Vibration-based structural health monitoring using output-only measurements under changing environment". In: *Mechanical Systems and Signal Processing* 22.1 (2008), pp. 34–56.

[37] D. Di Francesco, M. Chryssanthopoulos, M. H. Faber, and U. Bharadwaj. "Decision-theoretic inspection planning using imperfect and incomplete data". In: *Data-Centric Engineering* 2 (2021), e18.

[38] O. Ditlevsen and H. Madsen. *Structural Reliability Methods*. Wiley New York, 1996.

[39] P. Do, A. Voisin, E. Levrat, and B. Iung. "A proactive condition-based maintenance strategy with both perfect and imperfect maintenance actions". In: *Reliability Engineering & System Safety* 133 (2015), pp. 22–32.

[40] A. Doucet, N. de Freitas, and N. Gordon. *Sequential Monte Carlo Methods in Practice*. Springer-Verlag New York, 2001.

[41] A. Doucet and A. M. Johansen. "A Tutorial on Particle Filtering and Smoothing: Fifteen years later". In: *Handbook of Nonlinear Filtering* (2008).

[42] L. Eichner, R. Schneider, P. Simon, and M. Baeßler. "Optimal sensor placement for vibration-based structural health monitoring obtained via value of information analysis as part of a digital structural integrity management of offshore structures". In: 2022.

[43] B. Ellingwood. "Risk-informed condition assessment of civil infrastructure: state of practice and research issues". In: *Structure and Infrastructure Engineering* 1(1) (2005), pp. 7–18.

[44] B. R. Ellingwood and Y. Mori. "Probabilistic methods for condition assessment and life prediction of concrete structures in nuclear power plants". In: *Nuclear Engineering and Design* 142.2 (1993), pp. 155–166.

[45] G. Evensen. *Data Assimilation: The Ensemble Kalman Filter*. Berlin, Heidelberg: Springer-Verlag, 2006.

[46] M. H. Faber. "On the Treatment of Uncertainties and Probabilities in Engineering Decision Analysis". In: *Journal of Offshore Mechanics and Arctic Engineering* 127.3 (Mar. 2005), pp. 243–248.

[47] C. R. Farrar and K. Worden. "An introduction to structural health monitoring". In: *Philosophical Transactions of the Royal Society A.* 365 (2007), pp. 303–315.

[48] C. R. Farrar and K. Worden. *Structural Health Monitoring: A Machine Learning Perspective*. John Wiley & Sons, Ltd, 2013.

[49] C. R. Farrar and N. A. Lieven. "Damage prognosis: the future of structural health monitoring". In: *Philosophical Transactions of the Royal Society A: Mathematical, Physical and Engineering Sciences* 365.1851 (2007), pp. 623–632.

[50] W. Fauriat and E. Zio. "Optimization of an aperiodic sequential inspection and condition-based maintenance policy driven by value of information". In: *Reliability Engineering & System Safety* 204 (2020), p. 107133.

[51] A. Fenerci, K. A. Kvåle, Ø. W. Petersen, A. Rønnquist, and O. Øiseth. "Data Set from Long-Term Wind and Acceleration Monitoring of the Hardanger Bridge". In: *Journal of Structural Engineering* 147.5 (2021), p. 04721003.

[52] E. Figueiredo, G. Park, J. Figueiras, C. Farrar, and K. Worden. "Structural health monitoring algorithm comparisons using standard data sets". In: (Mar. 2009).

[53] O. Fink. "Data-Driven Intelligent Predictive Maintenance of Industrial Assets". In: *Women in Industrial and Systems Engineering: Key Advances and Perspectives on Emerging Topics*. Springer International Publishing, 2020, pp. 589–605.

[54] O. Fink, Q. Wang, M. Svensén, P. Dersin, W.-J. Lee, and M. Ducoffe. "Potential, challenges and future directions for deep learning in prognostics and health management applications". In: *Engineering Applications of Artificial Intelligence* 92 (2020), p. 103678.

[55] C. W. Fox and S. J. Roberts. "A tutorial on variational Bayesian inference". In: *Artificial Intelligence Review* 38.2 (2012), pp. 85–95.

[56] D. Frangopol, M. Kallen, and J. van Noortwijk. "Probabilistic models for life-cycle performance of deteriorating structures: review and future directions". In: *Progress in Structural Engineering and Materials* 6 (2004), pp. 197–212.

[57] D. M. Frangopol, K.-Y. Lin, and A. C. Estes. "Life-Cycle Cost Design of Deteriorating Structures". In: *Journal of Structural Engineering* 123.10 (1997), pp. 1390–1401.

[58] D. Galar, K. Goebel, P. Sandborn, and U. Kumar. *Prognostics and Remaining Useful Life (RUL) Estimation: Predicting with Confidence (1st ed.)* CRC Press, 2021.

[59] C. Gao, Z. Fang, J. Lin, X. Guan, and J. He. "Model averaging and probability of detection estimation under hierarchical uncertainties for Lamb wave detection". In: *Mechanical Systems and Signal Processing* 165 (2022), p. 108302.

[60] P. Gardner, L. Bull, J. Gosliga, N. Dervilis, and K. Worden. "Foundations of population-based SHM, Part III: Heterogeneous populations – Mapping and transfer". In: *Mechanical Systems and Signal Processing* 149 (2021), p. 107142.

[61] P. Gardner. *On Novel Approaches to Model-Based Structural Health Monitoring*. PhD thesis, University of Sheffield, 2018.

[62] A. Gelman, J. B. Carlin, H. S. Stern, D. B. Dunson, A. Vehtari, and D. B. Rubin. *Bayesian data analysis (3rd edition)*. Chapman and Hall/CRC, 2013.

[63] W. Gilks, S. Richardson, and D. Spiegelhalter. *Markov Chain Monte Carlo in Practice*. Chapman & Hall/CRC Interdisciplinary Statistics. Taylor & Francis, 1995.

[64] W. R. Gilks and C. Berzuini. "Following a Moving Target-Monte Carlo Inference for Dynamic Bayesian Models". In: *Journal of the Royal Statistical Society. Series B (Statistical Methodology)* 63.1 (2001), pp. 127–146.

[65] P. F. Giordano and M. P. Limongelli. "The value of structural health monitoring in seismic emergency management of bridges". In: *Structure and Infrastructure Engineering* 18.4 (2022), pp. 537–553.

[66] P. F. Giordano, S. Quqa, and M. P. Limongelli. "The value of monitoring a structural health monitoring system". In: *Structural Safety* 100 (2023), p. 102280.

[67] K. Goebel and R. Rajamani. "Policy, regulations and standards in prognostics and health management". In: *International Journal of Prognostics and Health Management* 12.1 (2021).

[68] K. Goebel, B. Saha, A. Saxena, J. R. Celaya, and J. P. Christophersen. "Prognostics in Battery Health Management". In: *IEEE Instrumentation & Measurement Magazine* 11.4 (2008), pp. 33–40.

[69] J. Gosliga, P. Gardner, L. Bull, N. Dervilis, and K. Worden. "Foundations of Population-based SHM, Part II: Heterogeneous populations – Graphs, networks, and communities". In: *Mechanical Systems and Signal Processing* 148 (2021), p. 107144.

[70] A. Grall, C. Bérenguer, and L. Dieulle. "A condition-based maintenance policy for stochastically deteriorating systems". In: *Reliability Engineering & System Safety* 76.2 (2002), pp. 167–180.

[71] S. M. Hoseyni, F. D. Maio, and E. Zio. "Optimal sensor positioning on pressurized equipment based on Value of Information". In: *Proceedings of the Institution of Mechanical Engineers, Part O: Journal of Risk and Reliability* 235 (4 2021), pp. 533–544.

[72] R. A. Howard. *Dynamic programming and Markov Processes*. John Wiley, 1960.

[73] Y. Hu, P. Baraldi, F. Di Maio, and E. Zio. "Online Performance Assessment Method for a Model-Based Prognostic Approach". In: *IEEE Transactions on Reliability* 65.2 (2016), pp. 718–735.

[74] Y. Hu, X. Miao, Y. Si, E. Pan, and E. Zio. "Prognostics and health management: A review from the perspectives of design, development and decision". In: *Reliability Engineering & System Safety* 217 (2022), p. 108063.

[75] J. Huang, Q. Chang, and J. Arinez. "Deep reinforcement learning based preventive maintenance policy for serial production lines". In: *Expert Systems with Applications* 160 (2020), p. 113701.

[76] A. Hughes, L. Bull, P. Gardner, R. Barthorpe, N. Dervilis, and K. Worden. "On risk-based active learning for structural health monitoring". In: *Mechanical Systems and Signal Processing* 167 (2022), p. 108569.

[77] A. Hughes, L. Bull, P. Gardner, N. Dervilis, and K. Worden. "On robust risk-based active-learning algorithms for enhanced decision support". In: *Mechanical Systems and Signal Processing* 181 (2022), p. 109502.

[78] A. Hughes. *On risk-based decision-making for structural health monitoring*. PhD thesis, University of Sheffield, 2022.

[79] L. Iannacone, P. Giordano, P. Gardoni, and M. Limongelli. "Quantifying the value of information from inspecting and monitoring engineering systems subject to gradual and shock deterioration". In: *Structural Health Monitoring* 21(1) (2022), pp. 72–89.

[80] O. L. Ivanov, I. Björnsson, D. Honfi, and J. Leander. "The practical value of structural health information for time dependence in bridge maintenance". In: *Structure and Infrastructure Engineering* 18.4 (2022), pp. 476–491.

[81] A. K. Jardine, D. Lin, and D. Banjevic. "A review on machinery diagnostics and prognostics implementing condition-based maintenance". In: *Mechanical Systems and Signal Processing* 20.7 (2006), pp. 1483–1510.

[82] K. Javed, R. Gouriveau, and N. Zerhouni. "State of the art and taxonomy of prognostics approaches, trends of prognostics applications and open issues towards maturity at different technology readiness levels". In: *Mechanical Systems and Signal Processing* 94 (2017), pp. 214–236.

[83] F. Jensen and T. Nielsen. *Bayesian Networks and Decision Graphs, 2nd Edition*. New York: Springer, 2007.

[84] G. Jia and P. Gardoni. "State-dependent stochastic models: A general stochastic framework for modeling deteriorating engineering systems considering multiple deterioration processes and their interactions". In: *Structural Safety* 72 (2018), pp. 99–110.

[85] E. A. Johnson, H. F. Lam, L. S. Katafygiotis, and J. L. Beck. "Phase I IASC-ASCE Structural Health Monitoring Benchmark Problem Using Simulated Data". In: *Journal of Engineering Mechanics* 130.1 (2004), pp. 3–15.

[86] M. Jouin, R. Gouriveau, D. Hissel, M.-C. Péra, and N. Zerhouni. "Particle filter-based prognostics: Review, discussion and perspectives". In: *Mechanical Systems and Signal Processing* 72-73 (2016), pp. 2–31.

[87] R. Kalman. "A New Approach to Linear Filtering and Prediction Problems". In: *ASME Journal of Basic Engineering* 82 (1960), pp. 35–45.

[88] A. Kamariotis, E. Chatzi, and D. Straub. "A framework for quantifying the value of vibration-based structural health monitoring". In: *Mechanical Systems and Signal Processing* 184 (2023), p. 109708.

[89] A. Kamariotis, E. Chatzi, and D. Straub. "Value of information from vibration-based structural health monitoring extracted via Bayesian model updating". In: *Mechanical Systems and Signal Processing* 166 (2022), p. 108465.

[90] A. Kamariotis, L. Sardi, I. Papaioannou, E. Chatzi, and D. Straub. "On off-line and on-line Bayesian filtering for uncertainty quantification of structural deterioration". In: *Data-Centric Engineering* 4 (2023), e17.

[91] A. Kamariotis, K. Tatsis, E. Chatzi, K. Goebel, and D. Straub. "A metric for assessing and optimizing data-driven prognostic algorithms for predictive maintenance". In: *Reliability Engineering & System Safety* 242 (2024), p. 109723.

[92] N. Kantas, A. Doucet, S. S. Singh, J. Maciejowski, and N. Chopin. "On Particle Methods for Parameter Estimation in State-Space Models". In: *Statistical Science* 30.3 (2015), pp. 328–351.

[93] M. G. Kapteyn, J. V. R. Pretorius, and K. E. Willcox. "A probabilistic graphical model foundation for enabling predictive digital twins at scale". In: *Nature Computational Science* 1.5 (2021), pp. 337–347.

[94] M. S. Khan, C. Caprani, S. Ghosh, and J. Ghosh. "Value of strain-based structural health monitoring as decision support for heavy load access to bridges". In: *Structure and Infrastructure Engineering* 18.4 (2022), pp. 521–536.

[95] N.-H. Kim, D. An, and J.-H. Choi. *Prognostics and Health Management of Engineering Systems. An introduction*. Springer, 2017.

[96] D. P. Kingma and J. Ba. *Adam: A Method for Stochastic Optimization*. 2014.

[97] A. D. Kiureghian and O. Ditlevsen. "Aleatory or epistemic? Does it matter?" In: *Structural Safety* 31.2 (2009). Risk Acceptance and Risk Communication, pp. 105–112.

[98] W. J. Klerk, T. Schweckendiek, F. den Heijer, and M. Kok. "Value of Information of Structural Health Monitoring in Asset Management of Flood Defences". In: *Infrastructures* 4.3 (2019).

[99] M. J. Kochenderfer. *Decision making under uncertainty: Theory and application.* English. MIT Lincoln Laboratory Series. The MIT Press, 2015.

[100] K. Konakli, B. Sudret, and M. H. Faber. "Numerical Investigations into the Value of Information in Lifecycle Analysis of Structural Systems". In: *ASCE-ASME Journal of Risk and Uncertainty in Engineering Systems, Part A: Civil Engineering* 2(3) (2016), B4015007.

[101] A. Krause. "Optimizing sensing: Theory and applications". English. Copyright - Database copyright ProQuest LLC; ProQuest does not claim copyright in the individual underlying works; Last updated - 2022-10-29. PhD thesis. 2008, p. 328.

[102] R. Kumar and P. Gardoni. "Renewal theory-based life-cycle analysis of deteriorating engineering systems". In: *Structural Safety* 50 (2014), pp. 94–102.

[103] J. Lee, F. Wu, W. Zhao, M. Ghaffari, L. Liao, and D. Siegel. "Prognostics and health management design for rotary machinery systems—Reviews, methodology and applications". In: *Mechanical Systems and Signal Processing* 42.1 (2014), pp. 314–334.

[104] J. Lee and M. Mitici. "Deep reinforcement learning for predictive aircraft maintenance using probabilistic Remaining-Useful-Life prognostics". In: *Reliability Engineering & System Safety* 230 (2023), p. 108908.

[105] Y. Lei, N. Li, L. Guo, N. Li, T. Yan, and J. Lin. "Machinery health prognostics: A systematic review from data acquisition to RUL prediction". In: *Mechanical Systems and Signal Processing* 104 (2018), pp. 799–834.

[106] S. Li and M. Pozzi. "What makes long-term monitoring convenient? A parametric analysis of value of information in infrastructure maintenance". In: *Structural Control and Health Monitoring* 26.5 (2019), e2329.

[107] X. Li, Q. Ding, and J.-Q. Sun. "Remaining useful life estimation in prognostics using deep convolution neural networks". In: *Reliability Engineering & System Safety* 172 (2018), pp. 1–11.

[108] X. Li, W. Zhang, and Q. Ding. "Deep learning-based remaining useful life estimation of bearings using multi-scale feature extraction". In: *Reliability Engineering & System Safety* 182 (2019), pp. 208–218.

[109] C. Lin, J. Song, and M. Pozzi. "Optimal inspection of binary systems via Value of Information analysis". In: *Reliability Engineering & System Safety* 217 (2022), p. 107944.

[110] L. Long, M. Döhler, and S. Thöns. "Determination of structural and damage detection system influencing parameters on the value of information". In: *Structural Health Monitoring* 21.1 (2022), pp. 19–36.

[111] R. Luce and H. Raiffa. *Games and decisions: Introduction and critical survey.* Harvard University, Boston: Dover Publications Inc., 1989.

[112] J. Luque and D. Straub. "Risk-based optimal inspection strategies for structural systems using dynamic Bayesian Networks". In: *Structural Safety* 76 (2019), pp. 68–80.

[113] C. Malings and M. Pozzi. "Value-of-information in spatio-temporal systems: Sensor placement and scheduling". In: *Reliability Engineering & System Safety* 172 (2018), pp. 45–57.

[114] C. Malings and M. Pozzi. "Conditional entropy and value of information metrics for optimal sensing in infrastructure systems". In: *Structural Safety* 60 (2016), pp. 77–90.

[115] C. Malings and M. Pozzi. "Value of information for spatially distributed systems: Application to sensor placement". In: *Reliability Engineering & System Safety* 154 (2016), pp. 219–233.

[116] H. Martín-Sanz, K. Tatsis, V. K. Dertimanis, L. D. Avendaño-Valencia, E. Brühwiler, and E. Chatzi. "Monitoring of the UHPFRC strengthened Chillon viaduct under environmental and operational variability". In: *Structure and Infrastructure Engineering* 16.1 (2020), pp. 138–168.

[117] R. E. Melchers. "Probabilistic Model for Marine Corrosion of Steel for Structural Reliability Assessment". In: *Journal of Structural Engineering* 129.11 (2003), pp. 1484–1493.

[118] R. E. Melchers. "Probabilistic Models for Corrosion in Structural Reliability Assessment—Part 1: Empirical Models ". In: *Journal of Offshore Mechanics and Arctic Engineering* 125.4 (Oct. 2003), pp. 264–271.

[119] R. E. Melchers. "Reliability-Based Service-Life Assessment of Aging Concrete Structures". In: *Journal of Structural Engineering* 119(5) (1993).

[120] R. E. Melchers and A. Beck. *Structural Reliability Analysis and Prediction, 3rd Edition*. John Wiley & Sons, Ltd, 2017.

[121] M. Memarzadeh and M. Pozzi. "Value of information in sequential decision making: Component inspection, permanent monitoring and system-level scheduling". In: *Reliability Engineering & System Safety* 154 (2016), pp. 137–151.

[122] R. van der Merwe and E. Wan. "Gaussian mixture sigma-point particle filters for sequential probabilistic inference in dynamic state-space models". In: *2003 IEEE International Conference on Acoustics, Speech, and Signal Processing, 2003. Proceedings. (ICASSP '03).* Vol. 6. 2003, pp. VI–701.

[123] P. D. Moral, A. Doucet, and A. Jasra. "Sequential Monte Carlo Samplers". In: *Journal of the Royal Statistical Society. Series B (Statistical Methodology)* 68.3 (2006), pp. 411–436.

[124] P. Morato, K. Papakonstantinou, C. Andriotis, J. Nielsen, and P. Rigo. "Optimal inspection and maintenance planning for deteriorating structural components through dynamic Bayesian networks and Markov decision processes". In: *Structural Safety* 94 (2022), p. 102140.

[125] Y. Mori and B. Ellingwood. "Reliability-Based Service-Life Assessment of Aging Concrete Structures". In: *Journal of Structural Engineering* 119(5) (1993).

[126] K. P. Murphy. *Machine Learning: A Probabilistic Perspective*. The MIT Press, 2012.

[127] *NASA Ames Prognostics Data Repository, NASA Ames Research Center*. https://www.nasa.gov/content/prognostics-center-of-excellence-data-set-repository.

[128] P. Nectoux, R. Gouriveau, K. Medjaher, E. Ramasso, B. Chebel-Morello, N. Zerhouni, and C. Varnier. "PRONOSTIA : An experimental platform for bearings accelerated degradation tests." In: *IEEE International Conference on Prognostics and Health Management, PHM'12.* Vol. sur CD ROM. Denver, Colorado, United States: IEEE Catalog Number : CPF12PHM-CDR, June 2012, pp. 1–8.

[129] A. C. Neves, J. Leander, I. González, and R. Karoumi. "An approach to decision-making analysis for implementation of structural health monitoring in bridges". In: *Structural Control and Health Monitoring* 26.6 (2019). e2352 STC-18-0244.R2, e2352.

[130] K. T. Nguyen and K. Medjaher. "A new dynamic predictive maintenance framework using deep learning for failure prognostics". In: *Reliability Engineering & System Safety* 188 (2019), pp. 251–262.

[131] J. Nielsen and J. D. Sorensen. "Risk-based decision making for deterioration processes using POMDP". In: *Proceedings of the 12th International Conference on Applications of Statistics and Probability in Civil Engineering*. Vancouver, Canada, 2015.

[132] J. S. Nielsen. "Value of information of structural health monitoring with temporally dependent observations". In: *Structural Health Monitoring* 21.1 (2022), pp. 165–184.

[133] J. S. Nielsen, D. Tcherniak, and M. D. Ulriksen. "A case study on risk-based maintenance of wind turbine blades with structural health monitoring". In: *Structure and Infrastructure Engineering* 17.3 (2021), pp. 302–318.

[134] Y. Ou, K. E. Tatsis, V. K. Dertimanis, M. D. Spiridonakos, and E. N. Chatzi. "Vibration-based monitoring of a small-scale wind turbine blade under varying climate conditions. Part I: An experimental benchmark". In: *Structural Control and Health Monitoring* 28.6 (2021), e2660.

[135] S. J. Pan and Q. Yang. "A Survey on Transfer Learning". In: *IEEE Transactions on Knowledge and Data Engineering* 22.10 (2010), pp. 1345–1359.

[136] M. D. Pandey and J. van der Weide. "Stochastic renewal process models for estimation of damage cost over the life-cycle of a structure". In: *Structural Safety* 67 (2017), pp. 27–38.

[137] C. Papadimitriou. "Optimal sensor placement methodology for parametric identification of structural systems". In: *Journal of Sound and Vibration* 278.4 (2004), pp. 923–947.

[138] K. Papakonstantinou and M. Shinozuka. "Planning structural inspection and maintenance policies via dynamic programming and Markov processes. Part I: Theory". In: *Reliability Engineering & System Safety* 130 (2014), pp. 202–213.

[139] P. Paris and F. Erdogan. "A Critical Analysis of Crack Propagation Laws". In: *Journal of Basic Engineering* 85.4 (1963), pp. 528–533.

[140] J. I. Park and S. J. Bae. "Direct Prediction Methods on Lifetime Distribution of Organic Light-Emitting Diodes From Accelerated Degradation Tests". In: *IEEE Transactions on Reliability* 59.1 (2010), pp. 74–90.

[141] I. de Pater and M. Mitici. "Novel metrics to evaluate probabilistic remaining useful life prognostics with applications to turbofan engines". In: *PHM Society European Conference*. Vol. 7(1). 2022, pp. 96–109.

[142] B. Peeters. *System identification and damage detection in civil engineering*. Belgium: PhD thesis, Katholieke Universiteit Leuven, 2000.

[143] B. Peeters and G. De Roeck. "One-year monitoring of the Z24-Bridge: environmental effects versus damage events". In: *Earthquake Engineering & Structural Dynamics* 30.2 (2001), pp. 149–171.

[144] W. B. Powell. *Reinforcement Learning and Stochastic Optimization: A Unified Framework for Sequential Decisions*. Wiley, 2022.

[145] M. Pozzi and A. D. Kiureghian. "Assessing the Value of Information for long-term structural health monitoring". In: *SPIE Conference on Health Monitoring of Structural and Biological Systems*. San Diego, California, USA, 2011.

[146] M. Pozzi, C. Malings, and A. Minca. "Information avoidance and overvaluation under epistemic constraints: Principles and implications for regulatory policies". In: *Reliability Engineering & System Safety* 197 (2020), p. 106814.

[147] S. Qin and W. Cui. "Effect of corrosion models on the time-dependent reliability of steel plated elements". In: *Marine Structures* 16.1 (2003), pp. 15–34.

[148] R. Rackwitz. "Optimizing systematically renewed structures". In: *Reliability Engineering & System Safety* 73.3 (2001), pp. 269–279.

[149] H. Raiffa and R. Schlaifer. *Applied statistical decision theory*. Harvard University, Boston: Division of Research, Graduate School of Business Administration, 1961.

[150] A. Rasheed, O. San, and T. Kvamsdal. "Digital Twin: Values, Challenges and Enablers From a Modeling Perspective". In: *IEEE Access* 8 (2020), pp. 21980–22012.

[151] C.-A. Robelin and S. M. Madanat. "History-Dependent Bridge Deck Maintenance and Replacement Optimization with Markov Decision Processes". In: *Journal of Infrastructure Systems* 13.3 (2007), pp. 195–201.

[152] C. P. Robert. *The Bayesian Choice. From Decision-Theoretic Foundations to Computational Implementation*. Springer Texts in Statistics, 2007.

[153] R. Rocchetta, L. Bellani, M. Compare, E. Zio, and E. Patelli. "A reinforcement learning framework for optimal operation and maintenance of power grids". In: *Applied Energy* 241 (2019), pp. 291–301.

[154] S. M. Ross. *Introduction to Probability Models, Twelfth Edition*. Academic Press, 2019.

[155] S. M. Ross. *Stochastic Processes, 2nd Edition*. Wiley Series in Probability and Mathematical Statistics, 1995.

[156] R. Y. Rubinstein and D. P. Kroese. *Simulation and the Monte Carlo Method*. 3rd. Wiley Publishing, 2016.

[157] C. Rudin. "Stop explaining black box machine learning models for high stakes decisions and use interpretable models instead". In: *Nature Machine Intelligence* 1.5 (2019), pp. 206–215.

[158] A. Rytter. "Vibrational Based Inspection of Civil Engineering Structures". English. Ph.D.-Thesis defended publicly at the University of Aalborg, April 20, 1993 PDF for print: 206 pp. PhD thesis. Denmark, 1993.

[159] M. Sanchez-Silva, G.-A. Klutke, and D. V. Rosowsky. "Life-cycle performance of structures subject to multiple deterioration mechanisms". In: *Structural Safety* 33.3 (2011), pp. 206–217.

[160] M. Sanchez-Silva, G.-A. Klutke, and D. V. Rosowsky. *Reliability and Life-Cycle Analysis of Deteriorating Systems*. Springer Series in Reliability Engineering, 2016.

[161] S. Sankararaman. "Significance, interpretation, and quantification of uncertainty in prognostics and remaining useful life prediction". In: *Mechanical Systems and Signal Processing* 52-53 (2015), pp. 228–247.

[162] S. Sankararaman and K. Goebel. "Why is the reamining useful life prediction uncertain?" In: *Annual Conference of the PHM Society* 5(1) (2013), pp. 134–147.

[163] S. Särkkä. *Bayesian Filtering and Smoothing*. English. United Kingdom: Cambridge University Press, 2013.

[164] A. Saxena, J. Celaya, E. Balaban, K. Goebel, B. Saha, S. Saha, and M. Schwabacher. "Metrics for evaluating performance of prognostic techniques". In: *2008 International Conference on Prognostics and Health Management*. 2008, pp. 1–17.

[165] R. Schöbi and E. N. Chatzi. "Maintenance planning using continuous-state partially observable Markov decision processes and non-linear action models". In: *Structure and Infrastructure Engineering* 12.8 (2016), pp. 977–994.

[166] X.-S. Si, W. Wang, C.-H. Hu, M.-Y. Chen, and D.-H. Zhou. "A Wiener-process-based degradation model with a recursive filter algorithm for remaining useful life estimation". In: *Mechanical Systems and Signal Processing* 35.1 (2013), pp. 219–237.

[167] J. Sikorska, M. Hodkiewicz, and L. Ma. "Prognostic modelling options for remaining useful life estimation by industry". In: *Mechanical Systems and Signal Processing* 25.5 (2011), pp. 1803–1836.

[168] E. Simoen, G. D. Roeck, and G. Lombaert. "Dealing with uncertainty in model updating for damage assessment: a review". In: *Mechanical Systems and Signal Processing* 56 (2015), pp. 123–149.

[169] C. Song, C. Zhang, A. Shafieezadeh, and R. Xiao. "Value of information analysis in non-stationary stochastic decision environments: A reliability-assisted POMDP approach". In: *Reliability Engineering & System Safety* 217 (2022), p. 108034.

[170] M. D. Spiridonakos, E. N. Chatzi, and B. Sudret. "Polynomial Chaos Expansion Models for the Monitoring of Structures under Operational Variability". In: *ASCE-ASME Journal of Risk and Uncertainty in Engineering Systems, Part A: Civil Engineering* 2.3 (2016), B4016003.

[171] R. Srinivasan and A. K. Parlikad. "Value of condition monitoring in infrastructure maintenance". In: *Computers & Industrial Engineering* 66.2 (2013), pp. 233–241.

[172] G. Storvik. "Particle filters for state-space models with the presence of unknown static parameters". In: *IEEE Transactions on Signal Processing* 50.2 (2002), pp. 281–289.

[173] D. Straub. *Lecture notes in Engineering Risk Analysis*. ERA Group, Technische Universität München, 2020.

[174] D. Straub. "Value of information analysis with structural reliability methods". In: *Structural Safety* 49 (2014), pp. 68–80.

[175] D. Straub, E. Chatzi, E. Bismut, et al. "Value of information: A roadmap to quantifying the benefit of structural health monitoring". In: *Proceedings of the 12th International Conference on Structural Safety and Reliability: ICOSSAR 2017*. Vienna, Austria, 2017, pp. 3018–3029.

[176] D. Straub and M. H. Faber. "Risk based inspection planning for structural systems". In: *Structural Safety* 27(4) (2005), pp. 335–355.

[177] D. Straub. *Generic approaches to risk based inspection planning for steel structures*. PhD thesis, ETH Zürich, Switzerland, 2004.

[178] D. Straub. "Reliability updating with equality information". In: *Probabilistic Engineering Mechanics* 26.2 (2011), pp. 254–258.

[179] D. Straub. "Stochastic Modeling of Deterioration Processes through Dynamic Bayesian Networks". In: *Journal of Engineering Mechanics* 135.10 (2009), pp. 1089–1099.

[180] D. Straub et al. "Value of information analysis for dummies". In: *manuscript in preparation* (2023).

[181] D. Straub, R. Schneider, E. Bismut, and H.-J. Kim. "Reliability analysis of deteriorating structural systems". In: *Structural Safety* 82 (2020), p. 101877.

[182] K. Tatsis and E. Chatzi. "A numerical benchmark for system identification under operational and environmental variability". In: *8th International Operational Modal Analysis Conference (IOMAC 19)*. Copenhagen, Denmark, 2019.

[183] A. Thelen, X. Zhang, O. Fink, Y. Lu, S. Ghosh, B. D. Youn, M. D. Todd, S. Mahadevan, C. Hu, and Z. Hu. "A comprehensive review of digital twin — part 1: modeling and twinning enabling technologies". In: *Structural and Multidisciplinary Optimization* 65.12 (2022), p. 354.

[184] S. Thöns. "On the value of monitoring information for the structural integrity and risk management". In: *Computer-Aided Civil and Infrastructure Engineering* 33(1) (2018), pp. 79–94.

[185] S. Thöns, R. Schneider, and M. Faber. "Quantification of the Value of Structural Health Monitoring Information for Fatigue Deteriorating Structural Systems". In: *Proceedings of the 12th International Conference on Applications of Statistics and Probability in Civil Engineering*. Vancouver, Canada, 2015.

[186] Z. Tian, T. Jin, B. Wu, and F. Ding. "Condition based maintenance optimization for wind power generation systems under continuous monitoring". In: *Renewable Energy* 36.5 (2011), pp. 1502–1509.

[187] H. C. Tijms. "Renewal-Reward Processes". In: *A First Course in Stochastic Models*. John Wiley & Sons, Ltd, 2003. Chap. 2, pp. 33–79.

[188] M. Torzoni, M. Tezzele, S. Mariani, A. Manzoni, and K. E. Willcox. "A digital twin framework for civil engineering structures". In: *Computer Methods in Applied Mechanics and Engineering* 418 (2024), p. 116584.

[189] G. Tsialiamanis, D. J. Wagg, N. Dervilis, and K. Worden. "On generative models as the basis for digital twins". In: *Data-Centric Engineering* 2 (2021), e11.

[190] J. van Noortwijk. "A survey of the application of gamma processes in maintenance". In: *Reliability Engineering and System Safety* 94.1 (2009), pp. 2–21.

[191] E. VanDerHorn and S. Mahadevan. "Digital Twin: Generalization, characterization and implementation". In: *Decision Support Systems* 145 (2021), p. 113524.

[192] E. Vanmarcke. *Random fields. Analysis and synthesis*. Cambridge, MA: MIT Press, 1983.

[193] E. Vereecken, W. Botte, G. Lombaert, and R. Caspele. "Bayesian decision analysis for the optimization of inspection and repair of spatially degrading concrete structures". In: *Engineering Structures* 220 (2020), p. 111028.

[194] E. Vereecken, W. Botte, G. Lombaert, and R. Caspeele. "VoI-Based Optimization of Structural Assessment for Spatially Degrading RC Structures". In: *Applied Sciences* 11.11 (2021).

[195] A. Verzobio, D. Bolognani, J. Quigley, and D. Zonta. "Quantifying the benefit of structural health monitoring: can the value of information be negative?" In: *Structure and Infrastructure Engineering* (2021), pp. 1–22.

[196] Z. Wang, C. Hu, W. Wang, X. Kong, and W. Zhang. "A prognostics-based spare part ordering and system replacement policy for a deteriorating system subjected to a random lead time". In: *International Journal of Production Research* 53.15 (2015), pp. 4511–4527.

[197] S. Wernitz, B. Hofmeister, C. Jonscher, T. Grießmann, and R. Rolfes. "A new open-database benchmark structure for vibration-based Structural Health Monitoring". In: *Structural Control and Health Monitoring* 29.11 (2022), e3077.

[198] K. Worden and J. M. Dulieu-Barton. "An Overview of Intelligent Fault Detection in Systems and Structures". In: *Structural Health Monitoring* 3.1 (2004), pp. 85–98.

[199] L. Wright and S. Davidson. "How to tell the difference between a model and a digital twin". In: *Advanced Modeling and Simulation in Engineering Sciences* 7(1) (2020).

[200] T. Yan, Y. Lei, N. Li, X. Si, L. Pintelon, and R. Dewil. "Online joint replacement-order optimization driven by a nonlinear ensemble remaining useful life prediction method". In: *Mechanical Systems and Signal Processing* 173 (2022), p. 109053.

[201] C. Ye, L. Butler, B. Calka, and M. I. et al. "A digital twin of bridges for structural health monitoring". In: *Structural Health Monitoring 2019: Enabling Intelligent Life-Cycle Health Management for Industry Internet of Things (IIOT) - Proceedings of the 12th International Workshop on Structural Health Monitoring*. Copenhagen, Denmark, 2019.

[202] F. Yokota and K. M. Thompson. "Value of Information Analysis in Environmental Health Risk Management Decisions: Past, Present, and Future". In: *Risk Analysis* 24.3 (2004), pp. 635–650.

[203] C. Zhang, Z. Wang, and A. Shafieezadeh. "Value of Information Analysis via Active Learning and Knowledge Sharing in Error-Controlled Adaptive Kriging". In: *IEEE Access* 8 (2020), pp. 51021–51034.

[204] W.-H. Zhang, D.-G. Lu, J. Qin, S. Thöns, and M. H. Faber. "Value of information analysis in civil and infrastructure engineering: a review". In: *Journal of Infrastructure Preservation and Resilience* 2.1 (2021), p. 16.

[205] W.-H. Zhang, J. Qin, D.-G. Lu, M. Liu, and M. H. Faber. "Quantifying the value of structural health monitoring information with measurement bias impacts in the framework of dynamic Bayesian Network". In: *Mechanical Systems and Signal Processing* 187 (2023), p. 109916.

[206] W.-H. Zhang, J. Qin, D.-G. Lu, M. Liu, and M. H. Faber. "VoI analysis of temporally continuous SHM information in the context of adaptive risk-based inspection planning". In: *Structural Safety* 99 (2022), p. 102258.

[207] W. Zhang, D. Yang, and H. Wang. "Data-Driven Methods for Predictive Maintenance of Industrial Equipment: A Survey". In: *IEEE Systems Journal* 13.3 (2019), pp. 2213–2227.

[208] Z. Zhang, X. Si, C. Hu, and Y. Lei. "Degradation data analysis and remaining useful life estimation: A review on Wiener-process-based methods". In: *European Journal of Operational Research* 271.3 (2018), pp. 775–796.

[209] E. Zio. "Prognostics and Health Management (PHM): Where are we and where do we (need to) go in theory and practice". In: *Reliability Engineering & System Safety* 218 (2022), p. 108119.

[210] E. Zio and G. Peloni. "Particle filtering prognostic estimation of the remaining useful life of nonlinear components". In: *Reliability Engineering & System Safety* 96.3 (2011), pp. 403–409.

[211] D. Zonta, B. Glisic, and S. Adriaenssens. "Value of Information: impact of monitoring on decision making". In: *Structural Control and Health Monitoring* 21(7) (2014), pp. 1043–1056.

[212] G. Zou, K. Banisoleiman, A. González, and M. H. Faber. "Probabilistic investigations into the value of information: A comparison of condition-based and time-based maintenance strategies". In: *Ocean Engineering* 188 (2019), p. 106181.

[213] G. Zou, M. H. Faber, A. González, and K. Banisoleiman. "Computing the value of information from periodic testing in holistic decision making under uncertainty". In: *Reliability Engineering & System Safety* 206 (2021), p. 107242.

Part II

Published Papers

Chapter 4

Value of information from vibration-based structural health monitoring extracted via Bayesian model updating

Original Publication

A. Kamariotis, E. Chatzi, and D. Straub. "Value of information from vibration-based structural health monitoring extracted via Bayesian model updating". In: *Mechanical Systems and Signal Processing* 166 (2022), p. 108465.

Author's contribution

Antonios Kamariotis: Conceptualization, Methodology, Software, Formal analysis, Visualization, Writing - original draft. **Eleni Chatzi**: Conceptualization, Methodology, Writing - review & editing, Funding acquisition. **Daniel Straub**: Conceptualization, Methodology, Writing - review & editing, Funding acquisition.

Abstract

Quantifying the value of the information extracted from a structural health monitoring (SHM) system is an important step towards convincing decision makers to implement these systems. We quantify this value by adaptation of the Bayesian decision analysis framework. In contrast to previous works, we model in detail the entire process of data generation to processing, model updating and reliability calculation, and investigate it on a deteriorating bridge system. The framework assumes that dynamic response data are obtained in a sequential fashion from deployed accelerometers, subsequently processed by an output-only operational modal analysis scheme for identifying the system's modal characteristics. We employ a classical Bayesian model updating methodology to sequentially learn the deterioration and estimate the structural damage evolution over time. This

leads to sequential updating of the structural reliability, which constitutes the basis for a preposterior Bayesian decision analysis. Alternative actions are defined and a heuristic-based approach is employed for the life-cycle optimization. By solving the preposterior Bayesian decision analysis, one is able to quantify the benefit of the availability of long-term SHM vibrational data. Numerical investigations show that this framework can provide quantitative measures on the optimality of an SHM system in a specific decision context.

4.1 Introduction

The advancements in the development of reliable and low-cost sensors, capable of measuring different structural response quantities (e.g. accelerations, displacements, strains, temperatures, loads, etc.) have led to vast scientific and practical developments in the field of Structural Health Monitoring (SHM) over the last four decades [10]. Techniques for processing the raw measurement data and obtaining indicators of structural "health" have been made readily available [20]. However, despite the advancements in the field, SHM still remains predominantly applied within the research community [11] and has not yet translated to extensive application on real-world structures and infrastructure systems. One main reason for this is that the effect and the potential benefit from the use of SHM systems can only be appraised on the basis of the decisions that are triggered by monitoring data. Key open-ended questions include [35]: How can information obtained from an SHM system provide optimal decision support? What is the Value of Information (VoI) from SHM systems? How can it be maximized?

Preposterior Bayesian decision analysis can be employed as a formal framework for quantifying the VoI [29], which adequately incorporates the uncertainties related to the structural performance and the associated costs, the monitoring measurements, etc. A VoI analysis provides the necessary mathematical framework for quantifying the benefit of an SHM system prior to its installation. In the civil and infrastructure engineering context, the computation of the VoI has been considered mainly related to optimal inspection planning for deteriorating structural systems [36, 21, 41]. Recent works [27, 46, 34, 39, 19, 1, 45, 14] use the VoI concept in an attempt to quantify the value of SHM on idealized structural systems within a Bayesian framework. All works to date, however, adopt rather simplified assumptions regarding the type of information offered by the SHM system. They thus largely rely on hypothetical likelihood functions or observation models, which render these demonstrations, although insightful, not easily transferable to realistic applications. A first attempt towards modeling the entire SHM process and the monitoring information has been made by the authors in [17], which is formalized and extended herein.

Installation of a continuous monitoring system on a structure allows for continuous measurement of the dynamic response of the structure (e.g., accelerations, strain). In an in-operation regime, a precise measurement of the acting loads, which are usually distributed along a system (e.g., wind, traffic), is a challenging task. Output-only operational modal analysis (OMA) [26, 3] techniques have been developed to alleviate the burden of the absence of acting load measurements. Using an OMA procedure one can identify the system eigenfrequencies and mode shapes of typical structures excited by unmeasured ambient (broadband) loads. This is beneficial, since the operation of the structure is not obstructed, as it would be in the case of forced vibration testing.

Further to data acquisition and system identification, model updating forms a popular subsequent step toward modeling the system performance on the basis of the monitoring information. This process is also referred to as the process of establishing a digital twin via model updating [43]. Bayesian model updating (BMU) using identified modal data has proved successful in identifying damage on a global or local level within a structure [40, 25, 4, 33, 44, 6]. These methods hold significant promise for application with actual full-scale structures [23, 5, 2]. The vast majority of studies are focused on investigating how the BMU framework performs in detecting, localizing and quantifying different types of artificially created damage given some fixed set of modal data. A few recent studies are concerned with BMU using vibrational data obtained in a continuous fashion from SHM systems [6, 31, 15]. However, no studies are available that systematically quantify the benefit of BMU using continuous SHM data towards driving optimal informed maintenance decision making.

This work embeds a sequential implementation of the BMU framework within a preposterior Bayesian decision analysis, to quantify the VoI from long-term vibrational data obtained from an SHM system. We employ a numerical benchmark for continuous monitoring under operational variability [38] to test and demonstrate the approach. The numerical benchmark serves as a tool to create continuous reference monitoring data from a two-span bridge system subject to different types of deterioration (scour, corrosion) at specific hotspots over its lifespan. The benchmark is used as a simulator for extracting dynamic response data, i.e. simulated measurements (accelerations), corresponding to a typical deployment of accelerometers on the structure. Acceleration measurements are provided as input to an output-only OMA algorithm, which identifies the system's modal characteristics. We implement Bayesian model and structural reliability updating methods in a sequential setting for incorporating the continuous OMA-identified modal data within a decision making framework. This proposed procedure follows the roadmap to quantifying the benefit of SHM presented in [35]. We employ a simple heuristic-based approach for the solution of the life-cycle optimization problem in the preposterior Bayesian decision analysis. The resulting optimal expected total life-cycle costs are computed in the preposterior case, and compared against the optimal expected total life-cycle costs obtained in the case of only prior knowledge, thus enabling the quantification of the VoI of SHM.

4.2 VoI from SHM analysis

The monitoring of a structural system through deployment of an appropriately designed SHM system is a viable means to support decision making related to infrastructure maintenance actions. But is gathering this information worth it? Preposterior Bayesian decision analysis provides the necessary formal mathematical framework for quantifying the VoI of an SHM system. A concise representation of a such an analysis with the use of an influence diagram (ID) has been introduced in [35]. An adaptation of this ID for the purposes of the VoI analysis that we propose and apply on a simulated SHM benchmark study in this paper is offered in Fig. 4.1. In the next paragraph, we lay out a brief introduction of this ID. For more in-depth explanations, the reader is referred to [35].

Influence diagrams build upon Bayesian networks (BN), which offer a concise graphical tool to model Bayesian probabilistic inference problems, and extend these through the addition of decision and utility nodes to model decision making under uncertainty [16]. In the ID of Fig. 4.1, green oval nodes model uncertain parameters and models/processes related to the structural system, the

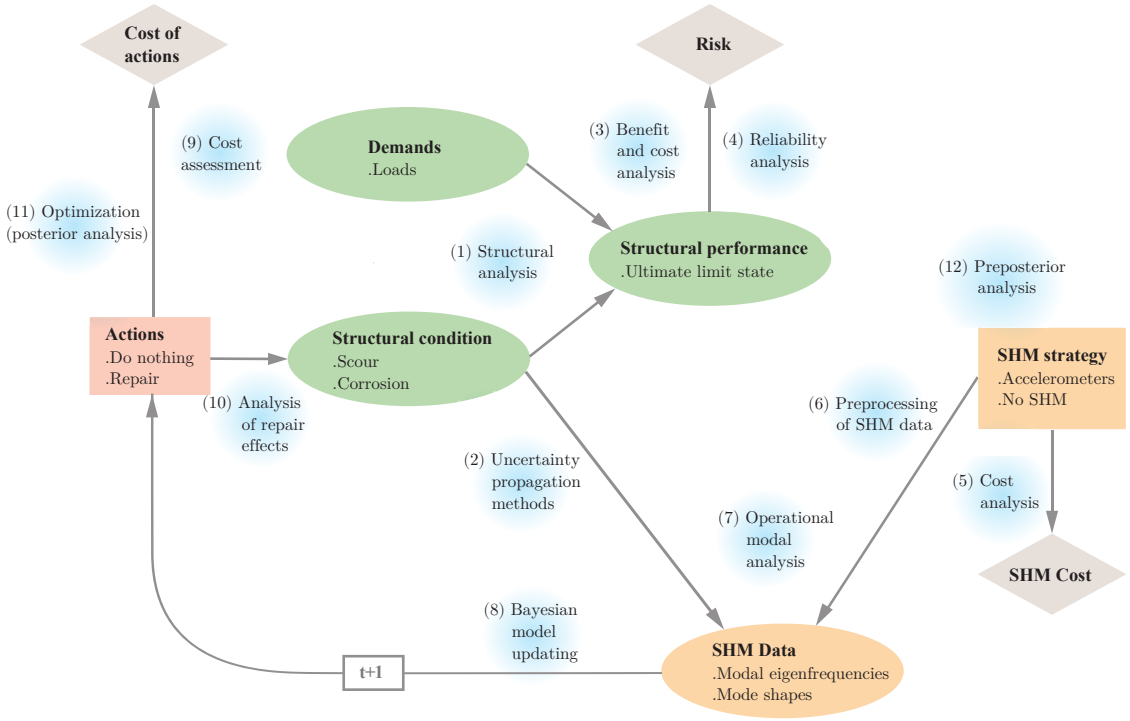

Figure 4.1: Influence diagram of the SHM process for a preposterior Bayesian decision analysis to quantify the VoI.

orange square node models the decision on the SHM system, while the orange oval node models the monitoring data that is extracted via use of a specific SHM system. This data can be used to learn the structural condition via Bayesian updating to then inform the decision on maintenance/repair actions (red square node). Finally, the grey diamond-shaped nodes represent the different costs that enter into the process. The decision to deploy an SHM system is associated with a corresponding SHM cost, the decision to perform a repair action induces a repair cost, and the risk (the expected cost of failures) can be quantified via the outcome of a structural reliability analysis. Causality is important for the direction of the links among the nodes of this ID. For example, the 'Structural condition' node points to the 'Structural performance' node, as one would expect, but also points to the 'SHM Data' node, which might not appear intuitive. However, the SHM measurement that one obtains causally depends on the actual condition of the monitored structure. Note, however, that the flow of information can go against the direction of the link; this is quantified via Bayesian analysis. The link to the 'Actions' node with the box [t+1] describes the flow of information and shows that this ID represents a decision process over the lifetime of the structure. Not explicitly shown here are the beginning and the end of the ID. The ID begins with the year when the installation of the SHM system is considered; it ends with the structural performance in the last year of the anticipated service life. The blue text bubbles introduce the different computational methods that are incorporated in the different parts of the process. The large number of these bubbles highlights the modeling and computational challenges associated with a full VoI analysis.

In this paper, for the first time in existing literature, we avoid overly simplifying assumptions in some parts of the modeling of the preposterior Bayesian decision analysis for quantifying the VoI from SHM, but we still model other parts of the process in a simplistic way. The main contribution lies in

the modeling of the SHM data. As can be seen in Fig. 4.1, we employ continuous SHM information over the lifetime of a deteriorating structural system in the form of acceleration time series, which are subsequently processed by an OMA procedure that identifies the modal eigenfrequencies and mode shapes. These SHM modal data are then used within a BMU procedure to sequentially identify the structural condition (see Section 4.3). The way in which the SHM data sets are sampled within a preposterior Bayesian decision analysis with the use of the benchmark structural model is described in detail in Section 4.6.3. We treat the modeling of the structural performance node of the ID, as well as the incorporation of the monitoring information within a reliability updating, in a realistic and computationally efficient approach (see Section 4.4). To provide a computationally viable solution to the VoI analysis, we adopt a rather simplified modeling of the action decision node, and we perform the life cycle optimization with the use of heuristics (see Section 4.5).

The solution of the preposterior Bayesian decision analysis leads to monitoring-informed optimization of the repair action, which in turn leads to the computation of the optimal expected total life-cycle cost in the case of having an SHM system installed. If the adopted SHM strategy is to implement no SHM system, then life-cycle optimization is conducted on the basis of prior information only. By comparing the optimal expected total life-cycle costs in the prior and preposterior cases, the VoI is implicitly quantified as the difference between the two.

4.3 Bayesian model updating

In this section, the Bayesian model updating framework with the use of OMA-identified modal data is presented. The Bayesian formulation presented here corresponds to the state-of-the-art formulation [33, 44, 5].

4.3.1 Bayesian formulation

We consider deterioration that leads to local stiffness reductions. The random variables (RVs) describing the uncertainty within the employed deterioration models are $\boldsymbol{\theta} \in \mathbb{R}^d$, with d being the total number of RVs. The goal of the Bayesian inverse problem is to infer the deterioration model parameters $\boldsymbol{\theta}$ given noisy OMA-identified modal data. These are the modal eigenvalues $\widetilde{\lambda}_m = (2\pi\widetilde{f}_m)^2$, where $\widetilde{f}_m$ are the modal eigenfrequencies, and/or mode shape vector components $\widetilde{\boldsymbol{\Phi}}_m \in \mathbb{R}^{N_s}$ at the N_s degrees of freedom (DOF) that correspond to the sensor locations, where $m = 1, ..., N_m$ is the number of identified modes. Modal eigenvalues can be identified quite accurately, but an accurate identification of the mode shape displacements requires the deployment of a relatively large number of sensors. Conditional on a fairly good representation of the mode shape vector, one can then derive other modal characteristics, such as the mode shape curvatures $\widetilde{\boldsymbol{K}}_m \in \mathbb{R}^{N_s}$, which are shown to be more sensitive to local damage [24]. If only the eigenvalue data is available, damage can be detected on a global level, while damage localization requires the existence of spatial information, in the form of mode shape (or mode shape curvature) data.

Consider a linear finite element (FE) model, which is parameterized through the parameters $\boldsymbol{\theta}$ of the deterioration models. The goal of the Bayesian probabilistic framework is to estimate the parameters $\boldsymbol{\theta}$, and their uncertainty, such that the FE model predicted modal eigenvalues $\lambda_m(\boldsymbol{\theta})$

and mode shapes $\boldsymbol{\Phi}_m(\boldsymbol{\theta})$, or mode shape curvatures $\boldsymbol{K}_m(\boldsymbol{\theta})$, best match the corresponding SHM modal data.

Using Bayes' theorem, the posterior probability density function π_{pos} of the deterioration model parameters $\boldsymbol{\theta}$ given an identified modal data set $[\widetilde{\boldsymbol{\lambda}}, \widetilde{\boldsymbol{\Phi}}]$ is computed via Eq. (4.1); it is proportional to the likelihood function $L(\boldsymbol{\theta}; \widetilde{\boldsymbol{\lambda}}, \widetilde{\boldsymbol{\Phi}})$ multiplied with the prior PDF of the model parameters $\pi_{\text{pr}}(\boldsymbol{\theta})$. The proportionality constant is the so-called model evidence c_{E} and requires the solution of a d-dimensional integral, shown in Eq. (4.2).

$$\pi_{\text{pos}}(\boldsymbol{\theta} \mid \widetilde{\boldsymbol{\lambda}}, \widetilde{\boldsymbol{\Phi}}) \propto L(\boldsymbol{\theta}; \widetilde{\boldsymbol{\lambda}}, \widetilde{\boldsymbol{\Phi}}) \pi_{\text{pr}}(\boldsymbol{\theta}) \tag{4.1}$$

$$c_{\text{E}} = \int_{\Omega_{\boldsymbol{\theta}}} L(\boldsymbol{\theta}; \widetilde{\boldsymbol{\lambda}}, \widetilde{\boldsymbol{\Phi}}) \pi_{\text{pr}}(\boldsymbol{\theta}) d\boldsymbol{\theta} \tag{4.2}$$

The model updating procedure contains significant uncertainties, which should be taken into account within the Bayesian framework. According to [33], these are classified into i) measurement uncertainty, including random measurement noise and variance or bias errors induced in the OMA procedure [30] (see Fig. 4.4), and ii) model uncertainty. In [6] the existence of inherent variability emerging from changing environmental conditions is highlighted. The combination of all the above uncertainties is called the total prediction error in literature [33, 6]. In order to construct the likelihood function, the eigenvalue and mode shape (similarly for mode shape curvature) prediction errors for a specific mode m are defined as in Eqs. (4.3) and (4.4).

$$\eta_{\lambda_m} = \widetilde{\lambda}_m - \lambda_m(\boldsymbol{\theta}) \in \mathbb{R} \tag{4.3}$$

$$\boldsymbol{\eta}_{\boldsymbol{\Phi}_m} = \gamma_m \widetilde{\boldsymbol{\Phi}}_m - \boldsymbol{\Phi}_m(\boldsymbol{\theta}) \in \mathbb{R}^{N_s}, \tag{4.4}$$

where γ_m is a normalization constant, which is computed as in Eq. (4.5). $\boldsymbol{\Gamma}$ is a binary matrix for selecting the FE degrees of freedom that correspond to the sensor locations.

$$\gamma_m = \frac{\widetilde{\boldsymbol{\Phi}}_m^{\mathsf{T}} \boldsymbol{\Gamma} \boldsymbol{\Phi}_m}{\left\| \widetilde{\boldsymbol{\Phi}}_m \right\|^2} \tag{4.5}$$

The probabilistic model of the eigenvalue prediction error is a zero-mean Gaussian random variable with standard deviation assumed to be proportional to the measured eigenvalues:

$$\eta_{\lambda_m} \sim \mathcal{N}\left(0, c_{\lambda m}^2 \widetilde{\lambda}_m^2\right) \tag{4.6}$$

All the N_s mode shape prediction error components in the vector $\boldsymbol{\eta}_{\boldsymbol{\Phi}_m}$ are assigned a zero-mean Gaussian random variable with the same standard deviation, assumed proportional to the L_2-norm of the measured mode shape vector. A multivariate Gaussian distribution is used to model this error. Eq. (4.7) implies that the errors for the different degrees of freedom are uncorrelated, which is a common assumption, but may be unrealistic [32].

$$\begin{aligned} \boldsymbol{\eta}_{\boldsymbol{\Phi}_m} &\sim \mathcal{N}(\mathbf{0}, \boldsymbol{\Sigma}_{\boldsymbol{\Phi}_m}) \\ \boldsymbol{\Sigma}_{\boldsymbol{\Phi}_m} &= \operatorname{diag}\left(c_{\Phi m}^2 \left\| \gamma_m \widetilde{\boldsymbol{\Phi}}_m \right\|^2 \right) \end{aligned} \tag{4.7}$$

The factors $c_{\lambda m}$ and $c_{\Phi m}$ can be regarded as assigned coefficients of variation, and their chosen values reflect the total prediction error. In practical applications, usually very little (if anything) is

known about the structure or the magnitude of the total prediction error. At the same time, even if the assumption of an uncorrelated zero mean Gaussian model for the errors has computational advantages and can be justified by the maximum entropy principle, the choice of the magnitude of the factors $c_{\lambda m}$ and $c_{\Phi m}$ clearly affects the results of the Bayesian updating procedure. It appears that most published works do not properly justify this particular choice of the magnitude of the error. Alternatively, these factors can be added as hyper-parameters with an assumed prior distribution and, thus, be included in the Bayesian parameter estimation [6].

Assuming statistical independence among the N_m identified modes, the likelihood function for a given modal data set can be written as in Eq. (4.8). $N(.)$ denotes the value of the normal probability density function at a specified location.

$$L\left(\boldsymbol{\theta}; \widetilde{\boldsymbol{\lambda}}, \widetilde{\boldsymbol{\Phi}}\right) = \prod_{m=1}^{N_m} N\left(\eta_{\lambda_m}; 0, c_{\lambda m}^2 \widetilde{\lambda}_m^2\right) N(\boldsymbol{\eta}_{\boldsymbol{\Phi}_m}; \mathbf{0}, \boldsymbol{\Sigma}_{\boldsymbol{\Phi}_m}) \tag{4.8}$$

The benefit of SHM is that the sensors can provide data in a continuous fashion, therefore resulting in an abundance of measurements received almost continuously. Assuming independence among N_t modal data sets obtained at different time instances, the likelihood can be expressed as:

$$L\left(\boldsymbol{\theta}; \widetilde{\boldsymbol{\lambda}}_1 ... \widetilde{\boldsymbol{\lambda}}_{N_t}, \widetilde{\boldsymbol{\Phi}}_1 ... \widetilde{\boldsymbol{\Phi}}_{N_t}\right) = \prod_{t=1}^{N_t} \prod_{m=1}^{N_m} N\left(\widetilde{\lambda}_{t_m} - \lambda_{t_m}(\boldsymbol{\theta}); 0, c_{\lambda m}^2 \widetilde{\lambda}_{t_m}^2\right) N\left(\gamma_{t_m} \widetilde{\boldsymbol{\Phi}}_{t_m} - \boldsymbol{\Phi}_{t_m}(\boldsymbol{\theta}); \mathbf{0}, \boldsymbol{\Sigma}_{\boldsymbol{\Phi}_{t_m}}\right) \tag{4.9}$$

where the index t_m indicates the modal data of mode m identified at time instance t. The formulation in Eq. (4.9) allows for sequential implementation of the Bayesian updating process. At any time step t_i when new data becomes available, the distribution of the parameters given all the data up to time t_i, $\pi_{\text{pos}}(\boldsymbol{\theta} \mid \widetilde{\boldsymbol{\lambda}}_{1:i}, \widetilde{\boldsymbol{\Phi}}_{1:i})$ or the one step ahead predictive distributions for time t_{i+1} can be obtained. The inclusion of data in a continuous fashion can increase the level of accuracy of the Bayesian model updating procedure. However, one should be aware that the assumption of independence in Eq. (4.9) typically does not hold. This could be addressed by a hierarchical modeling of $\boldsymbol{\theta}$ [6].

4.3.2 Solution methods

The solution of the Bayesian updating problem in the general case involves the solution of the d-dimensional integral for the computation of the model evidence. Analytic solutions to this integral are available only in special cases, otherwise numerical integration or sampling methods are deployed. The two solution methods that we employ within this work are the Laplace asymptotic approximation and an adaptive Markov Chain Monte Carlo (MCMC) algorithm.

4.3.2.1 Laplace approximation

A detailed presentation of this method can be found in [4, 25]. The main idea is that for globally identifiable cases [4], and for a sufficiently large number of experimental data, the posterior distribution can be approximated by a multivariate Gaussian distribution $N(\boldsymbol{\mu}, \boldsymbol{\Sigma})$. The mean vector $\boldsymbol{\mu}$ is set equal to the most probable value, or maximum aposteriori (MAP) estimate, of the parameter

vector, which is obtained by minimizing the negative logposterior:

$$\boldsymbol{\mu} = \boldsymbol{\theta}_{\text{MAP}} = \arg\min_{\boldsymbol{\theta}}(-\ln \pi_{\text{pos}}(\boldsymbol{\theta} \mid \widetilde{\boldsymbol{\lambda}}, \widetilde{\boldsymbol{\Phi}})) = \arg\min_{\boldsymbol{\theta}}(-\ln L(\boldsymbol{\theta}; \widetilde{\boldsymbol{\lambda}}, \widetilde{\boldsymbol{\Phi}}) - \ln \pi_{\text{pr}}(\boldsymbol{\theta})) \tag{4.10}$$

and the covariance matrix $\boldsymbol{\Sigma}$ is equal to the inverse of the Hessian of the log-posterior evaluated at the MAP estimate. When new data becomes available, the new posterior distribution has to be approximated. The MAP estimate of the previous time step is used as the initial point for the optimization at the current time step, to facilitate a faster convergence of the optimization algorithm.

4.3.2.2 MCMC sampling

For more accurate estimates of the posterior distributions than the one obtained by using the Laplace approximation, one can resort to MCMC sampling methods. Among the multiple available MCMC algorithms, here we employ the adaptive MCMC algorithm from [13], in which the adaptation is performed on the covariance matrix of the proposal PDF. Whenever new data becomes available, the MCMC algorithm has to be rerun to obtain the new posterior distribution. The posterior mean of the parameters estimated via MCMC at the previous time step is used as seed of the new Markov chain, which allows the chain to converge faster.

4.4 Structural reliability of a deteriorating structural system and its updating

Estimation of the structural reliability, and the use of vibrational data to update this, is instrumental for the framework that we are presenting here. A detailed review of the ideas presented in this section can be found in [22, 37].

4.4.1 Structural reliability analysis of a deteriorating structural system

In its simplest form, a failure event at time t can be described in terms of a structural system capacity $R(t)$ and a demand $S(t)$. Both R and S are random variables. With $D(\boldsymbol{\theta}, t)$ we define a parametric stochastic deterioration model. Herein we assume that the structural capacity $R(t)$ can be separated from the demand $S(t)$, and that the capacity is deterministic and known for a given deterioration $D(\boldsymbol{\theta}, t)$, hence we write $R\left(D(\boldsymbol{\theta}, t)\right)$. More details on how this deterministic curve can be obtained for specific cases are given in Section 4.6, which contains the numerical examples. Therefore, at a time t the structural capacity includes the effect of the deterioration process. The uncertain demand acting on the structure is here modeled by the distribution of the maximum load in a one-year time interval. The cumulative distribution function (CDF) of this distribution is denoted $F_{s_{max}}$. Such a modeling choice simplifies the estimation of the structural reliability, as will be made clear in what follows, which is vital within a computationally expensive VoI analysis framework.

We discretize time in intervals $j = 1, .., T$, where the j-th interval represents $t \in (t_{j-1}, t_j]$. For the type of problems that we are considering, the time-variant reliability problem can be replaced by

a series of time-invariant reliability problems [37]. F_j^* is defined as the event of failure in interval $(t_{j-1}, t_j]$. For a given value of the deterioration model parameters $\boldsymbol{\theta}$ and time t_j, the capacity $R\left(D(\boldsymbol{\theta}, t_j)\right)$ is fixed, and the conditional interval probability of failure is defined as:

$$\Pr(F_j^* \mid \boldsymbol{\theta}, t_j) = 1 - F_{s_{max}}\left(R\left(D(\boldsymbol{\theta}, t_j)\right)\right) \tag{4.11}$$

We define $\Pr[F(t_i)] = \Pr(F_1^* \cup F_2^* \cup ...F_i^*)$ as the accumulated probability of failure up to time t_i. One can compute $Pr[F(t_i)]$ through the conditional interval probabilities $Pr(F_j^*|R(\boldsymbol{\theta}, t_j))$ as:

$$\Pr[F(t_i) \mid \boldsymbol{\theta}] = 1 - \prod_{j=1}^{i}[1 - \Pr(F_j^* \mid \boldsymbol{\theta}, t_j)] \tag{4.12}$$

Following the total probability theorem, the unconditional accumulated probability of failure is:

$$\Pr[F(t_i)] = \int_{\Omega_{\boldsymbol{\theta}}} \Pr[F(t_i) \mid \boldsymbol{\theta}]\pi_{\text{pr}}(\boldsymbol{\theta})d\boldsymbol{\theta} \tag{4.13}$$

The solution to the above integral is approximated using Monte Carlo simulation (MCS). We draw samples from the prior distribution $\pi_{\text{pr}}(\boldsymbol{\theta})$ of the uncertain deterioration model parameters and the integral in Eq. (4.13) is approximated by:

$$\Pr[F(t_i)] \approx \frac{1}{n_{\text{MCS}}} \sum_{k=1}^{n_{\text{MCS}}} \Pr[F(t_i) \mid \boldsymbol{\theta}^{(k)}] \tag{4.14}$$

Having computed the probabilities $Pr[F(t_i)]$, one can compute the hazard function $h(t_i)$ for the different time intervals t_i, which expresses the failure rate of the structure conditional on survival up to time t_{i-1}:

$$h(t_i) = \frac{\Pr[F(t_i)] - \Pr[F(t_{i-1})]}{1 - \Pr[F(t_{i-1})]} \tag{4.15}$$

4.4.2 Structural reliability updating using SHM modal data

The goal of SHM is to identify structural damage. Monitoring data can be employed in order to identify the parameters $\boldsymbol{\theta}$ of the deterioration models and obtain their posterior distribution, as shown in Section 4.3. Consequently this leads to the updating of the accumulated probability of failure at time t_i, which can now be conditioned on data $\boldsymbol{Z}_{1:i-1}$ obtained up to time t_{i-1}.

$$\Pr[F(t_i) \mid \boldsymbol{Z}_{1:i-1}] = \Pr(F_1^* \cup F_2^* \cup ...F_i^* \mid \boldsymbol{Z}_{1:i-1}) \tag{4.16}$$

The accumulated probability of failure up to time t_i conditional on modal data obtained up to time t_{i-1} is:

$$\Pr[F(t_i) \mid \boldsymbol{Z}_{1:i-1}] = \int_{\Omega_{\boldsymbol{\theta}}} \Pr[F(t_i) \mid \boldsymbol{\theta}]\pi_{\text{pos}}(\boldsymbol{\theta}|\widetilde{\boldsymbol{\lambda}}_{1:i-1}, \widetilde{\boldsymbol{\Phi}}_{1:i-1})d\boldsymbol{\theta} \tag{4.17}$$

In Eq. (4.17), one needs to integrate over the posterior distribution of the parameters $\boldsymbol{\theta}$. As described in Section 4.3.2, two different methods for obtaining samples from this posterior distribution at each time step are implemented. In the case that an adaptive MCMC algorithm is used, at every step of the sequential updating we obtain the desired posterior distribution of the parameters in the form of correlated MCMC samples. In the case that the posterior distributions are approximated by

multivariate Gaussian distributions using the Laplace approximation, independent posterior samples can be drawn from this approximate posterior density. Using n_{pos} samples $\boldsymbol{\theta}^{(k)}$ from either MCMC or the asymptotic approximation, the integral in Eq. (4.17) can be approximated:

$$\Pr[F(t_i) \mid \boldsymbol{Z}_{1:i-1}] \approx \frac{1}{n_{\text{pos}}} \sum_{k=1}^{n_{\text{pos}}} \Pr[F(t_i) \mid \boldsymbol{\theta}^{(k)}] \tag{4.18}$$

The hazard function conditional on the monitoring data can then be obtained as:

$$h(t_i \mid \boldsymbol{Z}_{1:i-1}) = \frac{\Pr[F(t_i) \mid \boldsymbol{Z}_{1:i-1}] - \Pr[F(t_{i-1}) \mid \boldsymbol{Z}_{1:i-1}]}{1 - \Pr[F(t_{i-1}) \mid \boldsymbol{Z}_{1:i-1}]} \tag{4.19}$$

4.5 Life-cycle cost with SHM

4.5.1 Life-cycle optimization based on heuristics

The VoI is the difference in life-cycle cost between the cases with and without SHM system. To calculate the life-cycle cost we optimize the maintenance strategy. A strategy S is a set of policies that determine which action to take at any time step t_i, conditional on all the information at hand up to that time [16, 8]. One may define policies based on simple decision rules, also called heuristics, which may emerge from basic engineering understanding.

A detailed presentation of the use of heuristics in optimal inspection and maintenance planning can be found in [21, 8]. With the use of heuristics, the space of solutions to the decision problem is drastically reduced, but the problem is solved only approximately. Here, we utilize a simple heuristic for maintenance decisions. The simple heuristic chosen in this work is the following: Perform a repair action whenever the estimate of the hazard function (the conditional failure rate) is larger than a predefined threshold h_{thres}. The use of the hazard function as a decision criteria for condition assessment and maintenance planning is a popular choice in literature [9]. The parameter $w = h_{\text{thres}}$ describing the heuristic is a parameter of the strategy S. For simplicity, we assume herein that performing a repair action results in replacing the damaged components and bringing them back to the initial state, and that no failure will occur once a repair action has been performed. In this way, after a repair action, the computation of the total life cycle cost stops. This modeling choice is simplifying, but does allow for a viable computation of the VoI herein.

The total life-cycle cost C_{tot} is here taken as the total cost of maintenance and the risk of failure costs over the lifetime of the structure. The initial cost is not included in C_{tot}, because it is the same with or without SHM, therefore it cancels out when calculating the VoI.

With the use of heuristics, solving the decision problem boils down to finding the optimal value of the heuristic parameter w which minimizes the expected total cost, i.e., to the solution of the optimization problem:

$$w^* = \arg\min_{w} \mathbb{E}[C_{\text{tot}} \mid w] \tag{4.20}$$

4.5.2 Computation of the expected total life-cycle cost in the prior case

In the prior case, where only the prior deterioration model is available, the expectation in Eq. (4.20) is with respect to the system state, i.e. the deterioration model parameters $\boldsymbol{\theta}$. The total cost of maintenance and risk is the sum of the repair costs and the risk of failure costs over the lifetime of the bridge, $C_{\text{tot}}(w, \boldsymbol{\theta}) = C_{\text{R}}(w) + C_{\text{F}}(w, \boldsymbol{\theta})$, therefore the expected total life-cycle cost for a given heuristic parameter w is:

$$\mathbb{E}_{\boldsymbol{\theta}}[C_{\text{tot}} \mid w] = \mathbb{E}_{\boldsymbol{\theta}}[C_{\text{R}}(w) \mid w] + \mathbb{E}_{\boldsymbol{\theta}}[C_{\text{F}}(w, \boldsymbol{\theta}) \mid w] \tag{4.21}$$

The first part of the right hand side of Eq. (4.21) can be computed in the following way. We draw samples $\boldsymbol{\theta}^{(k)}, k = 1, .., n_{\text{MCS}}$, from the prior distribution $\pi_{\text{pr}}(\boldsymbol{\theta})$ and use them to compute the accumulated probability of failure via Eq. (4.14), and subsequently compute the hazard function with Eq. (4.15). When the hazard function exceeds the threshold, i.e. when $h(t_i) \geq w$, then we define $t_{\text{repair}}(w) = t_{i-1}$ as the time that the repair takes place. The time of repair is thus a function of our chosen heuristic. Hence the expected total cost of repair over the lifetime is given as:

$$\mathbb{E}_{\boldsymbol{\theta}}[C_{\text{R}}(w) \mid w] = \hat{c}_R \gamma(t_{\text{repair}}(w)) \tag{4.22}$$

where $\hat{c}_{\text{R}}$ is the fixed cost of the repair, and $\gamma(t) = \frac{1}{(1+r)^t}$ is the discounting function, r being the annually compounded discount rate.

The risk of failure over the lifetime can be computed via MCS, using the samples $\boldsymbol{\theta}^{(k)}$, $k = 1, .., n_{\text{MCS}}$, that were drawn from the prior distribution $\pi_{\text{pr}}(\boldsymbol{\theta})$, with the following formula:

$$\mathrm{E}_{\boldsymbol{\theta}}[C_{\text{F}}(w, \boldsymbol{\theta}) \mid w] \approx \frac{1}{n_{\text{MCS}}} \sum_{k=1}^{n_{\text{MCS}}} C_{\text{F}}(w, \boldsymbol{\theta}^{(k)}) \tag{4.23}$$

where:

$$C_{\text{F}}(w, \boldsymbol{\theta}^{(k)}) = \sum_{i=1}^{t_{\text{repair}}(w)} \hat{c}_{\text{F}} \gamma(t_i) \{\Pr[F(t_i) \mid \boldsymbol{\theta}^{(k)}] - \Pr[F(t_{i-1}) \mid \boldsymbol{\theta}^{(k)}]\} \tag{4.24}$$

and $\hat{c}_{\text{F}}$ is the fixed cost of the failure event.

Following the solution of the optimization problem in Eq. (4.20), the expected total life-cycle cost associated with the optimal decision in the prior case without any monitoring data is $\mathbb{E}_{\boldsymbol{\theta}}[C_{\text{tot}} \mid w_0^*]$.

4.5.3 Computation of the expected total life-cycle cost in the preposterior case

The goal of a preposterior analysis is to act as a decision tool on whether collecting SHM data is beneficial, and to quantify and optimize the VoI of an SHM system, prior to its installation. Therefore this type of analysis is performed before any actual SHM data are obtained. Instead, the SHM monitoring data histories must be sampled over the lifetime from the prior distribution of the uncertain deterioration model parameters $\boldsymbol{\theta}$, as will be explained shortly. A sampled monitoring data history vector $\boldsymbol{Z} = [\boldsymbol{Z}_1, ..., \boldsymbol{Z}_{n_T}]$ contains the OMA identified modal data at fixed time instances over the structure lifetime.

In a preposterior analysis, the expectation in Eq. (4.20) is operating over both the system state $\boldsymbol{\theta}$ and on the monitoring outcomes $\boldsymbol{Z}$.

$$\mathrm{E}_{\boldsymbol{\theta},\boldsymbol{Z}}[C_{\mathrm{tot}} \mid w] = \int_{\Omega_{\boldsymbol{\theta}}} \int_{\Omega_{\boldsymbol{Z}}} C_{\mathrm{tot}}(w, \boldsymbol{\theta}, \boldsymbol{z}) f_{\boldsymbol{\Theta},\boldsymbol{Z}}(\boldsymbol{\theta}, \boldsymbol{z}) d\boldsymbol{z} d\boldsymbol{\theta} \tag{4.25}$$

The total cost of maintenance and risk is again the sum of the repair cost and the risk of failure cost over the lifetime of the structure, which now both depend also on the monitoring outcomes $\boldsymbol{Z}$, $C_{\mathrm{tot}}(w, \boldsymbol{\theta}, \boldsymbol{Z}) = C_{\mathrm{R}}(w, \boldsymbol{Z}) + C_{\mathrm{F}}(w, \boldsymbol{\theta}, \boldsymbol{Z})$.

The integral in Eq. (4.25) is computed with crude MCS. We draw samples from the uncertain deterioration model parameters $\boldsymbol{\theta}$, which correspond to a deterioration history over the lifetime, as given by the deterioration model equation $D(\boldsymbol{\theta}, t)$. For each of these histories, we generate noisy acceleration measurements every year, feed them into the stochastic subspace identification (SSI) algorithm [26], and obtain one vector of monitoring modal data $\boldsymbol{Z}$ (one identified modal data set per year). In this way we are jointly sampling the system state space and monitoring data space, and Eq. (4.25) is approximated as:

$$\mathbb{E}_{\boldsymbol{\theta},\boldsymbol{Z}}[C_{\mathrm{tot}} \mid w] = \frac{1}{n_{\mathrm{MCS}}} \sum_{k=1}^{n_{\mathrm{MCS}}} [C_{\mathrm{R}}(w, \boldsymbol{z}^{(k)}) + C_{\mathrm{F}}(w, \boldsymbol{\theta}^{(k)}, \boldsymbol{z}^{(k)})] \tag{4.26}$$

For each of the sampled system states and corresponding monitoring data, we compute the updated hazard rate as given by Eq. (4.19), and when $h(t_i \mid \boldsymbol{z}_{1:i-1}^{(k)}) \geq w$, then $t_{\mathrm{repair}}(w, \boldsymbol{z}^{(k)}) = t_{i-1}$.

The cost of repair is:

$$C_{\mathrm{R}}(w, \boldsymbol{z}^{(k)}) = \hat{c}_{\mathrm{R}} \gamma(t_{\mathrm{repair}}(w, \boldsymbol{z}^{(k)})) \tag{4.27}$$

The risk of failure is:

$$C_{\mathrm{F}}(w, \boldsymbol{\theta}^{(k)}, \boldsymbol{z}^{(k)}) = \sum_{i=1}^{t_{\mathrm{repair}}(w, \boldsymbol{z}^{(k)})} \hat{c}_{\mathrm{F}} \gamma(t_i) \{\Pr[F(t_i) \mid \boldsymbol{\theta}^{(k)}] - \Pr[F(t_{i-1}) \mid \boldsymbol{\theta}^{(k)}]\} \tag{4.28}$$

Comparing Eqs. (4.24) and (4.28) it is evident that adoption of the same samples of $\boldsymbol{\theta}$ in both prior and preposterior analysis, leads to an identical estimate of the risk of failure for the two analyses up to the time of the repair. The only difference between prior and preposterior case is the resulting $t_{\mathrm{repair}}(w, \boldsymbol{z}^{(k)})$.

Solving Eq. (4.20), we obtain the optimal expected total life-cycle cost given the monitoring data, $\mathbb{E}_{\boldsymbol{\theta},\boldsymbol{Z}}[C_{\mathrm{tot}} \mid w^*_{\mathrm{mon}}]$.

4.5.4 Summary of the proposed methodology to calculate the VoI

The proposed procedure for the VoI analysis consists of the following steps:

1. Choose a prior stochastic deterioration model describing the structural condition over the lifetime of the structure. Define a decision analysis time discretization, maintenance/repair actions, costs of actions and cost of failure event. Choose a heuristic parameter w (threshold on hazard rate) for a heuristic-based solution of the decision problem.

2. Draw Monte Carlo samples $\boldsymbol{\theta}$ of the stochastic deterioration model parameters.

3. Perform a prior decision analysis:

   - Use the prior $\boldsymbol{\theta}$ samples to estimate the lifetime accumulated probability of failure $\Pr[F(t_i)]$ and the corresponding hazard rate $h(t_i)$.
   - Solve the LCC optimization problem to obtain the optimal value of the heuristic parameter w_0^* and the corresponding optimal t_{repair}. Obtain the optimal expected LCC in the prior case: $\mathbb{E}_{\boldsymbol{\theta}}[C_{\text{tot}}(\boldsymbol{\theta}, w) \mid w_0^*]$.

4. Perform a preposterior decision analysis:

   - For each individual prior sample $\boldsymbol{\theta}$ realization and given value of the heuristic parameter w do the following:
     (a) Sample the corresponding noisy acceleration time series data for every year over the lifetime of the structure. Feed the accelerations into the SSI algorithm to identify the structure's modal data vectors $\boldsymbol{Z}$.
     (b) Perform a posterior Bayesian analysis: BMU to sequentially learn the posterior distributions of $\boldsymbol{\theta}$ and subsequently obtain an updated estimate of the accumulated probability of failure $\Pr[F(t_i) \mid \boldsymbol{Z}_{1:i-1}]$ and the hazard rate $h(t_i \mid \boldsymbol{Z}_{1:i-1})$.
     (c) Find the time to perform the repair action for this specific deterioration and monitoring data realization, conditional on a value of the heuristic parameter w.
   - Solve the LCC optimization problem to obtain the optimal value of the heuristic parameter w_{mon}^* which minimizes the expected LCC in the preposterior case $\mathbb{E}_{\boldsymbol{\theta},\boldsymbol{Z}}[C_{\text{tot}}(\boldsymbol{\theta}, \boldsymbol{Z}, w) \mid w_{\text{mon}}^*]$.

5. Compute the VoI.

$$VoI = \mathbb{E}_{\boldsymbol{\theta}}[C_{\text{tot}}(\boldsymbol{\theta}, w) \mid w_0^*] - \mathbb{E}_{\boldsymbol{\theta},\boldsymbol{Z}}[C_{\text{tot}}(\boldsymbol{\theta}, \boldsymbol{Z}, w) \mid w_{\text{mon}}^*] \tag{4.29}$$

4.5.5 Value of Partial Perfect Information

The case of partial perfect information is related to a hypothetical situation, in which the SHM system provides perfect information on the condition of the structure. This means that there is no uncertainty on the parameters $\boldsymbol{\theta}$ of the deterioration model, and the optimal decision is found conditional on this perfect knowledge of $\boldsymbol{\theta}$. Because the SHM system is not able to provide any information about the load acting on the structure, which here is modeled by an uncertain Gumbel random variable, therefore one uses the term "partial".

Estimation of the value of partial perfect information is given by:

$$VPPI = \min_{w} \mathbb{E}_{\boldsymbol{\theta}}[C_{\text{tot}}(\boldsymbol{\theta}, w)] - \mathbb{E}_{\boldsymbol{\theta}}\{\min_{w}[C_{\text{tot}}(\boldsymbol{\theta}, w) \mid \boldsymbol{\theta}]\} \tag{4.30}$$

$\min_{w} \mathbb{E}_{\boldsymbol{\theta}}[C_{\text{tot}}(\boldsymbol{\theta}, w)]$ is the optimal expected total life-cycle cost in the prior case, exactly as presented in Section 4.5.2. To evaluate $\mathbb{E}_{\boldsymbol{\theta}}\{\min_{w}[C_{\text{tot}}(\boldsymbol{\theta}, w) \mid \boldsymbol{\theta}]\}$, first the optimal heuristic is found for a given value of $\boldsymbol{\theta}$, then the expected value of the total life-cycle costs associated with these optimal decisions

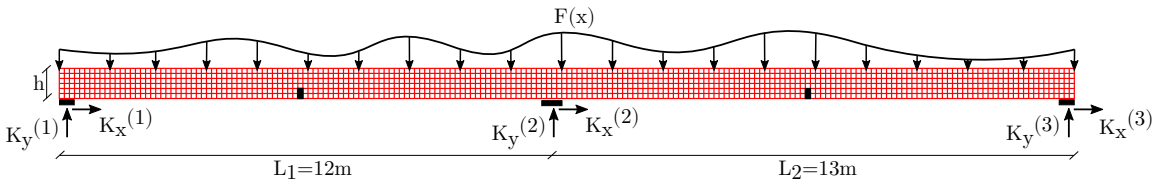

Figure 4.2: Benchmark model

is computed. This quantity corresponds to the value of information that one would obtain in the case of perfect monitoring and perfect decision making with the chosen heuristic.

The VPPI provides an upper limit on the value that the VoI can obtain. Since it can be computed much easier than the VoI, the VPPI can provide a first estimate on the maximum investment that should be made for SHM systems. Therefore, we motivate the idea that a VPPI computation should always be performed first.

4.6 Numerical investigations

4.6.1 Numerical benchmark: Continuously monitored bridge system subject to deterioration

We consider the two-span bridge model of Fig. 4.2, with its reference behavior [38] simulated by a FE model of isoparametric plane stress quadrilateral elements. This benchmark structure has been developed as part of the TU1402 COST Action and serves for verification of analysis methods and tools for SHM. 200 elements are employed to mesh the x direction, and 6 elements are assumed per height (y direction). The beam dimensions form configurable parameters of the benchmark and are set as: height $h = 0.6$m, width $w = 0.1$m, while the lengths are $L_1 = 12$m for the first span and $L_2 = 13$m for the second span. A linear elastic material with Young's modulus $E = 30$GPa, Poisson ratio $\nu = 0.2$, and material density $\rho = 2000$ kg/m^3 is assigned. Elastic boundaries in both directions are assumed for all three support points, in the form of translational springs with $K_x = 10^8$ N/m and $K_y = 10^7$ N/m.

It is assumed that the simulated two-span bridge is continuously monitored using a set of sensors measuring vertical acceleration, whose locations correspond to predefined FE nodes. A distributed Gaussian white noise excitation $F(x)$ is used as the load acting on the bridge, to simulate the unknown ambient excitation. A dynamic time history analysis of the model, for a given realization of the load, results in the measured vertical acceleration signals at the assigned sensor locations.

4.6.2 Deterioration modeling

A prior model describing structural deterioration is a prerequisite for a VoI analysis. A detailed presentation of probabilistic deterioration models for life-cycle performance assessment of structures can be found in [9, 12, 7]. For time-dependent reliability assessment purposes, the use of simple

empirical models, which are still flexible enough to model different kinds of deterioration mechanisms, can be adopted [9]. Within this work, we model structural deterioration with a simple rate equation of the form [9]:

$$D(t) = At^B \tag{4.31}$$

where $D(t)$ is the unit-less deterioration parameter (loss of stiffness) entering in the assumed damage model, and A, B are random variables driving the uncertainty in this model. Parameter A models the deterioration rate, while parameter B is related to the nonlinearity effect in terms of a power law in time. We consider herein the following two case studies related to structural deterioration of the bridge structure.

4.6.2.1 Bridge system subject to scour

We assume that the middle elastic support (pier) of the bridge structure is subjected to gradual deterioration, simulating the case of scour [28]. Damage is introduced as a progressive reduction of the stiffness in y-direction of the spring $K_y^{(2)}$ at the middle elastic support of the bridge (Fig. 4.2). The evolution of the stiffness reduction of the vertical spring support over the lifespan of the bridge is described by employing the damage model of Eq. (4.32), where $K_{y,0}^{(2)}$ is the initial undamaged value, and $D(t)$ is the stiffness reduction described by Eq. (4.31). We consider a lifespan of T=50 years for the structure. The uncertain parameters of the deterioration model are summarized in Tab. 4.1. The mean and coefficient of variation of the parameters A and B are chosen to reflect a significant a-priori uncertainty. They result in a 10% probability that $D(t = 50) > 9$ at the end of the lifespan.

$$K_y^{(2)}(t) = \frac{K_{y,0}^{(2)}}{(1 + D(t))} = \frac{K_{y,0}^{(2)}}{(1 + At^B)} \tag{4.32}$$

Table 4.1: Parameters of the stochastic deterioration model for scour.

Parameter	Distribution	Mean	CV
A	Lognormal	7.955×10^{-4}	0.5
B	Normal	2.0	0.15

4.6.2.2 Bridge system subject to corrosion deterioration

As a second separate case study, we assume that the bridge structure is subjected to gradual deterioration from corrosion in the middle of both midspans (elements in black in Fig. 4.2). At both locations, damage is introduced as a progressive reduction of the stiffness at the bottom 2 elements of the FE mesh. For the deterioration hotspots at the left and right midspans, the evolution of the elements' stiffness reduction over the lifespan of the bridge is described by employing the damage model of (Eq. (4.33)). $E^{(0)}$ is the initial undamaged value of the Young's modulus, and $D_1(t)$, $D_2(t)$ are the deterioration models (reduction of stiffness) employed for each location, as described by Eq. (4.31). The random variables of the deterioration models are summarized in Tab. 4.2. According to [9], for this simple empirical deterioration model, a value of B=0.5 corresponds to diffusion-controlled damage processes. Therefore the mean values of B_1 and B_2 have been chosen equal to 0.5. The mean and coefficient of variation of the four uncertain parameters are chosen so that they result in a 1% probability that $D(t = 50) >9$ at the end of the lifespan.

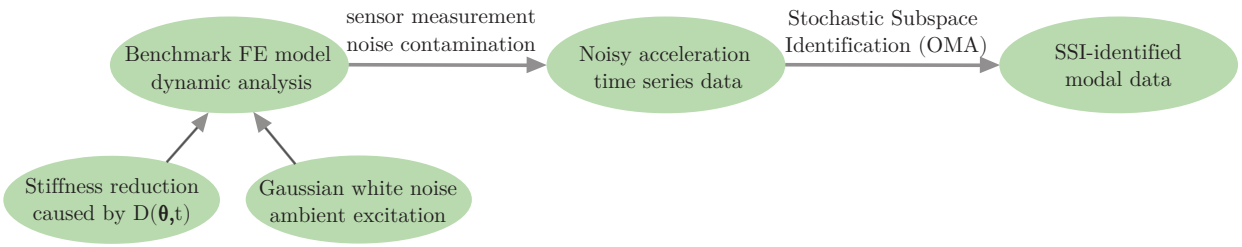

Figure 4.3: Process for generating the SHM data

$$E_j(t) = \frac{E^{(0)}}{(1 + D_j(t))} = \frac{E^{(0)}}{(1 + A_j t^{B_j})}, j = 1, 2 \tag{4.33}$$

Table 4.2: Parameters of the stochastic deterioration model for corrosion.

Parameters	Distribution	Mean	CV
A_1, A_2	Lognormal	0.506	0.4
B_1, B_2	Normal	0.5	0.15

4.6.3 Synthetic monitoring data creation

For the purpose of the VoI analysis, for every deterioration time instance at which one wants to simulate a monitoring data set obtained from the deployed SHM system, the corresponding stiffness reduction is implemented in the FE benchmark model, a dynamic time history analysis is run and the "true" vertical acceleration signals $\ddot{x}$ at the sensor locations (FE nodes) are obtained. This noise-free acceleration time series data set is then contaminated with Gaussian white noise of 2% root mean square noise-to-signal ratio, simulating a sensor measurement error. Subsequently, the noisy accelerations $\tilde{\ddot{x}}$ are fed into an output-only operational modal analysis (OMA) scheme. Specifically, the SSI algorithm is used to identify a set of the lower eigenvalues (squares of natural frequencies) and mode shapes [26].

The data creation process is summarized in Fig. 4.3. First, we draw samples of the deterioration parameters, defining the evolution of sample deterioration curves. For each of these deterioration curves we then create one monitoring history, i.e., we generate one set of OMA-identified modal data every year over the fifty years of the lifetime. Here, the influence of environmental (temperature, humidity) and operation (non stationary effects due to traffic) variability on the structural properties are not accounted for. We generate one data set for each year that the bridge is in service. Using this data, we then employ the sequential Bayesian deterioration model updating framework of Section 4.3.

4.6.4 Continuous Bayesian model updating

We demonstrate how the Bayesian framework performs in learning the parameters of the deterioration model on the basis of availability of the SHM modal data. In this work, the model predicting the eigenvalues and mode shapes for the Bayesian updating process is the same FE model as the

one described in Section 4.6.3 for the creation of the noise-contaminated synthetic data. Despite addition of artificial noise, adoption of the same model constitutes a so-called inverse crime [42]. However, this is a built-in feature of preposterior analysis.

Even in absence of model error and environmental/ambient effects, as assumed in this work, there remains measurement uncertainty, caused by the added random sensor measurement noise and by the variance or bias errors induced in the SSI procedure [30]. Fig. 4.4 demonstrates this measurement uncertainty. It shows the discrepancy between the "true" eigenfrequencies of the deteriorating structure over time, obtained via a modal analysis with the FE model, and the SSI-identified eigenfrequencies. The presence of noise is evident for all the displayed eigenfrequencies, while for the higher modes a clear bias in the estimation is present.

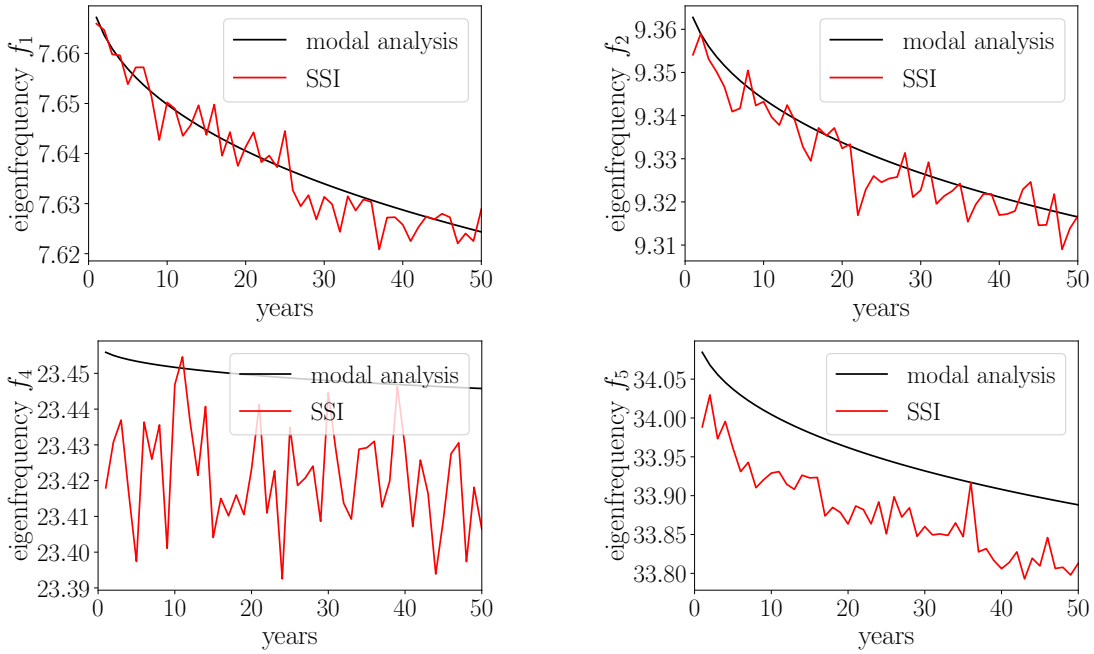

Figure 4.4: Demonstration of the measurement uncertainty. Identified eigenfrequencies (in red) against "true" underlying eigenfrequencies (in black) obtained from a realization of the structural deterioration following the second case study presented in Section 4.6.4.2.

We note that the noise shown in Fig. 4.4 depends on the amount of data considered in the analysis. Here, we make the simplifying assumption of considering one data point per year. Naturally, this is here a simplification for the purpose of our exploration. A continuous monitoring system (as is typically the requirement for SHM), can deliver more dense data and reduce the measurement noise (not the bias though), in the limit to a value of zero. The reason why we nevertheless choose to consider only a single data point per year is that, in this example which ignores other sources of uncertainty (such as environmental and operational variability), we wish to mimic the practical SHM setting, where the effects of noise cannot be eliminated. In a real SHM setting, the Bayesian analysis is subject to an unknown model error. As a result, the noise does not go to zero with increasing amounts of data [40, 6]. However, this is not reflected in preposterior analysis, which requires the use of the same model for generating the data and conducting the Bayesian analysis. As an alternative to using only a limited amount of data, one could also investigate the use of hierarchical models [6].

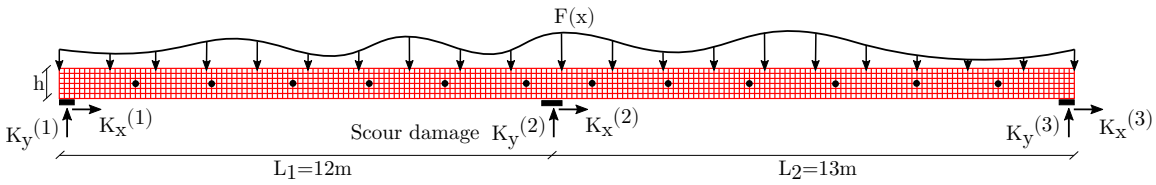

Figure 4.5: Bridge system subject to scour damage

However, the associated computational cost would be significantly larger.

The sequential Bayesian analysis framework requires a substantial number of evaluations of the likelihood function, implying multiple forward runs of the FE model. Within a VoI framework, Bayesian analysis must be performed numerous times. For this reason a VoI analysis can quickly become intractable. To enable the VoI analysis, we employ simple surrogate models to replace the structural FE model, which are described in the following two subsections.

4.6.4.1 Bridge system subject to scour deterioration - Global damage identification

In this assumed damage scenario we are interested in identifying damage in a global scale, for which use of the OMA-identified eigenvalue data alone may be sufficient. The benefit is that eigenvalue data can be successfully identified from an OMA procedure, even when only a rather small number of accelerometers are employed on the structure. The sensor placement that we assume here is the one corresponding to Fig. 4.5, with twelve employed sensors. This configuration is selected on the basis of engineering judgment, when seeking to identify the type of damage (local stiffness reduction) considered herein. Using the SSI algorithm, we identify the lower $N_m = 6$ modes, which we then use for the updating.

We employ a surrogate model to replace the structural FE model for facilitating the Bayesian updating procedure. To this end, we create a fine uniform grid of values for $D(t)$; for each of these, we execute a modal analysis using the FE model and store the output eigenvalues. Eventually, we replace the modal analysis run of the structural FE model with a simple nearest neighbor lookup in the precomputed database.

For illustrating the data sampling and updating process, we assume a scenario where the underlying "true" deterioration model corresponds to parameters values A^*=9.85×10^{-4} and $B^* = 2.28$. The "true" deterioration curve can be seen in black in all the subfigures of Fig. 4.7.

Fig. 4.6 demonstrates how the distribution of the deterioration model parameters is updated by comparing the prior PDF of A and B with the posterior PDF of A and B at year 25 and year 50. For this analysis, both factors $c_{\lambda m}$ and $c_{\Phi m}$ are assumed equal to 0.02, i.e. we assume that the total prediction error causes up to two percent deviation on the nominal model predicted values. 5000 MCMC samples are used for the Bayesian analysis at each time step. The posterior PDFs are given via a kernel density estimation using the 5000 posterior MCMC samples of the parameters. It is observed that using one SHM data set per year, the uncertainty in the deterioration model parameters gradually decreases, the PDFs become narrower and peak around the underlying "true" values for which the data was created.

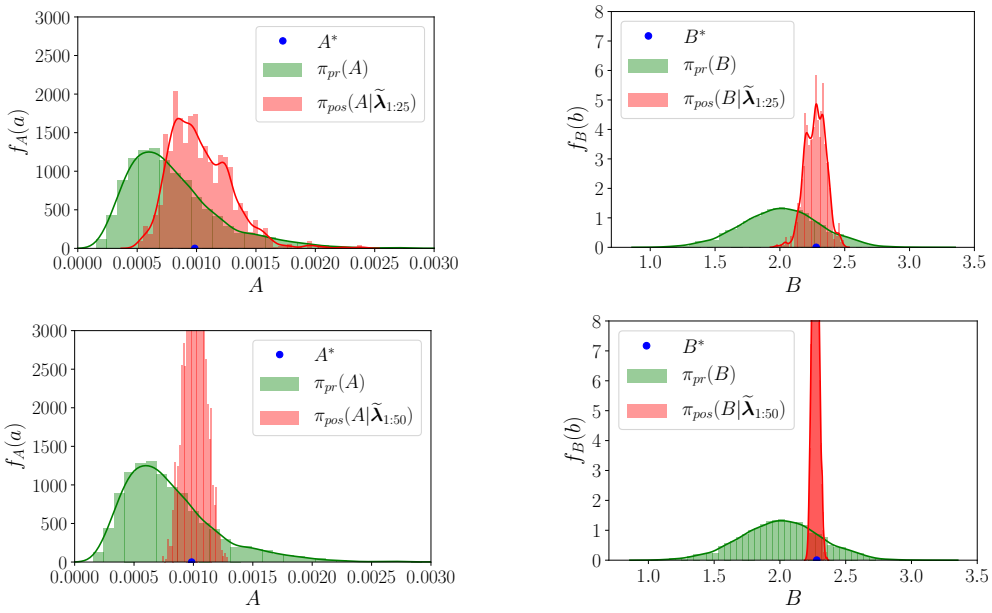

Figure 4.6: Prior PDF and posterior PDF at years 25 and 50 for deterioration model parameters ($c_{\lambda m} = c_{\Phi m} = 0.02$)

Fig. 4.7 contains the following: The mean estimated deterioration model together with its 90% credible interval in the prior case, obtained via a MCS from the prior distribution of the uncertain parameters, is plotted in the left panel in green. In red we plot the posterior predictive mean models together with their 90% credible intervals, which are estimated with posterior MCMC samples using monitoring data up to the three different time instances. For example in the second column, we use the monitoring data of the first ten years to obtain the posterior distribution $\pi_{\text{pos}}(\boldsymbol{\theta} \mid \tilde{\boldsymbol{\lambda}}_{1:10}, \tilde{\boldsymbol{\Phi}}_{1:10})$, and then we use the posterior MCMC samples to predict the evolution of the deterioration model over the structural lifetime. We observe that already the data obtained during the first few years of the deterioration process (up to year 10) help in shifting the mean posterior model towards the underlying "true" deterioration curve, however the posterior uncertainty in the estimation is still relatively large. The posterior uncertainty is reduced significantly as more SHM modal data become gradually available (year 25, year 50).

4.6.4.2 Bridge system subject to corrosion deterioration - Damage detection and localization

In the assumed scenario with two potential corrosion damage locations, the employed Bayesian model updating framework should be able to both detect and localize damage. Therefore both eigenvalue as well as mode shape displacement data should become available. As discussed in Section 4.3, a relatively large number of sensors is required for an accurate measurement and representation of the mode shape displacements. The sensor placement that we assume here is the one corresponding to Fig. 4.8, with 24 equally distributed accelerometers. By using a finite difference scheme, we can also obtain the mode shape curvatures, which are used instead of the mode shapes in the likelihood function, which seems to enhance the localization capabilities of the framework. Also in this case we identify the lower N_m=6 modes.

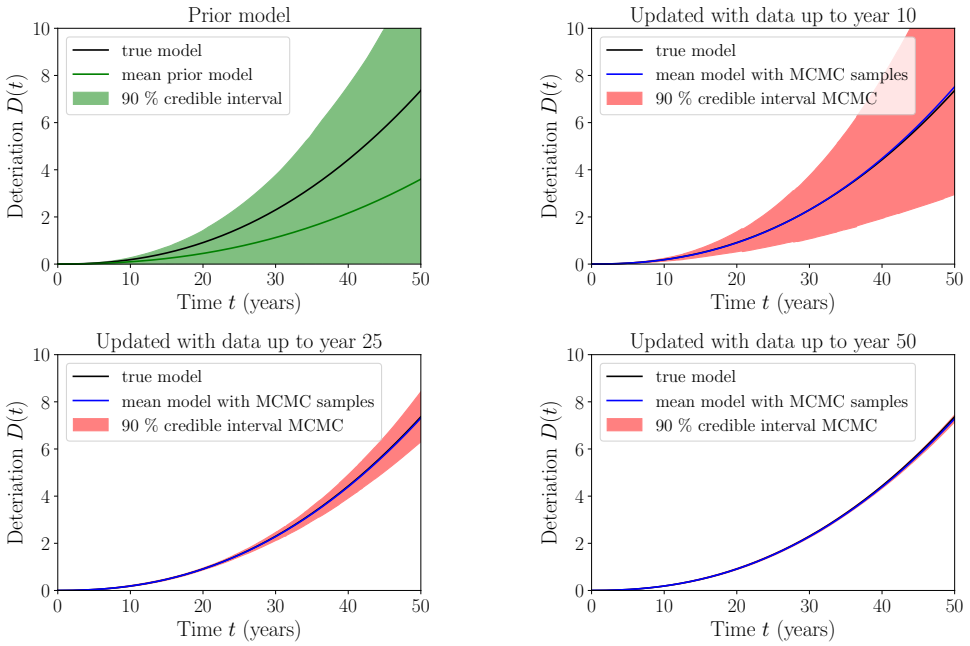

Figure 4.7: Sequential Bayesian learning of the scour deterioration model. The true model corresponds to a single randomly generated realization of the deterioration process.

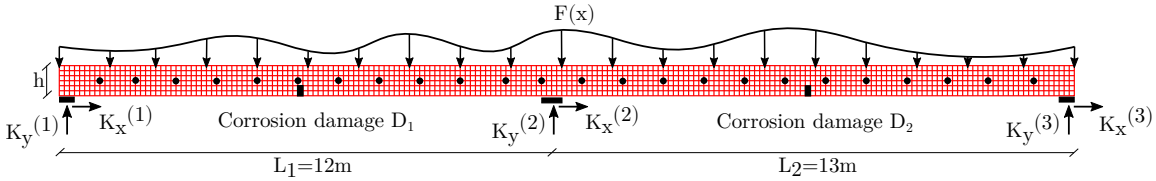

Figure 4.8: Bridge system subject to corrosion damage in two locations

For defining a surrogate model, we create a two-dimensional grid of values for $D_1(t), D_2(t)$, and for each of the grid points we run a modal analysis with the FE model, and we store the output eigenvalues and mode shape vectors. Eventually we employ the following surrogates: For each of the eigenvalues, we fit a two-dimensional polynomial regression response surface model. For the mode shape displacement vector data, we replace the run of the structural FE model with a simple nearest neighbor lookup in the precomputed two-dimensional database.

For illustration purposes, we draw one sample $\boldsymbol{\theta}^*$, which corresponds to the underlying "true" deterioration parameter values $A_1^* = 0.65$, $B_1^* = 0.55$, $A_2^* = 0.42$ and $B_2^* = 0.48$ ("true" deterioration curves can be seen in black in all the subfigures of Fig. 4.12).

Figs. 4.9 to 4.11 demonstrate how the distribution of the deterioration models' parameters is updated, by comparing the prior PDFs with the posterior PDFs at three different time instances. Both factors $c_{\lambda m}$ and $c_{\Phi m}$ in the likelihood function are assumed equal to 0.02. In Fig. 4.12, we compare the underlying "true" deterioration model with the deterioration model estimated using MCS in the prior case, and with the ones estimated with 5000 posterior MCMC samples at three different time instances.

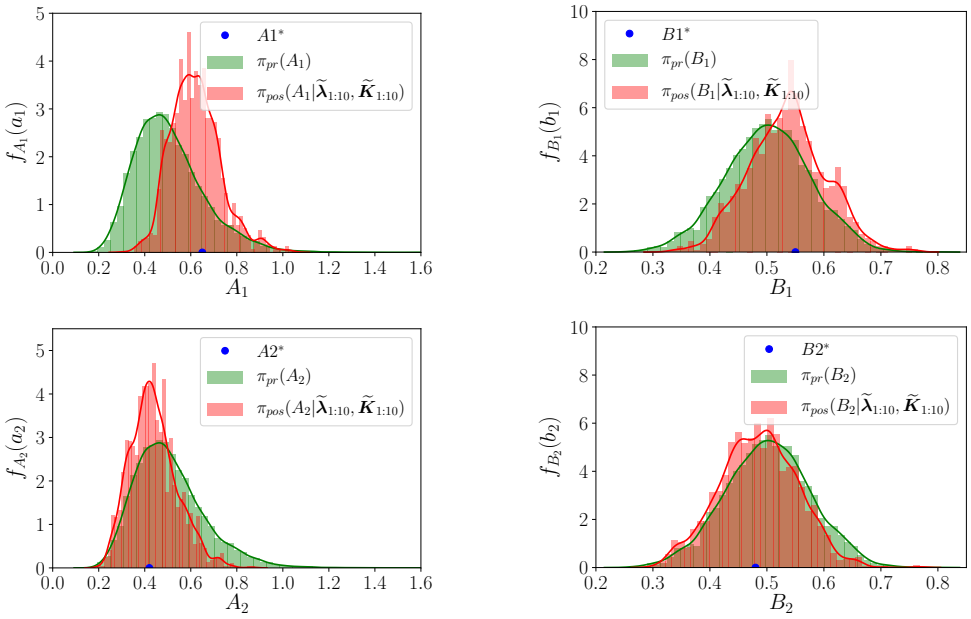

Figure 4.9: Prior PDF and posterior PDF at year 10 for deterioration models parameters ($c_{\lambda m} = c_{\Phi m} = 0.02$)

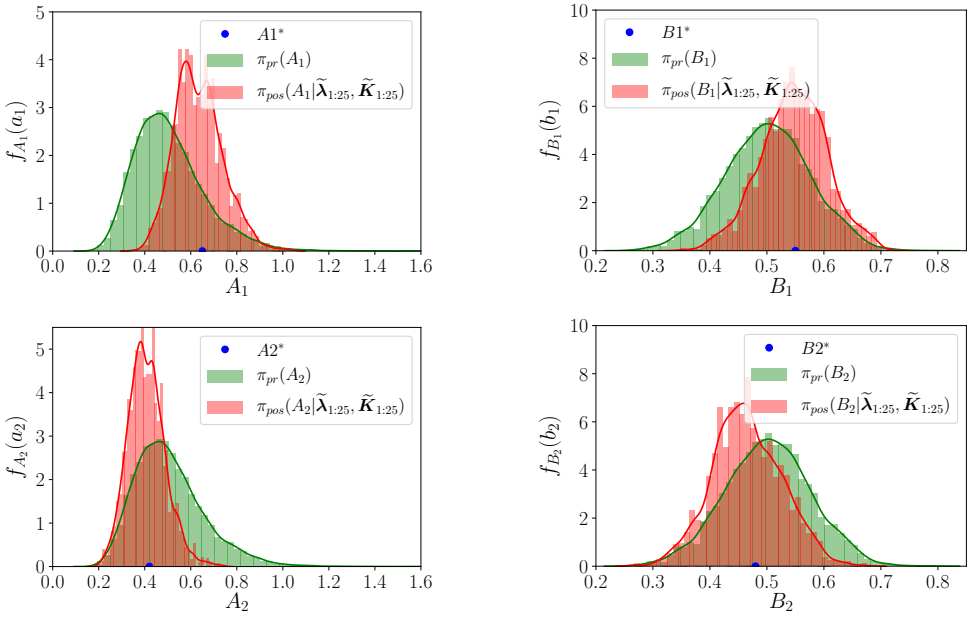

Figure 4.10: Prior PDF and posterior PDF at year 25 for deterioration models parameters ($c_{\lambda m} = c_{\Phi m} = 0.02$)

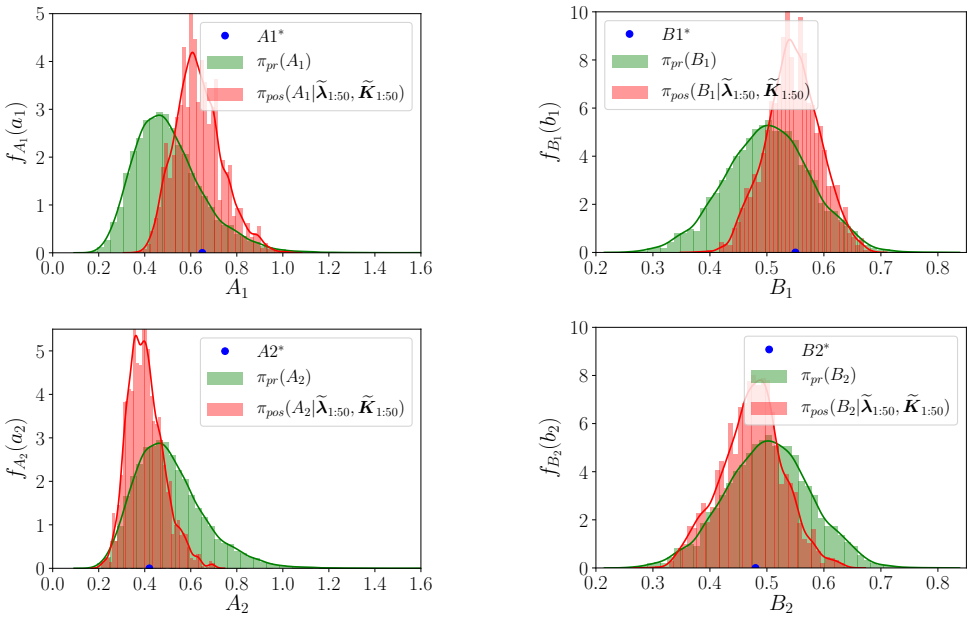

Figure 4.11: Prior PDF and posterior PDF at year 50 for deterioration models parameters ($c_{\lambda m} = c_{\Phi m} = 0.02$)

Section 4.3 discusses the fact that quite often the choice of the magnitude of factors $c_{\lambda m}$ and $c_{\Phi m}$ for constructing the likelihood function can be arbitrary, since usually very little is known about the magnitude of the total prediction error. Fig. 4.13 attempts to demonstrate how crucial this choice can be for the results of the Bayesian updating, by performing it additionally for $c_{\lambda m} = c_{\Phi m} = 0.05$. Comparing Fig. 4.13 to Fig. 4.11 (both at year 50), it can be clearly observed that the posterior distribution of the deterioration model parameters that one learns is significantly affected by the choice of these factors.

As discussed in Section 4.6.4, we employ one set of sampled OMA-identified modal data per year and use these to update the deterioration model. However, an SHM system can provide an abundance of measurement points (which produce corresponding modal estimates) in a continuous fashion. To investigate the effect of this choice, in Fig. 4.14 we plot the results of the posterior distribution of the deterioration model parameters at the final estimation time (year 50), in a case where we employ 50 OMA-identified modal estimates per each year (2500 modal estimates in total). Upon comparison of Fig. 4.14 and Fig. 4.11, it becomes evident that adoption of more sets of modal data leads in reduced uncertainty in the posterior estimate, although the posterior distributions seem to not be centered around the underlying "true" value of the parameters, which is possibly the result of a bias in the estimation of higher eigenfrequencies.

4.6.5 Time-dependent structural reliability and its updating using monitoring data

The uncertain demand acting on the structure is modeled by the maximum load in a one-year time interval with a Gumbel distribution (left panel of Fig. 4.15). The parameters of the Gumbel

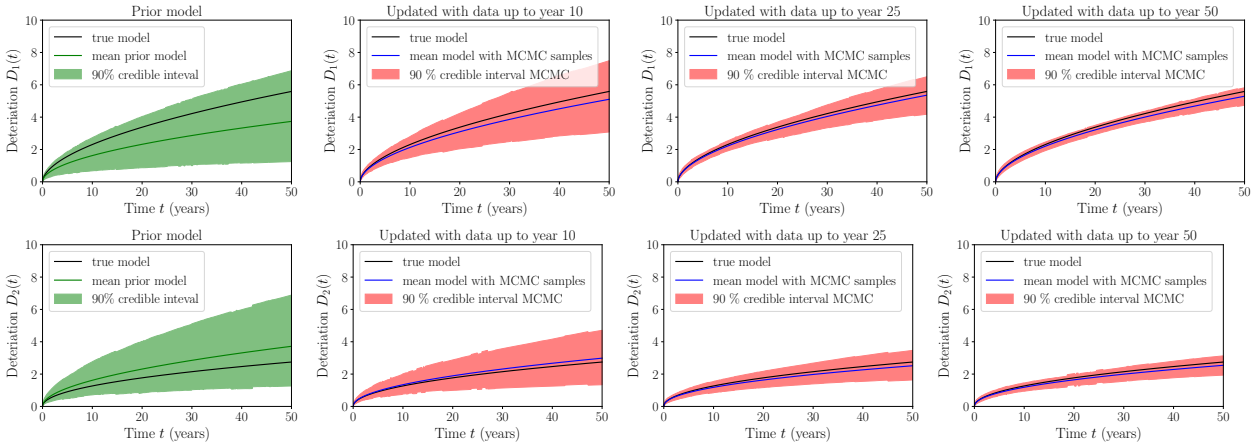

Figure 4.12: Sequential Bayesian learning of the two corrosion deterioration models. The true model corresponds to a single randomly generated realization of the deterioration process.

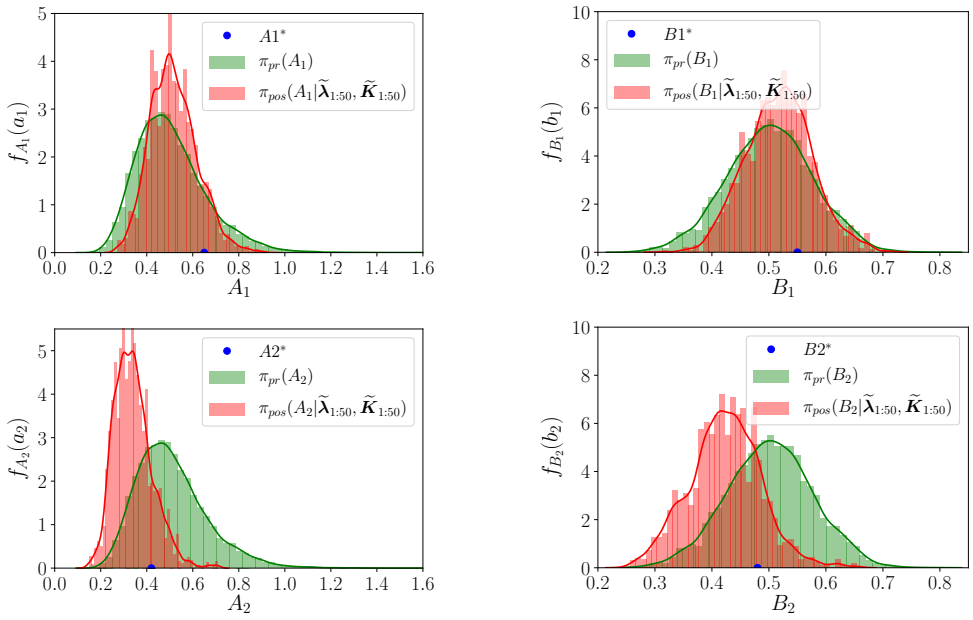

Figure 4.13: Prior PDF and posterior PDF at year 50 for deterioration models parameters ($c_{\lambda m} = c_{\Phi m} = 0.05$)

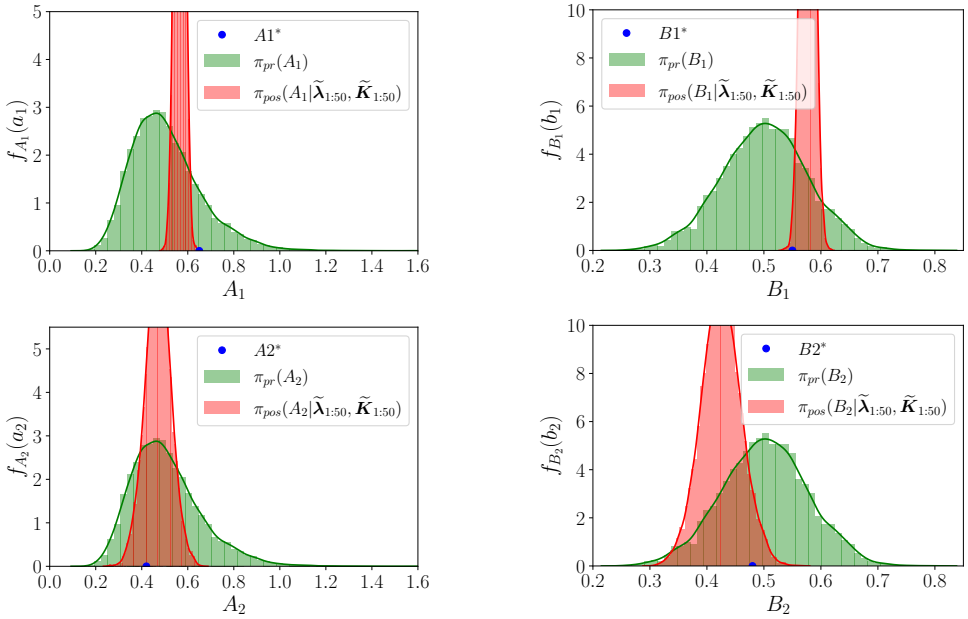

Figure 4.14: Prior PDF and posterior PDF at year 50 for deterioration models parameters ($c_{\lambda m} = c_{\Phi m} = 0.02$) in the case when 50 OMA-identified modal data per year are used (2500 modal estimates from the different years are employed for the updating at year 50)

distribution are chosen such that the probability of failure in the initial undamaged state is equal to 10^{-6} and the coefficient of variation of the random load is 20%.

4.6.5.1 Bridge system subject to scour deterioration

The deterministic capacity curve $R(D(\boldsymbol{\theta}, t))$ of the damaged structure for any realization of the scour deterioration $D(\boldsymbol{\theta}, t)$ can be seen in the middle panel of Fig. 4.15. To determine this curve, we consider that when scour damage occurs in the middle support, the critical quantity that increases is the normal stress at the middle of the second, slightly longer, midspan. We create a fine one-dimensional grid of possible values as input for $D(\boldsymbol{\theta}, t)$, for each of those we run a static analysis of our model, and we evaluate the loss of load bearing capacity of the structure relative to the initial undamaged state.

In the right panel of Fig. 4.15 we plot the time-dependent accumulated probability of failure and the hazard function in the prior case, together with the 95% credible intervals, estimated using 10^4 prior samples. Because of the skewness of the assumed prior deterioration model, the mean estimated curves are not contained within the 95% credible intervals.

4.6.5.2 Bridge system subject to corrosion deterioration

When damage (stiffness reduction) occurs in the elements at the bottom of each midspan, the quantity that increases critically are the normal stresses at the top of each midspan. We create a

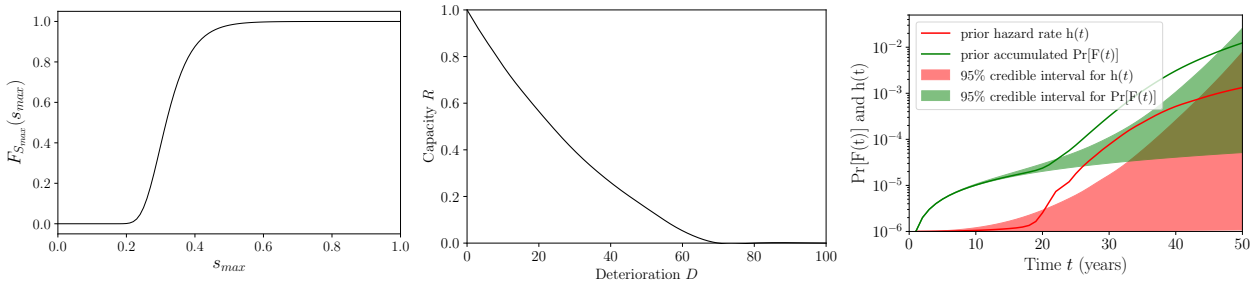

Figure 4.15: left: CDF of the Gumbel distribution for the load with location $a_n = 0.0509$, scale $b_n = 0.297$. middle: Structural capacity in function of scour deterioration, right: Time-dependent structural reliability curves estimated with the prior model in the scour deterioration case.

two-dimensional grid of possible values of the two corrosion deteriorations D_1 and D_2. For each of those possible combinations, we run a static analysis with our model, and we evaluate the loss of load bearing capacity of the bridge structure relative to the undamaged state. Eventually we fit a two-dimensional polynomial regression response surface curve that describes $R(\boldsymbol{D}(\boldsymbol{\theta}, t))$; it can be seen in the left panel of Fig. 4.16.

As presented in Section 4.4.2, learning the parameters of the deterioration models, and the reduction of the uncertainty in their estimation through the sequential acquisition of SHM modal data, affects the estimation of the time-dependent structural reliability. In Fig. 4.16, we plot in green the accumulated probability of failure and the hazard rate of the bridge structure in the case of using the prior deterioration model, and we compare it with the red plots of the accumulated probability of failure and the hazard rate conditional on the continuous monitoring data (1 data set per year), which correspond to the underlying "true" deterioration models described by $A_1^* = 0.65$, $B_1^* = 0.55$, $A_2^* = 0.42$ and $B_2^* = 0.48$. The prior estimates are obtained with 5000 Monte Carlo samples following Eqs. (4.14) and (4.15). The posterior estimates are obtained via Eqs. (4.18) and (4.19) using 5000 MCMC samples at each time step. The 95% credible intervals are computed using the Monte Carlo prior samples in the prior case, and the MCMC posterior samples in the posterior case. It is observed that the uncertainty in the estimation of the structural reliability is reduced in the posterior case. This reduction of the uncertainty and the updated estimate of the structural reliability form the basis for the VoI analysis.

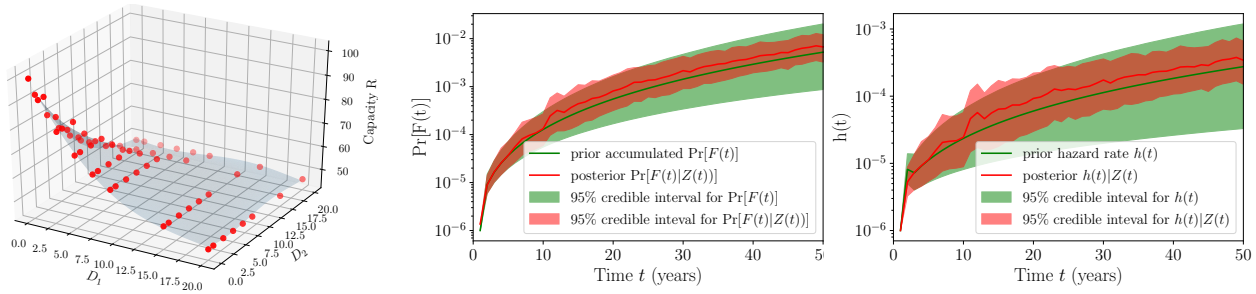

Figure 4.16: left: Polynomial regression response surface for structural capacity in function of corrosion deterioration, right: time dependent structural reliability curves in the prior/posterior corrosion case.

4.6.6 VoI analysis

The VoI is computed with Eq. (4.29) following the Bayesian preposterior decision analysis framework presented in Section 4.5. The expected total life-cycle costs, $\mathbb{E}_{\boldsymbol{\theta}}[C_{\text{tot}} \mid w]$ in the prior case and $\mathbb{E}_{\boldsymbol{\theta},\boldsymbol{Z}}[C_{\text{tot}}|w]$ in the preposterior case, are both computed with MCS. In the preposterior case, as already explained in Section 4.5.3, the system state space $\boldsymbol{\theta}$ and the monitoring data space $\boldsymbol{Z}$ are jointly sampled. For each full history of modal data, one sequential Bayesian posterior analysis has to be performed, which is a costly procedure by itself. It is clear that such an analysis can be very computationally expensive, therefore some considerations on the available computational budget, and how to distribute it, have to be made in advance. The computational cost of the VoI analysis is approximately proportional to the number of MCS samples used in the expected life-cycle cost computation and the necessary corresponding synthetic monitoring data creation, and by the computational cost of the employed method for performing the sequential Bayesian updating.

For our investigation we assume $\hat{c}_{\text{F}} = 10^7$€, and for the repair cost $\hat{c}_{\text{R}}$ we investigate different ratios $\frac{\hat{c}_{\text{R}}}{\hat{c}_{\text{F}}} = [10^{-1}, 10^{-2}, 10^{-3}]$, and for each of those we calculate the VoI. The discount rate is taken as $r = 2\%$.

The solution to the stochastic life-cycle optimization problem of Eq. (4.20) is performed through an exhaustive search among a large discrete set of values of the heuristic parameter (the threshold at which a repair is performed).

4.6.6.1 VoI results for bridge system subject to scour deterioration

For this example, we draw 1000 samples of $\boldsymbol{\theta}$, which are used in both prior and preposterior analysis. In the preposterior case, for each $\boldsymbol{\theta}$ sample we create one continuous set of identified modal data $\boldsymbol{Z}_{1:50}$. For the 1000 different sequential Bayesian analyses that have to be performed, we employ the adaptive MCMC algorithm. For the estimation of the different posterior accumulated probabilities of failure in Eq. (4.18), 2000 posterior MCMC samples are used.

Tabs. 4.3a and 4.3b summarize the results of the life cycle optimization, documenting the optimal value of the heuristic parameter w^*, and the optimal expected total life cycle costs that correspond to w^*. Table 4.3a documents also the optimal time for a repair action in the prior case. This is not documented in Tab. 4.3b, since in the preposterior case there is not one single optimal t_{repair} value, but t_{repair} varies for each sample $\boldsymbol{\theta}$ and the corresponding monitoring history.

Tab. 4.3c documents the resulting VoI values that we obtain with the 1000 samples via Eq. (4.29) for the three different cost ratios, while Tab. 4.3d reports the VPPI values obtained via Eq. (4.30), related to the hypothetical case when we learn perfectly the condition of the structure from the SHM system. We also include the coefficient of variation (CV) of the mean VoI, VPPI estimates, which quantifies the uncertainty in the estimates obtained via MCS. In cost ratio cases for which the optimal action in the prior case is not to perform any repair, the VoI estimate has a quite large variability. This is because the samples in the preposterior analysis that lead to a different optimal t_{repair} than in the prior case are only a few, which is an indication that a larger number of Monte Carlo samples or more efficient sampling techniques (e.g., importance sampling) should be used to reduce the variance. It is important to take into account that Eq. (4.30) for computing the VPPI

Table 4.3: Results of preposterior Bayesian decision analysis for the scour example

(a) Life-cycle optimization in the prior case.

$\frac{\hat{c}_R}{\hat{c}_F}$	w_0^*	$E[C_{tot}\|w_0^*]$	t_{repair}
10^{-1}	$\geq 2 \times 10^{-3}$	45395	no repair
10^{-2}	$\geq 2 \times 10^{-3}$	45395	no repair
10^{-3}	$2{\times}10^{-5}$	5924	year 31

(b) Life-cycle optimization in the preposterior case.

$\frac{\hat{c}_R}{\hat{c}_F}$	w_{mon}^*	$E[C_{tot}\|w_{mon}^*]$
10^{-1}	$2.1{\times}10^{-2}$	12552
10^{-2}	$1.2{\times}10^{-3}$	3125
10^{-3}	$9.9{\times}10^{-5}$	1109

(c) Value of information (VoI)

$\frac{\hat{c}_R}{\hat{c}_F}$	VoI (CV)
10^{-1}	32843 (0.34)
10^{-2}	42270 (0.30)
10^{-3}	4815 (0.02)

(d) Value of partial perfect information (VPPI)

$\frac{\hat{c}_R}{\hat{c}_F}$	VPPI (CV)
10^{-1}	35013 (0.23)
10^{-2}	42717 (0.21)
10^{-3}	4918 (0.02)

can easily be solved even for a very large number of MC samples, which would reduce the variability of the estimate shown here.

For all the cost ratio cases, the VoI is positive, which indicates a potential benefit of installing an SHM system on the deteriorating bridge structure. It is interesting to compare the obtained VoI values to the VPPI values. We observe that in this example the VoI from SHM extracted via Bayesian model updating is close to optimal, as it is very close to the VPPI value. This indicates that the choice of using only a single data point each year does not lead to a relevant reduction of the information content in the monitoring data. Clearly, in this case the monitoring system is able to identify damage with little uncertainty and can be used effectively for decision making.

4.6.6.2 VoI results for bridge system subject to corrosion deterioration

For this second example, we draw 2000 samples of $\boldsymbol{\theta}$, which are used in both prior and preposterior analysis. In the preposterior case, for each $\boldsymbol{\theta}$ sample we create one continuous set of identified modal data $\boldsymbol{Z}_{1:50}$. For the 2000 different sequential Bayesian analyses that have to be performed, we employ the Laplace approximation method of Section 4.3.2.1 for the solution, which introduces an approximation error in the posterior solution, especially in the initial years, when the data set is not so large, yet is computationally much faster than an MCMC solution. For the estimation of the posterior accumulated probability of failure in Eq. (4.18)), 10000 samples are drawn from the approximate multivariate Gaussian posterior distribution.

The computed VoI and VPPI estimates can be seen in Tab. 4.4. We observe that the VoI is 0 in the case when the costs have a ratio $\frac{\hat{c}_R}{\hat{c}_F} = 10^{-1}$, which means that one does not get any benefit from the data obtained from the SHM system. This is related to the fact that, for this cost ratio, the optimal decision is to not perform a repair action in the lifespan of the bridge, in both the prior and all the preposterior samples, since at all time steps the cost of a repair is much larger than the the risk of failure cost. For the cost ratio $\frac{\hat{c}_R}{\hat{c}_F} = 10^{-2}$, we observe that the VoI from SHM extracted via Bayesian model updating is not optimal, as it does not provide the full VPPI value, but 51% of this value, while for the cost ratio $\frac{\hat{c}_R}{\hat{c}_F} = 10^{-3}$ it only provides around 22% of the VPPI value.

We note that the VoI depends on the assumed prior uncertainty of the deterioration model, and how this propagates in time, among other factors. For the purpose of the numerical investigations

Table 4.4: Results of preposterior Bayesian decision analysis for the corrosion example

(a) Life-cycle optimization in the prior case.

$\frac{\hat{c}_R}{\hat{c}_F}$	w_0^*	$E[C_{tot}\|w_0^*]$	t_{repair}
10^{-1}	$\geq 2.8 \times 10^{-4}$	26792	no repair
10^{-2}	$\geq 2.8 \times 10^{-4}$	26792	no repair
10^{-3}	2×10^{-5}	9308	year 8

(b) Life-cycle optimization in the preposterior case.

$\frac{\hat{c}_R}{\hat{c}_F}$	w_{mon}^*	$E[C_{tot}\|w_{mon}^*]$
10^{-1}	$\geq 9 \times 10^{-3}$	26792
10^{-2}	7.5×10^{-4}	25334
10^{-3}	1.83×10^{-5}	9200

(c) Value of information (VoI)

$\frac{\hat{c}_R}{\hat{c}_F}$	VoI (CV)
10^{-1}	0
10^{-2}	1458 (0.42)
10^{-3}	108 (0.08)

(d) Value of partial perfect information (VPPI)

$\frac{\hat{c}_R}{\hat{c}_F}$	VPPI (CV)
10^{-1}	132 (0.30)
10^{-2}	2871 (0.22)
10^{-3}	497 (0.05)

that are conducted in this paper, we chose prior models which reflect sufficiently large uncertainty apriori. In practice, it is expected that the analyst has a prior model of the uncertainty and will use this to perform a VoI analysis. Without a prior model of this uncertainty, it is not possible to quantify the value of SHM a-priori.

4.6.6.3 VoI results - Sensor placement study

The purpose of this section is to demonstrate that the presented VoI analysis can be employed as a formal decision analysis tool for performing various parametric studies related to different choices in designing the SHM system and performing the Bayesian model updating procedure.

One critical choice when designing an SHM system is the number and position of the sensors to be employed on the structure. One could employ the proposed VoI analysis to perform optimal sensor placement studies for a deteriorating structural system. Each sensor arrangement choice will result in a VoI value, and the choice which leads to the highest VoI would be the preferred one.

Herein we demonstrate this with the use of the second example of the bridge system subject to corrosion deterioration at two locations. For the decision problem, we now fix the cost of failure to $\hat{c}_F = 10^7$€ and the cost of repair to $\hat{c}_R = 3.5 \times 10^4$€. We consider the following two different arrangements of the sensors: i) 24 uniformly distributed accelerometers along the structure, ii) 12 uniformly distributed accelerometers along the structure. In both cases the VoI analysis is performed by drawing 1000 samples of $\boldsymbol{\theta}$.

It becomes evident that in the case that the structure is subjected to deterioration at two different damage locations, the number of sensors and consequently the quality of the mode shape displacement or curvature information that one obtains clearly affects the BMU results and therefore leads to a notable difference in the heuristic-based life-cycle optimization and the VoI result that we obtain.

Table 4.5: Parametric study for the effect of the number of sensors on VoI result

(a) Life-cycle optimization in the prior case.

w_0^*	t_{repair}^*
6.1×10^{-5}	21

(b) Life-cycle optimization in the preposterior case.

sensors	w_{mon}^*
24	1×10^{-4}
12	3.2×10^{-4}

(c) Effect of number of sensors on the VoI

VPPI (CV)	sensors	VoI (CV)	$\frac{\text{VoI}}{\text{VPPI}}$
7681 (2.6%)	24	4614 (5.3%)	60%
	12	2711 (15%)	35%

4.7 Concluding remarks

This paper investigates the quantification of the VoI yielded via adoption of SHM systems acting in long-term prognostic mode for cases of deterioration. It focuses on demonstrating, for the first time, a VoI analysis on the full SHM chain, from data acquisition to utilization of a structural model for the purpose of the updating and reliability calculation. A preposterior Bayesian decision analysis for quantifying the VoI, specifically tailored for application on an employed numerical benchmark structural model, is presented. Two different structural damage case studies are investigated, for which a simple stochastic deterioration model with prior parameter uncertainties is assumed to be available. The modeling of the acquired SHM data is done in a realistic way, following a state-of-the-art operational modal analysis procedure. The data is used within a Bayesian model updating framework, implemented in a sequential setting, to continuously update the uncertain structural condition, which subsequently leads to the updating of the estimate of the structural reliability. A heuristic-based solution to the simplified decision problem is provided for finding the optimal time to perform a single repair action, which might be needed during the lifetime of the structure. We discuss specific computational aspects of a VoI calculation. The VoI analysis requires the integration over the monitoring data, which are here modeled in a realistic way, adding an extra computationally expensive layer in the analysis. In addition to the VoI solution, an upper limit to the VoI through the value of partial perfect information is also provided, related to hypothetical situations of perfect knowledge on the system condition.

It should be noted that the resulting VoI estimates are affected by the fact that only a single repair action case is explored. In the present exemplary analysis, we do not take into account nonlinearities of the underlying system, dependence on varying ambient/environmental effects (e.g dependence on temperature), or modeling errors. To partly account for these effects, as well as unknown errors in the structural model, we consider only a limited number of data points from the SHM. However, further investigations are necessary into how these types of uncertainties can be addressed within a VoI analysis.

Acknowledgment

The work of A. Kamariotis and E. Chatzi has been carried out with the support of the Technical University of Munich - Institute for Advanced Study, Germany, funded by the German Excellence Initiative and the TÜV SÜD Foundation.

References

[1] C. P. Andriotis, K. G. Papakonstantinou, and E. N. Chatzi. "Value of structural health information in partially observable stochastic environments". In: *Structural Safety* 93 (2021), p. 102072.

[2] C. Argyris, C. Papadimitriou, P. Panetsos, and P. Tsopelas. "Bayesian Model-Updating Using Features of Modal Data: Application to the Metsovo Bridge". In: *Sensors and Actuator Networks* 9(2) (2020), p. 27.

[3] S. Au, F. Zhang, and Y. Ni. "Bayesian operational modal analysis: theory, computation, practice". In: *Computers and Structures* 126 (2013), pp. 3–14.

[4] J. Beck and S. Au. "Bayesian Updating of Structural Models and Reliability using Markov Chain Monte Carlo Simulation". In: *Journal of Engineering Mechanics* 128(4) (2002), p. 380.

[5] I. Behmanesh and B. Moaveni. "Probabilistic identification of simulated damage on the Dowling Hall footbridge through Bayesian finite element model updating". In: *Structural Control and Health Monitoring* 22 (2015), pp. 463–483.

[6] I. Behmanesh, B. Moaveni, G. Lombaert, and C. Papadimitriou. "Hierarchical Bayesian model updating for structural identification". In: *Mechanical Systems and Signal Processing* 64-65 (2015), pp. 360–376.

[7] F. Biondini and D. Frangopol. "Life-cycle performance of deteriorating structural systems under uncertainty". In: *Journal of Structural Engineering* 142 (2016), F4016001.

[8] E. Bismut and D. Straub. "Optimal Adaptive Inspection and Maintenance Planning for Deteriorating Structural Systems". In: *Reliability Engineering and System Safety* 215 (2021), p. 107891.

[9] B. Ellingwood. "Risk-informed condition assessment of civil infrastructure: state of practice and research issues". In: *Structure and Infrastructure Engineering* 1(1) (2005), pp. 7–18.

[10] C. R. Farrar and K. Worden. "An introduction to structural health monitoring". In: *Philosophical Transactions of the Royal Society A.* 365 (2007), pp. 303–315.

[11] C. R. Farrar and K. Worden. *Structural Health Monitoring: A Machine Learning Perspective.* John Wiley & Sons, Ltd, 2013.

[12] D. Frangopol, M. Kallen, and J. van Noortwijk. "Probabilistic models for life-cycle performance of deteriorating structures: review and future directions". In: *Progress in Structural Engineering and Materials* 6 (2004), pp. 197–212.

[13] H. Haario, M. Laine, A. Mira, and E. Saksman. "DRAM: Efficient adaptive MCMC". In: *Statistics and Computing* 16 (2006), pp. 339–354.

[14] L. Iannacone, P. Giordano, P. Gardoni, and M. Limongelli. "Quantifying the value of information from inspecting and monitoring engineering systems subject to gradual and shock deterioration". In: *Structural Health Monitoring* 21(1) (2022), pp. 72–89.

[15] L. Ierimonti, I. Venanzi, N. Cavalagli, F. Comodini, and F. Ubertini. "An innovative continuous Bayesian model updating method for base-isolated RC buildings using vibration monitoring data". In: *Mechanical Systems and Signal Processing* 139 (2020), p. 106600.

[16] F. Jensen and T. Nielsen. *Bayesian Networks and Decision Graphs, 2nd Edition.* New York: Springer, 2007.

[17] A. Kamariotis, D. Straub, and E. Chatzi. "Optimal maintenance decisions supported by SHM: A benchmark study". In: *Life-Cycle Civil Engineering: Innovation, Theory and Practice. Proceedings of the 7th International Symposium on Life-Cycle Civil Engineering.* 2021.

[18] A. Kamariotis, E. Chatzi, and D. Straub. "Value of information from vibration-based structural health monitoring extracted via Bayesian model updating". In: *Mechanical Systems and Signal Processing* 166 (2022), p. 108465.

[19] K. Konakli, B. Sudret, and M. H. Faber. "Numerical Investigations into the Value of Information in Lifecycle Analysis of Structural Systems". In: *ASCE-ASME Journal of Risk and Uncertainty in Engineering Systems, Part A: Civil Engineering* 2(3) (2016), B4015007.

[20] M. Limongelli, E. Chatzi, E. Reynders, and G. Lombaert. "Towards extraction of vibration-based damage indicators". In: *Proceedings of the 8th European Workshop On Structural Health Monitoring (EWSHM 2016).* Bilbao, Spain, 2016, pp. 546–555.

[21] J. Luque and D. Straub. "Risk-based optimal inspection strategies for structural systems using dynamic Bayesian Networks". In: *Structural Safety* 76 (2019), pp. 68–80.

[22] R. E. Melchers and A. Beck. *Structural Reliability Analysis and Prediction, 3rd Edition.* John Wiley & Sons, Ltd, 2017.

[23] E. Ntotsios, C. Papadimitriou, P. Panetsos, G. Karaiskos, K. Perros, and P. Perdikaris. "Bridge health monitoring system based on vibration measurements". In: *Bull Earthquake Engineering* 7 (2009), pp. 469–483.

[24] A. Pandey, M. Biswas, and M. Samman. "Damage detection from changes in curvature mode shapes". In: *Journal of Sound and Vibration* 226(2) (1991), pp. 217–235.

[25] K. Papakonstantinou and M. Shinozuka. "Planning structural inspection and maintenance policies via dynamic programming and Markov processes. Part I: Theory". In: *Reliability Engineering & System Safety* 130 (2014), pp. 202–213.

[26] B. Peeters and G. D. Roeck. "Reference-based stochastic subspace identification for output-only modal analysis". In: *Mechanical Systems and Signal Processing* 13(6) (1999), pp. 855–878.

[27] M. Pozzi and A. D. Kiureghian. "Assessing the Value of Information for long-term structural health monitoring". In: *SPIE Conference on Health Monitoring of Structural and Biological Systems.* San Diego, California, USA, 2011.

[28] L. Prendergast and K. Gavin. "A review of bridge scour monitoring techniques". In: *Journal of Rock Mechanics and Geotechnical Engineering* 6 (2014), pp. 138–149.

[29] H. Raiffa and R. Schlaifer. *Applied statistical decision theory.* Harvard University, Boston: Division of Research, Graduate School of Business Administration, 1961.

[30] E. Reynders, R. Pintelon, and G. D. Roeck. "Uncertainty bounds on modal parameters obtained from stochastic subspace identification". In: *Mechanical Systems and Signal Processing* 22 (2008), pp. 948–969.

[31] E. Simoen, B. Moaveni, J. P. Conte, and G. Lombaert. "Uncertainty Quantification in the Assessment of Progressive Damage in a 7-Story Full-Scale Building Slice". In: *Journal of Engineering Mechanics* 139(12) (2013), pp. 1818–1830.

[32] E. Simoen, C. Papadimitriou, and G. Lombaert. "On prediction error correlation in Bayesian model updating". In: *Journal of Sound and Vibration* 18 (2013), pp. 4136–4152.

[33] E. Simoen, G. D. Roeck, and G. Lombaert. "Dealing with uncertainty in model updating for damage assessment: a review". In: *Mechanical Systems and Signal Processing* 56 (2015), pp. 123–149.

[34] D. Straub. "Value of information analysis with structural reliability methods". In: *Structural Safety* 49 (2014), pp. 68–80.

[35] D. Straub, E. Chatzi, E. Bismut, et al. "Value of information: A roadmap to quantifying the benefit of structural health monitoring". In: *Proceedings of the 12th International Conference on Structural Safety and Reliability: ICOSSAR 2017*. Vienna, Austria, 2017, pp. 3018–3029.

[36] D. Straub and M. H. Faber. "Risk based inspection planning for structural systems". In: *Structural Safety* 27(4) (2005), pp. 335–355.

[37] D. Straub, R. Schneider, E. Bismut, and H.-J. Kim. "Reliability analysis of deteriorating structural systems". In: *Structural Safety* 82 (2020), p. 101877.

[38] K. Tatsis and E. Chatzi. "A numerical benchmark for system identification under operational and environmental variability". In: *8th International Operational Modal Analysis Conference (IOMAC 19)*. Copenhagen, Denmark, 2019.

[39] S. Thöns, R. Schneider, and M. Faber. "Quantification of the Value of Structural Health Monitoring Information for Fatigue Deteriorating Structural Systems". In: *Proceedings of the 12th International Conference on Applications of Statistics and Probability in Civil Engineering*. Vancouver, Canada, 2015.

[40] M. Vanik, J. Beck, and S. Au. "Bayesian Probabilistic approach to Structural Health Monitoring". In: *Journal of Engineering Mechanics* 126(7) (2000), pp. 738–745.

[41] E. Vereecken, W. Botte, G. Lombaert, and R. Caspele. "Bayesian decision analysis for the optimization of inspection and repair of spatially degrading concrete structures". In: *Engineering Structures* 220 (2020), p. 111028.

[42] A. Wirgin. "The inverse crime". In: *arXiv e-prints*, math-ph/0401050 (2004), math–ph/0401050.

[43] L. Wright and S. Davidson. "How to tell the difference between a model and a digital twin". In: *Advanced Modeling and Simulation in Engineering Sciences* 7(1) (2020).

[44] K. Yueng and S. Kuok. "Bayesian methods for updating dynamical models". In: *Applied Mechanics Reviews* 64 (2011), pp. 010802–1.

[45] W. Zhang, J. Qin, D. Lu, S. Thöns, and M. H. Faber. "VoI-informed decision-making for SHM system arrangement". In: *Structural Health Monitoring* 21(1) (2022), pp. 37–58.

[46] D. Zonta, B. Glisic, and S. Adriaenssens. "Value of Information: impact of monitoring on decision making". In: *Structural Control and Health Monitoring* 21(7) (2014), pp. 1043–1056.

Chapter 5

A framework for quantifying the value of vibration-based structural health monitoring

Original Publication

A. Kamariotis, E. Chatzi, and D. Straub. "A framework for quantifying the value of vibration-based structural health monitoring". In: *Mechanical Systems and Signal Processing* 184 (2023), p. 109708.

Author's contribution

Antonios Kamariotis: Conceptualization, Methodology, Software, Formal analysis, Visualization, Writing - original draft. **Eleni Chatzi**: Conceptualization, Methodology, Writing - review & editing, Funding acquisition. **Daniel Straub**: Conceptualization, Methodology, Writing - review & editing, Funding acquisition.

Abstract

The difficulty in quantifying the benefit of Structural Health Monitoring (SHM) for decision support is one of the bottlenecks to an extensive adoption of SHM on real-world structures. In this paper, we present a framework for such a quantification of the value of vibration-based SHM, which can be flexibly applied to different use cases. These cover SHM-based decisions at different time scales, from near-real time diagnostics to the prognosis of slowly evolving deterioration processes over the lifetime of a structure. The framework includes an advanced model of the SHM system. It employs a Bayesian filter for the tasks of sequential joint deterioration state-parameter estimation and structural reliability updating, using continuously identified modal and intermittent visual inspection data. It also includes a realistic model of the inspection and maintenance decisions throughout the structural life-cycle. On this basis, the Value of SHM is quantified by the difference in expected total

life-cycle costs with and without the SHM. We investigate the framework through application on a numerical model of a two-span bridge system, subjected to gradual and shock deterioration, as well as to changing environmental conditions, over its lifetime. The results show that this framework can be used as an a-priori decision support tool to inform the decision on whether or not to install a vibration-based SHM system on a structure, for a wide range of SHM use cases.

5.1 Introduction

Operation and maintenance (O&M) of structures and infrastructures addresses various potential threats (e.g., gradual deterioration, extreme events) that can adversely affect the intended performance of these systems. This creates the need for inspection, maintenance and repair actions throughout a system's life-cycle, which come at a large cost [51, 37]. In the current approach to O&M, visual inspection still remains the primary, and oftentimes sole, source of information on the condition of a structure over its life-cycle.

Structural Health Monitoring (SHM) is defined as a continuous, automated, on-line process for damage assessment, whose ultimate goal is to provide cradle-to-grave system state awareness [13]. Continuous vibration-based SHM systems offer a great potential for facilitating and enhancing the O&M decision making process. Despite comprehensive scientific and practical developments in the field of SHM [12], adoption of SHM systems on real-world structures and infrastructure systems falls short of the mark [9], due to a number of challenges. These include the fact that damage-sensitive features can be very sensitive to changes in environmental and operational conditions (EOCs) [41, 35]. Furthermore, since there exist only a limited number of deployments of such systems on real-world structures, and since data from damage states are rarely available, it is often not clear how to make efficient use of acquired monitoring data for statistical decision making in a supervised learning mode. Besides, it is difficult to convince owners and operators of the potential economic benefit of installing SHM systems [67].

A clear need exists for offering actionable use cases, elaborating on the manner in which SHM systems can lead to enhanced management of structural deterioration, and how these can eventually inform optimal maintenance decisions over the structural life-cycle. A wide range of diverse SHM systems is continuously being developed and made available for application on a wide range of structures for performing various damage detection tasks. In designing a case-specific SHM system, one should start by defining the specific target structure and the associated damages that one pursues to detect with this system [12].

Bayesian decision analysis [46] offers a formal mathematical framework which enables investigating a-priori, i.e., prior to the installation of the SHM system, how monitoring data from a specific SHM system can inform inspection, maintenance or repair actions over the life-cycle of a structure subjected to a certain type of damage. Bayesian decision analysis further enables quantification of the effect of SHM systems on structural life-cycle costs through the Value of Information (VoI) [42, 54, 61, 18, 64, 38, 25].

The current paper presents a Bayesian decision analysis framework for the quantification of the value of continuous vibration-based SHM, which is applicable across different time scales. In contrast to

most works to date, which utilize simple idealized models of the information obtained from monitoring, we employ a realistic model of a vibration-based SHM system, considering modal data that is continuously identified via operational modal analysis (OMA) schemes. Our analysis also includes the effect of environmental variability on the identified modal data, a key issue in vibration-based SHM. Finally, the framework includes the full sequence of inspection and maintenance decisions throughout the structural life-cycle rather than just individual decisions, as in most of the literature.

The paper is organized as follows. Section 5.2 offers a fundamental classification of SHM use cases in terms of the associated time scales for decision making. Section 5.3 presents the proposed Bayesian decision analysis framework and the associated Value of SHM (VoSHM) metric. Section 5.4 introduces an environmental variability model and a structural deterioration model, and discusses sequential Bayesian learning of these models using continuous SHM data and inspection data. Section 5.5 contains an algorithmic summary of the presented framework for quantifying the VoSHM. Section 5.6 demonstrates application of this framework on different SHM use cases with the aid of a numerical model of a deteriorating two-span bridge system. Finally, Section 5.7 discusses and concludes this work.

5.2 SHM use cases across different time scales

In this section, we discuss various SHM use cases in relation to the different time scales at which they support decision making for infrastructure (Fig. 5.1), with a particular focus on application of SHM systems on civil structures. The main challenges associated with an efficient use of the data provided by an SHM system for decision support at each time scale are laid out.

5.2.1 Real-time or near real-time diagnostics (seconds to hours)

At this time scale, fast, almost on-line, detection of flaws or abnormalities is sought. When discussing a scale of seconds, one typically refers to real-time tracking and diagnostic tasks. This is particularly relevant in the context of control, where a possible failure of the control system (e.g., active vibration control) should be computed almost instantly. Near real-time tasks relax the requirements on the speed of reaction but still call for accelerated diagnosis, typically linked to emergency operations (e.g., smart tagging of buildings after an earthquake, powering down a wind turbine after a lightning strike, promptly deciding on whether to close down a bridge after a flood occurrence [43]). SHM can be valuable in informing near real-time decisions for avoiding catastrophic failures (e.g., bridge support or wind turbine blade failure), or avoiding unnecessary closures and down-time after the occurrence of an extreme event (e.g., rapid seismic loss assessment of structures using near real-time data [62]). Quantifying the VoSHM over the system lifetime requires a model of the occurrence of extreme events (shocks) [48, 21] that induce these abrupt failures (e.g., wind, flood, earthquake). A main challenge at this time scale stems from the real-time nature of required diagnostics, which implies fast computation, as well as from the masking influence of varying EOCs on the detection capabilities. Moreover, derivation of robust data-driven diagnostics in a fully unsupervised and automated manner is an intricate task. It is difficult to achieve higher-end SHM tasks beyond damage detection, such as damage localization or quantification, in a purely "on-line" data-driven

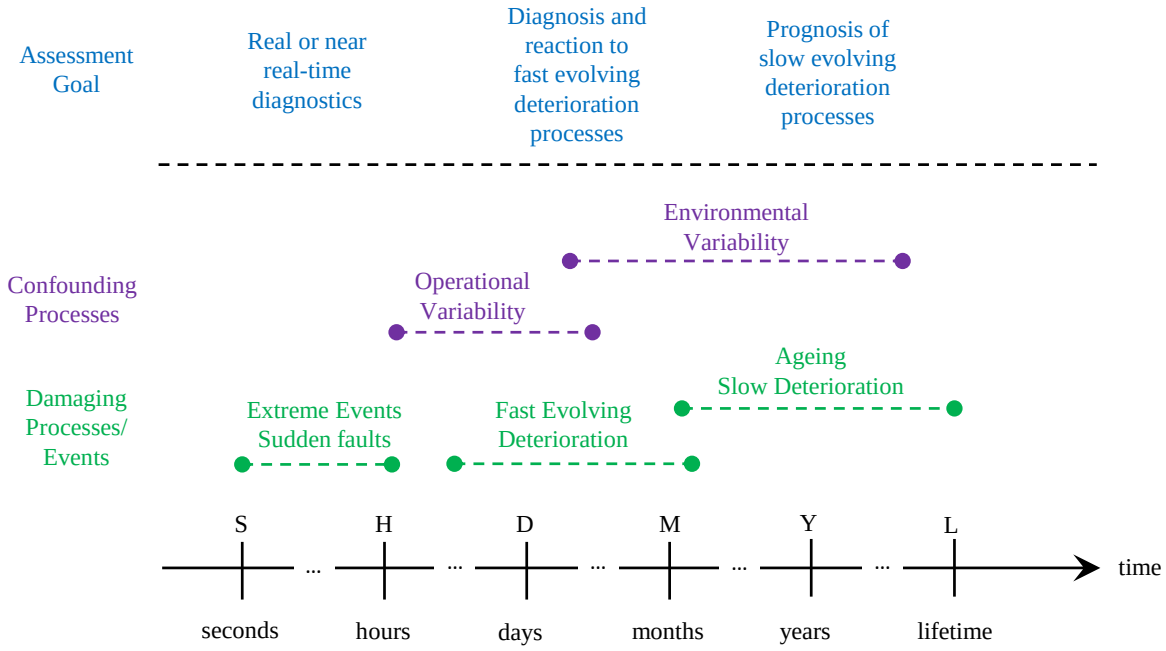

Figure 5.1: SHM use case-dependent time scales for decision making

fashion, without use of a dedicated model.

5.2.2 Fast-evolving deterioration processes (days to months)

Here, the objective lies in identifying structural deterioration processes with a rather fast rate of evolution, or capturing sudden damage increments caused by shock deterioration, which could endanger capacity, availability or serviceability. At this time scale, application of SHM should assist in avoiding failure and ensuring the desired safety and performance levels. Examples of damage types induced by effects at this time scale could be, e.g., a shaft failure on a train bogie after crack initiation, concrete bridge failure due to a fast evolving Akali-silica reaction (ASR) process [20], or freeze-thaw related damages [47]. Quantification of the VoSHM in such cases requires models for simulating such accelerated or shock deterioration processes [48, 21]. Furthermore, models are needed for the estimation of the structural reliability [33], which can be used as a metric to evaluate structural performance. Accounting for EOC variability can pose a significant challenge at this time scale as well.

5.2.3 Slow-evolving deterioration processes (years/life)

Over larger time spans, SHM can be used to support decisions on corrective, preventive or predictive maintenance associated with slowly-evolving gradual deterioration processes, such as fatigue or corrosion. Models for simulating such deterioration processes over the life-cycle [48, 21], as well as models for estimating the structural reliability and its updating using Bayesian methods [57], are

indispensable for a VoSHM analysis. At this time scale, main challenges include EOC variability, loads which are typically increasing over time (e.g. heavier trucks), abrupt changes in the assumed deterioration model (e.g., due to shock events).

5.2.4 Summary

The operation of real structural systems typically involves a combination of the above-mentioned potential threats. A successful management strategy should prescribe a plan for addressing these threats throughout the structural life-cycle. The main goal of this paper is to show that adoption of the proposed Bayesian decision analysis framework can lead to a comprehensive tool for performing quantitative VoSHM studies across these diverse time scales. Eventually, this framework can act as an a-priori decision support tool for the crucial decision on whether adoption of a specific SHM system can be cost-beneficial.

5.3 Bayesian decision analysis framework for the quantification of the VoSHM

In a decision analysis, the goal is to find the optimal set of actions which maximize the expected utility. For most engineering applications, utility can be equated with the negative total life-cycle costs [58]. Therefore, the problem translates to finding the optimal set of actions over the structural lifetime, that minimize the expected total life-cycle costs.

The total life-cycle costs $C_{\text{tot}}(\boldsymbol{X}, \boldsymbol{a})$ are defined as a function of a random vector $\boldsymbol{X}$, containing the parameters of the stochastic deterioration model and the structural response quantities, as well as a set of actions $\boldsymbol{a}$ that are performed on the system at different points in time over its life-cycle, such as inspection, repair or maintenance. Different cost components synthesize the overall costs $C_{\text{tot}}(\boldsymbol{X}, \boldsymbol{a})$ [15]. Because the initial cost of construction and the decommissioning cost at the end of the structure's lifetime are not affected by the SHM, they can be ignored for the VoSHM analysis. Therefore, $C_{\text{tot}}(\boldsymbol{X}, \boldsymbol{a})$ is the sum of the inspection costs C_{I}, the maintenance costs C_{M}, and the risk (the expected cost of failures) R_{F} over the lifetime of the structure:

$$C_{\text{tot}}(\boldsymbol{X}, \boldsymbol{a}) = C_{\text{I}}(\boldsymbol{X}, \boldsymbol{a}) + C_{\text{M}}(\boldsymbol{X}, \boldsymbol{a}) + R_{\text{F}}(\boldsymbol{X}, \boldsymbol{a}) \tag{5.1}$$

The goal is to find at any decision time step t the optimal set of inspection, repair and maintenance actions $\boldsymbol{a}_t$ that lead to a balance between the discounted cost of these actions and the failure risk [56, 39]. The risk of a failure event $F(t)$ at time step t, can be quantified via the outcome of a structural reliability analysis [57, 33].

A prior decision analysis is performed, where one only has access to prior information on the random vector $\boldsymbol{X}$. In a prior decision analysis, the optimal set of actions over the structural life-cycle is found as

$$\boldsymbol{a}_{\text{opt}} = \arg\min_{\boldsymbol{a}} \mathbb{E}_{\boldsymbol{X}}[C_{\text{tot}}(\boldsymbol{X}, \boldsymbol{a})], \tag{5.2}$$

where $\mathbb{E}_{\boldsymbol{X}}$ is the expectation with respect to the prior distribution $f_{\boldsymbol{X}}(\boldsymbol{x})$.

The benefit of monitoring is that it can provide information that reduces the uncertainty on the deterioration state and model parameters, thus enabling monitoring-informed risk estimation, which ultimately leads to better decisions. Once monitoring data $\boldsymbol{z}$ becomes available, one can perform a posterior decision analysis, in order to find the set of actions that are optimal conditional on the monitoring data. This requires solving the following optimization problem:

$$\boldsymbol{a}_{\text{opt}|\boldsymbol{z}} = \arg\min_{\boldsymbol{a}} \mathbb{E}_{\boldsymbol{X}|\boldsymbol{z}}[C_{\text{tot}}(\boldsymbol{X}, \boldsymbol{a})], \tag{5.3}$$

where the expectation $\mathbb{E}_{\boldsymbol{X}|\boldsymbol{z}}$ operates over the distribution of $\boldsymbol{X}$ conditional on $\boldsymbol{z}$. Therefore, prior to solving the optimization problem of Eq. (5.3), one has to perform Bayesian analysis [17, 50] to estimate the posterior distribution $f_{\boldsymbol{X}|\boldsymbol{z}}(\boldsymbol{x} \mid \boldsymbol{z})$, which is presented in Section 5.4.

The monitoring data $\boldsymbol{z}$ becomes available only after installation of an SHM system. However, typically one is interested in investigating the potential benefit of the deployment of a specific SHM system prior to its installation. In that case, a dedicated model of the SHM system must be employed to allow for probabilistic predictions of the monitoring information $\boldsymbol{Z}$ that one expects to extract with monitoring, for given sampled realizations of the random vector $\boldsymbol{X}$. Upper case $\boldsymbol{Z}$ therefore denotes the yet unknown monitoring information, while a realization of $\boldsymbol{Z}$ is denoted by lower case $\boldsymbol{z}$. The value-of-information analysis is conducted prior to observing any actual monitoring data $\boldsymbol{z}$, relying instead on simulated data. Hence this is known as a preposterior analysis [46]. The expected total life-cycle cost in such a preposterior decision analysis is written as

$$\mathbb{E}_{\boldsymbol{X},\boldsymbol{Z}}[C_{\text{tot}}(\boldsymbol{X}, \boldsymbol{a}_{\text{opt}|\boldsymbol{z}})], \tag{5.4}$$

where one can observe that the expectation $\mathbb{E}_{\boldsymbol{X},\boldsymbol{Z}}$ jointly operates over $\boldsymbol{X}$ and $\boldsymbol{Z}$. Using a sampling-based approach, for a realization of the structural system's uncertain parameters and response state space, i.e., for a given $\boldsymbol{X}$, one has to employ a model of the investigated SHM system to probabilistically predict the monitoring data $\boldsymbol{z}$ (observations) that the SHM system will provide over the life-cycle. With such a model, one can sample one (or more) realizations of $\boldsymbol{z}$. Any type of information that can be extracted from the SHM system and that can be used as a damage sensitive feature can be considered as a sampled $\boldsymbol{z}$ realization (see Section 5.6.1). For each sampled $\boldsymbol{z}$ realization, one subsequently needs to perform a posterior decision analysis, as in Eq. (5.3), to find the posterior optimal set of actions $\boldsymbol{a}_{\text{opt}|\boldsymbol{z}}$. This analysis has to be performed multiple times, for a sufficiently large set of samples of $\boldsymbol{X}, \boldsymbol{Z}$. The Value of Information (VoI) is quantified by taking the difference between the expected total life-cycle cost in the prior decision analysis and the expected total life-cycle cost in the preposterior decision analysis, as follows:

$$VoI = \mathbb{E}_{\boldsymbol{X}}[C_{\text{tot}}(\boldsymbol{X}, \boldsymbol{a}_{\text{opt}})] - \mathbb{E}_{\boldsymbol{X},\boldsymbol{Z}}[C_{\text{tot}}(\boldsymbol{X}, \boldsymbol{a}_{\text{opt}|\boldsymbol{z}})] \tag{5.5}$$

A VoI analysis offers a formal framework for quantifying the effect of SHM systems on structural life-cycle costs [42, 54, 55]. However, quantifying the VoI in this way is not very informative for system owners and operators, as it assumes that in the reference case neither inspection nor monitoring data will be available. It is seldom the case that no inspection or monitoring takes place throughout the whole life-cycle of a structure. Typically, intermittent visual inspection schemes are adopted by operators, with targeted non-destructive evaluations also complementing inspection when needed [9]. Therefore, to demonstrate the potential benefit of deploying continuous SHM systems on structures, as compared against the typical case of intermittent visual inspections, a more specialized metric, the Value of Structural Health Monitoring (VoSHM)[3], can be introduced:

$$VoSHM = \mathbb{E}_{\boldsymbol{X},\boldsymbol{Z}_{\text{insp}}}[C_{\text{tot}}(\boldsymbol{X}, \boldsymbol{a}_{\text{opt}|\boldsymbol{z}_{\text{insp}}})] - \mathbb{E}_{\boldsymbol{X},\boldsymbol{Z}_{\text{insp}},\boldsymbol{Z}_{\text{SHM}}}[C_{\text{tot}}(\boldsymbol{X}, \boldsymbol{a}_{\text{opt}|\boldsymbol{z}_{\text{insp}},\boldsymbol{z}_{\text{SHM}}})] \tag{5.6}$$

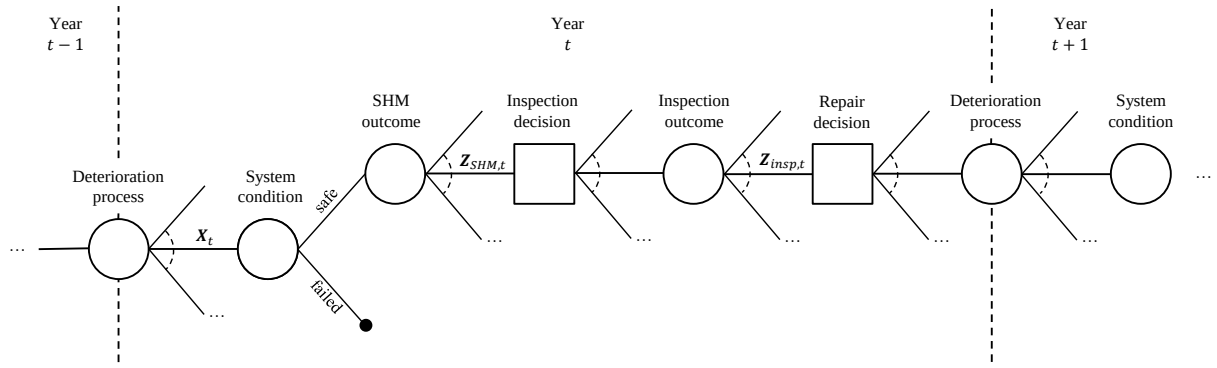

Figure 5.2: Decision tree illustrating a preposterior decision analysis for a deteriorating structure, which is continuously monitored from an SHM system, which can additionally be inspected and repaired.

The formulation of Eq. (5.6) implies that the quantification of the VoSHM emerges from the solution of two different preposterior decision analyses. In Eq. (5.6), we no longer use the generic variable $\boldsymbol{Z}$ to denote observations at large, but instead enforce a distinction between the data obtained from the continuous SHM system, denoted as $\boldsymbol{Z}_{\text{SHM}}$, and the data obtained via intermittent visual inspections, denoted as $\boldsymbol{Z}_{\text{insp}}$. Similarly to the requirement of a model of the monitoring system to probabilistically predict $\boldsymbol{Z}_{\text{SHM}}$, one further needs a model that enables probabilistic predictions of the inspection data $\boldsymbol{Z}_{\text{insp}}$. In $\mathbb{E}_{\boldsymbol{X},\boldsymbol{Z}_{\text{insp}}}[C_{\text{tot}}(\boldsymbol{X}, \boldsymbol{a}_{\text{opt}|\boldsymbol{z}_{\text{insp}}})]$ the total expected life-cycle cost is computed for the case when only inspection data is available. In $\mathbb{E}_{\boldsymbol{X},\boldsymbol{Z}_{\text{insp}},\boldsymbol{Z}_{\text{SHM}}}[C_{\text{tot}}(\boldsymbol{X}, \boldsymbol{a}_{\text{opt}|\boldsymbol{z}_{\text{insp}},\boldsymbol{z}_{\text{SHM}}})]$, the total expected life-cycle cost is computed for the case of continuous monitoring data, enriched by additional inspection information. The latter problem is illustrated by the decision tree in Fig. 5.2. The defined VoSHM metric assumes that an SHM system will be used in conjunction with some additional inspection policy (which will be informed by the SHM outcome), as -in a practical setting- operators would not allocate sufficient trust on a completely autonomous and unsupervised monitoring system, thus entirely replacing inspections.

5.3.1 Solution of the sequential decision problem via adoption of heuristics

A key challenge of a preposterior decision analysis is the identification of the optimal set of actions conditional on data $\boldsymbol{a}_{\text{opt}|\boldsymbol{z}}$. The optimization of inspection and maintenance plans forms a stochastic sequential decision problem [30, 28], the solution of which requires large computational efforts [54, 34]. Numerous algorithms are available for the solution of this problem, e.g., via proposal of a set of simple decision heuristics [30, 7], through partially observable Markov decision processes (POMDPs) [3, 34], or through deep reinforcement learning [2].

The concepts of policies and strategies have been introduced for the solution of sequential decision problems [19, 7]. A policy at time t is a set of rules which prescribes the decisions to be made at time t, based on all the structural state information available up to that time, i.e., past inspection and monitoring data $\boldsymbol{Z}$ and performed actions. Here, a policy at time t answers the following two questions: 1) 'Inspect the structure?', 2) 'Repair the structure?'. A strategy S is the set of policies for all time steps t of the decision time horizon, which typically reflects the intended lifetime of the

structure. If a strategy consists of policies which are the same at all times t, then the strategy is called stationary.

Heuristics, which are simple and intuitive rules that are easily understood by engineers and operators, can be used to parametrize a stationary strategy [30, 7]. The three heuristics applied herein are described below. These are based on the premise that structural performance at any time t conditional on inspection and monitoring results can be assessed via the structural reliability estimate. With Bayesian methods, past inspection and monitoring information can be used to update the structural reliability estimate [57].

1. *Reliability threshold for inspections* p_{th}^{I}. An inspection is performed at any time step before the updated estimate of the structural reliability exceeds p_{th}^{I}.
2. *Fixed-interval periodic inspections* Δt_{I}. Periodic inspections are performed every Δt_{I} years.
3. *Reliability threshold for repair* p_{th}^{R}. A repair is performed at any time step before the updated estimate of the structural reliability exceeds p_{th}^{R}.

We define the heuristic parameter vector $\boldsymbol{w} = [p_{\text{th}}^{\text{I}}, \Delta t_{\text{I}}, p_{\text{th}}^{\text{R}}]$. A strategy parametrized by the heuristic parameter vector $\boldsymbol{w}$ is denoted $S_{\boldsymbol{w}}$. With the use of heuristics, the optimal set of actions conditional on data $\boldsymbol{z}$, $\boldsymbol{a}_{\text{opt}|\boldsymbol{z}}$, is approximated by the applied optimal heuristic parameter values, which drastically reduces the space of solutions to the decision problem. In this way, the solution of the sequential decision problem boils down to finding the optimal set of heuristic parameter values $\boldsymbol{w}^*$ for which the strategy $S_{\boldsymbol{w}^*}$ is optimal, i.e., leads to the minimum expected total life-cycle costs.

$$S_{\boldsymbol{w}^*} = \arg\min_{\boldsymbol{w}} \mathbb{E}\left[C_{\text{tot}}\left(\boldsymbol{X}, \boldsymbol{Z}, \boldsymbol{w}\right)\right] \tag{5.7}$$

With the use of heuristics, Eq. (5.6) can be reformulated as follows:

$$VoSHM = \mathbb{E}_{\boldsymbol{X},\boldsymbol{Z}_{\text{insp}}}\left[C_{\text{tot}}\left(\boldsymbol{X}, \boldsymbol{Z}_{\text{insp}}, \boldsymbol{w}_1^*\right)\right] - \mathbb{E}_{\boldsymbol{X},\boldsymbol{Z}_{\text{insp}},\boldsymbol{Z}_{\text{SHM}}}\left[C_{\text{tot}}\left(\boldsymbol{X}, \boldsymbol{Z}_{\text{insp}}, \boldsymbol{Z}_{\text{SHM}}, \boldsymbol{w}_2^*\right)\right] \tag{5.8}$$

Eq. (5.8) indicates that the optimal heuristic parameter vectors $\boldsymbol{w}_1^*$ and $\boldsymbol{w}_2^*$ emerging from the solution of the two different preposterior decision analyses will differ. Obtaining $\boldsymbol{w}_2^*$ would typically require much larger computational effort than determining $\boldsymbol{w}_1^*$.

The problem can be further simplified by replacing the optimization of the heuristic parameters in Eq. (5.7) by a choice based on expert assessment, which better reflects what is typically done in practice, where optimization is rarely performed.

A Monte Carlo approach can be used to estimate the expected total life-cycle cost for given heuristic strategies for both terms in Eq. (5.8). The Monte Carlo approximation of the $VoSHM$ is

$$VoSHM \approx \frac{1}{n_{\text{MCS}}} \sum_{i=1}^{n_{\text{MCS}}} \left[C_{\text{tot}}\left(\boldsymbol{x}^{(i)}, \boldsymbol{z}_{\text{insp}}^{(i)}, \boldsymbol{w}_1^*\right) - C_{\text{tot}}\left(\boldsymbol{x}^{(i)}, \boldsymbol{z}_{\text{insp}}^{(i)}, \boldsymbol{z}_{\text{SHM}}^{(i)}, \boldsymbol{w}_2^*\right)\right] \tag{5.9}$$

wherein $\boldsymbol{x}^{(i)}$ are random samples drawn from the prior distribution $f_{\boldsymbol{X}}(\boldsymbol{x})$, $\boldsymbol{z}_{\text{insp}}^{(i)}$ are samples from the inspection likelihood function $f_{\boldsymbol{Z}_{\text{insp}}|\boldsymbol{X}}(\cdot|\boldsymbol{x}^{(i)})$ and $\boldsymbol{z}_{\text{SHM}}^{(i)}$ are sampled data from the model of the SHM system.

5.3.1.1 Cost breakdown

For a given heuristic strategy, i.e., for a given $\boldsymbol{w}$, and for given inspection $\boldsymbol{z}_{\text{insp}}^{(i)}$ and monitoring outcomes $\boldsymbol{z}_{\text{SHM}}^{(i)}$, the inspection and repair actions over the structural life-cycle are fixed, and the costs are computed as follows:

$$C_{\text{I}}\left(\boldsymbol{x}^{(i)}, \boldsymbol{z}_{\text{insp}}^{(i)}, \boldsymbol{z}_{\text{SHM}}^{(i)}, \boldsymbol{w}\right) = \sum_{j=1}^{n_{\text{insp}}} \gamma\left(t_{\text{insp}}^{(j)}\right) \widetilde{c}_{\text{I}} \tag{5.10}$$

$$C_{\text{R}}\left(\boldsymbol{x}^{(i)}, \boldsymbol{z}_{\text{insp}}^{(i)}, \boldsymbol{z}_{\text{SHM}}^{(i)}, \boldsymbol{w}\right) = \sum_{j=1}^{n_{\text{rep}}} \gamma\left(t_{\text{rep}}^{(j)}\right) \widetilde{c_{\text{R}}}, \tag{5.11}$$

where $\widetilde{c}_{\text{I}}$, $\widetilde{c_{\text{R}}}$ are the costs of an individual inspection and repair respectively, and $\gamma(t) = \frac{1}{(1+r)^t}$ is the discounting function, with r denoting the annually compounded discount rate.

The failure risk R_{F} is defined as

$$R_{\text{F}}\left(\boldsymbol{x}^{(i)}, \boldsymbol{z}_{\text{insp}}^{(i)}, \boldsymbol{z}_{\text{SHM}}^{(i)}, \boldsymbol{w}\right) = \sum_{j=1}^{T} \gamma(t_j) \widetilde{c_{\text{F}}} \left\{ \Pr[F(t_j)|\boldsymbol{x}^{(i)}] - \Pr[F(t_{j-1})|\boldsymbol{x}^{(i)}] \right\}, \tag{5.12}$$

where $\widetilde{c_{\text{F}}}$ is the cost of a failure event, and $Pr[F(t_j)|\boldsymbol{x}^{(i)}]$ is the conditional probability of failure of the structure up to time t_j, conditional on a sampled value $\boldsymbol{x}^{(i)}$ of the random vector $\boldsymbol{X}$. Its computation forms a structural reliability problem, which is laid out in Section 5.4.3.

5.3.2 Summary of the framework for quantifying the value of vibration-based SHM

Section 5.3 presents the Bayesian decision analysis framework in a general way, and then specifically introduces the VoSHM metric in Eq. (5.6), which forms the basis for the presented framework for the quantification of the value of vibration-based SHM.

Eq. (5.6) reveals that in order to perform a VoSHM analysis, one needs to specify different models and computational approaches. A probabilistic model of the random vector $\boldsymbol{X}$ needs to be defined, which in this paper is detailed in Section 5.4, where it is exemplified for a specific environmental variability model and deterioration model. A case-specific model of the vibration-based SHM system must be defined to allow for probabilistic predictions of the SHM outcomes $\boldsymbol{Z}_{\text{SHM}}$ (see Fig. 5.5), which can be made specific only in accordance with the case study at hand, while, lastly, a specific inspection model is required for sampling inspection outcomes $\boldsymbol{Z}_{\text{insp}}$ (see Eq. (5.25)). One further needs to define the stochastic sequential decision-making problem for the optimization of inspection and maintenance plans and choose the corresponding computational method for its solution. The solution to the latter problem using heuristics has been introduced in Section 5.3.1. Section 5.5 summarizes the algorithm for evaluation of Eq. (5.6), i.e., it provides the computational specifics of the framework.

5.4 Environmental variability modeling, deterioration modeling and Bayesian analysis

5.4.1 Environmental variability model

The premise of vibration-based SHM methods is that damage induces changes in the structural system's modal characteristics, e.g., the system's natural frequencies and mode shapes [13]. Thereby it must be considered that varying environmental and operational conditions also affect the system's modal characteristics. Temperature affects the stiffness (the effective Young's modulus) of civil structures [41, 35, 31]. The resulting changes in the system's modal characteristics owing to temperature variability can often be more prominent than the changes due to significant damage. Related to the effect of the temperature variability on the VoSHM, the authors have shown in [22] that not properly accounting for the environmental variability present in the SHM data can have a detrimental effect on the maintenance decisions triggered by the SHM system. Accounting for the effects of temperature variability is therefore of utmost importance within a vibration-based damage identification framework, and various ways to do that have been suggested in literature [35, 14, 53].

The dependence of the system's identified natural frequencies on temperature may often be nonlinear [35], especially in environments where the structure can experience below-freezing temperatures, and this nonlinearity has to be taken into account in the modeling. The following model for the Young's modulus as a function of temperature is employed, which was previously used to capture the dependence present in real data obtained from a bridge structure [4].

$$E(T_t) = \theta(T_t) \cdot E_0 \tag{5.13}$$

$$\theta(T_t) = Q + H \cdot T_t + U \cdot \left(1 - \text{erf}\left(\frac{T_t - Y}{\tau}\right)\right) \tag{5.14}$$

E_0 is the nominal value for the Young's modulus at a reference temperature of 20°C. The effective Young's modulus at a time instance t, for a given temperature T_t, is given by Eq. (5.13). The structural parameter θ is introduced as a modification factor for the effective Young's modulus at a given temperature T_t. $\theta(T_t)$ is a stochastic function of temperature, shown in Eq. (5.14), which is described by a parameter vector $[Q, H, U, Y, \tau]$ of independent random variables, each following an assigned prior probability distribution. Q models the intercept of the linear trend in the above-freezing temperature range, while H models the slope of the linear trends observed in both above and below-freezing temperatures, after the nonlinear transition around temperature Y. τ models the transition range, while U defines the size of increase in the Young's modulus at the end of the transition to the below-freezing temperature range.

5.4.1.1 Bayesian learning of the environmental variability model

Let us consider a case when an SHM system is installed on a civil structure from the beginning of its operation. Typically, vibration-based SHM systems rely on the deployment of acceleration sensors, which can provide continuous dynamic response measurements in the form of acceleration time series, for unknown ambient excitation. These can be subsequently processed by output-only operational modal analysis (OMA) schemes, e.g., the stochastic subspace identification (SSI) algorithm [40],

for identifying the system's modal characteristics. Temperature sensors can further be easily and inexpensively deployed on a structure, which can provide ambient temperature measurements. With the assumption that the structure will be in a healthy state and that no damage will be present at the beginning of its service life, one can make use of modal data identified at different temperatures in the first few months of operation (half a year to one year will usually be needed to get 'extreme' temperatures at both ends of the scale), in order to learn the underlying dependence of the Young's modulus on temperature ($E-T$) via Bayesian analysis.

The data obtained from such an SHM system, comprising acceleration and temperature sensors, can be summarized as different sets $\{\widetilde{\lambda}_{t_m}, \widetilde{T}_t; m=1,..,N_m\}$ of vectors of the N_m lower system eigenvalues $\widetilde{\lambda}_{t_m}$ identified via an OMA procedure at time t for a temperature $\widetilde{T}_t$. The modal eigenvalues are $\widetilde{\lambda}_{t_m} = (2\pi \widetilde{f}_{t_m})^2$, where $\widetilde{f}_{t_m}$ are the modal eigenfrequencies.

Consider a linear finite element (FE) model $\mathcal{G}$ of the structural system, parametrized via Eq. (5.13), which is used to predict the modal eigenvalues for different input values of the effective Young's modulus. The goal of the Bayesian inverse problem is to estimate the parameters $[Q, H, U, Y, \tau]$ of the stochastic model of Eq. (5.14), and their uncertainty, such that the FE model predicted modal eigenvalues $\left\{\lambda^{\mathcal{G}}_{t_m}\left(E=\theta(\widetilde{T}_t)\cdot E_0\right), m=1,..,N_m\right\}$ best match the corresponding OMA-identified modal eigenvalues. The joint posterior probability distribution of the updating parameters is obtained via Bayesian analysis.

The likelihood function can be formulated by assuming a probabilistic model for the discrepancy between the OMA-identified and the FE model predicted modal eigenvalues. The commonly assumed probabilistic model for this discrepancy is a zero-mean Gaussian random variable with standard deviation proportional to the identified eigenvalues. Assuming statistical independence among the N_m identified modes and among the N_t identified modal data sets obtained at different time instances, the likelihood function can be written

$$L\left(\widetilde{\lambda}_{t_m}, \widetilde{T}_t; Q, H, U, Y, \tau\right) = \prod_{t=1}^{N_t}\prod_{m=1}^{N_m} N\left(\widetilde{\lambda}_{t_m} - \lambda^{\mathcal{G}}_{t_m}\left(E=\theta(\widetilde{T}_t)\cdot E_0\right); 0, c^2_{\lambda m}\widetilde{\lambda}^2_{t_m}\right), \tag{5.15}$$

where $N(\,.\,;0,\sigma^2)$ denotes the value of the normal probability density function with mean zero and variance σ^2 at a specified location. The factor $c_{\lambda m}$ can be regarded as an assigned coefficient of variation, and its chosen value reflects the total prediction error [52], accounting for measurement and model uncertainty. For the numerical investigations of Section 5.6, $c_{\lambda m}$=0.02 [52, 25]. One should be aware that the assumption of independence in Eq. (5.15) typically does not hold. This could be addressed by a hierarchical modeling of the vector $[Q, H, U, Y, \tau]$ [5].

Once a certain number of N_t OMA-identified eigenvalue sets, identified at different temperatures in the initial undamaged state, becomes available, Bayesian analysis can be performed to estimate the posterior distribution of the environmental variability model parameters. One can then input the estimated posterior mean parameter values (denoted by μ'') in Eq. (5.14) and obtain a monitoring-informed estimate of the modification factor θ'' as a function of temperature

$$\theta''(T_t) = \mu''_Q + \mu''_H \cdot T_t + \mu''_U \cdot \left(1 - \text{erf}\left(\frac{T_t - \mu''_Y}{\mu''_\tau}\right)\right) \tag{5.16}$$

Within subsequent damage identification studies, an effective Young's modulus of $E(\widetilde{T}_t) = \theta''(\widetilde{T}_t)\cdot E_0$ is used for a measured temperature $\widetilde{T}_t$.

5.4.2 Deterioration model

Bayesian decision analysis relies on stochastic deterioration models for sampling many different potential "what-if" scenarios of the damage evolution over the life-cycle of a structure. Furthermore, a VoSHM analysis requires a model of the SHM system, which can provide probabilistic predictions of the life-cycle monitoring data for the different deterioration and temperature samples (see Fig. 5.5), as well as a model describing the uncertain outcome of visual inspections.

Structural deterioration can be classified in two main categories, 1) gradual deterioration (e.g., due to fatigue, corrosion, crack growth) and 2) shock deterioration (e.g. sudden damages due to extreme events such as earthquakes, floods, etc.), as described in Section 5.2. Herein, we employ an empirical deterioration model, which is a superposition of a gradual deterioration process and a shock deterioration process. The deterioration state at global time t (from the beginning of the structural lifetime) is described by the following equation:

$$X(t) = At^B \exp\left(\omega(t)\right) + \sum_{i=1}^{N(t)} D_i \tag{5.17}$$

The first part of Eq. (5.17) is a simple rate equation, which models the gradual deterioration process [11]. Random variable A models the deterioration rate, random variable B models the nonlinearity effect in terms of a power law in time, and $\omega(t)$ models a Gaussian stochastic process noise. The second part of Eq. (5.17) describes a homogeneous compound Poisson process (CPP) [63, 49], and is used to model deterioration due to sporadic shocks, which is typical of, e.g., earthquakes, floods. CPP models incorporate two types of randomness: i) random times of arrival of sporadic shock occurrences and ii) random damage increase due to an occurring shock. A CPP is a continuous-time stochastic process $\{V(t), t \geq 0\}$ of the form $V(t) = \sum_{i=1}^{N(t)} D_i$, where:

1. the number of jumps $\{N(t), t \geq 0\}$ is a Poisson process with rate λ,

2. the jumps $\{D_i, i = 1, .., N(t)\}$ are independent and identically distributed random variables following a specified probability distribution,

3. the process $\{N(t), t \geq 0\}$ and the damage increments $\{D_i, i = 1, .., N(t)\}$ are independent.

The model of Eq. (5.17) assumes that the gradual and shock deterioration processes are independent of each other. Furthermore, it is assumed that the shock deterioration magnitude is independent of the state of the system at the time of the shock event. Ten random realizations of this model are shown in Fig. 5.3.

The empirical deterioration model presented above is fairly general and flexible enough to capture a number of the challenges related to performing a VoSHM analysis at different time scales, as described in Section 5.2. The flexibility of this model is demonstrated in the numerical investigations for different SHM use cases presented in Section 5.6.

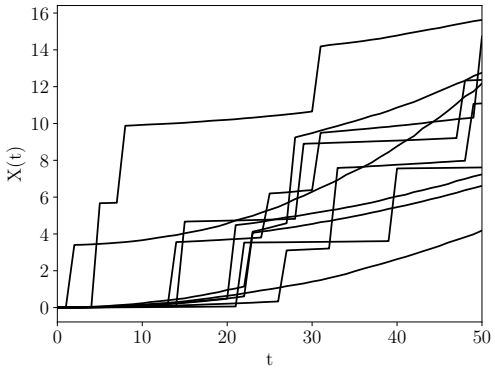

Figure 5.3: Random sampling from deterioration model of Eq. (5.17) using the parameters of Tab. 5.1

5.4.2.1 Sequential Bayesian estimation of deterioration state and parameters

The goal is to establish a model that uses the OMA-identified system eigenvalue data, obtained at different points in time and at different temperatures, to jointly update the distribution of the structural deterioration state $X(t)$ and the time-invariant gradual deterioration model parameters A, B of the model in Eq. (5.17). A discrete-time state-space model is defined, suitable for application of Bayesian filters for monitoring the deterioration. The state space is augmented to include the time-invariant random variables A and B in the estimation.

$$\widetilde{\boldsymbol{X}} = \begin{bmatrix} X(t) \\ A \\ B \end{bmatrix} \tag{5.18}$$

The continuous model of Eq. (5.17) is reformulated into a recursive process equation using a central finite difference scheme.

$$X_k = X_{k-1} + A_{k-1}B_{k-1}\left(\frac{t_{k-1}+t_k}{2}\right)^{B_{k-1}-1}\Delta t \cdot \exp(\omega_k) + \Delta D_k, \tag{5.19}$$

where k corresponds to the discrete time instance t_k. Time is discretized in yearly intervals $k = 1, ..., T$, where the k-th interval represents $t \in (t_{k-1}, t_k]$. ΔD_k is the distribution of the CPP jump increments within a time interval Δt, given by the following cumulative distribution function (CDF)

$$F_{\Delta D_k}(d) = \exp(-\lambda\Delta t) + \sum_{i=1}^{\infty}\frac{(\lambda\Delta t)^i}{i!}\exp(-\lambda\Delta t)\cdot F_{\sum_{j=1}^{i} D_j}(d), \tag{5.20}$$

where $F_{\sum_{j=1}^{i} D_j}(d)$ is the CDF of the i-fold convolution of the distribution of D with itself.

A CPP realization can occur at any point in time t_{cpp}. For certain decision cases, one can introduce new decision time intervals in order to incorporate decision making at time t_{cpp}, when an extreme event occurs. In such cases, the total number of intervals n_{int} is no longer equal to T, i.e, $k = 1, ..., n_{\text{int}}$.

For the time-invariant deterioration model parameters the process equation is as follows:

$$[A_k, B_k]^\intercal = [A_{k-1}, B_{k-1}]^\intercal \tag{5.21}$$

The measurement equation that links the OMA-identified modal eigenvalues with the unknown true deterioration state X_k at time instance t_k is given by

$$\boldsymbol{Z}_{\text{SHM},k} = \boldsymbol{Z}_k^{\mathcal{G}}\left(X_k, E = \theta''(\widetilde{T}_k)E_0\right) + \boldsymbol{\eta}_k \tag{5.22}$$

$\boldsymbol{Z}_{\text{SHM},k}$ is the vector of OMA-identified eigenvalues $\{\widetilde{\lambda}_{k_m}, m = 1, ..., N_m\}$ and $\boldsymbol{Z}_k^{\mathcal{G}}$ is the vector of N_m FE model predicted eigenvalues at time t_k and temperature $\widetilde{T}_k$. $\mathcal{G}$ is now parametrized by the deterioration state X_k and the effective Young's modulus. Note that for the effective Young's modulus, the monitoring-informed modification factor θ'' of Eq. (5.16) is used. To accelerate computations, a surrogate model of $\mathcal{G}$ can be employed. The error term $\boldsymbol{\eta}_k$ models the prediction error in the estimation of the modal eigenvalues, assumed to follow a zero-mean joint Gaussian distribution with variance proportional to the measured eigenvalues. With this assumption, the SHM likelihood function is

$$f_{\boldsymbol{Z}_{\text{SHM},k}|X_k}(\boldsymbol{Z}_{\text{SHM},k}|X_k) = \prod_{m=1}^{N_m} N\left(\widetilde{\lambda}_{k_m} - \lambda_{k_m}^{\mathcal{G}}\left(X_k, E = \theta''(\widetilde{T}_k)E_0\right); 0, c_{\lambda m}^2\widetilde{\lambda}_{k_m}^2\right) \tag{5.23}$$

Visual inspections might be required for complementing the monitoring at certain time instances over the structural life-cycle. At a time instance t_k, when a visual inspection is performed, the complementary inspection measurement equation is

$$Z_{\text{insp},k} = X_k + \epsilon_k, \tag{5.24}$$

where $Z_{\text{insp},k}$ is the uncertain outcome of a visual inspection and X_k is the unknown true deterioration state at time t_k. ϵ_k models the uncertainty of the visual inspection outcome, and is assumed to follow a zero-mean Gaussian distribution with an assigned coefficient of variation (cv_{insp}) reflecting the quality of the inspection (in the numerical investigations of Section 5.6, cv_{insp}=0.15). The resulting inspection likelihood function is

$$f_{Z_{\text{insp},k}|X_k}(Z_{\text{insp},k}|X_k) = N\left(Z_{\text{insp},k}; X_k, \text{cv}_{\text{insp}}\right) \tag{5.25}$$

A Bayesian filter [10, 50, 60] can be implemented to solve the sequential Bayesian joint state-parameter estimation problem. The Bayesian filter implemented within the presented VoSHM framework is provided in the algorithmic summary of Section 5.5. More specifically, we implement an on-line particle filter [27], which performs Gaussian mixture (GM)-based [32] resampling [26] whenever the effective sample size drops below a user-defined threshold (step 8 in the algorithmic summary of Section 5.5). The specific resampling scheme aims to counteract the issues of sample degeneracy and impoverishment that occur in on-line joint state-parameter estimation settings [50]. By running the filter, one obtains for each time step t_k the one-step ahead predictive posterior distribution $\pi_{\text{pos}}(\widetilde{\boldsymbol{X}}_k \mid \boldsymbol{Z}_{1:k-1})$ and the filtered posterior distribution $\pi_{\text{pos}}(\widetilde{\boldsymbol{X}}_k \mid \boldsymbol{Z}_{1:k})$. It is not the primary focus of this paper to provide a thorough elaboration on the use of Bayesian filtering; to this end, the interested reader is referred to [60, 26], where code is offered on an extended set of Bayesian algorithms. More specifically, the particle filter with GM resampling (PFGM) presented in [26] is the method that we employ in this work.

5.4.3 Structural reliability and its updating

In many instances, a failure event at time t can be expressed in terms of a structural capacity $R(t)$ and a demand $S(t)$, which are both random variables. We assume that the structural capacity

$R(t)$ can be separated from the demand $S(t)$, and that a deterministic function $R(X_k)$ that outputs the structural capacity for a given deterioration state X_k can be determined. Modeling $R(X_k)$ as deterministic is based on the assumption that the main uncertainties stem from the deterioration and the load, and that further physical and model uncertainties related to the structural capacity are not incorporated. More details on the definition of this problem-dependent deterministic function are provided for a specific structure in Section 5.6, as well as in previous work of the authors [25]. Such a simplified modeling choice is adopted here for the purpose of enabling a VoSHM analysis of practicable computational cost. The uncertain demand acting on the structure is modeled by the distribution of the maximum load S_{max} in a one-year time interval. $F_{s_{max}}$ denotes the cumulative distribution function (CDF) of this distribution.

The time-variant reliability problem can be replaced by a series of time-invariant reliability problems [57]. F_k^* is defined as the event of failure in interval $(t_{k-1}, t_k]$. For a given value of the deterioration state X_k, the structural capacity $R(X_k)$ is fixed and the conditional interval probability of failure is defined as:

$$\Pr(F_k^* \mid X_k) = \Pr\left(S_{max} > R(X_k)\right) = 1 - \Pr\left(S_{max} \leq R(X_k)\right) = 1 - F_{s_{max}}\big(R(X_k)\big) \tag{5.26}$$

The unconditional accumulated probability of failure up to time t_k, $\Pr(F_k) = \Pr(F_1^* \cup F_2^* \cup ...F_k^*)$, can be computed through the conditional interval probabilities $Pr(F_k^*|X_k)$,

$$\Pr(F_k|X_k) = 1 - \prod_{m=1}^{k} \left[1 - \Pr(F_m^* \mid X_m)\right] \tag{5.27}$$

and by use of the total probability theorem:

$$\Pr(F_k) = \int_{\Omega_{X_k}} \Pr(F_k \mid X_k)\pi(X_k)dX_k. \tag{5.28}$$

If one replaces $\pi(X_k)$ with $\pi_{\text{pos}}(X_k \mid \boldsymbol{Z}_{1:k})$ in Eq. (5.28), the updated estimate of the accumulated probability of failure is obtained:

$$\Pr(F_k|\boldsymbol{Z}_{1:k}) = \int_{\Omega_{X_k}} \Pr(F_k \mid X_k)\pi_{\text{pos}}(X_k \mid \boldsymbol{Z}_{1:k})dX_k \tag{5.29}$$

The above integral can be solved with random sampling-based techniques. Here we employ a particle filtering scheme [50] to obtain weighted samples following $\pi_{\text{pos}}(X_k \mid \boldsymbol{Z}_{1:k})$.

5.5 Algorithmic summary of the heuristic-based expected total life-cycle cost calculation

In this section, we present a detailed algorithmic summary of the proposed methodology for the heuristic-based total expected life-cycle cost computation in the SHM preposterior analysis, i.e., the computation of $\mathbb{E}_{\boldsymbol{X},\boldsymbol{Z}_{\text{insp}},\boldsymbol{Z}_{\text{SHM}}}\left[C_{\text{tot}}\left(\boldsymbol{X}, \boldsymbol{Z}_{\text{insp}}, \boldsymbol{Z}_{\text{SHM}}, \boldsymbol{w}\right)\right]$. For the sake of readability, in this section $\boldsymbol{Z} = [\boldsymbol{Z}_{\text{SHM}}, \boldsymbol{Z}_{\text{insp}}]$.

- Fix the heuristic parameter vector $\boldsymbol{w} = [p_{\text{th}}^{\text{I}}, \Delta t_{\text{I}}, p_{\text{th}}^{\text{R}}]$, which defines the heuristic strategy $S_{\boldsymbol{w}}$.

- Draw n_{MCS} samples of the parameter vector $[Q^{(i)}, H^{(i)}, U^{(i)}, Y^{(i)}, \tau^{(i)}]$ defining multiple potential underlying "true" realizations of the environmental variability model. For each realization, create eigenvalue (modal) "measurements" sampled at different temperatures in the initial undamaged structural state, and perform an offline Bayesian estimation, e.g., using the iTMCMC algorithm [6], to learn the posterior distribution of the environmental model parameters and subsequently obtain $\theta''^{(i)}$.

- Draw n_{MCS} samples from the prior model of the deterioration process, which define multiple potential underlying "true" realizations of the deterioration process $\widetilde{\boldsymbol{X}}^{(i)} = [X_k^{(i)}, A^{(i)}, B^{(i)}]^\intercal, \quad i = 1, .., n_{\text{MCS}}$.

- For each $\theta''^{(i)}$ and $\widetilde{\boldsymbol{X}}^{(i)}$ realization, do the following:

  – Draw n_{p} particles of the initial deterioration state $X_0^{(j)}$ and the time-invariant parameter vector $[A_0^{(j)}, B_0^{(j)}]$ and set particle weights $w_0^{(j)} = \frac{1}{n_{\text{p}}}, \quad j = 1, .., n_{\text{p}}$.

  – For each $k = 1, \ldots, T$ do the following:

  1. Draw a new point $X_k^{(j)}$ for each point in the particle set $\{X_{k-1}^{(j)}, j = 1, .., n_{\text{p}}\}$ from the deterioration state process equation:

$$X_k^{(j)} = X_{k-1}^{(j)} + A_{k-1}^{(j)} B_{k-1}^{(j)} \left(\frac{t_{k-1}+t_k}{2}\right)^{B_{k-1}^{(j)}-1} \Delta t \cdot \exp(\omega_k) + \Delta D_k^{(j)}$$

     and for the time-invariant parameters:

$$[A_k^{(j)}, B_k^{(j)}]^\intercal = [A_{k-1}^{(j)}, B_{k-1}^{(j)}]^\intercal$$

  2. Estimate the one-step-ahead prediction for the time-dependent accumulated failure probability and the hazard function h, which expresses the failure rate of the structure conditional on survival up to the previous time instance:

$$\Pr\left(F_k \mid \boldsymbol{Z}_{1:k-1}^{(i)}\right) \approx \textstyle\sum_{j=1}^{n_{\text{p}}} w_{k-1}^{(j)} \Pr(F_k \mid X_k^{(j)})$$

$$h_k\left(\boldsymbol{Z}_{1:k-1}^{(i)}\right) \approx \frac{\Pr\left(F_k|\boldsymbol{Z}_{1:k-1}^{(i)}\right) - \Pr\left(F_{k-1}|\boldsymbol{Z}_{1:k-1}^{(i)}\right)}{\Pr\left(F_{k-1}|\boldsymbol{Z}_{1:k-1}^{(i)}\right)}$$

  3. If $h_k\left(\boldsymbol{Z}_{1:k-1}^{(i)}\right) \geq p_{\text{th}}^{\text{R}}$: a repair is prescribed at time t_{k-1}. Set $\{X_{k-1}^{(j)} = 0, \quad j = 1, .., n_{\text{p}}\}$ and go back to step 1, i.e., after repair the structure is assumed to return back to its original undamaged state, and starts deteriorating anew.

  4. If $h_k\left(\boldsymbol{Z}_{1:k-1}^{(i)}\right) \geq p_{\text{th}}^{\text{I}}$: an inspection needs to be performed at time t_{k-1}. The uncertain inspection outcome $Z_{\text{insp},k-1}^{(i)}$ is sampled from the inspection likelihood function of Eq. (5.25).

  5. If $(t_k = t_{\text{cpp}})$, i.e., if an extreme event has occurred, an inspection needs to be performed at time t_k. The uncertain inspection outcome $Z_{\text{insp},k}^{(i)}$ is sampled from the inspection likelihood function of Eq. (5.25).

  6. Sample the measurement $\boldsymbol{Z}_{\text{SHM},k}^{(i)}$ from the SHM system model (see Fig. 5.5).

7. Perform the filtering step. Update the weights

$$w_k^{(j)} \propto f_{\boldsymbol{Z}_{\mathrm{SHM},k}|X_k}(\boldsymbol{Z}_{\mathrm{SHM},k}^{(i)}|X_k^{(i)}) \cdot f_{\boldsymbol{Z}_{\mathrm{insp},k}|X_k}(\boldsymbol{Z}_{\mathrm{insp},k}^{(i)}|X_k^{(i)}) \cdot w_{k-1}^{(j)}$$

and normalize these to sum to unity. Filter the accumulated probability of failure

$$\Pr\left[F_k \mid \boldsymbol{Z}_{1:k}^{(i)}\right] \approx \sum_{j=1}^{n_\mathrm{p}} w_k^{(j)} \Pr[F_k \mid X_k^{(j)}]$$

8. $N_{\mathrm{eff},k} = \frac{1}{\sum_{j=1}^{n_\mathrm{p}} (w_k^{(j)})^2} \leq c \cdot n_\mathrm{p}$ with $c \in [0,1]$ indicates sample degeneracy. To resolve that, fit a GM proposal distribution according to $\{\boldsymbol{X}_k^{(j)}, w_k^{(j)}\}$ [32], which approximates the current posterior, and sample n_p new particles from this GM proposal distribution. Reset particle weights to $w_k^{(j)} = \frac{1}{n_\mathrm{p}}$ [26].

– The lifetime inspection, repair and risk of failure costs corresponding to $\theta''^{(i)}$ and $\widetilde{\boldsymbol{X}}^{(i)}$ are:

$$C_\mathrm{I}^{(i)} = \sum_{m=1}^{n_\mathrm{insp}} \gamma\left(t_\mathrm{insp}^{(m)}\right) \widetilde{c}_\mathrm{I}$$

$$C_\mathrm{R}^{(i)} = \sum_{m=1}^{n_\mathrm{rep}} \gamma\left(t_\mathrm{rep}^{(m)}\right) \widetilde{c}_\mathrm{I}$$

$$R_\mathrm{F}^{(i)} = \sum_{k=1}^{T} \gamma(t_k) \widetilde{c}_\mathrm{F} \left\{\Pr[F_k|X_k^{(i)}] - \Pr[F_{k-1}|X_{k-1}^{(i)}]\right\}$$

- Compute the expected value:

$$\mathbb{E}_{\boldsymbol{X},\boldsymbol{Z}_\mathrm{insp},\boldsymbol{Z}_\mathrm{SHM}}\left[C_\mathrm{tot}\left(\boldsymbol{X}, \boldsymbol{Z}_\mathrm{insp}, \boldsymbol{Z}_\mathrm{SHM}, \boldsymbol{w}\right)\right] \approx \frac{1}{n_\mathrm{MCS}} \sum_{i=1}^{n_\mathrm{MCS}} \left(C_\mathrm{I}^{(i)} + C_\mathrm{R}^{(i)} + R_\mathrm{F}^{(i)}\right)$$

The methodology presented above can further be employed "as is" with only few modifications for the computation of $\mathbb{E}_{\boldsymbol{X},\boldsymbol{Z}_\mathrm{insp}}\left[C_\mathrm{tot}\left(\boldsymbol{X}, \boldsymbol{Z}_\mathrm{insp}, \boldsymbol{w}\right)\right]$, i.e., for the preposterior analysis in the case of only inspections.

5.6 Numerical investigations

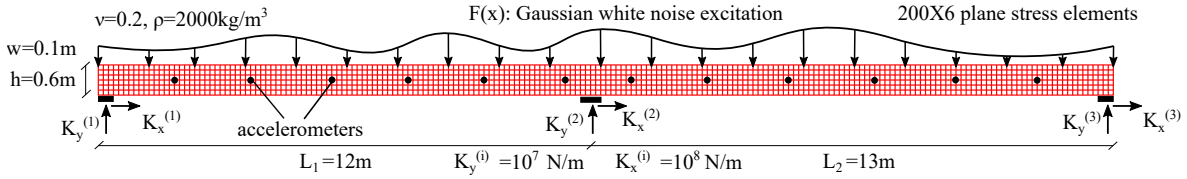

Figure 5.4: Bridge system subject to environmental variability and damage due to deterioration at the middle pier.

Fig. 5.4 shows the numerical benchmark model of a two-span bridge system [59], which has already been employed by the authors for a VoI analysis in [25, 23]. The model is used as a simulator

Table 5.1: Prior distribution of environmental variability and deterioration model parameters

Parameter	Distribution	Mean	cv
Q	Normal	-0.005	0.1
H	Normal	1.115	0.025
U	Normal	0.165	0.1
Y	Normal	-1.00	0.25
τ	Normal	3.00	0.20
A	Lognormal	$1.94{\cdot}10^{-4}$	0.4
B	Normal	2.0	0.10
ω_k	Normal	-0.005	0.10
D_i	Lognormal	3.75	0.25
$N(t)$	Poisson	$0.04{\cdot}t$	-

for creating dynamic response measurement samples from the bridge system, which is subjected to environmental variability and to gradual and shock deterioration at the middle elastic support, simulating the case of scour [45, 44, 16, 65, 51]. Scour is one of the main causes of failure events on bridges [44, 51].

Elastic boundaries in both directions are assumed for all three support points, in the form of translational springs with $K_x = 10^8$ N/m and $K_y = 10^7$ N/m. Damage is introduced as a reduction of the stiffness in the y-direction of the spring $K_y^{(2)}$. The evolution of damage over the bridge lifespan of $T = 50$ years is described by the damage model of Eq. (5.30), where $K_{y,0}^{(2)}$ is the initial undamaged value, and $X(t)$ is the gradual and shock (e.g., due to flood occurrences) deterioration process, described by the model in Eq. (5.17).

$$K_y^{(2)}(t) = \frac{K_{y,0}^{(2)}}{1 + X(t)} \tag{5.30}$$

Modeling scour damage as a stiffness reduction at the support is not straightforward. When doing so, we ensure that the implemented damage properly reflects percentual changes of the modal properties equivalent to ones reported in literature for cases of scour [45, 44]. As a result, the modeled deterioration $X(t)$ can lead to large reductions of the stiffness $K_y^{(2)}(t)$.

To model the environmental variability, a linear elastic material is assigned, with the Young's modulus assumed to vary with temperature, as described by Eq. (5.13). The nominal value for the Young's modulus at a reference temperature of 20°C is $E_0 = 29.11$GPa, intended to represent reinforced concrete. The prior probabilistic models for the random variables entering the models of Eqs. (5.13) and (5.17) are summarized in Tab. 5.1.

5.6.1 SHM probabilistic data sampling process

It is assumed that the two-span bridge system is continuously monitored from the beginning of its operation using a set of 12 sensors measuring vertical accelerations, whose locations correspond to predefined FE nodes (see Fig. 5.4), as well as temperature sensors continuously providing ambient temperature measurements. A distributed Gaussian white noise excitation F(x) is used as the load acting on the bridge, to simulate the unknown ambient excitation.

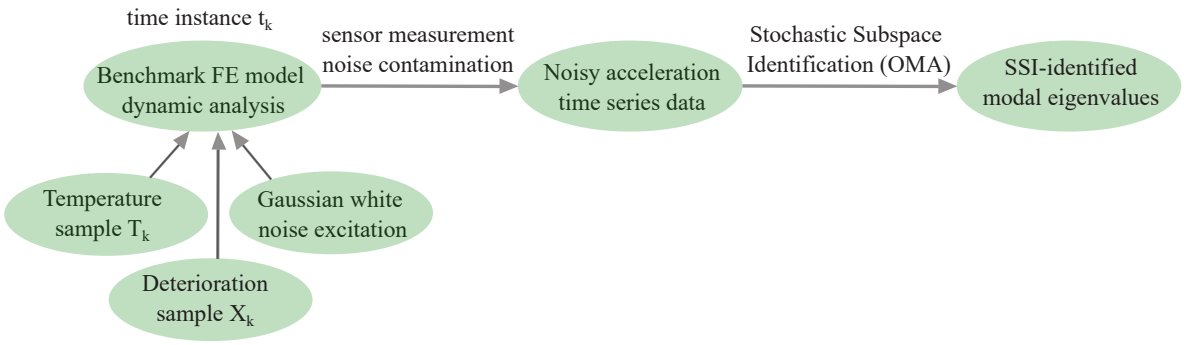

Figure 5.5: SHM modal data sampling process

As explained in Section 5.4, a VoSHM analysis requires a model of the SHM system, which can furnish probabilistic predictions of the life-cycle monitoring data. The SHM modal eigenvalue data sampling process is summarized in Fig. 5.5. At a time instance t_k, for a given input value of the deterioration state X_k and for a given temperature $\widetilde{T}_k$, a dynamic time history analysis is run and the "true" vertical acceleration signals $\ddot{x}$ at the sensor locations (FE nodes) are obtained. This noise-free acceleration time series data set is then contaminated with Gaussian white noise of 5% root mean square noise-to-signal ratio, simulating a sensor measurement error. Subsequently, the noisy accelerations $\tilde{\ddot{x}}$ are fed into the SSI algorithm [40], which identifies between $m = 3$ to 5 lower eigenvalues.

5.6.2 Bayesian learning of the environmental variability model

This section demonstrates the Bayesian learning of the environmental variability model, as explained in Section 5.4.1.1. The linear FE model $\mathcal{G}$ predicting the eigenvalues for the Bayesian updating process is the same FE model as the one used in the SHM modal data sampling process, which constitutes a so-called inverse crime [66]. However, this is a built-in feature of preposterior decision analysis. In a real SHM setting, the model is initially adjusted to reflect the true behavior as closely as possible, but existence of model uncertainty is inevitable, which will affect the accuracy of the VoSHM calculation. This, however, is a challenge pertinent to any engineering analysis.

For illustrating the updating process, we consider one underlying "true" realization of the environmental variability model, shown in black in the bottom right panel of Fig. 5.6, with associated parameter values $[Q^* = 1.101, H^* = -0.0057, U^* = 0.174, Y^* = -1.292, \tau^* = 3.464]$. We assume that N_t=50 eigenvalue sets, identified at different ambient temperature values via the SSI process, are available from the SHM in the initial operational period of the structure, when it is assumed that no damage is present. Via Bayesian analysis, the posterior distribution of the environmental variability model parameters is obtained. This is shown in Fig. 5.6, where the first five panels plot the prior and posterior distribution of the five parameters. The last panel (bottom right) plots the prior mean model of Eq. (5.13) with its 95% credible interval (CI), and the monitoring-informed estimate of the model $E(\widetilde{T}) = \theta''(\widetilde{T}) \cdot E_0$ with its 95% CI, obtained from posterior parameter samples generated from the iTMCMC algorithm [6]. One can observe that the underlying "true" model is captured very well and the posterior 95% CI is very narrow, reflecting small posterior uncertainty. For subsequent damage identification purposes, the learned blue model for the effective Young's

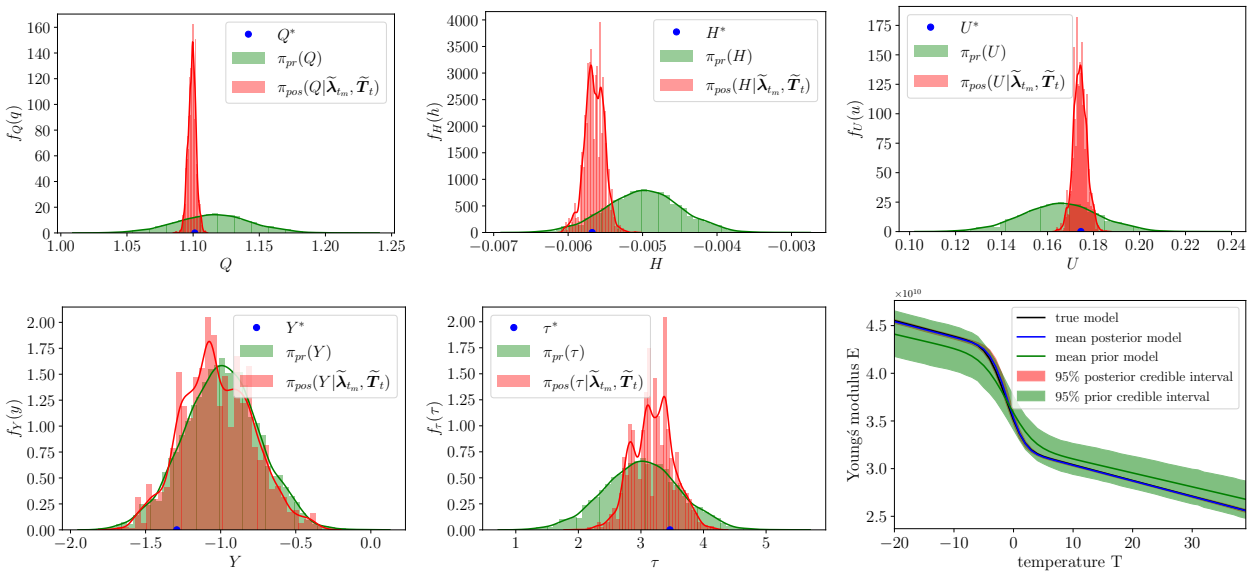

Figure 5.6: Bayesian learning of the parameters of the environmental variability model.

modulus is employed.

5.6.3 VoSHM quantification

In Section 5.3.1 the heuristic-based VoSHM quantification via Eq. (5.8) is presented. For the numerical investigations in this section, the optimal heuristic thresholds $p_{\text{th}}^{\text{I}*}$ and $p_{\text{th}}^{\text{R}*}$ are computed via a preposterior analysis for the case of visual inspections only. The periodic inspections interval Δt_I is set equal to 5 years, which is common practice for scour-specific inspections in many countries, and is not optimized, i.e., the heuristic parameters are $\boldsymbol{w}_1^* = [p_{\text{th}}^{\text{I}*}, p_{\text{th}}^{\text{R}*}, \Delta t_{\text{I}} = 5]$. Obtaining $\boldsymbol{w}_2^*$ can become computationally unaffordable, therefore we use for $\boldsymbol{w}_2^*$ the same heuristic thresholds $p_{\text{th}}^{\text{I}*}$ and $p_{\text{th}}^{\text{R}*}$ that were optimized in the case of visual inspections only. This leads to a potential underestimation of the VoSHM, as these choices may not be fully optimal. In the case of continuous SHM, we assume that no fixed-interval periodic inspections will be performed. Naturally, this choice is based on the assumption of a high level of trust in the adequate functionality of the SHM system throughout the whole life-cycle. Eventually, $\boldsymbol{w}_2^* = [p_{\text{th}}^{\text{I}*}, p_{\text{th}}^{\text{R}*}, \Delta t_{\text{I}} = \infty]$.

The following costs are assigned: $\widetilde{c}_{\text{F}} = 5 \cdot 10^7$€, $\widetilde{c}_{\text{I}} = 2 \cdot 10^4$€, $\widetilde{c}_{\text{R}} = 6 \cdot 10^5$€. The scour inspection cost is assigned based on [8], and the scour repair cost based on [44, 1]. The discount rate is taken as $r = 2\%$. The lifetime of $T = 50$ years is discretized into flexible decision-making intervals. "Inspect?" {yes, no} and "Repair?" {yes,no} decisions are made once per year, and potentially also at the specific time steps when an observed extreme event occurs.

It should be noted that the model describing the outcome of a visual inspection that we assume in this work, described by Eq. (5.25), is a hypothetical, simplified model, employed for the sake of performing a VoSHM analysis. In reality, an inspection outcome would not come in the form of an estimated stiffness loss, and a more detailed analysis would be needed to express the inspection outcome in this form. Even so, this simplified inspection model can still incorporate the expected

quality of the visual inspection by an appropriate choice of the assumed coefficient of variation cv_{insp} in Eq. (5.25). The effect of this choice on the VoSHM result has been investigated by the authors in [22].

For the structural reliability computation, the uncertain demand acting on the structure is modeled by the maximum load in each time interval with a Gumbel(a_n=0.0509, b_n=0.297) distribution. The parameters of the Gumbel distribution are chosen such that the probability of failure in the initial undamaged state is equal to 10^{-6}. In this work, we are interested in effects that are related to damage and are imprinted on monitored structural properties, in the form of residual stiffness reduction. We determine the deterministic function of the capacity for given deterioration state, $R(X_k)$, considering that for increasing stiffness reduction at the middle elastic support, the load bearing capacity of the bridge system decreases due to increase in the normal stresses at the middle of the right midspan. A one-dimensional grid of possible values of the deterioration X_k is created, and each of those values is given as input for a static analysis with the FE model. For each implemented X_k value, the loss of load bearing capacity of the structure relative to the initial undamaged state is evaluated, leading to the corresponding $R(X_k)$ value. The same modeling choice was employed by the authors in previous work (see Fig. 15 in [25]).

Finally, for the sequential Bayesian estimation of the deterioration state and parameters with continuous vibration-based SHM data, a polynomial ridge regression [36] surrogate model is used to replace each of the structural FE model $\mathcal{G}$-predicted eigenfrequencies entering Eq. (5.22). We create a two-dimensional grid of possible values for the deterioration $X(t)$ and for the effective Young's modulus as a function of temperature $E(T_t)$. For each point in this two-dimensional grid, we execute a modal analysis using the structural FE model and store the output eigenfrequencies. Eventually, for each eigenfrequency, we fit a two-dimensional polynomial ridge regression response surface model, as exemplarily shown in Fig. 5.7 for the first two eigenfrequencies, which we use as the surrogate model.

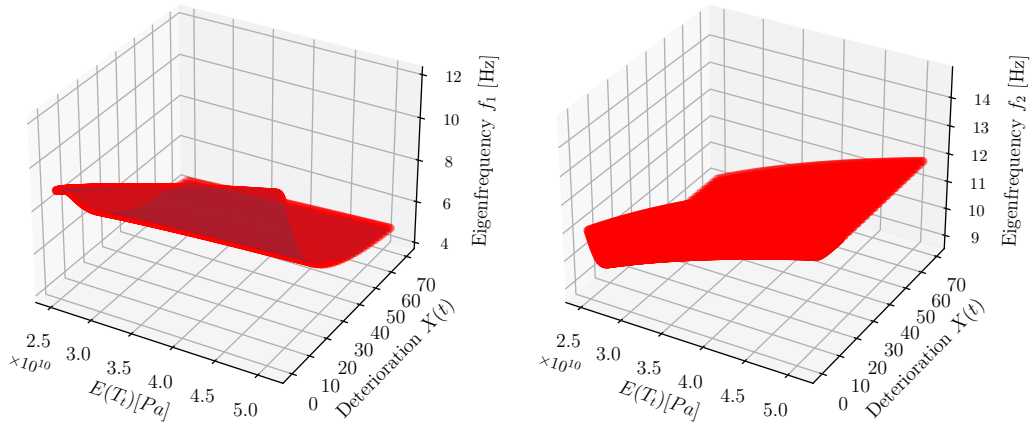

Figure 5.7: Polynomial ridge regression surrogate model for eigenfrequencies f_1 and f_2.

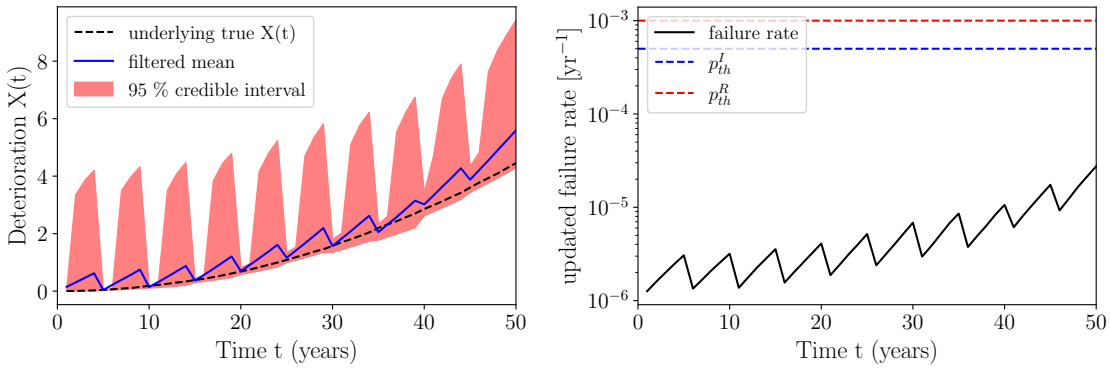

Figure 5.8: Bayesian filtering of the deterioration state and the reliability using intermittent visual inspection data.

5.6.3.1 First case study: Gradual deterioration and shock deterioration due to an observed extreme event

As a first case study, we assume a scenario with gradual and shock deterioration, where a CPP shock deterioration occurrence corresponds to an observed extreme event, e.g., a flood occurrence. In this case, both without and with continuous SHM, an additional visual inspection will take place right after the extreme event.

Performing a heuristic-based expected total life-cycle cost minimization without SHM, the optimal heuristic parameter vector $\boldsymbol{w}_1^* = [p_{\text{th}}^{\text{I}*} = 5 \cdot 10^{-4}, p_{\text{th}}^{\text{R}*} = 1 \cdot 10^{-3}, \Delta t_{\text{I}} = 5]$ is found. For the solution of the joint expectation $\mathbb{E}_{\boldsymbol{X},\boldsymbol{Z}_{\text{insp}}}$, as summarized in Section 5.5, $n_{\text{MCS}} = 1000$ samples were drawn, each defining one potential underlying "true" realization of the deterioration process and the corresponding visual inspection data.

We demonstrate how the sequential Bayesian estimation of the deterioration state and the corresponding sequential decision-making operates without and with continuous vibration-based SHM, by looking at one of these underlying "true" deterioration process realizations. The dashed black line in the first panel of Figs. 5.8 and 5.9, corresponds to this single underlying "true" realization. For this sample, no extreme event occurs, and the deterioration process is driven by gradual deterioration only. The left panel of Fig. 5.8 plots the filtered deterioration state estimate, and the right panel plots the filtered failure rate estimate, as obtained in view of intermittent visual inspection data. For $\boldsymbol{w}_1^* = [p_{\text{th}}^{\text{I}*} = 5 \cdot 10^{-4}, p_{\text{th}}^{\text{R}*} = 1 \cdot 10^{-3}, \Delta t_{\text{I}} = 5]$, a visual inspection is performed at $t_{\text{insp}} = [5, 10, 15, 20, 25, 30, 35, 40, 45]$ years, as dictated by $\Delta t_{\text{I}} = 5$. Since $p_{\text{th}}^{\text{I}*}$ and $p_{\text{th}}^{\text{R}*}$ are not exceeded, no additional inspection or repair takes place. Fig. 5.9 plots the corresponding estimates in the case when eigenvalue data from the investigated SHM system is continuously available. One can see that, in the presence of continuous SHM data, system state awareness at all times is accomplished, as opposed to Fig. 5.8, and the choice not to perform the periodic visual inspections leads to cost savings. More specifically, for this single realization $C_{\text{tot}}(\boldsymbol{x}, \boldsymbol{z}_{\text{insp}}, \boldsymbol{w}_1^*) - C_{\text{tot}}(\boldsymbol{x}, \boldsymbol{z}_{\text{insp}}, \boldsymbol{z}_{\text{SHM}}, \boldsymbol{w}_2^*) = 1.13 \cdot 10^5$€.

Figs. 5.10 and 5.11 plot the sequential Bayesian estimates for a second potential underlying "true" deterioration process realization. Without SHM, inspections are performed at Δt_{I}=5 year intervals, when p_{th}^{I} is exceeded, as well as when an extreme event occurs. More specifically, for the realization

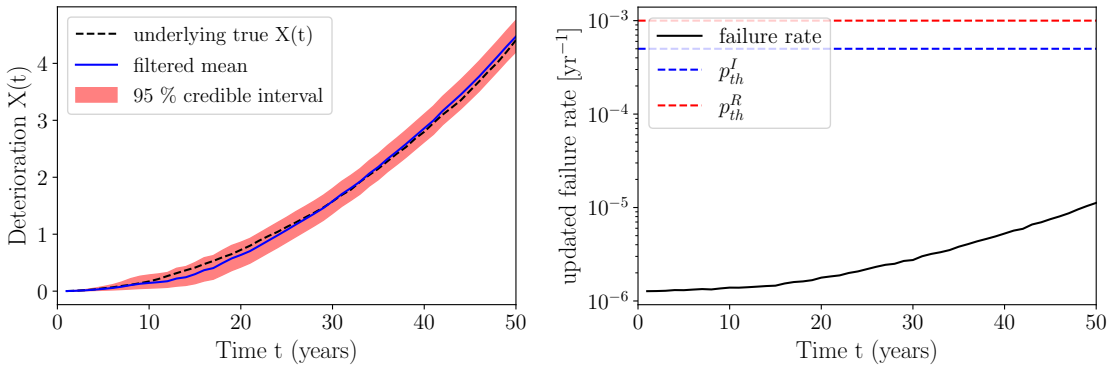

Figure 5.9: Bayesian filtering of the deterioration state and the reliability using continuous SHM and inspection data.

in Fig. 5.10, $t_{\text{insp}} = [5, 10, 15, 20, 25, 26.3, 31, 31.2, 36, 42, 47]$. A repair is performed at year 36, after an inspection triggered by p^{I}_{th} at year 36 causes the p^{R}_{th} to be exceeded. With SHM instead, $t_{\text{insp}} = [26.3, 31.2, 32, 33, 34, 35, 36]$ (this shows that the heuristic $\boldsymbol{w}_2^*$ is indeed suboptimal for the case with SHM). The inspections to complement the SHM are triggered when an extreme event occurs, and when p^{I}_{th} is exceeded. Also with SHM, a repair at year 36 is informed by p^{R}_{th}. For this second realization, $C_{\text{tot}}\left(\boldsymbol{x}, \boldsymbol{z}_{\text{insp}}, \boldsymbol{w}_1^*\right) - C_{\text{tot}}\left(\boldsymbol{x}, \boldsymbol{z}_{\text{insp}}, \boldsymbol{z}_{\text{SHM}}, \boldsymbol{w}_2^*\right) = 6.02 \cdot 10^4$€.

In Fig. 5.11, the bottom two panels further plot the estimates of the time-invariant gradual deterioration parameters A, B. Learning deterioration model parameters, and quantifying their uncertainty, is instrumental for predictive maintenance tasks.

In this subsection, we illustrated the sequential decision making process and the corresponding life-cycle cost calculation for two samples of the underlying "true" deterioration process and the corresponding sampled inspection and SHM data. Since the quantification of the $VoSHM$, as shown in Eq. (5.8), requires the evaluation of the expectation operator, one needs to draw a sufficiently large finite number of samples of $\boldsymbol{X}$ and $\boldsymbol{Z}_{\text{insp}}/\boldsymbol{Z}_{\text{SHM}}$ and compute the cost difference $C_{\text{tot}}\left(\boldsymbol{X}, \boldsymbol{Z}_{\text{insp}}, \boldsymbol{w}_1^*\right) - C_{\text{tot}}\left(\boldsymbol{X}, \boldsymbol{Z}_{\text{insp}}, \boldsymbol{Z}_{\text{SHM}}, \boldsymbol{w}_2^*\right)$ for each of those, and then take the mean value. For this first case study, with $n_{\text{MCS}} = 1000$ samples, $VoSHM = 1.11 \cdot 10^5$€, which indicates a potential benefit of installing an SHM system on the deteriorating bridge structure. This value does not contain the total life-cycle cost of the SHM system itself (cost of installation, maintenance, repair, etc.). One should compare the $VoSHM$ value with the expected total life-cycle cost of the SHM system, and then decide whether installing such a system can be cost-beneficial. Furthermore, the presented VoSHM analysis is based on the premise that the SHM system will be continuously operating in an unobstructed fashion, and that complete trust will be put on the SHM system to replace all periodic inspections, which seems unrealistic. In this regard, the obtained $VoSHM$ value provides an upper limit to the potential economic benefit that uninterrupted monitoring with the investigated SHM system would generate.

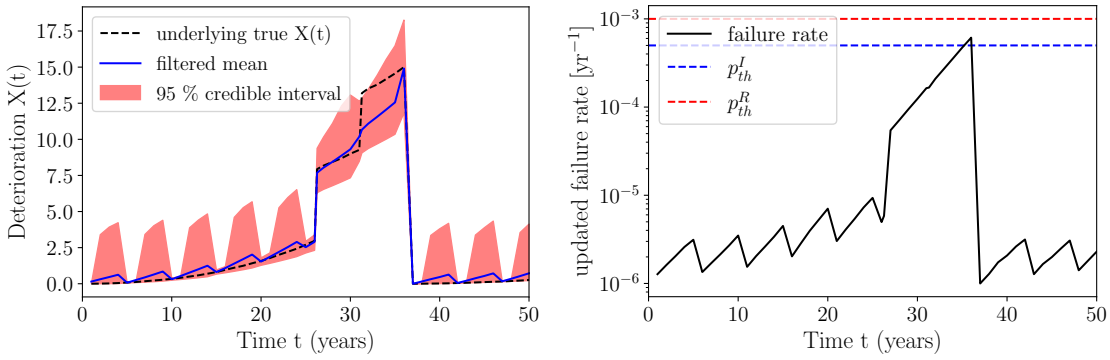

Figure 5.10: Bayesian filtering of the deterioration state and the reliability using intermittent visual inspection data.

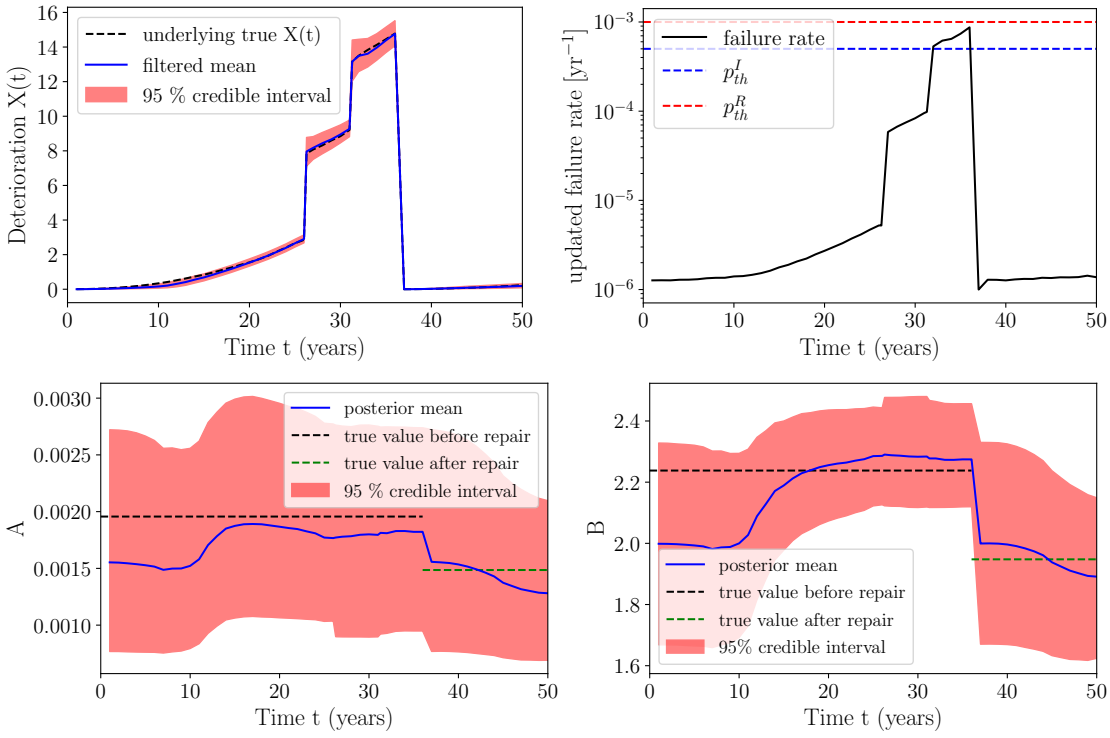

Figure 5.11: Bayesian filtering of the deterioration state, the time-invariant model parameters and the reliability using continuous SHM and inspection data. In the bottom two panels, A and B correspond to the time-invariant parameters of the deterioration model of Eq. (5.17)

.

5.6.3.2 Second case study: Gradual deterioration and shock deterioration due to an unobserved event

As a second case study, we assume scenarios when the CPP shock deterioration occurs due to an unobserved event, e.g., due to a sudden bridge bearing failure, or due to an extreme truck overloading. In such cases, without continuous SHM, no visual inspection will take place at the time of occurrence of this extreme event, since there is no knowledge of this occurrence. In contrast, with continuous vibration-based SHM in place, one will have access to continuous vibration data, and therefore data will be available right after the deterioration jump occurrence. This can lead to a timely tracking of the deterioration state increment and a subsequent prompt inspection or repair decision.

We consider the same single underlying true realization of the deterioration process as in Figs. 5.10 and 5.11, and demonstrate the corresponding sequential decision making in the second case study. Comparing the left panel of Fig. 5.12 to the top left panel of Fig. 5.11, one observes that the estimation with SHM barely differs between the two case studies, due to the continuity of the SHM data. The actions corresponding to Fig. 5.12 are inspections at $t_{\text{insp}} = [32, 33, 34, 35, 36]$, as informed by exceedance of p^{I}_{th}, and repair at $t_{\text{rep}} = 36$. On the other hand, comparing Fig. 5.13 to Fig. 5.10, it is clear that the absence of visual inspection measurements right after the deterioration jump events leads to a severe underestimation of the underlying true deterioration state. For the same heuristic thresholds as the ones in Fig. 5.10, the actions corresponding to Fig. 5.13 (without SHM) are inspections at $t_{\text{insp}} = [5, 10, 15, 20, 25, 30, 35, 37, 38, 44, 49]$ and repair at $t_{\text{rep}} = 38$, i.e., two years after the repair informed by SHM, with an increased risk of failure during this time period. For this single realization, in the second case study, $C_{\text{tot}}\left(\boldsymbol{x}, \boldsymbol{z}_{\text{insp}}, \boldsymbol{w}_1^*\right) - C_{\text{tot}}\left(\boldsymbol{x}, \boldsymbol{z}_{\text{insp}}, \boldsymbol{z}_{\text{SHM}}, \boldsymbol{w}_2^*\right) = 1.14 \cdot 10^5$€.

With $n_{\text{MCS}} = 1000$ samples, in the second case study we quantify $VoSHM = 1.42 \cdot 10^5$€, which is larger than the $VoSHM$ result obtained for the first case study. This increased $VoSHM$ value is expected.

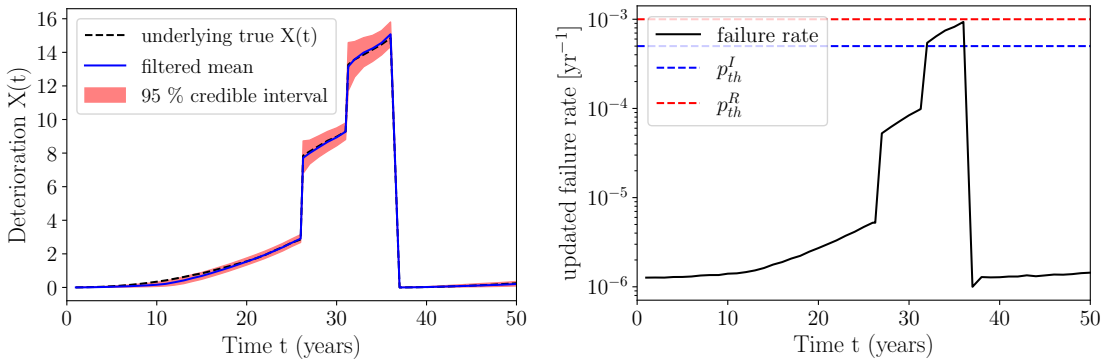

Figure 5.12: Bayesian filtering of the deterioration state and the reliability using continuous SHM and inspection data.

5.6.3.3 Third case study: Near-real time VoSHM in case of extreme event

As discussed in Section 5.2.1, SHM can be valuable in informing near real-time decisions for avoiding catastrophic failures, or avoiding unnecessary close-downs after the occurrence of an extreme event.

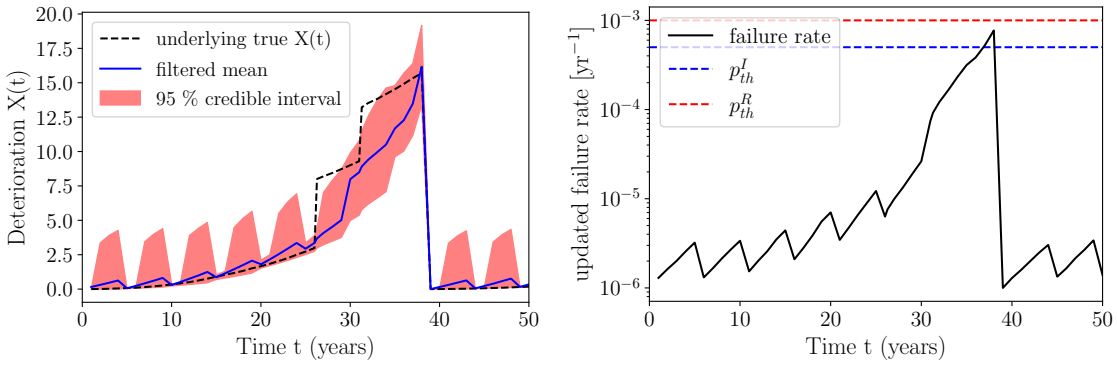

Figure 5.13: Bayesian filtering of the deterioration state and the reliability using intermittent inspection data.

As a third case study, we consider such an SHM for near-real time decision support.

As in the first case study of Section 5.6.3.1, we assume that a CPP shock deterioration corresponds to an observed extreme event. When such an event occurs, e.g., a flood, an inspection will have to take place right after the event, both in the case with and without SHM. However, we consider that it will only be possible to perform the inspection one week after the event, e.g., because inspectors cannot operate until the water level reduces or because they do not have the capacity to inspect all bridges in a short time. In this scenario, without SHM, an operator will have to close down the bridge for this one week until the inspection. This decision will induce a corresponding cost. According to [68], a close-down of a road bridge in the USA can cost up to $2 \cdot 10^5$ \$/day, while according to [29, 51], in the UK scour-related close-downs of a railway bridge can induce costs up to $1.65 \cdot 10^5$£/day. Herein, we assume a cost of close-down $c_{\text{clsdn}} = 1.5 \cdot 10^5$€/day. This cost is subject to discounting.

The benefit of continuous SHM is that the SHM system will be in operation also right after the extreme event, timely providing vibrational data from the state of the structural system. Already with the near-real time SHM data (hours) after the extreme event occurrence, the bridge operator will have an updated estimate of the state, and can therefore use this estimate to decide whether to close down the bridge for one week until the inspection, or whether to continue operating the bridge. We assume that in presence of the SHM data, the operator will be willing to accept a risk associated with continuation of the bridge operation if the updated estimate of the failure rate is lower than p^{I}_{th}. If p^{I}_{th} is exceeded, then the bridge will be closed down, with an associated cost of $c_{\text{clsdn}} = 1.5 \cdot 10^5$€/day.

To summarize, in the case without SHM, inspections take place every 5 years, when p^{I}_{th} is exceeded, and one week after an extreme event occurrence. The bridge is always closed down for this one week until the inspection. A repair is triggered when p^{R}_{th} is exceeded.

In the case with SHM, inspections take place when p^{I}_{th} is exceeded, and one week after an extreme event occurrence. If the near real-time SHM-informed estimate of the failure rate exceeds p^{I}_{th}, then the bridge is closed down for this one week until the inspection, otherwise it is allowed that the bridge continues operating. A repair is triggered when p^{R}_{th} is exceeded.

With the setup described above, we run the VoSHM analysis with $n_{\text{MCS}} = 1000$ samples, and we obtain an estimate of the near-real time $VoSHM = 1.34 \cdot 10^6$€. The $VoSHM$ in this third case study is one order of magnitude larger than in the previous two case studies. The reason for this is that the close-down cost per day is large, and hence the expected total close-down costs largely dominate the expected total life-cycle cost (the are one order of magnitude larger than the expected total inspection, repair, and risk costs).

This result shows that an effective SHM system for near real-time diagnostics might provide significant economic benefit, if it leads to avoidance of unnecessary close-downs.

5.6.3.4 Fourth case study: Reliability-based management

In all three case studies of Section 5.6.3.1-Section 5.6.3.3, we employ the heuristic parameter vector $\boldsymbol{w}_1^* = [p_{\text{th}}^{\text{I}*} = 5 \cdot 10^{-4}, p_{\text{th}}^{\text{R}*} = 1 \cdot 10^{-3}, \Delta t_{\text{I}} = 5]$, which is optimized for the case without SHM, and $\boldsymbol{w}_2^* = [p_{\text{th}}^{\text{I}*} = 5 \cdot 10^{-4}, p_{\text{th}}^{\text{R}*} = 1 \cdot 10^{-3}, \Delta t_{\text{I}} = \infty]$. The values $p_{\text{th}}^{\text{I}*}$ and $p_{\text{th}}^{\text{R}*}$ of the thresholds used for inspection and repair decisions imply failure rates that are higher than what is typically accepted by authorities. As mentioned in Section 5.3.1, the presented framework can also be used when replacing the optimization of the heuristic parameters by a choice based on expert assessment. The current subsection aims to demonstrate the VoSHM quantification in the case when reliability thresholds are imposed by authorities.

To this end, we revisit the first case study of Section 5.6.3.1, but we now assume that a threshold for repairs $p_{\text{th}}^{\text{R}} = 10^{-5}$ is imposed, and not subject to any optimization. We therefore optimize only the inspection threshold, and we find $p_{\text{th}}^{\text{I}*} = 7 \cdot 10^{-6}$. We eventually use the heuristic parameter vector $\boldsymbol{w}_1^* = [p_{\text{th}}^{\text{I}*} = 7 \cdot 10^{-6}, p_{\text{th}}^{\text{R}} = 10^{-5}, \Delta t_{\text{I}} = 5]$ for the case of inspections only, and $\boldsymbol{w}_2^* = [p_{\text{th}}^{\text{I}*} = 7 \cdot 10^{-6}, p_{\text{th}}^{\text{R}} = 10^{-5}, \Delta t_I = \infty]$ for the case with SHM, and we run a VoSHM analysis with $n_{\text{MCS}} = 1000$ samples. We quantify $VoSHM = 7.70 \cdot 10^4$€. This value is slightly lower than the VoSHM value from the first case study of Section 5.6.3.1, where both thresholds $p_{\text{th}}^{\text{I}}, p_{\text{th}}^{\text{R}}$ were optimized for the case without SHM.

5.7 Concluding remarks

This paper presents a Bayesian decision analysis framework for quantifying the expected gains that continuous vibration-based SHM-aided maintenance planning can provide when compared against the currently dominant approach of intermittent inspection-based maintenance planning; the Value of SHM (VoSHM) metric is adopted for formally computing this benefit. The framework requires the a-priori definition of damage scenarios and the associated stochastic deterioration models, describing the damage evolution over a target structure's lifetime. Furthermore, a case-specific SHM system model is necessary to allow for sampling of monitoring information. Contingent on these considerations, this framework can support the a-priori decision, in an operational evaluation level, on whether opting for an SHM system on a target structure can provide economic benefit.

We detail the computational aspects of a VoSHM analysis, which involves stochastic sequential decision making, Bayesian analysis and structural reliability analysis. The modal data, identified

sequentially over the structural life-cycle at different damage levels and for varying environmental conditions, is sampled in a realistic manner, following a state-of-the-art operational modal analysis procedure. The effect of the environmental variability present in the identified modal data is accounted for via Bayesian analysis. Sequential Bayesian updating of the deterioration state and model parameters, and consequently the structural reliability, is efficiently performed via adoption of a particle filtering scheme. Heuristic decision strategies, based on the updating of the risk estimation through inspection and monitoring, simplify the computationally challenging solution to the stochastic sequential decision making problem. A detailed algorithmic summary of a VoSHM analysis is provided, which is meant to act as an implementation template of the proposed framework for the interested reader.

We discuss a novel classification of SHM use cases in terms of the associated time scales for decision making for infrastructure management. A gradual and shock stochastic deterioration model is employed, which is flexible in simulating various of these use cases. By means of a numerical model of a deteriorating two-span bridge system, we showcase the VoSHM analysis for four different case studies, across different time scales. The results show that investing in SHM systems can potentially lead to large benefits. It should be noted that the VoSHM framework of this paper does not incorporate deterioration or failure of the SHM system itself, and does not take into account modeling errors; it thus provides an upper limit to the "true" VoSHM. For the purpose of illustration, in the presented numerical investigations, only a single deteriorating component has been considered, which tends to underestimate the VoSHM. The framework can, however, be extended to multiple deteriorating components. In general, the models utilized to showcase the illustrated framework in this paper can be extended to incorporate additional factors and uncertainties. While this can lead to increased computation, the main challenge to such extensions lies in the need for more detailed modeling, which is often difficult to justify in real-world projects. Hence, we believe that the level of detailing and accuracy reflected in the illustration in this paper is representative of what one can do when assessing the benefit of real-world SHM systems.

This framework can be applied for optimal sensor placement studies as well. In this regard, the sensor placement which leads to the optimal balance between a large VoSHM and a low life-cycle cost of the SHM system would be the preferred arrangement.

Acknowledgments

The work of A. Kamariotis and E. Chatzi has been carried out with the support of the Technical University of Munich - Institute for Advanced Study, Germany, funded by the German Excellence Initiative and the TÜV SÜD Foundation. We thank Dr. Konstantinos Tatsis for providing the code for the stochastic subspace identification algorithm and for the support provided for seamless integration of the SSI algortihm within the presented framework.

References

[1] I. Anderson. *Improving Detection And Prediction Of Bridge Scour Damage And Vulnerability Under Extreme Flood Events Using Geomorphic And Watershed Data.* USA: PhD thesis, University of Vermont, 2018.

[2] C. P. Andriotis and K. G. Papakonstantinou. "Managing engineering systems with large state and action spaces through deep reinforcement learning". In: *Reliability Engineering & System Safety* 191 (2019), p. 106483.

[3] C. P. Andriotis, K. G. Papakonstantinou, and E. N. Chatzi. "Value of structural health information in partially observable stochastic environments". In: *Structural Safety* 93 (2021), p. 102072.

[4] I. Behmanesh and B. Moaveni. "Accounting for environmental variability, modeling errors,and parameter estimation uncertainties in structural identification". In: *Journal of Sound and Vibration* 374 (2016), pp. 92–110.

[5] I. Behmanesh, B. Moaveni, G. Lombaert, and C. Papadimitriou. "Hierarchical Bayesian model updating for structural identification". In: *Mechanical Systems and Signal Processing* 64-65 (2015), pp. 360–376.

[6] W. Betz, I. Papaioannou, and D. Straub. "Transitional Markov Chain Monte Carlo: Observations and Improvements". In: *Journal of Engineering Mechanics* 142.5 (2016).

[7] E. Bismut and D. Straub. "Optimal Adaptive Inspection and Maintenance Planning for Deteriorating Structural Systems". In: *Reliability Engineering and System Safety* 215 (2021), p. 107891.

[8] J. Briaud, S. Hurlebaus, K. Chang, C. Yao, H. Sharma, O. Yu, and et al. "Realtime monitoring of bridge scour using remote monitoring technology". In: (2011).

[9] P. Cawley. "Structural health monitoring: Closing the gap between research and industrial deployment". In: *Structural Health Monitoring* 17(5) (2018), pp. 1225–1244.

[10] A. Doucet, N. de Freitas, and N. Gordon. *Sequential Monte Carlo Methods in Practice.* Springer-Verlag New York, 2001.

[11] B. Ellingwood. "Risk-informed condition assessment of civil infrastructure: state of practice and research issues". In: *Structure and Infrastructure Engineering* 1(1) (2005), pp. 7–18.

[12] C. R. Farrar and K. Worden. "An introduction to structural health monitoring". In: *Philosophical Transactions of the Royal Society A.* 365 (2007), pp. 303–315.

[13] C. R. Farrar and K. Worden. *Structural Health Monitoring: A Machine Learning Perspective.* John Wiley & Sons, Ltd, 2013.

[14] E. Figueiredo, G. Park, C. R. Farrar, K. Worden, and J. Figueiras. "Machine learning algorithms for damage detection under operational and environmental variability". In: *Structural Health Monitoring* 10.6 (2011), pp. 559–572.

[15] D. M. Frangopol, K.-Y. Lin, and A. C. Estes. "Life-Cycle Cost Design of Deteriorating Structures". In: *Journal of Structural Engineering* 123.10 (1997), pp. 1390–1401.

[16] A. J. Garcia-Palencia, E. Santini-Bell, J. D. Sipple, and M. Sanayei. "Structural model updating of an in-service bridge using dynamic data". In: *Struct. Control Health Monit.* (2015).

[17] A. Gelman, J. B. Carlin, H. S. Stern, D. B. Dunson, A. Vehtari, and D. B. Rubin. *Bayesian data analysis (3rd edition)*. Chapman and Hall/CRC, 2013.

[18] P. F. Giordano, L. J. Prendergast, and M. P. Limongelli. "A framework for assessing the value of information for health monitoring of scoured bridges". In: *Journal of Civil Structural Health Monitoring* 10(3) (2020), pp. 485–496.

[19] F. Jensen and T. Nielsen. *Bayesian Networks and Decision Graphs, 2nd Edition*. New York: Springer, 2007.

[20] V. Jensen. "Alkali-silica reaction damage to Elgeseter Bridge, Trondheim, Norway: a review of construction, research and repair up to 2003". In: *Materials Characterization* 53.2 (2004), pp. 155–170.

[21] G. Jia and P. Gardoni. "State-dependent stochastic models: A general stochastic framework for modeling deteriorating engineering systems considering multiple deterioration processes and their interactions". In: *Structural Safety* 72 (2018), pp. 99–110.

[22] A. Kamariotis, E. Chatzi, and D. Straub. "Quantifying the value of vibration-based structural health monitoring considering environmental variability". In: *Structural Health Monitoring 2021. Proceedings of the 13th International Workshop on Structural Health Monitoring*. Stanford University, CA, USA, 2022, pp. 1033–1040.

[23] A. Kamariotis, E. Chatzi, and D. Straub. "Value of Information from SHM via estimating deterioration jump processes with particle filtering". In: *Engineering Mechanics Institute Conference and Probabilistic Mechanics & Reliability Conference (EMI/PMC 2021)*. 2021.

[24] A. Kamariotis, E. Chatzi, and D. Straub. "A framework for quantifying the value of vibration-based structural health monitoring". In: *Mechanical Systems and Signal Processing* 184 (2023), p. 109708.

[25] A. Kamariotis, E. Chatzi, and D. Straub. "Value of information from vibration-based structural health monitoring extracted via Bayesian model updating". In: *Mechanical Systems and Signal Processing* 166 (2022), p. 108465.

[26] A. Kamariotis, L. Sardi, I. Papaioannou, E. Chatzi, and D. Straub. "On off-line and on-line Bayesian filtering for uncertainty quantification of structural deterioration". In: *Data-Centric Engineering* 4 (2023), e17.

[27] N. Kantas, A. Doucet, S. S. Singh, J. Maciejowski, and N. Chopin. "On Particle Methods for Parameter Estimation in State-Space Models". In: *Statistical Science* 30.3 (2015), pp. 328–351.

[28] M. J. Kochenderfer. *Decision making under uncertainty: Theory and application*. English. MIT Lincoln Laboratory Series. The MIT Press, 2015.

[29] R. Lamb, P. Garside, R. Pant, and J. W. Hall. "A Probabilistic Model of the Economic Risk to Britain's Railway Network from Bridge Scour During Floods". In: *Risk analysis* 39.11 (2019), pp. 2457–2478.

[30] J. Luque and D. Straub. "Risk-based optimal inspection strategies for structural systems using dynamic Bayesian Networks". In: *Structural Safety* 76 (2019), pp. 68–80.

[31] H. Martin-Sanz, K. Tatsis, V. K. Dertimanis, L. D. Avendaño-Valencia, E. Brühwiler, and E. Chatzi. "Monitoring of the UHPFRC strengthened Chillon viaduct under environmental and operational variability". In: *Structure and Infrastructure Engineering* 16.1 (2020), pp. 138–168.

[32] G. J. McLachlan and T. Krishnan. *The EM Algorithm and Extensions, Second Edition*. John Wiley & Sons, Ltd, 2007.

[33] R. E. Melchers and A. Beck. *Structural Reliability Analysis and Prediction, 3rd Edition*. John Wiley & Sons, Ltd, 2017.

[34] P. Morato, K. Papakonstantinou, C. Andriotis, J. Nielsen, and P. Rigo. "Optimal inspection and maintenance planning for deteriorating structural components through dynamic Bayesian networks and Markov decision processes". In: *Structural Safety* 94 (2022), p. 102140.

[35] P. Moser and B. Moaveni. "Environmental effects on the identified natural frequencies of the Dowling Hall Footbridge". In: *Mechanical Systems and Signal Processing* 25(7) (2011), pp. 2336–2357.

[36] K. P. Murphy. *Machine Learning: A Probabilistic Perspective*. The MIT Press, 2012.

[37] J. Nielsen and J. Sorensen. "Risk-based operation and maintenance planning for offshore wind turbines". In: *Proceedings of the reliability and optimization of structural systems*. Munich, Germany, 2010.

[38] J. S. Nielsen, D. Tcherniak, and M. D. Ulriksen. "A case study on risk-based maintenance of wind turbine blades with structural health monitoring". In: *Structure and Infrastructure Engineering* 17.3 (2021), pp. 302–318.

[39] K. Papakonstantinou and M. Shinozuka. "Planning structural inspection and maintenance policies via dynamic programming and Markov processes. Part I: Theory". In: *Reliability Engineering & System Safety* 130 (2014), pp. 202–213.

[40] B. Peeters and G. D. Roeck. "Reference-based stochastic subspace identification for output-only modal analysis". In: *Mechanical Systems and Signal Processing* 13(6) (1999), pp. 855–878.

[41] B. Peeters. *System identification and damage detection in civil engineering*. Belgium: PhD thesis, Katholieke Universiteit Leuven, 2000.

[42] M. Pozzi and A. D. Kiureghian. "Assessing the Value of Information for long-term structural health monitoring". In: *SPIE Conference on Health Monitoring of Structural and Biological Systems*. San Diego, California, USA, 2011.

[43] M. Pregnolato, A. Ford, S. M. Wilkinson, and R. J. Dawson. "The impact of flooding on road transport: A depth-disruption function". In: *Transportation Research Part D: Transport and Environment* 55 (2017), pp. 67–81.

[44] L. Prendergast and K. Gavin. "A review of bridge scour monitoring techniques". In: *Journal of Rock Mechanics and Geotechnical Engineering* 6 (2014), pp. 138–149.

[45] L. Prendergast, D. Hester, K. Gavin, and J. O'Sullivan. "An investigation of the changes in the natural frequency of a pile affected by scour". In: *Journal of Sound and Vibration* 332.25 (2013), pp. 6685–6702.

[46] H. Raiffa and R. Schlaifer. *Applied statistical decision theory*. Harvard University, Boston: Division of Research, Graduate School of Business Administration, 1961.

[47] A. R. Sakulich and D. P. Bentz. "Increasing the Service Life of Bridge Decks by Incorporating Phase-Change Materials to Reduce Freeze-Thaw Cycles". In: *Journal of Materials in Civil Engineering* 24.8 (2012), pp. 1034–1042.

[48] M. Sanchez-Silva, G.-A. Klutke, and D. V. Rosowsky. "Life-cycle performance of structures subject to multiple deterioration mechanisms". In: *Structural Safety* 33.3 (2011), pp. 206–217.

[49] M. Sanchez-Silva, G.-A. Klutke, and D. V. Rosowsky. *Reliability and Life-Cycle Analysis of Deteriorating Systems*. Springer Series in Reliability Engineering, 2016.

[50] S. Särkkä. *Bayesian Filtering and Smoothing*. English. United Kingdom: Cambridge University Press, 2013.

[51] M. Sasidharan, A. K. Parlikad, and J. Schooling. "Risk-informed asset management to tackle scouring on bridges across transport networks". In: *Structure and Infrastructure Engineering* (2021), pp. 1–17.

[52] E. Simoen, G. D. Roeck, and G. Lombaert. "Dealing with uncertainty in model updating for damage assessment: a review". In: *Mechanical Systems and Signal Processing* 56 (2015), pp. 123–149.

[53] M. D. Spiridonakos, E. N. Chatzi, and B. Sudret. "Polynomial Chaos Expansion Models for the Monitoring of Structures under Operational Variability". In: *ASCE-ASME Journal of Risk and Uncertainty in Engineering Systems, Part A: Civil Engineering* 2.3 (2016), B4016003.

[54] D. Straub. "Value of information analysis with structural reliability methods". In: *Structural Safety* 49 (2014), pp. 68–80.

[55] D. Straub, E. Chatzi, E. Bismut, et al. "Value of information: A roadmap to quantifying the benefit of structural health monitoring". In: *Proceedings of the 12th International Conference on Structural Safety and Reliability: ICOSSAR 2017*. Vienna, Austria, 2017, pp. 3018–3029.

[56] D. Straub and M. H. Faber. "Risk based inspection planning for structural systems". In: *Structural Safety* 27(4) (2005), pp. 335–355.

[57] D. Straub, R. Schneider, E. Bismut, and H.-J. Kim. "Reliability analysis of deteriorating structural systems". In: *Structural Safety* 82 (2020), p. 101877.

[58] H. Streicher and R. Rackwitz. "Time-variant reliability-oriented structural optimization and a renewal model for life-cycle costing". In: *Probabilistic Engineering Mechanics* 19.1 (2004), pp. 171–183.

[59] K. Tatsis and E. Chatzi. "A numerical benchmark for system identification under operational and environmental variability". In: *8th International Operational Modal Analysis Conference (IOMAC 19)*. Copenhagen, Denmark, 2019.

[60] K. E. Tatsis, V. K. Dertimanis, and E. N. Chatzi. "Sequential Bayesian Inference for Uncertain Nonlinear Dynamic Systems: A Tutorial". In: *Journal of Structural Dynamics* (2022), pp. 236–262.

[61] S. Thöns. "On the value of monitoring information for the structural integrity and risk management". In: *Computer-Aided Civil and Infrastructure Engineering* 33(1) (2018), pp. 79–94.

[62] E. Tubaldi, E. Ozer, J. Douglas, and P. Gehl. "Examining the contribution of near real-time data for rapid seismic loss assessment of structures". In: *Structural Health Monitoring* 21.1 (2022), pp. 118–137.

[63] J. van Noortwijk. "A survey of the application of gamma processes in maintenance". In: *Reliability Engineering and System Safety* 94.1 (2009), pp. 2–21.

[64] A. Verzobio, D. Bolognani, J. Quigley, and D. Zonta. "Quantifying the benefit of structural health monitoring: can the value of information be negative?" In: *Structure and Infrastructure Engineering* (2021), pp. 1–22.

[65] C. Wang, X. Yu, and F. Liang. "A review of bridge scour: mechanism, estimation, monitoring and countermeasures". In: *Nat Hazards* 87 (2017), pp. 1881–1906.

[66] A. Wirgin. "The inverse crime". In: *arXiv e-prints*, math-ph/0401050 (2004), math–ph/0401050.

[67] C. Ye, S. C. Kuok, L. J. Butler, and C. R. Middleton. "Implementing bridge model updating for operation and maintenance purposes: examination based on UK practitioners' views". In: *Structure and Infrastructure Engineering* (2021), pp. 1–20.

[68] S. Zhu and D. Levison. "A review of research on planned and unplanned disruptions to transporation networks". In: *Transportation Research Record* 89 (2010), pp. 1–11.

Chapter 6

On off-line and on-line Bayesian filtering for uncertainty quantification of structural deterioration

Original Publication

A. Kamariotis, L. Sardi, I. Papaioannou, E. Chatzi, and D. Straub. "On off-line and on-line Bayesian filtering for uncertainty quantification of structural deterioration". In: *Data-Centric Engineering* 4 (2023), e17.

Author's contribution

Antonios Kamariotis: Conceptualization, Methodology, Software, Formal analysis, Visualization, Writing - original draft. **Luca Sardi**: Conceptualization, Methodology, Software, Formal analysis, Visualization. **Iason Papaioannou**: Conceptualization, Methodology, Writing - review & editing. **Eleni Chatzi**: Conceptualization, Methodology, Writing - review & editing, Funding acquisition. **Daniel Straub**: Conceptualization, Methodology, Writing - review & editing, Funding acquisition.

Abstract

Data-informed predictive maintenance planning largely relies on stochastic deterioration models. Monitoring information can be utilized to update sequentially the knowledge on model parameters. In this context, on-line (recursive) Bayesian filtering algorithms typically fail to properly quantify the full posterior uncertainty of time-invariant deterioration model parameters. Off-line (batch) algorithms are - in principle - better suited for the uncertainty quantification task, yet they are computationally prohibitive in sequential settings. In this work, we adapt and investigate selected Bayesian filters for parameter estimation: an on-line particle filter, an on-line iterated batch importance sampling filter, which performs Markov chain Monte Carlo (MCMC) move steps, and an

off-line MCMC-based sequential Monte Carlo filter. A Gaussian mixture model is used to approximate the posterior distribution within the resampling process in all three filters. Two numerical examples serve as the basis for a comparative assessment. The first case study considers a low-dimensional, nonlinear, non-Gaussian probabilistic fatigue crack growth model that is updated with sequential monitoring measurements. The second high-dimensional, linear, Gaussian case study employs a random field to model corrosion deterioration across a beam, which is updated with sequential sensor measurements. The numerical investigations provide insights into the performance of off-line and on-line filters in terms of the accuracy of posterior estimates and the computational cost, when applied to problems of different nature, increasing dimensionality and varying sensor information amount. Importantly, they show that a tailored implementation of the on-line particle filter proves competitive with the computationally demanding MCMC-based filters. Suggestions on the choice of the appropriate method in function of problem characteristics are provided.

Impact Statement

Stochastic models describing time-evolving deterioration processes are widespread in engineering. In the modern data-rich engineering landscape, Bayesian methods can exploit monitoring data to sequentially update knowledge on underlying model parameters. The precise probabilistic characterization of these parameters is indispensable for several real-world tasks, where decisions need to be taken in view of the evaluated margins of risk and uncertainty. This work investigates and compares on-line and off-line Bayesian filters and adapts the former for posterior uncertainty quantification of time-invariant parameters. We show that tailored on-line particle filters are competitive alternatives to off-line Bayesian filters, especially in certain high-dimensional settings.

6.1 Introduction

Structural deterioration of various forms is present in most mechanical and civil structures and infrastructure systems. Accurate and effective tracking of structural deterioration processes can help to effectively manage it and minimize the total life-cycle costs [8, 30, 51, 46]. The deployment of sensors on structural components/systems can enable long-term monitoring of such processes. Monitoring data obtained sequentially at different points in time must be utilized in an efficient manner within a Bayesian framework to enable data-informed estimation and prediction of the deterioration process evolution.

Monitored structural deterioration processes are commonly modeled using Markovian state-space representations [63, 9, 5], whereby the deterioration state evolution is represented by a recursive Markov process equation, and is subject to stochastic process noise [19]. Monitoring information is incorporated by means of the measurement equation. The deterioration models further contain time-invariant uncertain parameters. The state-space can be augmented to include these parameters, if one wishes to obtain updated estimates thereof conditional on the monitoring information [80, 72, 83, 19, 90, 21, 45]; this is referred to as joint state-parameter estimation [73, 48].

A different approach entails defining the structural deterioration state evolution solely as a function

of uncertain time-invariant model parameters [25, 87, 28, 78], which can be updated in view of the monitoring data. This updating, referred to herein as Bayesian parameter estimation, is often the primary task of interest. In this approach, the deterioration state variables are obtained as outputs of the calibrated deterioration model with posterior parameter estimates [50, 69]. The parameter estimation problem can be cast into a Markovian state-space representation. Quantifying the full posterior uncertainty of the time-invariant model parameters is essential for performing monitoring-informed predictions on the deterioration process evolution, the subsequent monitoring-informed estimation of the time-variant structural reliability [81, 59] or the remaining useful life [83, 51], and eventually for predictive maintenance planning.

Bayesian estimation of time-invariant deterioration model parameters is the main focus of this paper. In long-term deterioration monitoring settings, where data is obtained sequentially at different points in time, Bayesian inference can be performed either in an on-line or an off-line framework [79, 48, 4]. In literature, these are also referred to as recursive (on-line) and batch (off-line) estimation [73]. Parameter estimation is cast into a state-space setup to render it suitable for application with on-line Bayesian filtering algorithms [48], such as the Kalman filter [44] and its nonlinear variants [42, 43, 22, 76], the ensemble Kalman filter [29], and particle filters [26, 18, 27, 40, 73, 84]. We employ on-line particle filter methods for pure recursive estimation of time-invariant deterioration model parameters. This is not the typical use case for such methods, which often yield degenerate and impoverished posterior estimates, hence, failing to effectively characterize the posterior uncertainty [61, 73]. In this work we tailor on-line particle filters for quantifying the full posterior uncertainty of time-invariant model parameters. Subsequently, we provide a formal investigation and discussion on their suitability with respect to this task.

In its most typical setting within engineering applications, Bayesian parameter estimation is commonly performed with the use of off-line Markov Chain Monte Carlo (MCMC) methods, which have been used extensively in statistics and engineering to sample from complex posterior distributions of model parameters [39, 35, 6, 38, 15, 65, 89, 57]. However, use of off-line methods for on-line estimation tasks is computationally prohibitive [61, 48]. Additionally, when considering off-line inference, in settings when measurements are obtained sequentially at different points in time, off-line MCMC methods tend to induce a larger computational cost than on-line particle filter methods, which can be important, e.g., when optimizing inspection and monitoring [67, 56, 45]. Questions that we investigate in this context include: Can one precisely quantify the posterior uncertainty of time-invariant parameters when employing on-line particle filter methods? How does this quantification compare against the posterior estimates obtained with off-line MCMC methods? How does the estimation accuracy depend on the nature of the problem, i.e., dimensionality, nonlinearity, or non-Gaussianity? What is the computational cost induced by the different methods? Ideally, one would opt for the method which can provide sufficiently accurate posterior results at the expense of the least computational cost. To address these questions, this paper selects and adapts algorithms in view of parameter estimation, and performs a comparative assessment of selected off-line and on-line Bayesian filters specifically tailored for posterior uncertainty quantification of time-invariant parameters. The innovative comparative assessment results in a set of suggestions on the choice of the appropriate algorithm in function of problem characteristics.

The paper is structured as follows. Section 6.2 provides a detailed description of on-line and off-line Bayesian inference in the context of parameter estimation. Three different selected and adapted Bayesian filters are presented in algorithmic detail, namely an on-line particle filter with Gaussian mixture-based resampling (PFGM) [60, 58], the on-line iterated batch importance sampling filter

(IBIS) [17], which performs off-line MCMC steps with a Gaussian mixture as a proposal distribution, and an off-line MCMC-based sequential Monte Carlo (SMC) filter [61], which enforces tempering of the likelihood function (known as simulated annealing) to sequentially arrive to the single final posterior density of interest [64, 41]. The tPFGM and tIBIS variants, which adapt the PFGM and IBIS filters by employing tempering of the likelihood function of each new measurement, are further presented and proposed for problems with high sensor information amount. Section 6.3 describes the two case studies that serve as the basis for numerical investigations, one non-linear, non-Gaussian and low-dimensional and one linear, Gaussian and high-dimensional. MATLAB codes implementing the different algorithms and applying them on the two case studies introduced in this paper are made publicly available via a GitHub repository[1]. Section 6.4 summarizes the findings of this comparative assessment, provides suggestions on choice of the appropriate method according to the nature of the problem, discusses cases which are not treated in our investigations, and concludes this work.

6.2 On-line and off-line Bayesian filtering for time-invariant parameter estimation

This work assumes the availability of a stochastic deterioration model D, parametrized by a vector $\boldsymbol{\theta} \in \mathbb{R}^d$ containing the d uncertain time-invariant model parameters. We collect the uncertain parameters influencing the deterioration process in the vector $\boldsymbol{\theta}$. In the Bayesian framework, $\boldsymbol{\theta}$ is modeled as a vector of random variables with a prior distribution $\pi_{\text{pr}}(\boldsymbol{\theta})$. We assume that the deterioration process is monitored via a permanently installed monitoring system. Long-term monitoring of a deterioration process leads to sets of noisy measurements $\{y_1, \ldots, y_n\}$ obtained sequentially at different points in time $\{t_1, \ldots, t_n\}$ throughout the lifetime of a structural component/system. Such measurements can be used to update the distribution of $\boldsymbol{\theta}$; this task is referred to as Bayesian parameter estimation. Within a deterioration monitoring setting, Bayesian parameter estimation can be performed either in an on-line or an off-line framework [48], depending on the task of interest.

In an on-line framework, one is interested in updating the distribution of $\boldsymbol{\theta}$ in a sequential manner, i.e., at every time step t_n when a new measurement y_n becomes available, conditional on all measurements available up to t_n. Thus, in an on-line framework, inference of the sequence of posterior densities $\{\pi_{\text{pos}}(\boldsymbol{\theta}|\mathbf{y}_{1:n})\}_{n\geq 1}$ is the goal, where $\mathbf{y}_{1:n}$ denotes the components $\{y_1, \ldots, y_n\}$. We point out that in this paper the term on-line does not relate to "real-time" estimation, although on-line algorithms are also used in real-time estimation [13, 71].

In contrast, in an off-line framework, inference of $\boldsymbol{\theta}$ is performed at a fixed time step t_N using a fixed set of measurements $\{y_1, \ldots, y_N\}$, and the single posterior density $\pi_{\text{pos}}(\boldsymbol{\theta}|\mathbf{y}_{1:N})$ is sought, which can be estimated via Bayes' rule as

$$\pi_{\text{pos}}(\boldsymbol{\theta}|\mathbf{y}_{1:N}) \propto L(\mathbf{y}_{1:N}|\boldsymbol{\theta})\pi_{\text{pr}}(\boldsymbol{\theta}), \tag{6.1}$$

where $L(\mathbf{y}_{1:N}|\boldsymbol{\theta})$ denotes the likelihood function of the whole measurement set $\mathbf{y}_{1:N}$ given the parameters $\boldsymbol{\theta}$. With the assumption that measurements are independent given the parameter state,

[1] https://github.com/antoniskam/Offline_online_Bayes

$L(\mathbf{y}_{1:N}|\boldsymbol{\theta})$ can be expressed as a product of the likelihoods $L(y_n|\boldsymbol{\theta})$ as

$$L(\mathbf{y}_{1:N}|\boldsymbol{\theta}) = \prod_{n=1}^{N} L(y_n|\boldsymbol{\theta}). \tag{6.2}$$

MCMC methods sample from $\pi_{\text{pos}}(\boldsymbol{\theta}|\mathbf{y}_{1:N})$ via simulation of a Markov chain with $\pi_{\text{pos}}(\boldsymbol{\theta}|\mathbf{y}_{1:N})$ as its stationary distribution, e.g., by performing Metropolis Hastings (MH) steps [39]. MCMC methods do not require estimation of the normalization constant in Eq. (6.1). However, in the on-line framework, MCMC methods are impractical, since they require simulating anew a different Markov chain for each new posterior $\pi_{\text{pos}}(\boldsymbol{\theta}|\mathbf{y}_{1:n})$, and the previously generated Markov chain for the posterior estimation of $\pi_{\text{pos}}(\boldsymbol{\theta}|\mathbf{y}_{1:n-1})$ is not accounted for, except when choosing the seed for initializing the new Markov chain. This implies that MCMC methods quickly become computationally prohibitive in the on-line framework, already for a small n. An additional computational burden stems from the fact that each step within the MCMC sampling process requires evaluation of the full likelihood function $L(\mathbf{y}_{1:n}|\boldsymbol{\theta})$, i.e., the whole set of measurements $\mathbf{y}_{1:n}$ needs to be processed. This leads to increasing computational complexity for increasing n, and can render use of MCMC methods computationally inefficient even for off-line inference, especially when N is large.

On-line particle filters [73, 48] operate in a sequential fashion by making use of the Markovian property of the employed state-space representation, i.e., they compute $\pi_{\text{pos}}(\boldsymbol{\theta}|\mathbf{y}_{1:n})$ solely based on $\pi_{\text{pos}}(\boldsymbol{\theta}|\mathbf{y}_{1:n-1})$ and the new measurement y_n. The typical use of particle filters targets the tracking of a system's response (dynamic state) by means of a state-space representation [37, 73], while they are often also used also for joint state-parameter estimation tasks, wherein the state-space is augmented to include the model parameters to be estimated [73, 48]. In addition, particle filters can also be applied for pure recursive estimation of time-invariant parameters, for which the noise in the dynamic model is formally zero [61, 73], although this is not the typical setting for application of particle filters. A model of the Markovian discrete time state-space representation for the case of time-invariant parameter estimation is given in Eqs. (6.3a) and (6.3b)

$$\boldsymbol{\theta}_n = \boldsymbol{\theta}_{n-1} \tag{6.3a}$$

$$y_n = D_n\left(\boldsymbol{\theta}_n\right) \exp\left(\epsilon_n\right), \tag{6.3b}$$

where ϵ_n models the error/noise of the measurement at time t_n, and $\boldsymbol{\theta}_n$ denotes the time-invariant parameter vector at time step n. The dynamic equation for the time-invariant parameters Eq. (6.3a) is introduced for the sole purpose of casting the problem into a state-space representation. Since the measurements are assumed independent given the parameter state, the errors ϵ_n in Eq. (6.3b) are independent. It should be noted that the measurement error, which is introduced in multiplicative form in Eq. (6.3b), is commonly expressed in an additive form [19]. Indeed, Eq. (6.3b) can be reformulated in the logarithmic scale, whereby the measurement error is expressed in an additive form. The multiplicative form of the measurement error in Eq. (6.3b) is consistent with the fact that - in the context of structural deterioration - measurements y_n cannot be negative. All target distributions of interest in the sequence $\pi_{\text{pos}}(\boldsymbol{\theta}_n|\mathbf{y}_{1:n})$ are defined on the same space of $\boldsymbol{\theta} \in \mathbb{R}^d$. In the remainder of this paper, the subscript n will therefore be dropped from $\boldsymbol{\theta}_n$. As previously discussed, particle filters are mainly used for on-line inference. However, these can also be used in exactly the same way for off-line inference, where only a single posterior density $\pi_{\text{pos}}(\boldsymbol{\theta}|\mathbf{y}_{1:N})$ is of interest. In this case, particle filters use the sequence of measurements successively to sequentially arrive to the final single posterior density of interest via estimating all the intermediate distributions.

6.2.1 On-line Particle Filter

Particle filter (PF) methods, also referred to as sequential Monte Carlo (SMC) methods, are importance sampling-based techniques that use a set of weighted samples $\{(\boldsymbol{\theta}_n^{(i)}, w_n^{(i)}) : \ i = 1, \ldots, N_{\text{par}}\}$, called particles, to represent the posterior distribution of interest at estimation time step n, $\pi_{\text{pos}}(\boldsymbol{\theta}|\mathbf{y}_{1:n})$. PFs form the following approximation to the posterior distribution of interest:

$$\pi_{\text{pos}}(\boldsymbol{\theta}|\mathbf{y}_{1:n}) \approx \sum_{i=1}^{N_{\text{par}}} w_n^{(i)} \delta(\boldsymbol{\theta} - \boldsymbol{\theta}_n^{(i)}), \tag{6.4}$$

where δ denotes the Dirac delta function.

When a new measurement y_n becomes available, PFs shift from $\pi_{\text{pos}}(\boldsymbol{\theta}|\mathbf{y}_{1:n-1})$ to $\pi_{\text{pos}}(\boldsymbol{\theta}|\mathbf{y}_{1:n})$ by importance sampling using an appropriately chosen importance distribution, which results in a reweighting procedure (updating of the weights). An important issue that arises from this weight updating procedure is the sample degeneracy problem [73]. This relates to the fact that the importance weights $w_n^{(i)}$ become more unevenly distributed with each updating step. In most cases, after a certain number of updating steps, the weights of almost all the particles assume values close to zero (see Fig. 6.1). This problem is alleviated by the use of adaptive resampling procedures based on the effective sample size $N_{\text{eff}} = 1/\sum_{i=1}^{N_{\text{par}}}(w_n^{(i)})^2$ [55]. Most commonly, resampling is performed with replacement according to the particle weights whenever N_{eff} drops below a user-defined threshold $N_{\text{T}} = cN_{\text{par}}, \ c \in [0, 1]$. Resampling introduces additional variance to the parameter estimates [73]. In the version of the PF algorithm presented in Alg. 1, the dynamic model of Eq. (6.3) is used as the importance distribution, as originally proposed in the bootstrap filter by [37]. Theoretical analysis of PF algorithms can be found in numerous seminal sources, e.g., [18, 61, 40].

Algorithm 1 Particle Filter (PF)

1: generate N_{par} initial particles $\boldsymbol{\theta}^{(i)}$ from $\pi_{\text{pr}}(\boldsymbol{\theta})$, $\quad i = 1, \ldots, N_{\text{par}}$
2: assign initial weights $w_0^{(i)} = 1/N_{\text{par}}$, $\quad i = 1, \ldots, N_{\text{par}}$
3: **for** $n = 1, \ldots, N$ **do**
4: evaluate likelihood of the particles based on new measurement y_n, $L_n^{(i)} = L\left(y_n \mid \boldsymbol{\theta}^{(i)}\right)$
5: update particle weights $w_n^{(i)} \propto L_n^{(i)} \cdot w_{n-1}^{(i)}$ and normalize s.t. $\sum_{i=1}^{N_{\text{par}}} w_n^{(i)} = 1$
6: evaluate $N_{\text{eff}} = \frac{1}{\sum_{i=1}^{N_{\text{par}}}\left(w_n^{(i)}\right)^2}$
7: **if** $N_{\text{eff}} < N_{\text{T}}$ **then**
8: resample particles $\boldsymbol{\theta}^{(i)}$ with replacement according to $w_n^{(i)}$
9: reset particle weights to $w_n^{(i)} = 1/N_{\text{par}}$
10: **end if**
11: **end for**

When using PFs to estimate time-invariant parameters, for which the process noise in the dynamic equation is zero, one runs into the issue of sample impoverishment [73]. The origin of this issue is the resampling process. More specifically, after a few resampling steps, most (or in extreme cases all) of the particles in the sample set end up assuming the exact same value, i.e., the particle set consists of only few (or one) distinct particles (see Fig. 6.1). The sample impoverishment issue poses the greatest obstacle for time-invariant parameter estimation with PFs. A multitude of techniques have

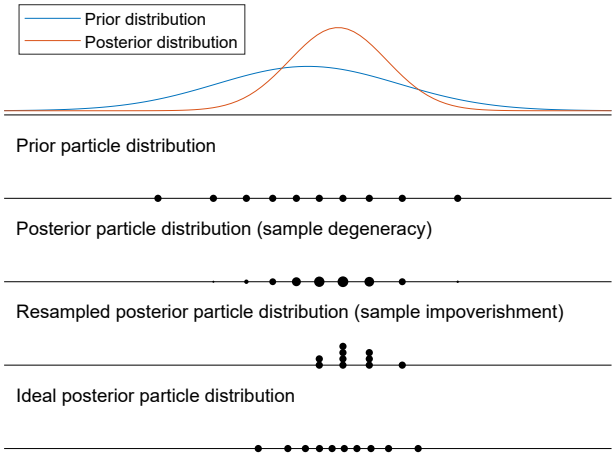

Figure 6.1: Sample degeneracy and impoverishment

been suggested in literature to alleviate the sample impoverishment issue in joint state-parameter estimation setups [see, e.g., 36, 54, 62, 79, 1, 10, 2, 16, 12]. Fewer works have proposed solutions for resolving this issue in parameter estimation setups [see, e.g., 17, 61]. One of the simplest and most commonly used approaches consists in introducing artificial dynamics in the dynamic model of the parameter vector, i.e., the dynamic model $\boldsymbol{\theta}_n = \boldsymbol{\theta}_{n-1} + \boldsymbol{\epsilon}_{n-1}$ is employed, where $\boldsymbol{\epsilon}_{n-1}$ is a small artificial process noise [52]. In this way, the time-invariant parameter vector is transformed into a time-variant one, therefore, the parameter estimation problem deviates from the original one [73, 48]. This approach can introduce a bias and an artificial variance inflation in the estimates [48]. For these reasons, this approach is not considered in this paper.

To resolve the sample impoverishment issue encountered when using the PF Alg. 1 for parameter estimation, this work employs the particle filter with Gaussian mixture resampling (PFGM), described in Alg. 2. The PFGM algorithm relates to pre-existing concepts [60, 86], and is here specifically tailored for the parameter estimation task, with its main goal being, in contrast to previous works, the quantification of the full posterior parameter uncertainty. A comparison between Algs. 1 and 2 shows that the only difference lies in the way that the resampling step is performed. PFGM replaces the standard resampling process of PF by first approximating the posterior distribution at estimation step n by a Gaussian mixture model (GMM), which is fitted via the Expectation-Maximization (EM) algorithm [58, 14] on the weighted particle set. The degenerating particle set is then rejuvenated by sampling N_{par} new particles from the GMM of Eq. (6.5),

$$p\left(\boldsymbol{\theta} \mid \mathbf{y}_{1:n}\right) \approx \sum_{i=1}^{N_{\text{GM}}} \phi_i \mathcal{N}\left(\boldsymbol{\theta}; \boldsymbol{\mu}_{\mathbf{i}}, \boldsymbol{\Sigma}_{\mathbf{i}}\right), \tag{6.5}$$

where ϕ_i represents the weight of the Gaussian component i, while $\boldsymbol{\mu}_{\mathbf{i}}$ and $\boldsymbol{\Sigma}_{\mathbf{i}}$ are the respective mean vector and covariance matrix. The number of Gaussians in the mixture N_{GM}, has to be chosen in advance, or can be estimated by use of appropriate algorithms [74, 11, 33]. In the numerical investigations of Section 6.3, we set N_{GM}=8. We point out that the efficacy of PFGM strongly depends on the quality of the GMM posterior approximation. The reason for applying a GMM (and not a single Gaussian) is that the posterior distribution can deviate from the normal distribution, and can even be multimodal or heavy-tailed.

Algorithm 2 Particle Filter with Gaussian mixture resampling (PFGM)

1: generate N_{par} initial particles $\boldsymbol{\theta}^{(i)}$ from $\pi_{\text{pr}}(\boldsymbol{\theta})$, $\quad i = 1, \ldots, N_{\text{par}}$
2: assign initial weights $w_0^{(i)} = 1/N_{\text{par}}$, $\quad i = 1, \ldots, N_{\text{par}}$
3: **for** $n = 1, \ldots, N$ **do**
4: evaluate likelihood of the particles based on new measurement y_n, $L_n^{(i)} = L\left(y_n \mid \boldsymbol{\theta}^{(i)}\right)$
5: update particle weights $w_n^{(i)} \propto L_n^{(i)} \cdot w_{n-1}^{(i)}$ and normalize s.t. $\sum_{i=1}^{N_{\text{par}}} w_n^{(i)} = 1$
6: evaluate $N_{\text{eff}} = \frac{1}{\sum_{i=1}^{N_{\text{par}}} \left(w_n^{(i)}\right)^2}$
7: **if** $N_{\text{eff}} < N_{\text{T}}$ **then**
8: EM: fit a Gaussian mixture proposal distribution $g_{\text{GM}}(\boldsymbol{\theta})$ according to $\{\boldsymbol{\theta}^{(i)}, w_n^{(i)}\}$
9: sample N_{par} new particles $\boldsymbol{\theta}^{(i)}$ from $g_{\text{GM}}(\boldsymbol{\theta})$
10: reset particle weights to $w_n^{(i)} = 1/N_{\text{par}}$
11: **end if**
12: **end for**

The simple reweighting procedure used in the on-line PFs is based on the premise that $\pi_{\text{pos}}(\boldsymbol{\theta}|\mathbf{y}_{1:n-1})$ and $\pi_{\text{pos}}(\boldsymbol{\theta}|\mathbf{y}_{1:n})$ are likely to be similar, i.e., that the new measurement y_n will not cause a very large change in the posterior. However, when that is not the case, this simple reweighting procedure is bound to perform poorly, leading to very fast degeneration of the particle set. In cases where already the first measurement set y_1 is strongly informative relative to the prior, the PF is bound to strongly degenerate already in the first weight updating step (e.g., we observe this in the second case study of Section 6.3.2 in the case of 10 sensors). To counteract this issue, in this paper we incorporate the idea of simulated annealing (enforcing tempering of the likelihood function) [64] when needed within the on-line PFGM algorithm, which we term the tPFGM Alg. 3. The tPFGM algorithm draws inspiration from previous works [31, 24], but is here tailored for the parameter estimation task, opting for the quantification of the full posterior parameter uncertainty. The algorithm operates as follows: At estimation time step n, before performing the reweighting operation, the algorithm first checks the updated effective sample size for indication of sample degeneracy. If no degeneracy is detected, tPFGM operates exactly like PFGM. When sample degeneracy occurs, tPFGM employs adaptive tempering of the likelihood $L\left(y_n \mid \boldsymbol{\theta}\right)$ of the new measurement y_n in order to "sequentially" sample from $\pi_{\text{pos}}(\boldsymbol{\theta}|\mathbf{y}_{1:n-1})$ to $\pi_{\text{pos}}(\boldsymbol{\theta}|\mathbf{y}_{1:n})$ by visiting a sequence of artificial intermediate posteriors, as defined by the tempered likelihood function $L^q\left(y_n \mid \boldsymbol{\theta}\right)$. The tempering factor q takes values between 0 and 1. When $q = 0$, the new measurement y_n is neglected, while $q = 1$ entails considering the whole likelihood function of y_n, thus reaching to $\pi_{\text{pos}}(\boldsymbol{\theta}|\mathbf{y}_{1:n})$. The intermediate values of q are adaptively selected via solution of the optimization problem in line 11 of Alg. 3, which ensures that the effective sample size does not drop below the threshold N_{T} for the chosen q value. Naturally, use of tPFGM can trigger more resampling events than PFGM, as resampling can occur more than once within a time step n.

The PFGM and tPFGM filters rely entirely on the posterior approximation via a GMM for sampling N_{par} new particles during the resampling process. However, there is no guarantee that these new particles follow the true posterior distribution of interest. The IBIS filter of the following Section 6.2.2 aims at addressing this issue.

Algorithm 3 Particle Filter with Gaussian mixture resampling and likelihood tempering (tPFGM)

generate N_{par} initial particles $\boldsymbol{\theta}^{(i)}$ from $\pi_{\text{pr}}(\boldsymbol{\theta})$, $\quad i = 1, \ldots, N_{\text{par}}$
assign initial weights $w_0^{(i)} = 1/N_{\text{par}}$, $\quad i = 1, \ldots, N_{\text{par}}$
for $n = 1, \ldots, N$ **do**
  evaluate likelihood of the particles based on new measurement y_n, $L_n^{(i)} = L\left(y_n \mid \boldsymbol{\theta}^{(i)}\right)$
  set $q = 0$ and create auxiliary particle weights $w_a^{(i)} = w_{n-1}^{(i)}$
  while $q \neq 1$ **do**
    if $N_{\text{eff}} = \left(\sum_{i=1}^{N_{\text{par}}} w_a^{(i)} \cdot {L_n^{(i)}}^{1-q}\right)^2 / \sum_{i=1}^{N_{\text{par}}} \left(w_a^{(i)} \cdot {L_n^{(i)}}^{1-q}\right)^2 > N_{\text{T}}$ **then**
      update auxiliary particle weights $w_a^{(i)} \propto w_a^{(i)} \cdot {L_n^{(i)}}^{1-q}$ and normalize s.t. $\sum_{i=1}^{N_{\text{par}}} w_a^{(i)} = 1$
      set $q = 1$
    else
      solve $\left(\sum_{i=1}^{N_{\text{par}}} w_a^{(i)} \cdot {L_n^{(i)}}^{dq}\right)^2 / \sum_{i=1}^{N_{\text{par}}} \left(w_a^{(i)} \cdot {L_n^{(i)}}^{dq}\right)^2 - N_{\text{T}} = 0$ for dq
      set $q_{\text{new}} = \min\left[q + dq, 1\right]$
      set $dq = q_{\text{new}} - q$ and $q = q_{\text{new}}$
      update auxiliary particle weights $w_a^{(i)} \propto w_a^{(i)} \cdot {L_n^{(i)}}^{dq}$ and normalize s.t. $\sum_{i=1}^{N_{\text{par}}} w_a^{(i)} = 1$
      EM: fit a Gaussian mixture proposal distribution $g_{\text{GM}}(\boldsymbol{\theta})$ according to $\{\boldsymbol{\theta}^{(i)}, w_a^{(i)}\}$
      sample N_{par} new particles $\boldsymbol{\theta}^{(i)}$ from $g_{\text{GM}}(\boldsymbol{\theta})$
      reset auxiliary particle weights to $w_a^{(i)} = 1/N_{\text{par}}$
    end if
  end while
  set $w_n^{(i)} = w_a^{(i)}$
end for

6.2.2 Iterated Batch Importance Sampling

Implementing MCMC steps within PF methods to move the particles after a resampling step was originally proposed by [36], in the so-called resample-move algorithm. [17] introduced a special case of the resample-move algorithm, specifically tailored for application to static parameter estimation purposes, namely the iterated batch importance sampling (IBIS) filter. IBIS was originally introduced as an iterative method for solving off-line estimation tasks by incorporating the sequence of measurements one at a time. In doing this, the algorithm visits the sequence of intermediate posteriors within its process, and can therefore also be used to perform on-line estimation tasks. An on-line version of the IBIS filter is presented in Alg. 5, used in conjuction with the MCMC routine of Alg. 4.

The core idea of the IBIS filter is the following: At estimation step n, if sample degeneracy is identified, first the particles are resampled with replacement, and subsequently the resampled particles are moved with a Markov chain transition kernel whose stationary distribution is $\pi_{\text{pos}}(\boldsymbol{\theta}|\mathbf{y}_{1:n})$. More specifically, each of the N_{par} resampled particles is used as the seed to perform a single MCMC step. This approach is inherently different to standard applications of MCMC, where a transition kernel is applied multiple times on one particle.

A question that arises is how to choose the Markov chain transition kernel. [17] argues for choosing a transition kernel that ensures that the proposed particle only weakly depends on the seed particle value. It is therefore recommended to use an independent Metropolis-Hastings (IMH) kernel, wherein the proposed particle is sampled from a proposal distribution g, which has to be as close as possible to the target distribution $\pi_{\text{pos}}(\boldsymbol{\theta}|\mathbf{y}_{1:n})$. In obtaining such a proposal distribution, along the lines of what is described in Section 6.2.1, in this work we employ a GMM approximation (see Eq. (6.5)) of the target distribution as the proposal density $g_{\text{GM}}(\boldsymbol{\theta})$ within the IMH kernel [66, 77]. The IMH kernel with a GMM proposal distribution is denoted IMH-GM herein. The acceptance probability (line 6 of Alg. 4) of the IMH-GM kernel is a function of both the initial seed particle and the GMM proposed particle. The acceptance rate can indicate how efficient the IMH-GM kernel is in performing the MCMC move step within the IBIS algorithm. It is important to note that when computing the acceptance probability, a call of the full likelihood function is invoked, which requires the whole set of measurements $y_{1:n}$ to be processed; this leads to a significant additional computational demand, which pure on-line methods are not supposed to accommodate [26].

The performance of the IBIS sampler depends highly on the mixing properties of the IMH-GM kernel. If the kernel leads to slowly decreasing chain auto-correlation, the moved particles are bound to remain in regions close to the particles obtained by the resampling step. This can lead to an underrepresentation of the parameter space of the intermediate posterior distribution. It might therefore be beneficial to add a burn-in period within the IMH-GM kernel [61]. Implementing that is straightforward and is shown in Alg. 4, where n_{B} is the user-defined number of burn-in steps. Naturally, the computational cost of the IMH-GM routine increases linearly with the number of burn-in steps.

Algorithm 4 Independent Metropolis Hastings with GM proposal (IMH-GM)

1: **IMH-GM Input**: $\{\boldsymbol{\theta}^{(i)}, L^{(i)} \cdot \pi_{\text{pr}}(\boldsymbol{\theta}^{(i)})\}$, $\pi_{\text{pr}}(\boldsymbol{\theta})$, $L(\mathbf{y}_{1:n}|\boldsymbol{\theta})$ and $g_{\text{GM}}(\boldsymbol{\theta})$
2: **for** $i = 1, \ldots, N_{\text{par}}$ **do**
3: **for** $j = 1, \ldots, n_{\text{B}} + 1$ **do**
4: sample candidate particle $\boldsymbol{\theta}_{c,j}^{(i)}$ from $g_{\text{GM}}(\boldsymbol{\theta})$
5: evaluate $L_{c,j}^{(i)} = L(\mathbf{y}_{1:n}|\boldsymbol{\theta}_{c,j}^{(i)})$ for candidate particle
6: evaluate acceptance ratio $\alpha = \min\left[1, \frac{L_{c,j}^{(i)} \cdot \pi_{\text{pr}}(\boldsymbol{\theta}_{c,j}^{(i)}) \cdot g_{\text{GM}}(\boldsymbol{\theta}^{(i)})}{L^{(i)} \cdot \pi_{\text{pr}}(\boldsymbol{\theta}^{(i)}) \cdot g_{\text{GM}}(\boldsymbol{\theta}_{c,j}^{(i)})}\right]$
7: generate uniform random number $u \in [0, 1]$
8: **if** $u < \alpha$ **then**
9: replace $\{\boldsymbol{\theta}^{(i)}, L^{(i)} \cdot \pi_{\text{pr}}(\boldsymbol{\theta}^{(i)})\}$ with $\{\boldsymbol{\theta}_{c,j}^{(i)}, L_{c,j}^{(i)} \cdot \pi_{\text{pr}}(\boldsymbol{\theta}_{c,j}^{(i)})\}$
10: **end if**
11: **end for**
12: **end for**
13: **IMH-GM Output**: $\{\boldsymbol{\theta}^{(i)}, L^{(i)} \cdot \pi_{\text{pr}}(\boldsymbol{\theta}^{(i)})\}$

Alg. 5 details the workings of the IMH-GM-based IBIS filter used in this work. In line 11 of this algorithm, the IMH-GM routine of Alg. 4 is called, which implements the IMH-GM kernel for the MCMC move step. Comparing Algs. 2 and 5, it is clear that both filters can be used for on-line inference within a single run, but the IBIS filter has significantly larger computational cost, as will also be demonstrated in the numerical investigations of Section 6.3. In the same spirit as the proposed tPFGM Alg. 3, which enforces simulated annealing (tempering of the likelihood function)

in cases when $\pi_{\text{pos}}(\boldsymbol{\theta}|\mathbf{y}_{1:n-1})$ and $\pi_{\text{pos}}(\boldsymbol{\theta}|\mathbf{y}_{1:n})$ are likely to be quite different, the same idea can be implemented also within the IBIS algorithm. That leads to what we refer to as the tIBIS algorithm in this paper.

Algorithm 5 IMH-GM-based Iterated Batch Importance Sampling (IBIS)

1: generate N_{par} initial particles $\boldsymbol{\theta}^{(i)}$ from $\pi_{\text{pr}}(\boldsymbol{\theta})$, $\quad i = 1, \ldots, N_{\text{par}}$
2: assign initial weights $w_0^{(i)} = 1/N_{\text{par}}$, $\quad i = 1, \ldots, N_{\text{par}}$
3: **for** $n = 1, \ldots, N$ **do**
4: evaluate likelihood of the particles based on new measurement y_n, $L_n^{(i)} = L\left(y_n \mid \boldsymbol{\theta}^{(i)}\right)$
5: evaluate the new target distribution, $L(\mathbf{y}_{1:n}|\boldsymbol{\theta}^{(i)}) \cdot \pi_{\text{pr}}\left(\boldsymbol{\theta}^{(i)}\right) = L_n^{(i)} \cdot L(\mathbf{y}_{1:n-1}|\boldsymbol{\theta}^{(i)}) \cdot \pi_{\text{pr}}\left(\boldsymbol{\theta}^{(i)}\right)$
6: update particle weights $w_n^{(i)} \propto L_n^{(i)} \cdot w_{n-1}^{(i)}$ and normalize s.t. $\sum_{i=1}^{N_{\text{par}}} w_n^{(i)} = 1$
7: evaluate $N_{\text{eff}} = \frac{1}{\sum_{i=1}^{N_{\text{par}}} \left(w_n^{(i)}\right)^2}$
8: **if** $N_{\text{eff}} < N_{\text{T}}$ **then**
9: EM: fit a Gaussian mixture proposal distribution $g_{\text{GM}}(\boldsymbol{\theta})$ according to $\{\boldsymbol{\theta}^{(i)}, w_n^{(i)}\}$
10: resample N_{par} new particles $\{\boldsymbol{\theta}^{(i)}, L(\mathbf{y}_{1:n}|\boldsymbol{\theta}^{(i)}) \cdot \pi_{\text{pr}}(\boldsymbol{\theta}^{(i)})\}$ with replacement according to $w_n^{(i)}$
11: IMH-GM step with inputs $\{\boldsymbol{\theta}^{(i)}, L(\mathbf{y}_{1:n}|\boldsymbol{\theta}^{(i)}) \cdot \pi_{\text{pr}}(\boldsymbol{\theta}^{(i)})\}$, $\pi_{\text{pr}}(\boldsymbol{\theta})$, $L(\mathbf{y}_{1:n}|\boldsymbol{\theta})$ and $g_{\text{GM}}(\boldsymbol{\theta})$
12: reset particle weights to $w_n^{(i)} = 1/N_{\text{par}}$
13: **end if**
14: **end for**

6.2.3 Off-line Sequential Monte Carlo sampler

In Section 4 of [61], the authors presented a generic approach to convert an off-line MCMC sampler into a sequential Monte Carlo (SMC) sampler tailored for performing off-line estimation tasks, i.e., for estimating the single posterior density of interest $\pi_{\text{pos}}(\boldsymbol{\theta}|\mathbf{y}_{1:N})$. The off-line SMC sampler used in this work is presented in Alg. 6 based on [61] and [41]. The key idea of this sampler is to adaptively construct the following artificial sequence of densities,

$$\pi_j(\boldsymbol{\theta}|\mathbf{y}_{1:N}) \propto L^{q_j}(\mathbf{y}_{1:N}|\boldsymbol{\theta})\pi_{\text{pr}}(\boldsymbol{\theta}), \tag{6.6}$$

where q_j is a tempering parameter which obtains values between 0 and 1, in order to "sequentially" sample in a smooth manner from the prior to the final single posterior density of interest. Once $q_j = 1$, $\pi_{\text{pos}}(\boldsymbol{\theta}|\mathbf{y}_{1:N})$ is reached. Similar to what was described in tPFGM, the intermediate values of q_j are adaptively found via solution of the optimization problem in line 5 of Alg. 6. The GMM approximation of the intermediate posteriors and the IMH-GM kernel of Alg. 4 in order to move the particles after resampling are also key ingredients of this SMC sampler. Unlike PFGM and IBIS, this SMC algorithm cannot provide the on-line solution within a single run, and has to be rerun from scratch for every new target posterior of interest. In this regard, use of Alg. 6 for on-line inference is impractical. We choose to include this algorithm for the purpose of the comparative assessment in this paper, as off-line algorithms are generally considered to be better suited for the full posterior uncertainty quantification of time-invariant parameters.

Algorithm 6 IMH-GM-based Sequential Monte Carlo (SMC)

generate N_{par} initial particles $\boldsymbol{\theta}^{(i)}$ from $\pi_{\text{pr}}(\boldsymbol{\theta})$, $\quad i = 1, \ldots, N_{\text{par}}$
evaluate for every particle the full likelihood $L^{(i)} = L(\mathbf{y}_{1:N} \mid \boldsymbol{\theta}^{(i)})$ and the prior $\pi_{\text{pr}}(\boldsymbol{\theta}^{(i)})$
set $q = 0$
while $q \neq 1$ **do**
  solve $\left(\sum_{i=1}^{N_{\text{par}}} {L^{(i)}}^{dq}\right)^2 / \sum_{i=1}^{N_{\text{par}}} {L^{(i)}}^{2 \cdot dq} - N_{\text{T}} = 0$ for dq
  set $q_{\text{new}} = \min\left[q + dq, 1\right]$
  set $dq = q_{\text{new}} - q$ and $q = q_{\text{new}}$
  evaluate particle weights $w^{(i)} \propto {L^{(i)}}^{dq}$ and normalize s.t. $\sum_{i=1}^{N_{\text{par}}} w^{(i)} = 1$
  EM: fit a Gaussian mixture proposal distribution $g_{\text{GM}}(\boldsymbol{\theta})$ according to $\{\boldsymbol{\theta}^{(i)}, w^{(i)}\}$
  resample N_{par} new particles $\{\boldsymbol{\theta}^{(i)}, {L^{(i)}}^{q} \cdot \pi_{\text{pr}}(\boldsymbol{\theta}^{(i)})\}$ with replacement according to $w^{(i)}$
  IMH-GM step with inputs $\{\boldsymbol{\theta}^{(i)}, {L^{(i)}}^{q} \cdot \pi_{\text{pr}}(\boldsymbol{\theta}^{(i)})\}$, $\pi_{\text{pr}}(\boldsymbol{\theta})$, $L^{q}(\mathbf{y}_{1:N}|\boldsymbol{\theta})$ and $g_{\text{GM}}(\boldsymbol{\theta})$
  reset particle weights to $w^{(i)} = 1/N_{\text{par}}$
end while

6.2.4 Computational remarks

The algebraic operations in all presented algorithms are implemented in the logarithmic scale, which employs evaluations of the logarithm of the likelihood function and, hence, ensures computational stability. Furthermore, the EM step for fitting the GMM is performed after initially transforming the prior joint probability density function of $\boldsymbol{\theta}$ to an underlying vector $\boldsymbol{u}$ of independent standard normal random variables [53]. In standard normal space, the parameters are decorrelated, which enhances the performance of the EM algorithm.

6.3 Numerical investigations

6.3.1 Low-dimensional case study: Paris-Erdogan fatigue crack growth model

A fracture mechanics-based model serves as the first case study. This describes the fatigue crack growth evolution under increasing stress cycles [68, 25]. The crack growth follows the following first-order differential Eq. (6.7), known as Paris-Erdogan law,

$$\frac{da\,(n, \boldsymbol{\theta})}{dn} = \exp\left(C_{\ln}\right) \left[\Delta S \sqrt{\pi a\,(n)}\right]^{m} \tag{6.7}$$

where $\boldsymbol{\theta} = [a, \Delta S, C_{ln}, m]$ is a vector containing the uncertain time-invariant model parameters. Specifically, a is the crack length, n is the number of stress cycles, ΔS is the stress range per cycle when assuming constant stress amplitudes, C and m represent empirically determined model parameters; $C_{\ln}$ corresponds to the natural logarithm of C.

The solution to this differential equation, with boundary condition $a\,(n = 0) = a_0$, can be written as a function of the number of stress cycles n and the vector $\boldsymbol{\theta} = [a_0, \Delta S, C_{ln}, m]$ as (for the derivation

see, e.g., [25]):

$$a\left(n,\boldsymbol{\theta}\right)=\left[\left(1-\frac{m}{2}\right)\exp\left(C_{\ln}\right)\Delta S^{m}\pi^{m/2}n+a_{0}^{(1-m/2)}\right]^{(1-m/2)^{-1}}. \tag{6.8}$$

We assume that noisy measurements of the crack y_n are obtained sequentially at different values of n. The measurement Eq. (6.9) assumes a multiplicative lognormal measurement error, $\exp\left(\epsilon_n\right)$.

$$y_n = a(n,\boldsymbol{\theta})\exp\left(\epsilon_n\right) \tag{6.9}$$

In numerical investigations that follow, the measurement Eq. (6.9) is used for generating synthetic measurements of the deterioration state. In this context, a multiplicative lognormal measurement error ensures that non-negative generated measurements of the deterioration state are not feasible.

Under this assumption, the likelihood function for a measurement at a given n is shown in Eq. (6.10).

$$L\big(y_n;a\left(n,\boldsymbol{\theta}\right)\big)=\frac{1}{\sigma_{\epsilon_n}\sqrt{2\pi}}\exp\left[-\frac{1}{2}\left(\frac{\ln\left(y_n\right)-\mu_{\epsilon_n}-\ln\big(a\left(n,\boldsymbol{\theta}\right)\big)}{\sigma_{\epsilon_n}}\right)^{2}\right] \tag{6.10}$$

Tab. 6.1 shows the prior probability distribution model for each random variable in the vector $\boldsymbol{\theta}$ [25, 80], as well as the assumed probabilistic model of the measurement error. In this case study we are dealing with a non-linear model and a parameter vector with non-Gaussian prior distribution.

Table 6.1: Prior distribution model for the fatigue crack growth model parameters and the measurement error.

Parameter	Distribution	Mean	Standard Deviation	Correlation
a_0	Exponential	1	1	–
ΔS	Normal	60	10	–
$C_{\ln}$, m	Bi-Normal	$(-33;\ 3.5)$	$(0.47;\ 0.3)$	$\rho_{C_{\ln},m}=-0.9$
$\exp\left(\epsilon_n\right)$	Log-normal	1.0	0.1508	–

6.3.1.1 Markovian state-space representation for application of on-line filters

A Markovian state-space representation of the deterioration process is required for application of on-line filters. The number of stress cycles is discretized as $n=k\Delta n$, with $k=1,\ldots,100$ denoting the estimation time step and $\Delta n=1\times10^{5}$ the number of stress cycles per time step. The dynamic and measurement equations of the discrete-time state-space representation of the fatigue crack growth model with unknown time-invariant parameters $\boldsymbol{\theta}=[a_0,\Delta S,C_{ln},m]$ are shown below:

$$\boldsymbol{\theta}_k=\boldsymbol{\theta}_{k-1}$$

$$y_k=a\left(k\Delta n,\boldsymbol{\theta}_k\right)\exp\left(\epsilon_k\right)=\left[\left(1-\frac{m_k}{2}\right)\exp\left(C_{ln_k}\right)\Delta S_k^{m_k}\pi^{m_k/2}k\Delta n+a_0^{(1-m_k/2)}\right]^{(1-m_k/2)^{-1}}\exp\left(\epsilon_k\right). \tag{6.11}$$

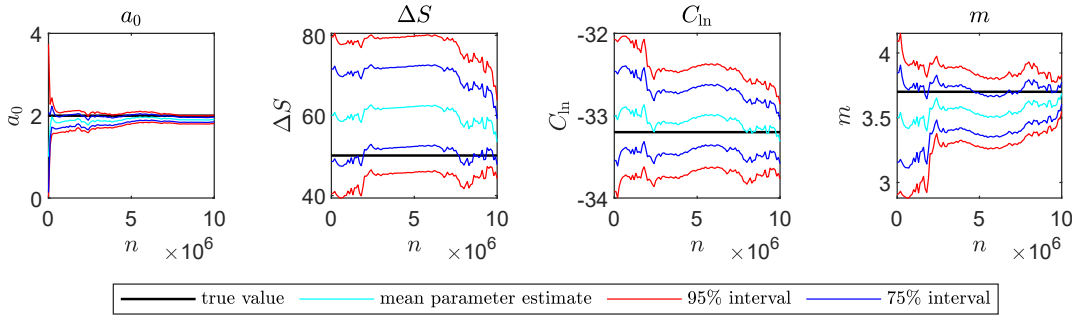

Figure 6.2: Reference posterior solution: mean and credible intervals for the sequence of posterior distributions $\pi_{\text{pos}}(\boldsymbol{\theta}|\mathbf{y}_{1:k})$.

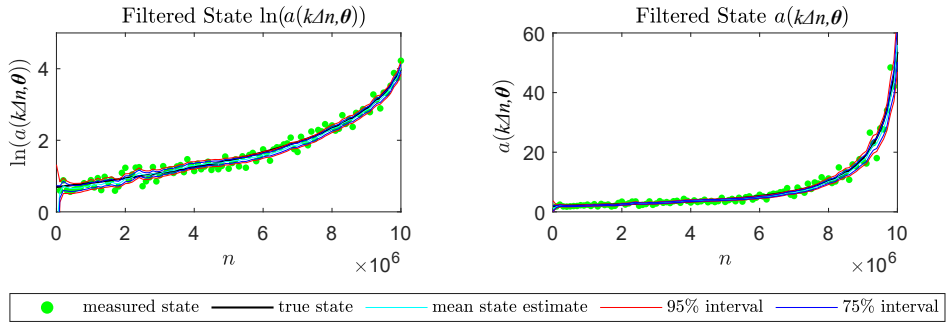

Figure 6.3: Reference mean and credible intervals for the filtered crack growth state $a(k\Delta n, \boldsymbol{\theta})$.

The state-space model of Eq. (6.11) is nonlinear and the prior is non-Gaussian. For reasons explained in Section 6.2, the subscript k in $\boldsymbol{\theta}_k$ is dropped in the remainder of this section.

6.3.1.2 Reference posterior solution

For the purpose of performing a comparative assessment of the different filters, an underlying "true" realization of the fatigue crack growth process $a^*(n, \boldsymbol{\theta})$ is generated for $n = k\Delta n$, with $k = 1, \ldots, 100$ and $\Delta n = 1 \times 10^5$. This realization corresponds to the randomly generated "true" vector of time-invariant parameters $\boldsymbol{\theta}^* = [a_0^* = 2.0, \Delta S^* = 50.0, C_{ln}^* = -33.5, m^* = 3.7]$. Sequential synthetic crack monitoring measurements y_k are sampled from the measurement Eq. (6.9) for $a(k\Delta n, \boldsymbol{\theta}^*)$, and for randomly generated measurement noise samples $\exp(\epsilon_k)$. These measurements are scattered in green in Fig. 6.3.

Based on the generated measurements, the sequence of reference posterior distributions $\pi_{\text{pos}}(\boldsymbol{\theta}|\mathbf{y}_{1:k})$ is obtained using the prior distribution as an envelope distribution for rejection sampling [75, 70]. More specifically, for each of the 100 posterior distributions of interest $\pi_{\text{pos}}(\boldsymbol{\theta}|\mathbf{y}_{1:k})$, 10^5 independent samples are generated. The results of this reference posterior estimation of the four time-invariant model parameters are plotted in Fig. 6.2. With posterior samples, the reference filtered estimate of the crack length $a(k\Delta n, \boldsymbol{\theta})$ at each estimation step is also obtained via the model of Eq. (6.8) and plotted in Fig. 6.3. In the left panel of this figure, the filtered state is plotted in logarithmic scale. In an off-line estimation, a single posterior density is of interest. One such reference posterior estimation result for the last estimation step, $\pi_{\text{pos}}(\boldsymbol{\theta}|\mathbf{y}_{1:100})$, is plotted for illustration in Fig. 6.4.

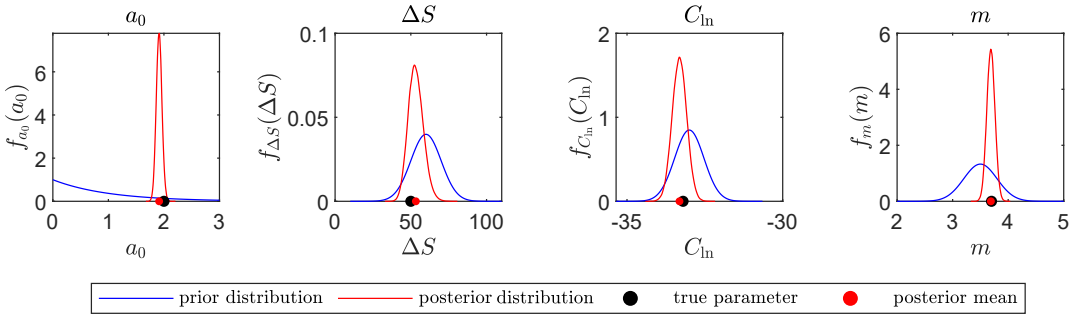

Figure 6.4: Reference final posterior: prior and single posterior distribution of interest $\pi_{\text{pos}}(\boldsymbol{\theta}|\mathbf{y}_{1:100})$.

6.3.1.3 Comparative assessment of the investigated on-line and off-line filters

We apply the PFGM filter with 5000 and 50000 particles, the IBIS filter with 5000 particles, and the SMC filter with 5000 particles for performing on-line and off-line time-invariant parameter estimation tasks. We evaluate the performance of each filter by taking the relative error of the estimated mean and standard deviation of each of the four parameters with respect to the reference posterior solution. For example, the relative error in the estimation of the mean of parameter a_0 at a certain estimation step k is computed as $|\frac{\mu_{a_0,k}-\hat{\mu}_{a_0,k}}{\mu_{a_0,k}}|$, where $\mu_{a_0,k}$ is the reference posterior mean from rejection-sampling (Section 6.3.1.2), and $\hat{\mu}_{a_0,k}$ is the posterior mean estimated with each filter. Each filter is run 50 times, and the mean relative error of the mean and the standard deviation of each parameter, together with the 90% credible intervals (CI), are obtained. These are plotted in Fig. 6.5.

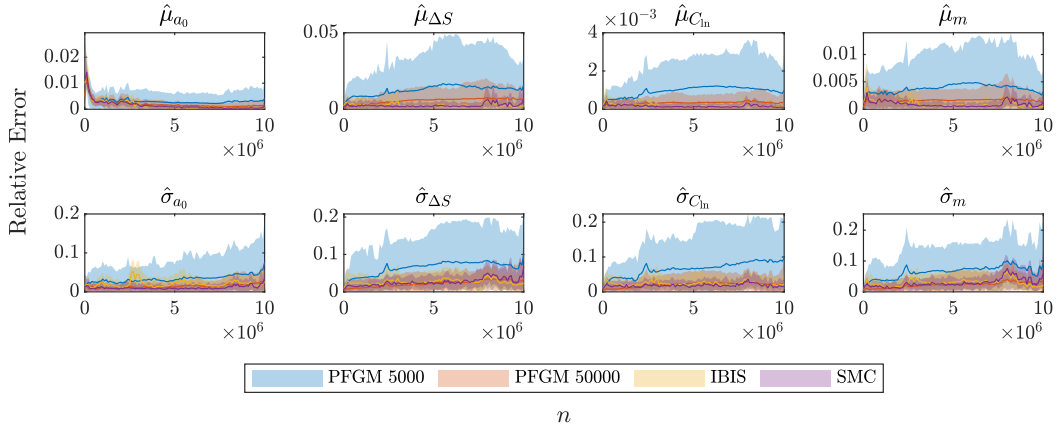

Figure 6.5: Comparison of the relative error of the mean and standard deviation of the parameters evaluated for each filter. The solid lines show the mean and the shaded areas the 90% credible intervals inferred from 50 repeated runs of each filter. In the horizontal axis, n is the number of stress cycles.

Fig. 6.6 plots the L^2 relative error norm of the mean and the standard deviation of all four parameters, i.e., the quantity of Eq. (6.12) (here formulated for the mean at estimation step k)

$$\sqrt{\frac{\sum_{i=1}^{d}\left(\mu_{i,k}-\hat{\mu}_{i,k}\right)^2}{\sum_{i=1}^{d}\left(\mu_{i,k}\right)^2}}, \tag{6.12}$$

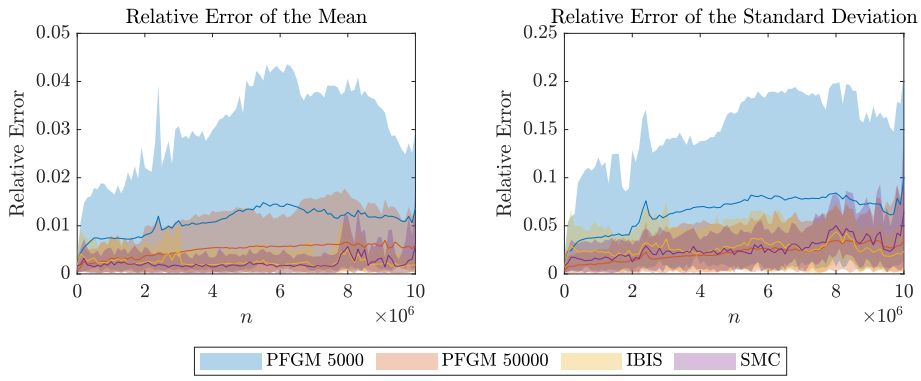

Figure 6.6: Comparison of the L^2 relative error norm of the mean and the standard deviation of the parameters evaluated for each filter. The solid lines show the mean and the shaded areas the 90% credible intervals inferred from 50 repeated runs of each filter. In the horizontal axis, n is the number of stress cycles.

Table 6.2: Average number of model evaluations (Eq. (6.8)) for the fatigue crack growth model parameter estimation.

method	PFGM 5000	PFGM 50000	IBIS	SMC (final posterior)	SMC (all posteriors)
model evaluations	5×10^5	5×10^6	3.4×10^6	4.5×10^6	1.9×10^8

where d is the dimensionality of the time-invariant parameter vector $\boldsymbol{\theta}$ (in this example $d = 4$). More specifically, Fig. 6.6 plots the mean and credible intervals of the L^2 relative error norm of the estimated mean and standard deviation, as obtained from 50 runs of each filter.

Figs. 6.5 and 6.6 reveal that, when all three filters are run with the same number of particles, the IBIS and SMC filters yield superior performance over PFGM. When the number of particles in the PFGM filter is increased to 50000, the PFGM filter performance is comparable to the one of the IBIS and SMC filters. In estimating the mean, the mean L^2 relative error norm obtained from the PFGM filter with 50000 particles is slightly larger than the corresponding error obtained from IBIS and SMC with 5000 particles, while the 90% credible intervals of the PFGM filter estimation are still wider. In estimating the standard deviation, the PFGM filter with 50000 particles proves competitive.

Figs. 6.5 and 6.6 show the estimation accuracy of each filter when used for on-line inference, i.e., for estimating the whole sequence of 100 posterior distributions $\pi_{\text{pos}}(\boldsymbol{\theta}|\mathbf{y}_{1:k})$, $k = 1, \ldots, 100$. The PFGM and IBIS filters, being intrinsically on-line filters, provide the whole posterior sequence with one run. On the other hand, the off-line SMC filter is run anew for each of the 100 required posterior estimations. Hence, Figs. 6.5 and 6.6 enclose the results of both the on-line and the off-line inference. If one is interested in the off-line estimation accuracy at a specific stress cycle n, one can simply consider a vertical "cut" at n.

Tab. 6.2 documents the computational cost associated with each filter, expressed in the form of required model evaluations induced by calls of the likelihood function. When using the term model, we refer to the model defined in Eq. (6.8), which corresponds to an analytical expression with negligible associated runtime. However, unlike the simple measurement equation that we have assumed

in this example, in many realistic deterioration monitoring settings, the deterioration state cannot be measured directly (e.g., in vibration-based structural health monitoring [46]). In such cases, each deterioration model evaluation often entails evaluation of a finite element (FE) model, which has substantial runtime. It therefore appears appropriate to evaluate the filters' computational cost in terms of required model evaluations. The on-line PFGM filter with 5000 particles requires 5×10^5 model evaluations, and yields by far the smallest computational cost, while at the same time providing the solution to both on-line and off-line estimation tasks. However, it also yields the worst performance in terms of accuracy of the posterior estimates. Running the IBIS filter with 5000 particles, which performs MCMC move steps, leads to 3.4×10^6 model evaluations. Comparing this value against the 5×10^5 model evaluations required by the PFGM filter with 5000 particles for performing the same task distinctly shows the computational burden associated with MCMC move steps, which require a complete browsing of the whole measurement data set in estimating the acceptance probability. However, the IBIS filter also leads to enhanced estimation accuracy, which might prove significant when the subsequent tasks entail prognosis of the deterioration evolution, the structural reliability or the remaining useful lifetime, and eventually the predictive maintenance planning. Using 50000 particles, the PFGM filter performance increases significantly with a computational cost that is comparable to the IBIS filter with 5000 particles. For the off-line SMC algorithm, 4.5×10^6 model evaluations are required only for the task of estimating the final posterior density. The 1.9×10^8 model evaluations required by the SMC for obtaining the whole sequence of posteriors $\pi_{\text{pos}}(\boldsymbol{\theta}|\mathbf{y}_{1:k})$, $k = 1, \ldots, 100$, clearly demonstrate that off-line MCMC techniques are unsuited to on-line estimation tasks.

6.3.2 High-dimensional case study: Corrosion deterioration spatially distributed across beam

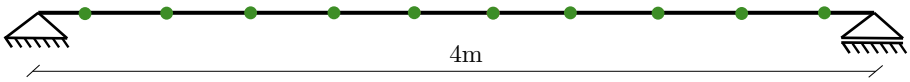

Figure 6.7: Structural beam subjected to spatially and temporally varying corrosion deterioration. The deterioration process is monitored from sensors deployed at specific sensor locations (in green).

As a second case study, we employ the deterioration model of Eq. (6.13), which describes the spatially and temporally varying corrosion deterioration across the structural beam shown in Fig. 6.7.

$$D(t,x) = A(x)t^{B(x)}, \qquad t = 0, \ldots, 50. \tag{6.13}$$

$A(x), B(x), x \in \Omega$ are random fields defined on $\Omega = [0, L]$, with L denoting the length of the beam taken as $L = 4$m. $A(x)$ models the deterioration rate, while $B(x)$ models the nonlinearity effect of the deterioration process in terms of a power law in time. The corrosion deterioration $D(t,x)$ is therefore also a spatial random field.

A random field, by definition, contains an infinite number of random variables, and must therefore be discretized [85]. One of the most common methods for discretization of random fields is the midpoint method [23]. Thereby the spatial domain Ω is discretized into m elements, and the random field is approximated within each element through the random variable that corresponds to midpoint of the element. In that case, the uncertain time-invariant deterioration model parameter vector

is $\boldsymbol{\theta} = [A_1, \ldots, A_m, B_1, \ldots, B_m]$, where $A_i := A(x_i), B_i := B(x_i), i = 1, \ldots, m$, are the random variables corresponding to the element midpoints. With the midpoint discretization, the spatial deterioration $D(t, x)$ is parametrized by $\boldsymbol{\theta}$.

We assume that noisy measurements of the corrosion deterioration state $D_{t,l}(\boldsymbol{\theta}) := D(t, x_l, \boldsymbol{\theta})$ at time t and at certain locations l of the beam are obtained sequentially (summarized in one measurement per year) from n_l sensors deployed at these locations ($n_l = 10$ sensor locations are shown in Fig. 6.7). The measurement Eq. (6.14), describing the corrosion measurement at time t and sensor location l, assumes a multiplicative measurement error, $\exp(\epsilon_{t,l})$,

$$y_{t,l} = D_{t,l}(\boldsymbol{\theta}) \exp(\epsilon_{t,l}) = A_{i_l} t^{B_{i_l}} \exp(\epsilon_{t,l}), \tag{6.14}$$

where i_l returns the discrete element number of the midpoint discretization within which the measurement location l lies. Tab. 6.3 shows the prior distribution model for the two random fields of the deterioration model of Eq. (6.13) and the assumed probabilistic model of the multiplicative measurement error. Since $A(x)$ models a lognormal random field, $\ln(A(x))$ follows the normal distribution. For both random fields $\ln(A(x))$ and $B(x)$, the exponential correlation model with correlation length of 2m is applied [82].

Table 6.3: Prior distribution model for the corrosion deterioration model parameters and the measurement error.

Parameter	Distribution	Mean	Standard Deviation	Corr. length (m)
$A(x)$	Lognormal	0.8	0.24	2
$B(x)$	Normal	0.8	0.12	2
$\exp(\epsilon_{t,l})$	Lognormal	1.0	0.101	-

The goal is to update the time-invariant deterioration model parameters $\boldsymbol{\theta} = [A_1, \ldots, A_m, B_1, \ldots, B_m]$ given sequential noisy corrosion measurements $y_{t,l}$ from n_l deployed sensors. The dimensionality of the problem is $d = 2 \times m$. Hence, the more elements in the midpoint discretization, the higher the dimensionality of the parameter vector.

The main goal of this second case study is to investigate the effect of the problem dimensionality and the amount of sensor information on the posterior results obtained with each filter. We choose the following three midpoint discretization schemes:

1. $m = 25$ elements: $d = 50$ time-invariant parameters to estimate.
2. $m = 50$ elements: $d = 100$ time-invariant parameters to estimate.
3. $m = 100$ elements: $d = 200$ time-invariant parameters to estimate.

Furthermore, we choose the following three potential sensor arrangements:

1. $n_l = 2$ sensors (the 4^{th} and 7^{th} sensors of Fig. 6.7).
2. $n_l = 4$ sensors (the $1^{st}, 4^{th}, 7^{th}$ and 10^{th} sensors of Fig. 6.7).
3. $n_l = 10$ sensors of Fig. 6.7.

We therefore study nine different cases of varying problem dimensionality and number of sensors.

6.3.2.1 Markovian state-space representation for application of on-line filters

A Markovian state-space representation of the deterioration process is required for application of on-line filters. The dynamic and measurement equations are shown in Eq. (6.15). The measurement equation is written in the logarithmic scale. Time t is discretized in yearly estimation time steps k, i.e., $k = 1, \ldots, 50$, and the subscript $l = 1, \ldots, n_l$ corresponds to the sensor location.

$$\begin{aligned} \boldsymbol{\theta}_k &= \boldsymbol{\theta}_{k-1} \\ \ln(y_{k,l}) = \ln(D_{k,l}(\boldsymbol{\theta}_k)) + \epsilon_{k,l} &\Rightarrow \ln(y_{k,l}) = \ln(A_{k,i_l}) + B_{k,i_l} \ln(t_k) + \epsilon_{k,l}, \end{aligned} \tag{6.15}$$

where $\boldsymbol{\theta}_k$ denotes the time-invariant parameter vector at time step k. In the logarithmic scale, both the dynamic and measurement equations are linear functions of Gaussian random variables. For reasons explained in Section 6.2, the subscript k in $\boldsymbol{\theta}_k$ is dropped in the following.

6.3.2.2 Underlying "true" realization

To generate a high-resolution underlying "true" realization of the two random fields $A(x)$ and $B(x)$, and the corresponding synthetic monitoring data set, we employ the Karhunen-Loève (KL) expansion using the first 400 KL modes. The KL expansion is an alternative random field discretization scheme to the midpoint method that represents the random field in terms of the eigenfunctions of its autocovariance function [82, 34]. The implementation of the KL expansion can be found in the Matlab codes accompanying this article[2]. We remark that a fine resolution KL expansion is chosen to represent the "true" realization in order to avoid the inverse crime [88]. These realizations are shown in the left panel of Fig. 6.8. Given these $A(x)$ and $B(x)$ realizations, the underlying "true" realizations of the deterioration process at ten specific beam locations are generated, which correspond to the ten potential sensor placement locations shown in Fig. 6.7. Subsequently, a synthetic corrosion sensor measurement data set (one measurement per year) at these 10 locations is generated from the measurement Eq. (6.14). These are shown in the right panel of Fig. 6.8.

6.3.2.3 Reference posterior solution

For the investigated linear Gaussian state space representation of Eq. (6.15), we create reference on-line posterior solutions for each of the nine considered cases by applying the Kalman filter (KF) [44], which is the closed form solution to the Bayesian filtering equations. The process noise covariance matrix in the KF equations is set equal to zero. The linear Gaussian nature of the chosen problem ensures existence of an analytical reference posterior solution obtained with the KF. One such reference on-line posterior solution for the case described by $m = 25$ elements ($d = 50$) and $n_l = 4$ sensors is shown in Fig. 6.9.

[2] https://github.com/antoniskam/Offline_online_Bayes

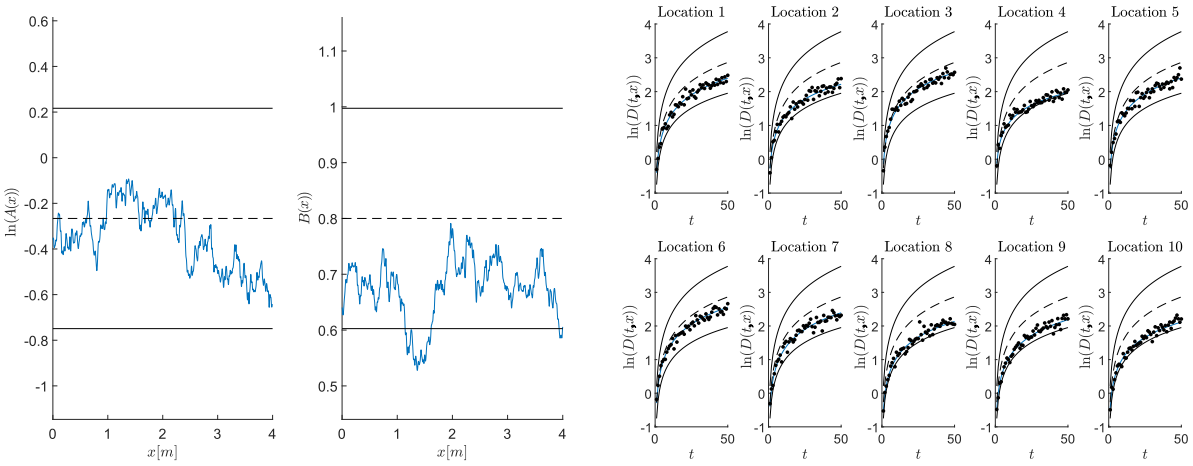

Figure 6.8: Left: the blue solid line plots the underlying "true" realization of $\ln(A(x))$ and $B(x)$ created using the KL expansion. Right: the blue solid line plots the underlying "true" realization of $\ln(D(t,x))$ at 10 specific sensor locations and the corresponding synthetic sensor monitoring data are scattered in black. In both figures, the black dashed lines plot the prior mean and the black solid lines the prior 90% credible intervals

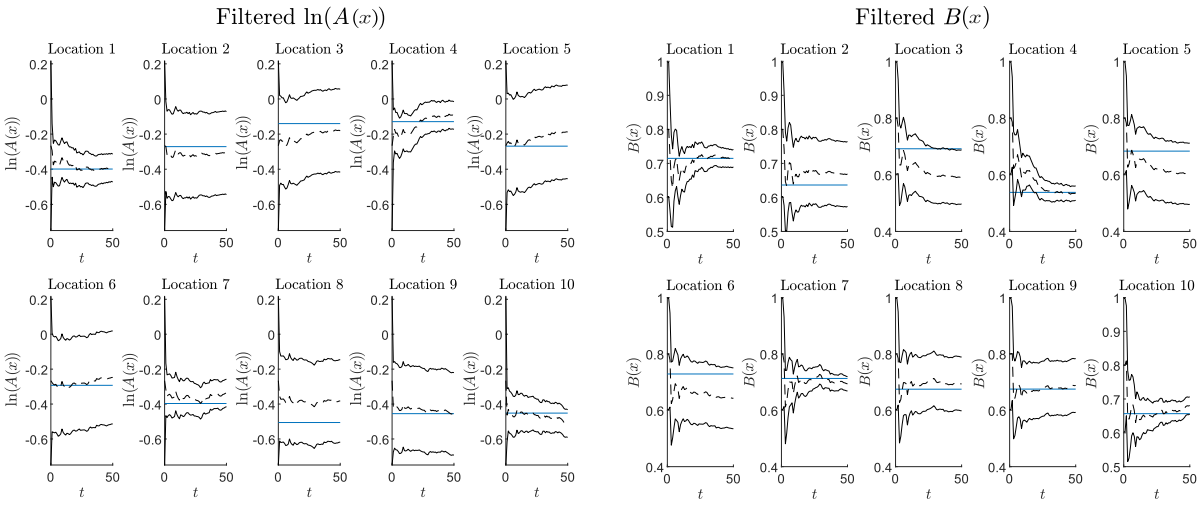

Figure 6.9: Case with $m = 25, n_l = 4$: reference on-line posterior solution at 10 locations across the beam obtained by applying the Kalman filter for solving Eq. (6.15). The solid blue horizontal line represents the underlying "true" values of $ln(A(x))$ and $B(x)$ at these locations. The black dashed lines plot the posterior mean and the black solid lines the posterior 90% credible intervals. Locations 1,4,7,10 correspond to the four assumed sensor placement locations

6.3.2.4 Comparative assessment of the investigated on-line and off-line filters

The goal of this section is to offer a comparative assessment among the three Bayesian filtering algorithms presented in this paper when applied on a high-dimensional problem. To be able to derive a reference solution, as described above, a linear Gaussian state space representation of a structural deterioration problem has been defined (Eq. (6.15)). We apply the tPFGM filter, the tIBIS filter, and the SMC filter, all with N_{par}=2000 particles, for estimating the time-invariant parameter vector

$\boldsymbol{\theta}$. For each of the nine cases of varying problem dimensionality and number of sensors described above, we compute the L^2 relative error norm of the estimated means, correlation coefficients, and standard deviations of the parameters with respect to the corresponding KF reference posterior solution, i.e., we estimate a quantity as in Eq. (6.12) for all estimation steps $k = 1, \ldots, 50$. In Figs. 6.10 to 6.12 we plot the mean and credible intervals of these relative errors as obtained from 50 different runs. The off-line SMC filter, which does not provide the on-line solution within a single run, is run anew for estimating the single posterior density of interest at years 10, 20, 30, 40, 50, and in between, the relative error is linearly interpolated. Although each of the nine panels in the figures corresponds to a different case with a different underlying KF reference solution, their y axes have the same scaling. Tab. 6.4 documents the computational cost of each filter in each considered case, measured by average number of evaluations of the model of Eq. (6.13).

Figs. 6.10 and 6.11 show that the off-line IMH-GM-based SMC filter yields the best performance in estimating the KF reference posterior mean and correlation, for all nine considered cases, while at the same time producing the narrowest credible intervals. Comparison of the relative errors obtained with the SMC and tIBIS filters reveals that, although they are both reliant on the IMH-GM MCMC move step, the on-line tIBIS filter leads to larger estimation errors. The on-line tPFGM and tIBIS filters generate quite similar results in estimating the reference posterior mean and correlation, thus rendering the benefit of the MCMC move step in tIBIS unclear, except in cases with more sensors and lower parameter dimension. Figs. 6.10 and 6.11 reveal a slight trend, indicating that for fixed dimensionality, availability of more sensors (i.e., stronger information content in the likelihood function) leads to a slight decrease in the relative errors when using the SMC and tIBIS filters, whereas the opposite trend can be identified for the tPFGM filter. Increasing problem dimensionality (for fixed number of sensors) does not appear to have strong influence on the posterior results in any of the columns of Figs. 6.10 to 6.12, a result that initially appears puzzling.

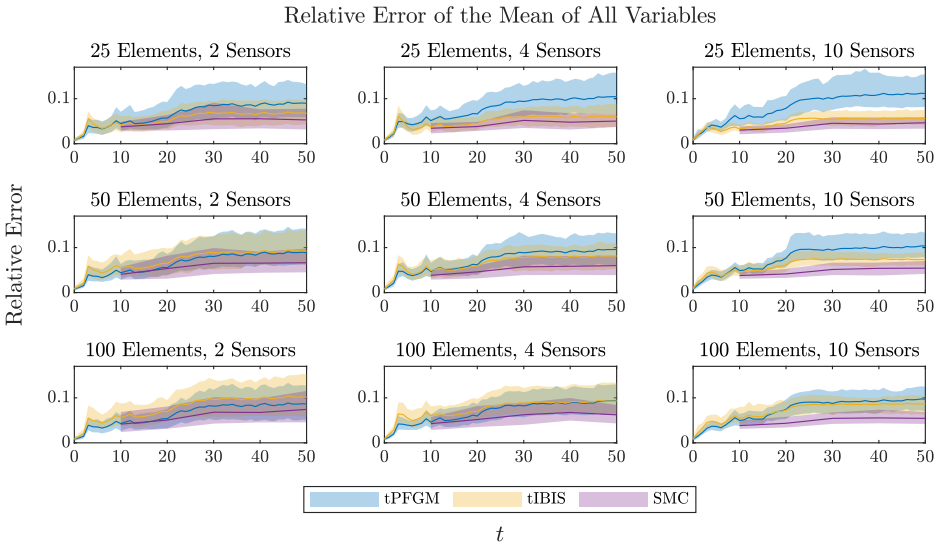

Figure 6.10: Comparison of the L^2 relative error norm of the means of the parameters evaluated for each filter. The solid lines show the mean and the shaded areas the 90% credible intervals inferred from 50 repeated runs of each filter.

Fig. 6.12 conveys that the tPFGM filter, which entirely depends on the GMM posterior approximation, induces the smallest relative errors for the estimation of the standard deviation of the parameters in all considered cases. This result reveals a potential inadequacy of the single applica-

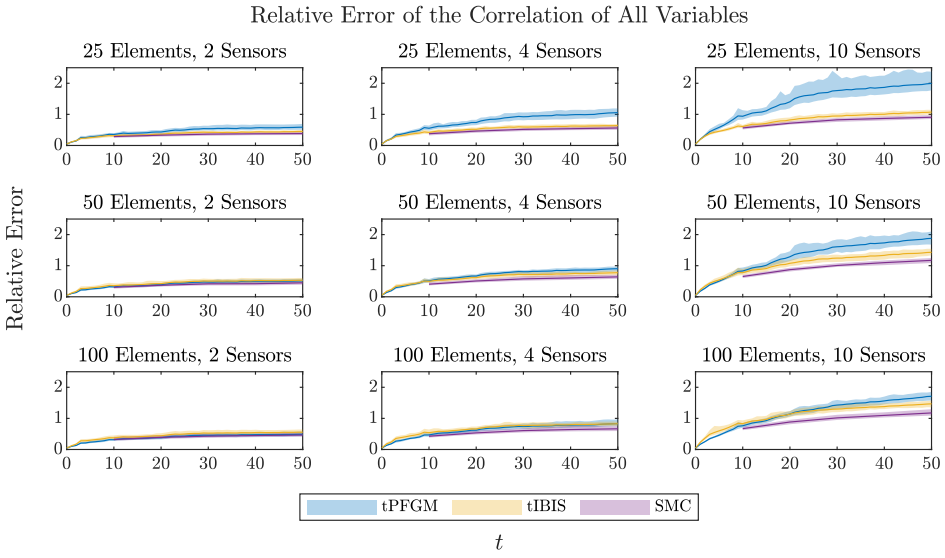

Figure 6.11: Comparison of the L^2 relative error norm of the correlation coefficients of the parameters evaluated for each filter. The solid lines show the mean and the shaded areas the 90% credible intervals inferred from 50 repeated runs of each filter.

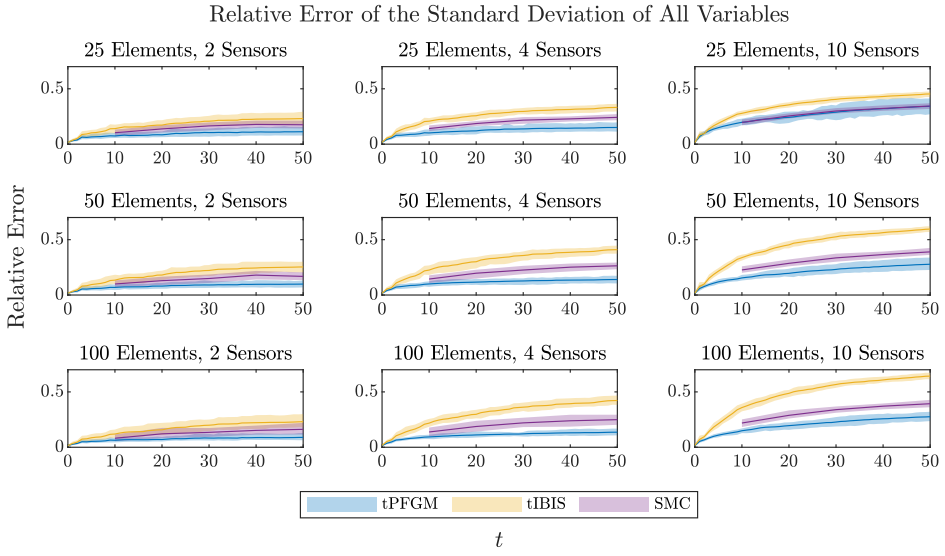

Figure 6.12: Comparison of the L^2 relative error norm of the standard deviations of the parameters evaluated for each filter. The solid lines show the mean and the shaded areas the 90% credible intervals inferred from 50 repeated runs of each filter.

tion of the IHM-GM kernel for the move step within the tIBIS and SMC filters in properly exploring the space of $\boldsymbol{\theta}$. In all 50 runs of the tIBIS and SMC filters, the standard deviation of the parameters is consistently underestimated compared to the reference, unlike when applying the tPFGM filter.

Based on the discussion of Section 6.2.2, we introduce a burn-in period of n_{B}=5 in the IMH-GM kernel of Alg. 4 and perform 50 new runs of the tIBIS and SMC filters. One can expect that inclusion of a burn-in is more likely to ensure sufficient exploration of the intermediate posterior distributions.

Table 6.4: Average number of model evaluations (Eq. (6.8)) for the high-dimensional case study. For the SMC, the required model evaluations for obtaining the single final posterior density are reported.

elements	25			50			100		
sensors	2	4	10	2	4	10	2	4	10
tPFGM	129,480	154,000	194,440	129,440	155,560	195,760	130,480	157,120	199,040
tIBIS	602,400	1,038,440	1,878,000	603,240	1,049,400	1,909,880	567,720	1,017,280	1,876,240
SMC	1,130,000	1,596,000	2,298,000	1,108,000	1,582,000	2,250,000	1,100,000	1,504,000	2,150,000

However, at the same time the computational cost of tIBIS and SMC increases significantly, with a much larger number of required model evaluations than in Tab. 6.4. In Figs. 6.13 and 6.14 we plot the mean and credible intervals for the relative errors in the estimation of the mean and standard deviation of the parameters. Comparing Fig. 6.10 and Fig. 6.13, inclusion of burn-in is shown to lead to an improved performance of tIBIS and SMC in estimating the mean of the parameters in all cases. This improvement is more evident in the lower-dimensional case with 25 elements, and lessens as the problem dimension increases. Hence, it is only after the inclusion of burn-in, which leads to an enhanced posterior solution, that one starts observing the anticipated deterioration of the tIBIS and SMC filters' performance with increasing dimensionality. This effect was masked in the results of Fig. 6.10 without burn-in. This point becomes more evident when looking at the relative errors of the estimated standard deviation in Fig. 6.14. With burn-in, the tIBIS and SMC filters provide better results than the tPFGM filter in estimating the standard deviation in the case of 25 elements, but perform progressively worse as the dimensionality increases, where they underestimate the KF reference standard deviation. This underestimation is clearly illustrated in Fig. 6.15. The reason for this behavior is the poor performance of the IMH-GM algorithm in high dimensions, which is numerically demonstrated in [66]. We suspect that this behavior is related to the degeneracy of the acceptance probability of MH samplers in high dimensions, which has been extensively discussed in the literature for random walk samplers, e.g., in [32, 3, 49, 7, 20, 65]. Single application of the IHM-GM kernel without burn-in yielded acceptance rates of around 50% for all cases. With inclusion of burn-in, in higher dimensions, the acceptance rate in IMH-GM drops significantly in the later burn-in steps, leading to rejection of most proposed particles. To alleviate this issue, one could consider using the preconditioned Crank Nicolson (pCN) sampler to perform the move step within the IBIS and SMC filters, whose performance is shown to be independent of the dimension of the parameter space when the prior is Gaussian [20].

Increase of dimensionality does not seem to have any influence on the results obtained with the tPFGM filter. The illustrated efficacy of the tPFGM filter in estimating the time-invariant parameters in all considered cases of increasing dimensionality is related to the nature of the studied problem. The tPFGM filter relies entirely on the GMM approximation of the posterior distribution within its resampling process, in that it simply "accepts" all the N_{par} GMM-proposed particles, unlike the tIBIS and SMC filters, which contain the degenerating acceptance-rejection step within the IMH-GM move step. Clearly, the worse the GMM fit, the worse the expected performance of the tPFGM filter. The particular case investigated here has a Gaussian reference posterior solution, hence the GMM fitted by EM proves effective in approximating the posterior with a relatively small number of particles, even when going up to d=200 dimensions, thus leading to a good proposal distribution for sampling N_{par} new particles in tPFGM. As reported in Tab. 6.4, the tPFGM filter is associated with a significantly lower computational cost than its MCMC-based counterparts.

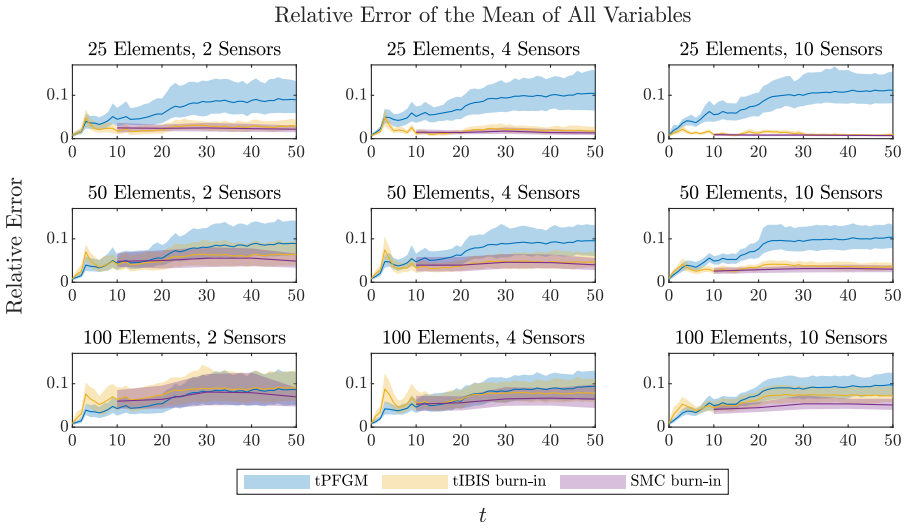

Figure 6.13: Comparison of the L^2 relative error norm of the mean of the parameters evaluated for each filter. The solid lines show the mean and the shaded areas the 90% credible intervals inferred from 50 repeated runs of each filter. Burn-in n_{B}=5.

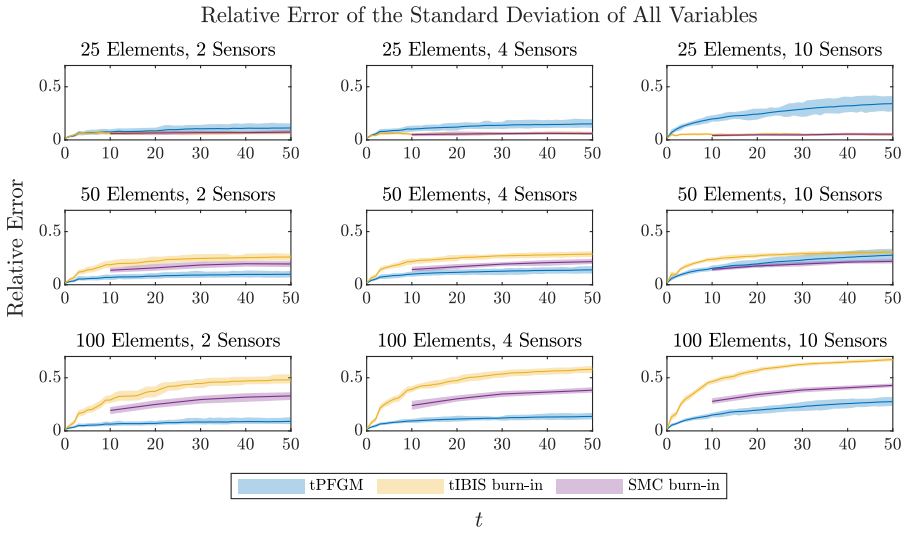

Figure 6.14: Comparison of the L^2 relative error norm of the standard deviation of the parameters evaluated for each filter. The solid lines show the mean and the shaded areas the 90% credible intervals inferred from 50 repeated runs of each filter. Burn-in n_{B}=5.

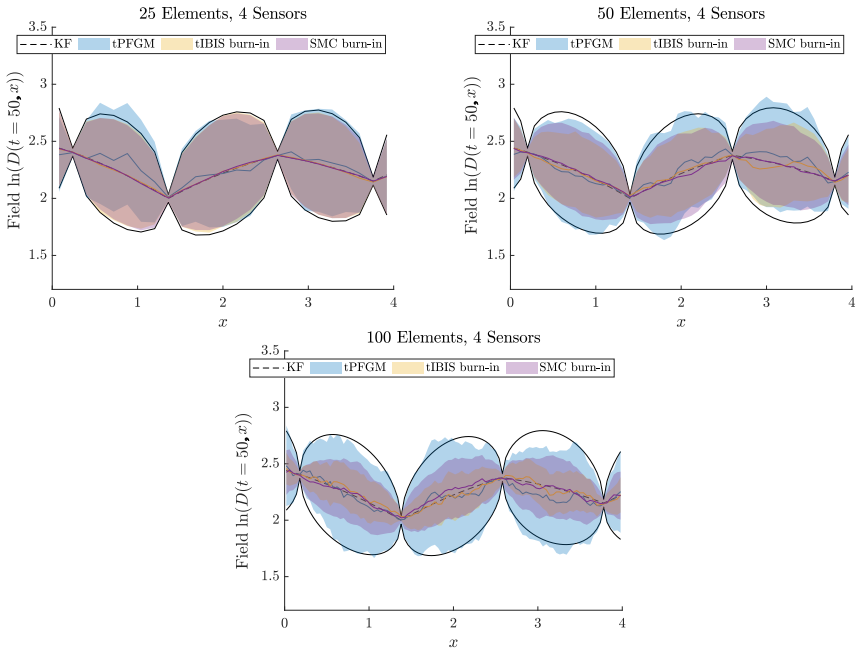

Figure 6.15: Updating of the random field $\ln(D(t=50,x))$ in three different cases of varying problem dimensionality. The solid lines show the mean and the shaded areas the 90% credible intervals inferred from 10 repeated runs of each filter. The black dashed line represented the posterior mean obtained via the KF, and the black solid lines the KF 90% credible intervals

6.4 Concluding remarks

In this article, we present in algorithmic detail three different on-line and off-line Bayesian filters. The on-line filters are specifically tailored for quantifying the full posterior uncertainty of time-invariant deterioration model parameters in long-term monitoring settings. Specifically, the three presented methods are an on-line particle filter with Gaussian mixture resampling (PFGM), an on-line iterated batch importance sampling (IBIS) filter, and an off-line sequential Monte Carlo (SMC) filter, which applies simulated annealing to sequentially arrive to a single posterior density of interest. The IBIS and SMC filters perform Markov Chain Monte Carlo (MCMC) move steps via application of an independent Metropolis Hastings kernel with a Gaussian mixture proposal distribution (IMH-GM) whenever degeneracy is identified. A simulated annealing process (tempering of the likelihood function) is further incorporated within the update step of the on-line PFGM and IBIS filters for cases when each new measurement is expected to have a strong information content; this leads to the presented tPFGM and tIBIS filters. The SMC filter can be employed only for off-line inference, while the PFGM, tPFGM, IBIS and tIBIS filters can perform both on-line and off-line inference tasks.

With the aid of two numerical examples, a comparative assessment of these algorithms for off-line and on-line Bayesian filtering of time-invariant deterioration model parameters is performed. In contrast to other works, the main focus here lies on the efficacy of the investigated Bayesian filters in quantifying the full posterior uncertainty of deterioration model parameters, as well as on the induced computational cost.

For the first non-linear, non-Gaussian and low-dimensional case study, the IBIS and SMC filters, which both contain IMH-GM-based MCMC move steps, are shown to consistently outperform the purely on-line PFGM filter in estimating the parameters' reference posterior distributions. However, they induce a computational cost of at least an order of magnitude larger than the PFGM filter, when the same initial number of particles is used in all three filters. With similar computational cost, i.e., when increasing the number of particles in PFGM, it achieves enhanced posterior accuracy, comparable to the IBIS and SMC filters.

The second case study involves a linear, Gaussian and high-dimensional model. The focus here lies on evaluating the performance of the investigated filters in increasing dimensions. The linear Gaussian nature of the problem allows access to an exact reference posterior solution with the Kalman filter. For this case study, the results vary with increasing problem dimensionality and number of sensors. The on-line tPFGM filter achieves a consistently satisfactory quality with increasing dimensionality, a behavior explained by the linear Gaussian nature of the problem, while a slight drop in the posterior quality is observed for increasing amount of sensor information. The tIBIS and SMC filters are shown to consistently outperform the tPFGM filter in lower dimensions, they however perform progressively worse in higher dimensions, a behavior likely explained by the degeneracy of the acceptance probability of MH samplers in high dimensions. The computational cost of the tIBIS and SMC filters is an order of magnitude larger than the tPFGM filter.

Some general conclusions drawn from the delivered comparative assessment are listed below.

- The purely on-line PFGM (and its tPFGM variant) filter is competitive with MCMC-based filters, especially for higher-dimensional well-behaved problems.

- The IBIS (and its tIBIS variant) and SMC filters, which contain MCMC move steps, offer better approximations of the posterior mean of the model parameters than the purely on-line PFGM (and its tPFGM variant) filter with the same number of samples, as shown in both studied examples.

- The independent Metropolis Hastings (IMH)-based MCMC move step performed within the IBIS, tIBIS and SMC filters proves inadequate in properly exploring the posterior parameter space in high-dimensional problems.

Finally, to support the reader with the selection of the appropriate algorithm for a designated scenario, we provide Tab. 6.5, which contains an assessment of the methods presented in this paper in function of problem characteristics.

This paper does not investigate the performance of these filters when applied to high-dimensional and highly non-Gaussian problems. Such problems are bottlenecks for most existing filters and we expect the investigated filters to be confronted with difficulties in approximating the posterior distributions.

Table 6.5: Set of suggestions on choice of the appropriate method in function of problem characteristics.

	Criterion	PFGM (tPFGM)	IMH-GM-based IBIS (tIBIS)	IMH-GM-based SMC
	On-line inference	✓	○	×
	Computational cost	C_1	C_2	C_3
Applicability to various problems	Mean estimation in low-dimensional, nonlinear, non-Gaussian problems	Q_3	Q_4	Q_4
	Uncertainty quantification in low-dimensional, nonlinear, non-Gaussian problems	Q_3	Q_4	Q_4
	Mean estimation in high-dimensional, well-behaved problems	Q_2	Q_3	Q_4
	Uncertainty quantification in high-dimensional, well-behaved problems	Q_3	Q_1	Q_1
	Increasing sensor information amount	× (✓)	× (✓)	✓

Q_1: low quality
Q_2: moderate quality
Q_3: moderate to high quality
Q_4: high quality

✓: applicable
○: partly applicable
×: not applicable

C_1: moderate
C_2: moderate to high
C_3: high

Acknowledgments

The work of A. Kamariotis and E. Chatzi has been carried out with the support of the Technical University of Munich - Institute for Advanced Study, Germany, funded by the German Excellence Initiative and the TÜV SÜD Foundation.

References

[1] C. Andrieu, A. Doucet, S. Singh, and V. Tadic. "Particle methods for change detection, system identification, and control". In: *Proceedings of the IEEE* 92.3 (2004), pp. 423–438.

[2] C. Andrieu, A. Doucet, and R. Holenstein. "Particle Markov chain Monte Carlo methods". In: *Journal of the Royal Statistical Society: Series B (Statistical Methodology)* 72.3 (2010), pp. 269–342.

[3] S.-K. Au and J. L. Beck. "Estimation of small failure probabilities in high dimensions by subset simulation". In: *Probabilistic Engineering Mechanics* 16.4 (2001), pp. 263–277.

[4] S. E. Azam, E. Chatzi, C. Papadimitriou, and A. Smyth. "Experimental validation of the Kalman-type filters for online and real-time state and input estimation". In: *Journal of Vibration and Control* 23.15 (2017), pp. 2494–2519.

[5] P. Baraldi, F. Cadini, F. Mangili, and E. Zio. "Model-based and data-driven prognostics under different available information". In: *Probabilistic Engineering Mechanics* 32 (2013), pp. 66–79.

[6] J. Beck and S. Au. "Bayesian Updating of Structural Models and Reliability using Markov Chain Monte Carlo Simulation". In: *Journal of Engineering Mechanics* 128(4) (2002), p. 380.

[7] A. Beskos and A. Stuart. "Computational Complexity of Metropolis-Hastings Methods in High Dimensions". In: *Monte Carlo and Quasi-Monte Carlo Methods 2008*. Ed. by P. L' Ecuyer and A. B. Owen. Berlin, Heidelberg: Springer Berlin Heidelberg, 2009, pp. 61–71.

[8] F. Cadini, E. Zio, and D. Avram. "Model-based Monte Carlo state estimation for condition-based component replacement". In: *Reliability Engineering & System Safety* 94.3 (2009), pp. 752–758.

[9] F. Cadini, E. Zio, and D. Avram. "Monte Carlo-based filtering for fatigue crack growth estimation". In: *Probabilistic Engineering Mechanics* 24.3 (2009), pp. 367–373.

[10] C. M. Carvalho, M. S. Johannes, H. F. Lopes, and N. G. Polson. "Particle Learning and Smoothing". In: *Statistical Science* 25.1 (2010), pp. 88–106.

[11] G. Celeux, S. Fruewirth-Schnatter, and C. P. Robert. "Model Selection for Mixture Models - Perspectives and Strategies". In: *Handbook of Mixture Analysis* (2019).

[12] E. Chatzi and A. Smyth. "Particle filter scheme with mutation for the estimation of time-invariant parameters in structural health monitoring applications". In: *Structural Control and Health Monitoring* 20 (2013), pp. 1081–1095.

[13] E. N. Chatzi and A. W. Smyth. "The unscented Kalman filter and particle filter methods for nonlinear structural system identification with non-collocated heterogeneous sensing". In: *Structural Control and Health Monitoring* 16.1 (2009), pp. 99–123.

[14] Y. Chen, M. R. Gupta, Y. Chen, and M. R. Gupta. "EM demystified: An expectation-maximization tutorial". In: *University of Washington, Dept. of EE* (2010).

[15] J. Ching and Y.-C. Chen. "Transitional Markov Chain Monte Carlo Method for Bayesian Model Updating, Model Class Selection, and Model Averaging". In: *Journal of Engineering Mechanics* 133.7 (2007), pp. 816–832.

[16] N. Chopin, P. E. Jacob, and O. Papaspiliopoulos. "SMC2: an efficient algorithm for sequential analysis of state space models". In: *Journal of the Royal Statistical Society: Series B (Statistical Methodology)* 75.3 (2013), pp. 397–426.

[17] N. Chopin. "A Sequential Particle Filter Method for Static Models". In: *Biometrika* 89(3) (Aug. 2002), pp. 539–552.

[18] N. Chopin. "Central limit theorem for sequential Monte Carlo methods and its application to Bayesian inference". In: *The Annals of Statistics* 32.6 (2004), pp. 2385–2411.

[19] M. Corbetta, C. Sbarufatti, M. Giglio, and M. D. Todd. "Optimization of nonlinear, non-Gaussian Bayesian filtering for diagnosis and prognosis of monotonic degradation processes". In: *Mechanical Systems and Signal Processing* 104 (2018), pp. 305–322.

[20] S. L. Cotter, G. O. Roberts, A. M. Stuart, and D. White. "MCMC Methods for Functions: Modifying Old Algorithms to Make Them Faster". In: *Statistical Science* 28.3 (2013), pp. 424–446.

[21] D. Cristiani, C. Sbarufatti, and M. Giglio. "Damage diagnosis and prognosis in composite double cantilever beam coupons by particle filtering and surrogate modelling". In: *Structural Health Monitoring* 20.3 (2021), pp. 1030–1050.

[22] F. Daum. "Nonlinear filters: beyond the Kalman filter". In: *IEEE Aerospace and Electronic Systems Magazine* 20.8 (2005), pp. 57–69.

[23] A. Der Kiureghian and J.-B. Ke. "The stochastic finite element method in structural reliability". In: *Probabilistic Engineering Mechanics* 3.2 (1988), pp. 83–91.

[24] J. Deutscher, A. Blake, and I. Reid. "Articulated body motion capture by annealed particle filtering". In: *Proceedings IEEE Conference on Computer Vision and Pattern Recognition. CVPR 2000 (Cat. No.PR00662)*. Vol. 2. 2000, 126–133 vol.2.

[25] O. Ditlevsen and H. Madsen. *Structural Reliability Methods*. Wiley New York, 1996.

[26] A. Doucet, N. de Freitas, and N. Gordon. *Sequential Monte Carlo Methods in Practice*. Springer-Verlag New York, 2001.

[27] A. Doucet and A. M. Johansen. "A Tutorial on Particle Filtering and Smoothing: Fifteen years later". In: *Handbook of Nonlinear Filtering* (2008).

[28] B. Ellingwood. "Risk-informed condition assessment of civil infrastructure: state of practice and research issues". In: *Structure and Infrastructure Engineering* 1(1) (2005), pp. 7–18.

[29] G. Evensen. *Data Assimilation: The Ensemble Kalman Filter*. Berlin, Heidelberg: Springer-Verlag, 2006.

[30] D. M. Frangopol. "Life-cycle performance, management, and optimisation of structural systems under uncertainty: accomplishments and challenges". In: *Structure and Infrastructure Engineering* 7.6 (2011), pp. 389–413.

[31] J. Gall, J. Potthoff, C. Schnörr, B. Rosenhahn, and H.-P. Seidel. "Interacting and Annealing Particle Filters: Mathematics and a Recipe for Applications". In: *J Math Imaging Vis* 28 (2007), pp. 1–18.

[32] A. Gelman, W. R. Gilks, and G. O. Roberts. "Weak convergence and optimal scaling of random walk Metropolis algorithms". In: *The Annals of Applied Probability* 7.1 (1997), pp. 110–120.

[33] S. Geyer, I. Papaioannou, and D. Straub. "Cross entropy-based importance sampling using Gaussian densities revisited". In: *Structural Safety* 76 (2019), pp. 15–27.

[34] R. G. Ghanem and P. D. Spanos. *Stochastic Finite Elements: A Spectral Approach*. Springer, 1991.

[35] W. Gilks, S. Richardson, and D. Spiegelhalter. *Markov Chain Monte Carlo in Practice*. Chapman & Hall/CRC Interdisciplinary Statistics. Taylor & Francis, 1995.

[36] W. R. Gilks and C. Berzuini. "Following a Moving Target-Monte Carlo Inference for Dynamic Bayesian Models". In: *Journal of the Royal Statistical Society. Series B (Statistical Methodology)* 63.1 (2001), pp. 127–146.

[37] N. Gordon, D. Salmond, and A. Smith. "Novel approach to nonlinear/non-Gaussian Bayesian state estimation". In: *IEE Proc. F Radar Signal Process. UK* 140.2 (1993), p. 107.

[38] H. Haario, M. Laine, A. Mira, and E. Saksman. "DRAM: Efficient adaptive MCMC". In: *Statistics and Computing* 16 (2006), pp. 339–354.

[39] W. K. Hastings. "Monte Carlo Sampling Methods Using Markov Chains and Their Applications". In: *Biometrika* 57.1 (1970), pp. 97–109.

[40] X.-L. Hu, T. B. Schon, and L. Ljung. "A Basic Convergence Result for Particle Filtering". In: *IEEE Transactions on Signal Processing* 56.4 (2008), pp. 1337–1348.

[41] A. Jasra, D. A. Stephens, A. Doucet, and T. Tsagaris. "Inference for Lévy-Driven Stochastic Volatility Models via Adaptive Sequential Monte Carlo". In: *Scandinavian Journal of Statistics* 38.1 (2011), pp. 1–22.

[42] A. Jazwinski. *Stochastic Processes and Filtering Theory*. Mathematics in Science and Engineering. Elsevier Science, 1970.

[43] S. Julier and J. Uhlmann. "A new extension of the Kalman filter to nonlinear systems". In: *The Proceedings of AeroSense Symposium* (1997), pp. 54–65.

[44] R. Kalman. "A New Approach to Linear Filtering and Prediction Problems". In: *ASME Journal of Basic Engineering* 82 (1960), pp. 35–45.

[45] A. Kamariotis, E. Chatzi, and D. Straub. "A framework for quantifying the value of vibration-based structural health monitoring". In: *Mechanical Systems and Signal Processing* 184 (2023), p. 109708.

[46] A. Kamariotis, E. Chatzi, and D. Straub. "Value of information from vibration-based structural health monitoring extracted via Bayesian model updating". In: *Mechanical Systems and Signal Processing* 166 (2022), p. 108465.

[47] A. Kamariotis, L. Sardi, I. Papaioannou, E. Chatzi, and D. Straub. "On off-line and on-line Bayesian filtering for uncertainty quantification of structural deterioration". In: *Data-Centric Engineering* 4 (2023), e17.

[48] N. Kantas, A. Doucet, S. S. Singh, J. Maciejowski, and N. Chopin. "On Particle Methods for Parameter Estimation in State-Space Models". In: *Statistical Science* 30.3 (2015), pp. 328–351.

[49] L. Katafygiotis and K. Zuev. "Geometric insight into the challenges of solving high-dimensional reliability problems". In: *Probabilistic Engineering Mechanics* 23.2 (2008), pp. 208–218.

[50] M. C. Kennedy and A. O'Hagan. "Bayesian calibration of computer models". In: *Journal of the Royal Statistical Society: Series B (Statistical Methodology)* 63.3 (2001), pp. 425–464.

[51] N.-H. Kim, D. An, and J.-H. Choi. *Prognostics and Health Management of Engineering Systems. An introduction*. Springer, 2017.

[52] G. Kitagawa. "A Self-Organizing State-Space Model". In: *Journal of the American Statistical Association* 93.443 (1998), pp. 1203–1215.

[53] A. D. Kiureghian and P.-L. Liu. "Structural Reliability under Incomplete Probability Information". In: *Journal of Engineering Mechanics* 112.1 (1986), pp. 85–104.

[54] J. Liu and M. West. *Combined Parameter and State Estimation in Simulation-Based Filtering*. New York, NY: Springer New York, 2001, pp. 197–223.

[55] J. S. Liu and R. Chen. "Sequential Monte Carlo Methods for Dynamic Systems". In: *Journal of the American Statistical Association* 93.443 (1998), pp. 1032–1044.

[56] J. Luque and D. Straub. "Risk-based optimal inspection strategies for structural systems using dynamic Bayesian Networks". In: *Structural Safety* 76 (2019), pp. 68–80.

[57] A. Lye, A. Cicirello, and E. Patelli. "Sampling methods for solving Bayesian model updating problems: A tutorial". In: *Mechanical Systems and Signal Processing* 159 (2021), p. 107760.

[58] G. J. McLachlan and T. Krishnan. *The EM Algorithm and Extensions, Second Edition*. John Wiley & Sons, Ltd, 2007.

[59] R. E. Melchers and A. Beck. *Structural Reliability Analysis and Prediction, 3rd Edition*. John Wiley & Sons, Ltd, 2017.

[60] R. van der Merwe and E. Wan. "Gaussian mixture sigma-point particle filters for sequential probabilistic inference in dynamic state-space models". In: *2003 IEEE International Conference on Acoustics, Speech, and Signal Processing, 2003. Proceedings. (ICASSP '03).* Vol. 6. 2003, pp. VI–701.

[61] P. D. Moral, A. Doucet, and A. Jasra. "Sequential Monte Carlo Samplers". In: *Journal of the Royal Statistical Society. Series B (Statistical Methodology)* 68.3 (2006), pp. 411–436.

[62] C. Musso, N. Oudjane, and F. Le Gland. *Improving Regularised Particle Filters.* New York, NY: Springer New York, 2001, pp. 247–271.

[63] E. Myötyri, U. Pulkkinen, and K. Simola. "Application of stochastic filtering for lifetime prediction". In: *Reliability Engineering & System Safety* 91.2 (2006), pp. 200–208.

[64] R. M. Neal. "Annealed importance sampling". In: *Statistics and Computing* 11 (2001), pp. 125–139.

[65] I. Papaioannou, W. Betz, K. Zwirglmaier, and D. Straub. "MCMC algorithms for Subset Simulation". In: *Probabilistic Engineering Mechanics* 41 (2015), pp. 89–103.

[66] I. Papaioannou, C. Papadimitriou, and D. Straub. "Sequential importance sampling for structural reliability analysis". In: *Structural Safety* 62 (2016), pp. 66–75.

[67] K. Papakonstantinou and M. Shinozuka. "Planning structural inspection and maintenance policies via dynamic programming and Markov processes. Part II: POMDP implementation". In: *Reliability Engineering & System Safety* 130 (2014), pp. 214–224.

[68] P. Paris and F. Erdogan. "A Critical Analysis of Crack Propagation Laws". In: *Journal of Basic Engineering* 85.4 (1963), pp. 528–533.

[69] M. K. Ramancha, R. Astroza, R. Madarshahian, and J. P. Conte. "Bayesian updating and identifiability assessment of nonlinear finite element models". In: *Mechanical Systems and Signal Processing* 167 (2022), p. 108517.

[70] R. Y. Rubinstein and D. P. Kroese. *Simulation and the Monte Carlo Method.* 3rd. Wiley Publishing, 2016.

[71] S. J. Russell and P. Norvig. *Artificial intelligence: A modern approach, 4th Edition.* Pearson Education, Inc, 2021.

[72] B. Saha, K. Goebel, S. Poll, and J. Christophersen. "Prognostics Methods for Battery Health Monitoring Using a Bayesian Framework". In: *IEEE Transactions on Instrumentation and Measurement* 58.2 (2009), pp. 291–296.

[73] S. Särkkä. *Bayesian Filtering and Smoothing.* English. United Kingdom: Cambridge University Press, 2013.

[74] E. Schubert, J. Sander, M. Ester, H. P. Kriegel, and X. Xu. "DBSCAN Revisited, Revisited: Why and How You Should (Still) Use DBSCAN". In: *ACM Trans. Database Syst.* 42.3 (2017).

[75] A. F. M. Smith and A. E. Gelfand. "Bayesian Statistics without Tears: A Sampling-Resampling Perspective". In: *The American Statistician* 46.2 (1992), pp. 84–88.

[76] M. Song, R. Astroza, H. Ebrahimian, B. Moaveni, and C. Papadimitriou. "Adaptive Kalman filters for nonlinear finite element model updating". In: *Mechanical Systems and Signal Processing* 143 (2020), p. 106837.

[77] L. F. South, A. N. Pettitt, and C. C. Drovandi. "Sequential Monte Carlo Samplers with Independent Markov Chain Monte Carlo Proposals". In: *Bayesian Analysis* 14.3 (2019), pp. 753–776.

[78] M. G. Stewart and J. A. Mullard. "Spatial time-dependent reliability analysis of corrosion damage and the timing of first repair for RC structures". In: *Engineering Structures* 29.7 (2007), pp. 1457–1464.

[79] G. Storvik. "Particle filters for state-space models with the presence of unknown static parameters". In: *IEEE Transactions on Signal Processing* 50.2 (2002), pp. 281–289.

[80] D. Straub. "Stochastic Modeling of Deterioration Processes through Dynamic Bayesian Networks". In: *Journal of Engineering Mechanics* 135.10 (2009), pp. 1089–1099.

[81] D. Straub, R. Schneider, E. Bismut, and H.-J. Kim. "Reliability analysis of deteriorating structural systems". In: *Structural Safety* 82 (2020), p. 101877.

[82] B. Sudret and A. Der Kiureghian. "Stochastic Finite Element Methods and Reliability A State-of-the-Art Report". In: (2000).

[83] J. Sun, H. Zuo, W. Wang, and M. G. Pecht. "Prognostics uncertainty reduction by fusing on-line monitoring data based on a state-space-based degradation model". In: *Mechanical Systems and Signal Processing* 45.2 (2014), pp. 396–407.

[84] K. E. Tatsis, V. K. Dertimanis, and E. N. Chatzi. "Sequential Bayesian Inference for Uncertain Nonlinear Dynamic Systems: A Tutorial". In: *Journal of Structural Dynamics* (2022), pp. 236–262.

[85] E. Vanmarcke. *Random fields. Analysis and synthesis*. Cambridge, MA: MIT Press, 1983.

[86] D. R. A. Veettil and S. Chakravorty. *Particle Gaussian Mixture (PGM) Filters*. 2016.

[87] K. A. T. Vu and M. G. Stewart. "Structural reliability of concrete bridges including improved chloride-induced corrosion models". In: *Structural Safety* 22.4 (2000), pp. 313–333.

[88] A. Wirgin. "The inverse crime". In: *arXiv e-prints*, math-ph/0401050 (2004), math–ph/0401050.

[89] S. Wu, P. Angelikopoulos, C. Papadimitriou, and P. Koumoutsakos. "Bayesian Annealed Sequential Importance Sampling: An Unbiased Version of Transitional Markov Chain Monte Carlo". In: *ASCE-ASME J Risk and Uncert in Engrg Sys Part B Mech Engrg* 4.1 (2017).

[90] S.-r. Yi and J. Song. "Particle Filter Based Monitoring and Prediction of Spatiotemporal Corrosion Using Successive Measurements of Structural Responses". In: *Sensors* 18.11 (2018).

Chapter 7

A metric for assessing and optimizing data-driven prognostic algorithms for predictive maintenance

Original Publication

A. Kamariotis, K. Tatsis, E. Chatzi, K. Goebel, and D. Straub. "A metric for assessing and optimizing data-driven prognostic algorithms for predictive maintenance". In: *Reliability Engineering & System Safety* 242 (2024), p. 109723

Author's contribution

Antonios Kamariotis: Conceptualization, Methodology, Software, Formal analysis, Visualization, Writing - original draft. **Konstantinos Tatsis**: Methodology, Software, Visualization, Writing - original draft. **Eleni Chatzi**: Conceptualization, Methodology, Writing - review & editing, Funding acquisition. **Kai Goebel**: Writing - review & editing. **Daniel Straub**: Conceptualization, Methodology, Writing - review & editing, Funding acquisition.

Abstract

Prognostic Health Management aims to predict the Remaining Useful Life (RUL) of degrading components/systems utilizing monitoring data. These RUL predictions form the basis for optimizing maintenance planning in a Predictive Maintenance (PdM) paradigm. We here propose a metric for assessing data-driven prognostic algorithms based on their impact on downstream PdM decisions. The metric is defined in association with a decision setting and a corresponding PdM policy. We consider two typical PdM decision settings, namely component ordering and/or replacement planning, for which we investigate and improve PdM policies that are commonly utilized in the literature. All policies are evaluated via the data-based estimation of the long-run expected maintenance cost

per unit time, using monitored run-to-failure experiments. The policy evaluation enables the estimation of the proposed metric. We employ the metric as an objective function for optimizing heuristic PdM policies and algorithms' hyperparameters. The effect of different PdM policies on the metric is initially investigated through a theoretical numerical example. Subsequently, we employ four data-driven prognostic algorithms on a simulated turbofan engine degradation problem, and investigate the joint effect of prognostic algorithm and PdM policy on the metric, resulting in a decision-oriented performance assessment of these algorithms.

7.1 Introduction

Prognostics is primarily concerned with the prediction of the time instance when a system or component loses its functionality [30]. In the context of an on-line monitoring strategy, this typically implies the use of a prognostic model, which furnishes estimates of the Remaining Useful Life (RUL) on the basis of available measurements of the system's response [18]. The subsequent task of optimal maintenance planning informed by the prognostic model output is known as health management. Prognostic Health Management (PHM) [30, 18, 70] is the umbrella term used to define this procedure. Multiple sources of uncertainty enter the prognostics process, which motivates the adoption of a stochastic approach to the estimation of the RUL [15]. Consequently, the associated maintenance planning can be defined as a sequential decision problem under uncertainty [32, 49, 41, 39, 2].

One can distinguish between model-based and data-driven prognostic methods [30]. A recent review paper [35] classified prognostic approaches into four distinct categories: physics model-based approaches, statistical model-based approaches, artificial intelligence (AI) approaches and hybrid approaches. An overview of recent literature reveals the increasing popularity of data-driven AI approaches [37, 64, 38], owing amongst other factors, to their applicability in case where the degradation pattern cannot be easily represented a-priori via physics-based or statistical models [45, 35]. On the downside, it is often not straightforward to capture the uncertainty in machine learning (ML) predictions [15, 47]. The task of quantifying such an uncertainty, that is inherent in RUL predictions, is essential for subsequent maintenance planning tasks.

The PHM community has established various experimental and numerical prognostic datasets, which typically contain multivariate time series data obtained from continuous monitoring of run-to-failure experiments on deteriorating components/systems, such as rolling bearings [45], batteries [54], turbofan engines [59] and industrial machines [52]. Several of these datasets have been made publicly available by the NASA Prognostics Center of Excellence [44]. The availability of such datasets has paved the way for the development and training of a multitude of data-driven prognostic algorithms. These are reviewed in [60, 23, 35]. Most of the available literature focuses on the RUL prediction task [37, 64, 38, 3], and does not consider the subsequent health management task.

For the task of health management on the basis of RUL predictions, the predictive maintenance (PdM) paradigm stands out [19, 8, 14]. PdM tasks usually relate to planning intermittent inspections and maintenance [11, 31], and planning maintenance actions informed via continuous monitoring [10, 46, 65]. PdM can be classified as either model-based PdM or data-driven PdM [46, 14]. The former is based on the assumption that a physics-based model, e.g., the Paris-Erdogan law for fatigue crack growth [50], or a statistical process model, e.g., a Gamma process [63] or a Wiener process [68], is

available for describing the deterioration process. The performance of model-based PdM depends on the adopted model. Most PdM studies to date either employ model-based PdM [11, 21, 40, 9, 65, 26], or simplistically consider hypothetical models of the prognostics information and only focus on the maintenance decision optimization [12, 5]. End-to-end data-driven PdM frameworks (from data-driven prognostics to data-driven PdM planning) have recently been introduced and applied on prognostic datasets [46, 10, 7, 42, 69]. The data-driven PdM framework relies on availability of a sufficient amount of monitoring data from run-to-failure experiments. These are required both for the training of data-driven prognostic algorithms as well as for the data-driven evaluation of PdM policies.

Given the diversity of prognostic models, the definition of metrics for assessing and comparing the performance of prognostic algorithms can be of defining importance in decision making [57, 58, 45, 22, 20, 4, 51]. Recent papers review such metrics [35, 36]. Most of these metrics only implicitly account for the subsequent health management task in their design, e.g., how early the algorithm allows for prediction [58, 45]. Our conjecture is that the choice of a performance metric should be guided by the type of PdM decisions that are to be triggered by the algorithms' outcome.

The current paper proposes a metric for assessing the efficacy of data-driven prognostic models based on their impact on downstream PdM decisions. We clarify the role that PdM policies play in the definition of this metric. The metric can be applied within any given decision setting. In this paper, two PdM decision settings are considered, namely i) component replacement planning and ii) component ordering-replacement planning, which are fairly common for industrial components. We thoroughly investigate some PdM policies of different complexity that are utilized in the literature. These dynamically receive as input the RUL prediction from prognostics and opt for the actions that should lead to an optimal balance between the predicted risk of failure/risk of late order for a new component, and the benefit of extending the life-cycle of a component/not keeping a spare component in the inventory, respectively. Alternatives and improvements to these PdM policies are proposed. We evaluate these in terms of the estimation of the long-run expected maintenance cost per unit time [11, 13], upon applying the policies on a run-to-failure dataset. The proposed metric is evaluated on the basis of this estimation.

The paper is organized as follows. Section 7.2 introduces the proposed decision-oriented metric and discusses its data-driven estimation via samples of run-to-failure experiments. Subsequently, the metric is described within the context of two typical PdM decision settings, for which specific PdM policies are presented and discussed. Section 7.3 introduces a virtual RUL simulator, which serves as an initial test-bed for investigating different aspects of optimality/sub-optimality of the presented PdM policies and their effect on the metric. Section 7.4 contains numerical investigations on an actual case study related to degrading turbofan engines, by use of the well-known CMAPSS prognostic dataset [59]. Four different data-driven prognostic algorithms, three classifiers and one regression model, are implemented and compared on the basis of the proposed decision-oriented metric. The interplay between RUL prediction algorithm and PdM policy on the metric is also investigated. Finally, Section 7.5 discusses and concludes this work.

7.2 Predictive maintenance decision policies on the basis of RUL predictions

To evaluate the quality of different prognostic algorithms that deliver RUL predictions, we compare their performance on subsequent PdM decision making. To evaluate the RUL-based decisions, policies are introduced [24]. A policy is a rule that determines the action to take at time t, based on the available information up to that time, i.e., past monitoring data and performed actions. For example, a policy answers the following question: "Preventively replace the component?" {yes, no}. In this work, we consider only decision settings in which the policy is the same at all times, and we refer to this stationary policy [32] as the *PdM policy*.

7.2.1 Decision-oriented metric for prognostics performance evaluation

Towards the goal of providing a formal decision-oriented framework for assessing and optimizing the performance of prognostic algorithms, this section proposes a metric that quantifies the optimality of the resulting maintenance decisions triggered by the algorithm's RUL predictions within any given decision setting. The proposed framework is summarized in Fig. 7.1.

7.2.1.1 Data-based evaluation of a generic PdM policy

The long-run expected maintenance cost per unit time (over an infinite time horizon) is typically the quantity of interest when evaluating a PdM policy. According to renewal theory [62, 11, 13], specifically the renewal-reward theorem, the long-run expected maintenance cost per unit time corresponds to the ratio:

$$R = \frac{\mathrm{E}[C_\mathrm{m}]}{\mathrm{E}[T_\mathrm{lc}]}, \tag{7.1}$$

where $\mathrm{E}[C_\mathrm{m}]$ is the expected maintenance cost induced within one life-cycle of the component when following a certain PdM policy, and $\mathrm{E}[T_\mathrm{lc}]$ is the expected length of one life-cycle. This result is valid without discounting [63]; for renewal theory with discounting, see, e.g., [48]. It allows evaluating the above expectations for a PdM policy by applying it on n independent single life-cycles. In the vast majority of the literature, this evaluation is done with the aid of a model, with which a large number of life-cycle realizations is simulated [11]. In cases where data from multiple run-to-failure experiments are available, the expectations in Eq. (7.1) can be evaluated based on the data. More specifically, a PdM policy can be applied on n independent components of the same type (e.g., n engines of the same type in the CMAPSS dataset [59]) and the cost of maintenance C_m and the lifetime T_lc (also known as a renewal cycle in the context of renewal theory [62]) of each component can be evaluated. The expectations in the numerator and denominator of Eq. (7.1) can then be approximated as:

$$\frac{\mathrm{E}[C_\mathrm{m}]}{\mathrm{E}[T_\mathrm{lc}]} \approx \hat{R} = \frac{\frac{1}{n}\sum_{i=1}^{n} C_\mathrm{m}^{(i)}}{\frac{1}{n}\sum_{i=1}^{n} T_\mathrm{lc}^{(i)}}, \tag{7.2}$$

where $\hat{R}$ denotes the data-based estimator of the quantity in Eq. (7.1), $C_\mathrm{m}^{(i)}$ and $T_\mathrm{lc}^{(i)}$ are the cost of maintenance and the lifetime of the i-th component, respectively. The lifetime $T_\mathrm{lc}^{(i)}$ is the time to

failure or replacement of the component.

With finite n, the estimate of R provided by Eq. (7.2) is subject to uncertainty. A first-order approximation of the variance of the estimator in Eq. (7.2) is [29]:

$$\mathrm{Var}[\hat{R}] \approx \frac{1}{n}\left[\frac{\mathrm{Var}[C_\mathrm{m}]}{\mathrm{E}[T_\mathrm{lc}]^2} + \frac{\mathrm{E}[C_\mathrm{m}]^2 \cdot \mathrm{Var}[T_\mathrm{lc}]}{\mathrm{E}[T_\mathrm{lc}]^4} - 2 \cdot \frac{\mathrm{E}[C_\mathrm{m}] \cdot \mathrm{Cov}[C_\mathrm{m}, T_\mathrm{lc}]}{\mathrm{E}[T_\mathrm{lc}]^3}\right]. \tag{7.3}$$

It is noted that occasionally in literature the expectation of the ratio $\mathrm{E}\left[\frac{C_\mathrm{m}}{T_\mathrm{lc}}\right]$ is evaluated, instead of the ratio of the expectations of Eqs. (7.1) and (7.2). This is only an approximation, which can be poor if the variance of the denominator is large.

7.2.1.2 Data-based evaluation of the perfect PdM policy

As a reference, we consider the hypothetical scenario of perfect prognostics, in which the time to failure is known exactly. Perfect prognostics would lead to perfect PdM decisions for each component. Based on the n run-to-failure experiments, the long-run expected maintenance cost per unit time of the perfect PdM policy can be estimated via Eq. (7.4):

$$R_\mathrm{perfect} = \frac{\mathrm{E}[C_\mathrm{m,perfect}]}{\mathrm{E}[T_\mathrm{lc,perfect}]} \approx \hat{R}_\mathrm{perfect} = \frac{\frac{1}{n}\sum_{i=1}^{n} C_\mathrm{m,perfect}^{(i)}}{\frac{1}{n}\sum_{i=1}^{n} T_\mathrm{lc,perfect}^{(i)}}, \tag{7.4}$$

where $C_\mathrm{m,perfect}^{(i)}$ and $T_\mathrm{lc,perfect}^{(i)}$ are the optimal cost of maintenance and length of the first life-cycle of the i-th component, respectively.

7.2.1.3 Proposed metric

To specify the decision-oriented metric for assessing prognostic algorithms, we evaluate the long-run expected maintenance cost per unit time that is achieved with a specific prognostic algorithm in combination with a PdM policy, which is then compared with the respective quantity obtained from perfect prognostics. We define a scalar metric M as the relative difference between the two, based on which the performance of a prognostic algorithm can be assessed with respect to the PdM decisions that are triggered by its outcome:

$$M = \frac{\frac{\mathrm{E}[C_\mathrm{m}]}{\mathrm{E}[T_\mathrm{lc}]} - \frac{\mathrm{E}[C_\mathrm{m,perfect}]}{\mathrm{E}[T_\mathrm{lc,perfect}]}}{\frac{\mathrm{E}[C_\mathrm{m,perfect}]}{\mathrm{E}[T_\mathrm{lc,perfect}]}}. \tag{7.5}$$

Based on the n run-to-failure experiments, the metric M can be estimated as:

$$\hat{M} = \frac{\hat{R} - \hat{R}_\mathrm{perfect}}{\hat{R}_\mathrm{perfect}}. \tag{7.6}$$

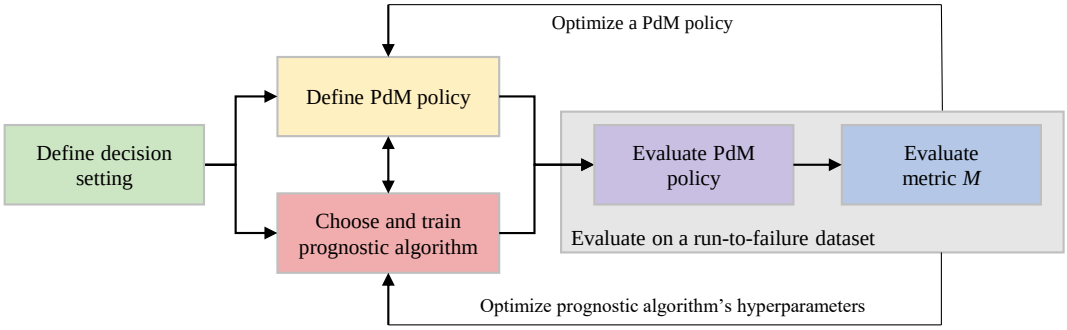

Figure 7.1: Summary of the proposed framework for a decision-oriented performance assessment and optimization of data-driven prognostic algorithms based on the proposed metric M.

$M = 0$ is the optimal result; the larger the value of the metric M, the worse the performance of the prognostic algorithm. M cannot assume a negative value. In a loose sense, a connection can be identified between the metric M and the Value of Information (VoI) metric [13, 25] from Bayesian decision theory [53].

The estimate of Eq. (7.6) for the metric M is subject to uncertainty. Assuming that the variance of $\hat{R}_{\text{perfect}}$ is negligible, the variance of $\hat{M}$ is quantified as:

$$\text{Var}[\hat{M}] = \text{Var}\left[\frac{\hat{R} - \hat{R}_{\text{perfect}}}{\hat{R}_{\text{perfect}}}\right] = \text{Var}\left[\frac{\hat{R}}{\hat{R}_{\text{perfect}}} - 1\right] \approx \frac{1}{\hat{R}^2_{\text{perfect}}} \cdot \text{Var}[\hat{R}] \tag{7.7}$$

Due to the assumption that the variance of $\hat{R}_{\text{perfect}}$ is negligible, the covariance of $\hat{R}$ and $\hat{R}_{\text{perfect}}$ is neglected.

The decision-oriented metric M can further serve as an objective function for optimizing PdM policies and for optimizing the training process of prognostics algorithms (e.g., hyperparameter tuning, see Eq. (7.27)) directly with respect to subsequent PdM decision-making (see Fig. 7.1). This will be demonstrated in the numerical investigations of Sections 7.3 and 7.4.

The metric M is generally applicable in any given decision setting in conjunction with a PdM policy. The sections that follow specify the metric M for two common decision settings.

7.2.2 PdM decision settings

In this paper, we consider and discuss two PdM decision settings that are typical for industrial assets. In the first basic setting (Section 7.2.3), the only decision that has to be taken is when to replace a component. In the second setting (Section 7.2.4), we additionally consider a decision on ordering and keeping a replacement component in the inventory. Both considered decision settings have the following characteristics:

- We study single component problems.
- Continuous monitoring of a component is available.
- The monitoring data is employed to derive a probabilistic RUL prediction.

- Inspections are not considered.
- Decisions on maintenance actions can only be made at discrete points in time, defined by $t_k = k \cdot \Delta T$, for a fixed time interval ΔT and integer $k = 1, 2, \ldots, N$. The choice of ΔT is problem-dependent. For example, in the case of aeroengines, a value of $\Delta T = 5 - 10$ flight cycles is deemed realistic based on the authors' expertise.
- Two types of replacement actions are considered:
  1. Preventive replacement with cost c_{p}.
  2. Corrective replacement with cost c_{c}, which occurs upon component failure before a preventive replacement. Corrective replacement induces a larger cost than preventive replacement, which also accounts for longer downtime: $c_{\mathrm{c}} > c_{\mathrm{p}}$.
- A replacement is assumed to be a perfect replacement, bringing the component back to a pristine state. Replacement at t leads to the end of one life-cycle of the component, and the component starts deteriorating anew. The stochastic deterioration process starting at time t is a probabilistic copy of the process starting at time 0. These assumptions allow for use of renewal theory [62]. Within renewal theory, the time interval between two successive replacements defines a renewal cycle.
- Maintenance is a viable decision, i.e., it is possible to assume remediative action within the decision horizon.
- It is assumed that failure is self-announcing.
- We do not include discounting of future costs.

7.2.3 Predictive maintenance (PdM) planning for replacement

We first consider the simple dynamic PdM decision setting, in which one determines at each time step t_k whether a component should be preventively replaced or not. The assumption here is that the new component is readily available when a preventive replacement is decided or a corrective replacement is imposed.

7.2.3.1 Metric for prognostic performance evaluation with respect to PdM planning for replacement

Following a certain PdM policy for planning replacement (specific PdM policies are introduced in Sections 7.2.3.2 to 7.2.3.4), each i-th component life ends with a preventive replacement informed at time $T_{\mathrm{R}}^{(i)}$, or a corrective replacement in case of component failure at time $T_{\mathrm{F}}^{(i)}$. A preventive replacement can only be performed at discrete points in time, i.e., $T_{\mathrm{R}}^{(i)}$ lies in the set $\{t_k = k \cdot \Delta T, k = 1, 2, \ldots\}$. A corrective replacement is performed immediately upon failure at $T_{\mathrm{F}}^{(i)}$. The (non-discounted) cost of the replacement action for the i-th component is

$$C_{\mathrm{rep}}^{(i)} = \begin{cases} c_{\mathrm{p}}, & \text{if } T_{\mathrm{R}}^{(i)} < T_{\mathrm{F}}^{(i)} \\ c_{\mathrm{c}}, & \text{else.} \end{cases} \tag{7.8}$$

Replacement (preventive or corrective) leads to the end of one life-cycle of a component. The length of the life-cycle of the i-th component is thus $T_{\mathrm{lc}}^{(i)} = \min[T_{\mathrm{R}}^{(i)}, T_{\mathrm{F}}^{(i)}]$. In this setting, the cost of maintenance for the i-th component is equal to the cost of the replacement action, i.e., $C_{\mathrm{m}}^{(i)} = C_{\mathrm{rep}}^{(i)}$.

Within the current decision setting, the perfect PdM policy would not lead to any corrective replacement, as this is more costly, or any early preventive replacement, as this leads to shortening of the component life-cycle. Thus, the perfect PdM policy is a preventive replacement with cost $C^{(i)}_{\text{m,perfect}} = c_{\text{p}}$ at the optimal time step $t_k = k \cdot \Delta T$ directly before $T^{(i)}_{\text{F}}$ [1]. This is denoted by $T^{(i)}_{\text{R,perfect}}$. The long-run expected maintenance cost per unit time of the perfect PdM policy is evaluated via Eq. (7.4).

Eventually, the decision-oriented metric proposed in Eq. (7.5), in particular in conjunction with a PdM policy for replacement, is estimated as:

$$\hat{M} = \frac{\frac{\frac{1}{n}\sum_{i=1}^{n} C^{(i)}_{\text{rep}}}{\frac{1}{n}\sum_{i=1}^{n} T^{(i)}_{\text{lc}}} - \frac{c_{\text{p}}}{\frac{1}{n}\sum_{i=1}^{n} T^{(i)}_{\text{R,perfect}}}}{\frac{c_{\text{p}}}{\frac{1}{n}\sum_{i=1}^{n} T^{(i)}_{\text{R,perfect}}}}. \tag{7.9}$$

7.2.3.2 PdM policy 1: simple heuristic PdM policy for preventive replacement

The first PdM policy that we consider is a simple heuristic policy, similar to [46]. Heuristic policies employ simple and intuitive decision rules that are easily understood by engineers and operators [39]. Specifically, at each time step $t_k = k \cdot \Delta T$, the policy determines the action $a_{\text{rep},k}$ to take as:

$$a_{\text{rep},k} = \begin{cases} \text{DN}, & \text{if } \Pr(RUL_{\text{pred},k} \leq \Delta T) < p_{\text{thres}} \\ \text{PR} & \text{else,} \end{cases} \tag{7.10}$$

where DN denotes the do nothing action, PR denotes the preventive replacement action, $RUL_{\text{pred},k}$ is the RUL prediction estimated at time t_k from the employed prognostic algorithm, and p_{thres} is a variable heuristic threshold. In [46], a value of $p_{\text{thres}} = c_{\text{p}}/c_{\text{c}}$ has been used. The PR action is associated with a cost c_{p}, while the DN action entails the predicted risk of component failure within the next time step, $\Pr(RUL_{\text{pred},k} \leq \Delta T) \cdot c_{\text{c}}$. The reasoning behind $p_{\text{thres}} = c_{\text{p}}/c_{\text{c}}$ is that the PR action is performed at time t_k only when the associated cost is smaller than the predicted risk of component failure in the next time step. This is a simplification, as it does not account for the future time steps; after a replacement, one has a new component with - on average - lower maintenance costs. Hence the choice $p_{\text{thres}} = c_{\text{p}}/c_{\text{c}}$ leads to suboptimal decisions. An improvement can be reached by optimizing the heuristic threshold p_{thres}, as we demonstrate in the numerical investigations of Sections 7.3 and 7.4.

The simple heuristic PdM policy requires the predicted probability of RUL exceedance within the next decision time step, $\Pr(RUL_{\text{pred},k} \leq \Delta T)$, as sole input from the prognostics, in order to evaluate the DN versus PR decision at each time step. Different prognostic algorithms operate in distinct manners, and thus use different methods for deriving this probability. This can be specified as the probability of the $RUL_{\text{pred},k}$ belonging to a certain class (corresponding to $RUL_{\text{pred},k} \leq \Delta T$) in the case of a prognostic classifier [46]. For the case of prognostic regression models, uncertainty quantification in the RUL predictions is a prerequisite for obtaining this probability.

[1] In extreme cases, where c_{c} is very close to c_{p}, and where ΔT is small enough, the optimal action may be to allow the component to fail at $T^{(i)}_{\text{F}}$ with a cost $C^{(i)}_{\text{m,perfect}} = c_{\text{c}}$.

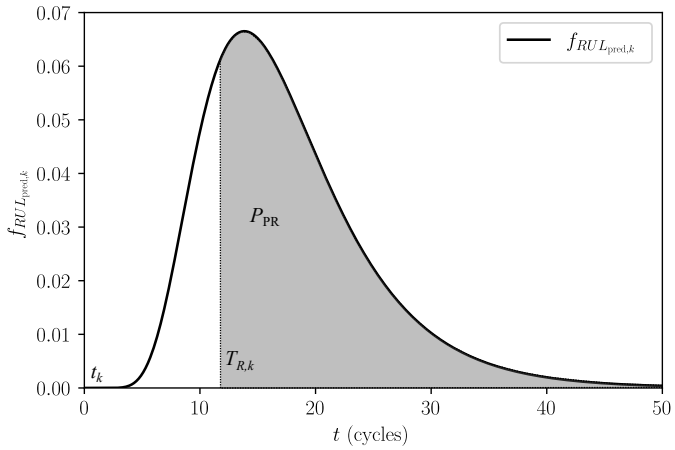

Figure 7.2: Optimization of $T_{\text{R},k}$. P_{PR} corresponds to the probability of a preventive replacement for a fixed $T_{\text{R},k}$, which appear in the objective function of Eq. (7.12)

Eventually, this heuristic PdM policy informs the replacement decision for each i-th component, leading to $C_{\text{rep}}^{(i)}$ and $T_{\text{lc}}^{(i)}$. The long-run expected maintenance cost per unit time associated with this heuristic PdM policy can then be evaluated via Eq. (7.2).

7.2.3.3 PdM policy 2: PdM policy for preventive replacement on the basis of the full RUL distribution.

We consider a second PdM policy for preventive replacement, which determines at each time step t_k the action $a_{\text{rep},k}$ to take as:

$$a_{\text{rep},k} = \begin{cases} \text{PR}, & \text{if } t_k + \Delta T \geq T_{\text{R},k}^* \\ \text{DN} & \text{else,} \end{cases} \tag{7.11}$$

where $T_{\text{R},k}^*$ is the optimal time to replacement found through solving an optimization problem at each time step t_k. A preventive replacement is thus decided when $T_{\text{R},k}^*$ is smaller or equal to $t_k + \Delta T$, where ΔT defines the time interval until the next decision.

The most commonly employed objective function for finding the optimal $T_{\text{R},k}^*$ in RUL-based PdM [13, 65, 66] is presented in this section. It can be employed when the full distribution of the RUL prediction at each time step t_k is available, denoted by $f_{RUL_{\text{pred},k}}(t)$. The distribution of the predicted time to failure (T_F) at time step t_k is $f_{T_{F\text{pred},k}}(t) = f_{RUL_{\text{pred},k}}(t - t_k)$, and is bounded below at t_k. The objective function for the optimization problem at each time step t_k is:

$$f(T_{\text{R},k}) = \frac{\text{E}[C_{\text{rep}}(T_{\text{R},k})]}{\text{E}[T_{\text{lc}}(T_{\text{R},k})]} = \frac{P_{\text{PR}} \cdot c_{\text{p}} + (1 - P_{\text{PR}}) \cdot c_{\text{c}}}{P_{\text{PR}} \cdot (T_{\text{R},k}) + \int_{t}^{T_{\text{R},k}} t \, f_{RUL_{\text{pred},k}}(t - t_k) \, \text{d}t}, \tag{7.12}$$

where:

$$P_{\text{PR}} = \int_{T_{\text{R},k}}^{\infty} f_{RUL_{\text{pred},k}}(t - t_k) \, \text{d}t \tag{7.13}$$

denotes the probability that the component will be preventively replaced at $T_{\mathrm{R},k}$, whereas $(1-P_{\mathrm{PR}})$ is the probability that the component will fail before $T_{\mathrm{R},k}$ with an induced cost c_{c}. These probabilities are graphically represented for a fixed $T_{\mathrm{R},k}$ in Fig. 7.2.

The objective function in Eq. (7.12) makes use of renewal theory and evaluates the long-run expected maintenance cost per unit time, in order to determine the optimal time for preventive replacement for a single component. The underlying assumption when using this objective function for optimizing replacement for a single component is that the predicted distribution of the time to failure of the component, $f_{T_{F\mathrm{pred},k}}(t)$, corresponds to the underlying distribution of the time to failure of the whole population of components. This (incorrect) assumption has not been clarified in the literature that uses this policy.

Eventually, this PdM policy optimizes the replacement decisions for each i-th component leading to $C_{\mathrm{rep}}^{(i)}$ and $T_{\mathrm{lc}}^{(i)}$. The long-run expected maintenance cost per unit time of this PdM policy can then be quantified via Eq. (7.2).

7.2.3.4 PdM policy 3: modified PdM policy for preventive replacement on the basis of the full RUL distribution

In this section we propose a modification of the objective function defined in Eq. (7.12) to overcome the implicit assumption pointed out above, i.e., we no longer assume that all future components have the same lifetime distribution as the one implied by the RUL prediction of the current component. Instead, we approximate the long-run expected maintenance cost per unit time of all future components, $\frac{\mathrm{E}_{\bar{T}_{\mathrm{F}}}[C_{\mathrm{rep}}]}{\mathrm{E}_{\bar{T}_{\mathrm{F}}}[T_{\mathrm{lc}}]}$, and utilize it to formulate the objective function for the time to replace the current component. This objective function is the sum of the cost associated with maintenance of the current component and the "opportunity" loss associated with replacing the component too early[2]. This opportunity loss is equal to the expected value of the lifetime of the current component beyond the time of replacement $T_{\mathrm{R},k}$ multiplied with $\frac{\mathrm{E}_{\bar{T}_{\mathrm{F}}}[C_{\mathrm{rep}}]}{\mathrm{E}_{\bar{T}_{\mathrm{F}}}[T_{\mathrm{lc}}]}$. The resulting objective function for finding the optimal $T_{\mathrm{R},k}^{*}$ at each time step t_k is:

$$f(T_{\mathrm{R},k}) = P_{\mathrm{PR}} \cdot c_{\mathrm{p}} + (1-P_{\mathrm{PR}}) \cdot c_{\mathrm{c}} + \frac{\mathrm{E}_{\bar{T}_{\mathrm{F}}}[C_{\mathrm{rep}}]}{\mathrm{E}_{\bar{T}_{\mathrm{F}}}[T_{\mathrm{lc}}]} \int_{T_{\mathrm{R},k}}^{\infty} (t - T_{\mathrm{R},k}) \cdot f_{RUL_{\mathrm{pred},k}}(t - t_k)\,\mathrm{d}t, \tag{7.14}$$

where P_{PR} is defined in Eq. (7.13). The first two terms of Eq. (7.14) (which correspond to the numerator of the objective function in Eq. (7.12)) are the expected replacement cost of the component. The integral in the last term of Eq. (7.14) is the expected lifetime of the component beyond $T_{\mathrm{R},k}$.

To approximate the long-run expected maintenance cost per unit time of all future components, $\frac{\mathrm{E}_{\bar{T}_{\mathrm{F}}}[C_{\mathrm{rep}}]}{\mathrm{E}_{\bar{T}_{\mathrm{F}}}[T_{\mathrm{lc}}]}$, we make use of the estimated distribution $f_{\bar{T}_{\mathrm{F}}}$ of the time to failure of the population of components. We consider the following assumptions to approximate $\frac{\mathrm{E}_{\bar{T}_{\mathrm{F}}}[C_{\mathrm{rep}}]}{\mathrm{E}_{\bar{T}_{\mathrm{F}}}[T_{\mathrm{lc}}]}$:

[2]Please note that the objective functions in Eqs. (7.12) and (7.14) have different units, as Eq. (7.12) quantifies a cost per unit time, while Eq. (7.14) quantifies a cost.

1. For an assumed case without monitoring, renewal theory can be used to find the optimal time for preventive replacement with respect to $f_{\bar{T}_\mathrm{F}}$. Then $\frac{\mathrm{E}_{\bar{T}_\mathrm{F}}[C_\mathrm{rep}]}{\mathrm{E}_{\bar{T}_\mathrm{F}}[T_\mathrm{lc}]}$ can be set equal to the corresponding optimal value of the long-run expected maintenance cost per unit time. This choice delivers an upper bound to the value of this term, causing early preventive replacements to be penalized more, and consequently delivers a less conservative PdM policy.
2. For an assumed "perfect" monitoring case, replacement of every component will be a preventive one, and the expected life-cycle length of the population of components will be equal to the mean $\mu_{\bar{T}_F}$ of the distribution $f_{\bar{T}_\mathrm{F}}$. Therefore, one can set $\frac{\mathrm{E}_{\bar{T}_\mathrm{F}}[C_\mathrm{rep}]}{\mathrm{E}_{\bar{T}_\mathrm{F}}[T_\mathrm{lc}]} = \frac{c_\mathrm{p}}{\mu_{\bar{T}_\mathrm{F}}}$. This choice yields a lower bound to the value of this term, leading to a more conservative PdM policy.
3. A value for $\frac{\mathrm{E}_{\bar{T}_\mathrm{F}}[C_\mathrm{rep}]}{\mathrm{E}_{\bar{T}_\mathrm{F}}[T_\mathrm{lc}]}$ between the upper bound of option 1 and the lower bound of option 2 can be chosen, e.g., the average of these bounds.

7.2.4 Predictive maintenance (PdM) planning for component ordering and replacement

In the first decision setting of Section 7.2.3, it is assumed that the new component will always be available for replacement. In this section, we consider a second decision setting, which includes ordering and replacement decisions. A deterministic lead time L is assumed from the time of component ordering T_order to the time of component delivery. We implicitly assume that L is a multiple of ΔT.

7.2.4.1 Metric for prognostic performance evaluation with respect to PdM planning for ordering & replacement

Following a certain PdM policy for component ordering and replacement (one specific policy is introduced in Section 7.2.4.2), different costs will be induced. The cost of the replacement action for the i-th component is given by Eq. (7.8).

The cost related to a late ordering of a component for replacement (preventive or corrective) is:

$$C^{(i)}_\mathrm{delay} = \max\big(T^{(i)}_\mathrm{order} + L - T^{(i)}_\mathrm{lc}, 0\big) \cdot c_\mathrm{unav}, \tag{7.15}$$

where c_unav is the system unavailability cost per unit time, related to necessary operation shutdown from $T^{(i)}_\mathrm{lc}$ until the time of component arrival, upon which a replacement can be performed.

The cost related to an early ordering of a component, i.e., the holding inventory cost, is:

$$C^{(i)}_\mathrm{stock} = \max\big(T^{(i)}_\mathrm{lc} - (T^{(i)}_\mathrm{order} + L), 0\big) \cdot c_\mathrm{inv}, \tag{7.16}$$

where c_inv is the holding inventory cost per unit time for a component.

The total maintenance cost, excluding the cost of the new component, is:

$$C^{(i)}_\mathrm{m} = C^{(i)}_\mathrm{rep} + C^{(i)}_\mathrm{delay} + C^{(i)}_\mathrm{stock} \tag{7.17}$$

The long-run expected maintenance cost per unit time that is achieved with a PdM policy is evaluated by applying the PdM policy on n independent components via Eq. (7.2).

In this second decision setting, the perfect PdM policy would replace the i-th component at $T^{(i)}_{\text{R,perfect}}$, which is the time step $k \cdot \Delta T$ directly before $T^{(i)}_{\text{F}}$, and order a component at $T^{(i)}_{\text{order,perfect}} = T^{(i)}_{\text{R,perfect}} - L$. Therefore, the costs induced when applying the perfect PdM policy to the i-th component are $C^{(i)}_{\text{stock,perfect}} = 0$, $C^{(i)}_{\text{delay,perfect}} = 0$, and $C^{(i)}_{\text{rep,perfect}} = c_{\text{p}}$, resulting in $C^{(i)}_{\text{m,perfect}} = c_{\text{p}}$.

Eventually, the decision-oriented metric for component ordering and replacement is estimated as:

$$\hat{M} = \frac{\frac{\frac{1}{n}\sum_{i=1}^{n}(C^{(i)}_{\text{rep}} + C^{(i)}_{\text{delay}} + C^{(i)}_{\text{stock}})}{\frac{1}{n}\sum_{i=1}^{n} T^{(i)}_{\text{lc}}} - \frac{c_{\text{p}}}{\frac{1}{n}\sum_{i=1}^{n} T^{(i)}_{\text{R,perfect}}}}{\frac{c_{\text{p}}}{\frac{1}{n}\sum_{i=1}^{n} T^{(i)}_{\text{R,perfect}}}}. \tag{7.18}$$

7.2.4.2 Simple heuristic PdM policy for component ordering and preventive replacement

At each time step t_k (as long as no replacement component has been ordered previously), the policy first determines based on the prognostics input whether a replacement component should be ordered (O), or not (NO). The considered simple policy determines the action to take as:

$$a_{\text{order},k} = \begin{cases} \text{O}, & \text{if } \Pr(RUL_{\text{pred},k} \leq w + \Delta T) \geq p^{\text{order}}_{\text{thres}} \\ \text{NO} & \text{else,} \end{cases} \tag{7.19}$$

where $w = \left\lceil \frac{L}{\Delta T} \right\rceil \cdot \Delta T$ is the ordering lead time adjusted for the discrete time steps. $p^{\text{order}}_{\text{thres}}$ is a variable heuristic threshold.

The reasoning behind the condition of Eq. (7.19) is the following: a lead time L is required for the component to become available upon ordering it. Therefore, if a component is ordered at time step t_k, the earliest future decision time at which the component will be available for replacement is $t_k + w$. The simple policy assumes that the critical threshold for the O-NO decision is based on the predicted probability that a preventive replacement will be necessary at time $t_k + (w + \Delta T)$. Once a component has been ordered, the O-NO decision is no longer relevant until a replacement action is performed.

At each time step t_k, the policy further determines whether the component is preventively replaced (PR) or nothing is done (DN). This applies independent of whether or not a new component is in stock, which, as discussed in Section 7.4.3, is not an optimal choice. Similar to Section 7.2.3.2, the policy determines the action to take $a_{\text{rep},k}$ as:

$$a_{\text{rep},k} = \begin{cases} \text{DN}, & \text{if } \Pr(RUL_{\text{pred},k} \leq \Delta T) < p^{\text{rep}}_{\text{thres}} \\ \text{PR} & \text{else.} \end{cases} \tag{7.20}$$

A value of $p_{\text{thres}}^{\text{rep}} = p_{\text{thres}}^{\text{order}} = c_{\text{p}}/c_{\text{c}}$ has been used in literature [46]. The values of the two heuristic thresholds may be optimized, leading to an improvement of this heuristic policy, as we demonstrate in Section 7.4.3.

The advantage of this heuristic PdM policy lies in its simplicity and universal applicability – it can be applied as long as the RUL prediction provides the probabilities in Eqs. (7.19) and (7.20). Other, more complex and possibly more optimal heuristic policies, or even algorithms such as partially observable Markov decision processes (POMDP) [49, 2], can be investigated, but we leave this for future work.

7.3 Numerical investigations on a virtual RUL simulator

This section investigates the proposed metric and the PdM policies presented in Section 7.2.3 in a hypothetical setup. For this purpose, a virtual RUL simulator serves as a test-bed, which enables the assessment and evaluation of PdM policies for varying data availability. The aim of this section is to investigate and quantitatively assess the performance and optimality of the three PdM policies for replacement and their effect on metric M, and eventually propose a set of directives towards optimizing decision heuristics.

7.3.1 Virtual RUL simulator

In this section we introduce a virtual RUL simulator, i.e., we establish a model with which to generate $RUL_{\text{pred},k}$ distributions over time, conditional on given underlying "true" realizations of the failure time of a component, emulating uncertain RUL predictions provided by a prognostic algorithm in a realistic setting.

We assume that the uncertain time to failure (expressed in cycles to failure) of a hypothetical population of mechanical components follows a normal distribution, specifically $T_{\text{F}} \sim N(\mu = 225, \sigma = 40)$, where N denotes the Gaussian probability density function (PDF) with mean μ and standard deviation σ. We draw samples from this distribution, each representing one underlying "true" realization of a component's failure time.

We define a PdM planning problem, wherein it is assumed that the maintenance actions can only be performed at discrete points in time t_k, defined by $t_k = k \cdot \Delta T$, for fixed $\Delta T = 10$ cycles and $k = 1, \ldots, N$. The predicted time to failure, yielded as an output of a prognostic algorithm at time step k, is denoted by $T_{\text{F,pred},k}$. Eq. (7.21) defines in logarithmic scale the modeled discrepancy between the prognostic RUL prediction at time step k, $RUL_{\text{pred},k} = T_{\text{F,pred},k} - t_k$, and the underlying "true" RUL value at time step k, $RUL_k = T_{\text{F}} - t_k$:

$$\ln\left(RUL_{\text{pred},k}\right) = \ln(RUL_k) + \ln(\epsilon_k), \tag{7.21}$$

where ϵ_k is the prognostic prediction error. We assume the following probabilistic model for the random vector containing the logarithm of the prediction errors over time

$$[\ln(\epsilon_1), \ldots, \ln(\epsilon_n)] \sim \text{MVN}\left(\mathbf{0}, \mathbf{\Sigma}\right), \tag{7.22}$$

where MVN() denotes the multivariate normal distribution with mean vector $\mathbf{0}$ and covariance matrix $\mathbf{\Sigma}$, which is constructed as

$$\mathbf{\Sigma} = \mathbf{D} \cdot \mathbf{R} \cdot \mathbf{D}, \tag{7.23}$$

where $\mathbf{D}$ is a diagonal matrix containing the standard deviation of the prediction errors $\sigma_{\ln(\epsilon_k)}$ in the diagonal, and $\mathbf{R}$ is a correlation coefficient matrix. The prediction errors over time are assumed to be correlated according to an exponential correlation model with correlation length l:

$$\mathbf{R} = [\rho_{ij}], \quad \text{where} \quad \rho_{ij} = \exp\left(-\frac{|t_i - t_j|}{l}\right) \tag{7.24}$$

With this model, the distributions $f_{RUL_{\text{pred},k}}$ are obtained as follows:

- Sample the mean values $\mu_{\ln\left(RUL_{\text{pred},k}\right)}$ of the different $\ln\left(RUL_{\text{pred},k}\right)$ predictions via Eq. (7.25) by drawing a sample $[\ln(\epsilon_1^{(i)}), \ldots, \ln(\epsilon_n^{(i)})]$ from the MVN distribution of Eq. (7.22).

$$\mu^{(i)}_{\ln(RUL_{\text{pred},k})} = \ln(RUL_k^{(i)}) + \ln(\epsilon_k^{(i)}) \tag{7.25}$$

- $\ln\left(RUL_{\text{pred},k}\right)$ then follows the normal distribution with mean equal to the value sampled in Eq. (7.25) and standard deviation $\sigma_{\ln(\epsilon_k)}$, i.e., $\ln\left(RUL_{\text{pred},k}\right) \sim N\left(\mu = \mu^{(i)}_{\ln\left(RUL_{\text{pred},k}\right)}, \sigma = \sigma_{\ln(\epsilon_k)}\right)$.

For an underlying "true" realization $T_{\text{F}}^{(i)} = 247$, a sampled realization of means of the different $RUL_{\text{pred},k}$ distributions over time and the 95% credible intervals (CI), are plotted in Fig. 7.3. For generating these distributions, we have assumed $\sigma_{\ln(\epsilon_k)} = 0.4$ and correlation length $l = 50$ cycles in the definition of the prediction errors.

The useful feature of this virtual RUL simulator is that one can generate a large number of virtual run-to-failure experiments via a Monte Carlo simulation. Each sample consists of a $T_{\text{F}}^{(i)}$ sample and associated $RUL_{\text{pred},k}$ distributions, assumed to be obtained via fusion of monitoring data with a prognostic algorithm, simplistically simulating realistic PHM settings. Using these samples, the ratio in Eq. (7.2) is evaluated for a PdM policy and subsequently the metric M corresponding to a decision setting is estimated via Eq. (7.6). Introducing this virtual RUL simulator allows the generation of a large number of samples, with which we investigate the performance of the three PdM policies for replacement of Section 7.2.3 and the uncertainty in estimating the metric M via Eq. (7.9) in function of the number of available run-to-failure experiments.

7.3.2 First decision setting: PdM planning for replacement

To investigate the first decision setting, we generate $n = 2 \cdot 10^3$ samples of $T_{\text{F}} \sim N(\mu = 225, \sigma = 40)$ and corresponding $RUL_{\text{pred},k}$ distributions (generated for $\sigma_{\ln(\epsilon_k)} = 0.4$). These correspond to $n = 2 \cdot 10^3$ hypothetical components, for which run-to-failure monitoring data, as well as predicted $RUL_{\text{pred},k}$ distributions provided by means of a prognostic algorithm, are assumed available. We employ all three PdM policies presented in Section 7.2.3, and for each component we compute the $C_{\text{rep}}^{(i)}$ and $T_{\text{lc}}^{(i)}$ for each of the three policies, for different cost ratios $c_{\text{p}}/c_{\text{c}}$. Subsequently, for each policy we evaluate the long-run expected maintenance cost per unit time via Eq. (7.2), and estimate

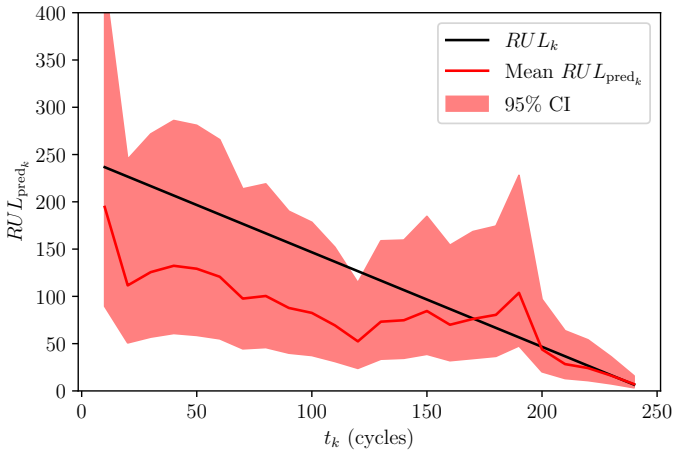

Figure 7.3: Demonstration of the virtual RUL simulator. Generated $RUL_{\text{pred},k}$ distributions conditional on an underlying true realization $T_{\text{F}}^{(i)} = 247$ cycles.

the metric M via Eq. (7.9). In Fig. 7.4a we plot the value of $\hat{M}$ and the associated uncertainty, represented with 95% CIs, in function of the cost ratio. The red line corresponds to the values of $\hat{M}$ when using the heuristic PdM policy 1 with $p_{\text{thres}} = c_{\text{p}}/c_{\text{c}}$. The blue line corresponds to use of the PdM policy 2, whereas the purple line corresponds to the PdM policy 3, where option 1 has been chosen for the value of $\frac{\text{E}_{\bar{T}_{\text{F}}}[C_{\text{rep}}]}{\text{E}_{\bar{T}_{\text{F}}}[T_{\text{lc}}]}$. Finally, the green line corresponds to the optimized heuristic PdM policy 1, wherein the heuristic threshold has been optimized. The optimal threshold p^*_{thres} is found as the argument that minimizes the metric M, when estimating it using Eq. (7.9), with $C_{\text{rep}}^{(i)}$ and $T_{\text{lc}}^{(i)}$ found by applying the heuristic PdM policy 1 on each of the $n = 2 \cdot 10^3$ components. The values that p^*_{thres} assumes for the different cost ratios are plotted in Fig. 7.4b. It is noted that for all cost ratios, the optimal value of p^*_{thres} is smaller than $c_{\text{p}}/c_{\text{c}}$.

Various conclusions can be drawn from the results of this numerical investigation. For most cost ratios, the PdM policies 2 and 3, which operate on the basis of the availability of the full RUL distribution, lead to better performance than the heuristic PdM policy 1 and to reduced uncertainty. For the relatively large level of prognostic uncertainty considered here ($\sigma_{\ln(\epsilon_k)} = 0.4$), the PdM policies 2 and 3 tend to be more conservative than the heuristic PdM policy, leading to earlier preventive replacements (for some components significantly earlier) in order to reduce the risk of corrective failure, but also reducing the life-cycle of the components, especially for low values of $c_{\text{p}}/c_{\text{c}}$. The heuristic PdM policy 1 instead informs later preventive replacements, which is favorable for many components, but at the same time leads to corrective replacements for some components, even for cases when c_{c} is significantly large. The latter is the reason for its seemingly worse performance and its associated increased uncertainty in the evaluation of the metric M. Naturally, as the ratio $c_{\text{p}}/c_{\text{c}}$ increases, corrective replacements become less critical, and all three policies do lead to some corrective replacements. It is noted that even with a relatively large number of samples, the evaluation of all considered PdM policies with Eq. (7.2), and the estimation of M with Eq. (7.6), seem to entail non-negligible uncertainty.

The PdM policy 3 that we propose in Section 7.2.3.4 proves somewhat less conservative, and thus delivers better results than the PdM policy 2, which is the one most widely used in literature.

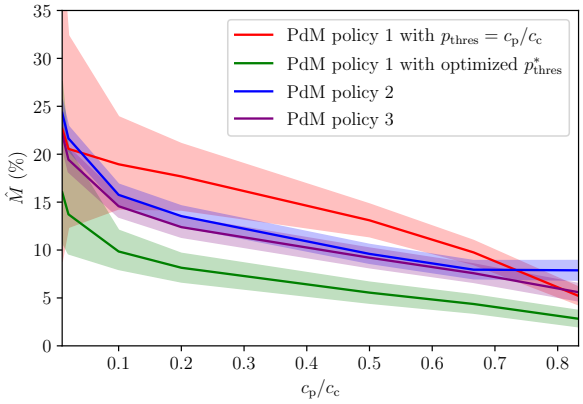

(a) Estimation of the metric M via Eq. (7.6), and the associated uncertainty (95% CIs), in combination with the PdM policies of Section 7.2.3, for different c_p/c_c ratios.

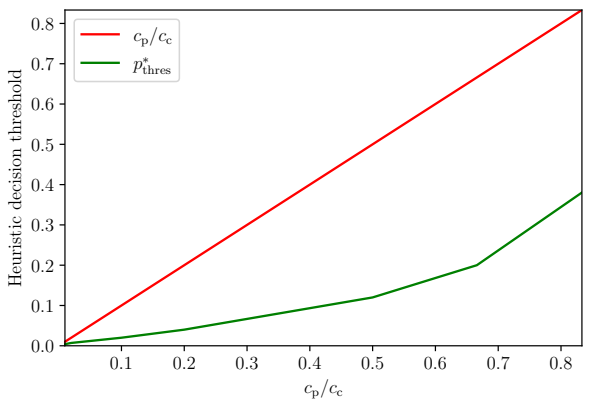

(b) The probability threshold that is used as a heuristic decision threshold in the PdM policy 1. The green line plots the optimal threshold value found for different c_p/c_c ratios.

Figure 7.4: Results from virtual RUL simulator with $n = 2{\cdot}10^3$ sampled components for $\sigma_{\ln(\epsilon_k)} = 0.4$.

Optimizing the heuristic PdM policy leads to a policy that delivers the best performance among all policies for all cost ratios. The PdM policy 1, and its optimized version, are characterized by simplicity, fast evaluation, and universal applicability - as long as the prognostics provide the $\Pr(RUL_{\text{pred},k} \leq \Delta T)$. Thus, when enough training data are available to optimize the heuristic threshold, this simple PdM policy can outperform other more involved policies. However, in reality, one is typically bounded by the availability of only a limited number of training data, which involves a rather large uncertainty in the estimation of the long-run expected maintenance cost per unit time and the metric M. This consequently complicates the task of finding a p^*_{thres} value that will be optimal also for future components.

The uncertainty in the RUL prognostics is propagated to the subsequent PdM planning task. It is expected that reduced uncertainty in the RUL predictions given by a prognostic algorithm leads to enhanced PdM policy performance, and thus to lower values for M. This can easily be shown in the context of the virtual RUL simulator. Assuming a smaller value of $\sigma_{\ln(\epsilon_k)}$ corresponds to less uncertain prognostics. Fig. 7.5a plots the uncertainty in $\hat{M}$ that we find with each of the employed PdM policies for the same $n = 2 \cdot 10^3$ sampled components as in Fig. 7.4, but for RUL predictions generated with $\sigma_{\ln(\epsilon_k)} = 0.15$. It is clear that the values of $\hat{M}$ are significantly reduced compared to the ones reported in Fig. 7.4. With less uncertain prognostics, the heuristic PdM policy 1 leads to fewer corrective replacements. At the same time, both PdM policies 2, 3 become less conservative. However, they can lead to corrective replacements even for cases with large c_c values, as does the heuristic PdM policy 1. This explains the increased uncertainty in quantifying the metric M with these two policies, when compared to Fig. 7.4. For small prognostic uncertainty, all three PdM policies lead to comparable results. The optimized heuristic PdM policy 1 again leads to superior performance, further showcasing the benefit of optimizing decision thresholds within simple heuristic PdM policies. Fig. 7.5b plots the optimal heuristic threshold p^*_{thres}.

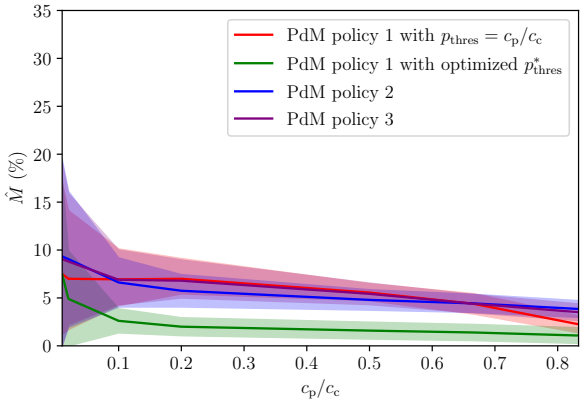

(a) Estimation of the metric M via Eq. (7.6), and the associated uncertainty (95% CIs), in combination with the PdM policies of Section 7.2.3, for different c_p/c_c ratios.

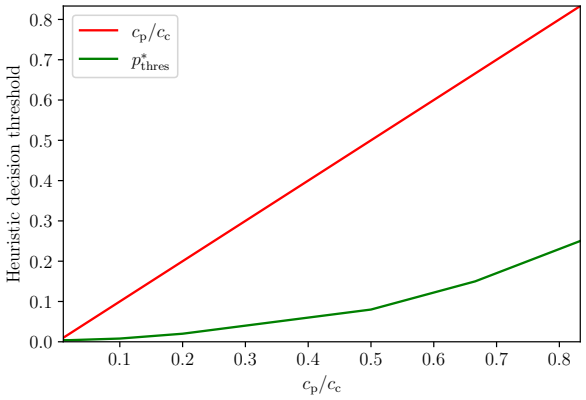

(b) The probability threshold that is used as a heuristic decision threshold in the PdM policy 1. The green line plots the optimal threshold value found for different c_p/c_c ratios.

Figure 7.5: Results from virtual RUL simulator with $n = 2 \cdot 10^3$ sampled components for $\sigma_{\ln(\epsilon_k)} = 0.15$.

7.4 Case study: predictive maintenance of degrading turbofan engines

Performance degradation histories of a turbofan engine due to wear and tear were numerically generated using the simulator C-MAPSS [16]. The engine is simulated under different flight conditions and the effect of performance degradation is introduced in one of the engine modules in the form of an exponential degradation model. The data consists of 14 input variables, which specify the configuration parameters of the simulation, 21 output variables, which provide a measurement snapshot of the response of the system during or after each flight, and 3 variables that describe the operation modes of the engine. The simulations are performed for a number of engine units and they are randomized in the sense that different initial conditions, degradation and noise parameters are selected for each scenario. The dataset contains four data subsets which have been generated with different simulation settings.

At the start of each unit simulation, the engine is normally operating and a fault is introduced in a certain time instance, with the parameters controlling the direction of the failure evolution trajectory randomly selected. The reader is referred to the paper describing the benchmark problem for further details [59]. The simulations and the corresponding datasets are split into two parts: i) a training set that contains simulation data, wherein the fault grows in magnitude up to system failure, and ii) a test set that contains simulation data up to a point before system failure. It should be noted that this benchmark dataset has been developed for prediction purposes, with the aim of challenging the development of RUL predictors that are to be evaluated on the test set. However, this study is concerned with the decisions towards optimal PdM planning and as such, the results reported in this section are derived using the FD001 training set, which contains simulation data up to system failure and therefore offers the possibility of exploring the entire decision space. The original training set is split into a training and a test subset, with the former used for the training of prognostic models, as described in the following section, and the latter used for the evaluation of

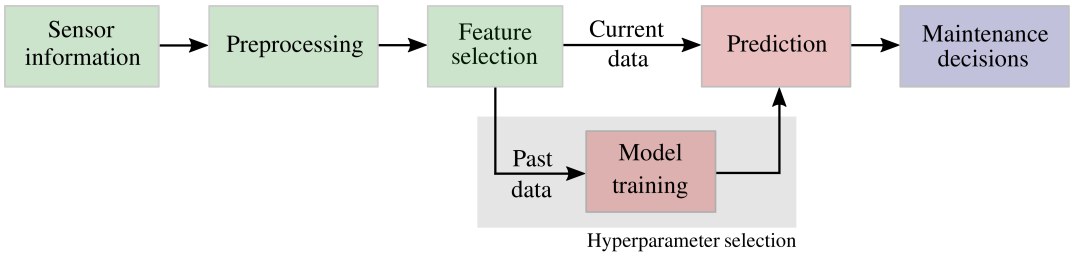

Figure 7.6: Flowchart of the adopted data-driven predictive maintenance decision process

these models with the PdM policies.

For the purpose of the investigations in this paper, the task of PdM planning for each engine unit is simplistically considered as a problem for planning order and replacement actions for a single component. Turbofan engines are complex machinery systems, whose maintenance is in practice planned by taking multiple system-level considerations and logistic constraints into account (e.g., shop loading, parts lead time, consolidated repair planning, etc.). These are not reflected in the simple PdM decision settings considered in this section, but may form part of future investigations.

7.4.1 Prognostic models

Data-driven prognostic models can be considered as mapping functions from a set of input parameters $\mathbf{x} \in \mathbb{R}^{n_\mathrm{x}}$, which represent the available system response information, to a set of output quantities of interest (QoI) $\mathbf{y} \in \mathbb{R}^{n_\mathrm{y}}$ [3], so that $\mathcal{F} : \mathbf{x} \rightarrow \mathbf{y}$. This mapping can be expressed by the following mathematical model

$$\mathbf{y} = \mathcal{F}_{\mathbf{H}}\left(\mathbf{x}, \mathbf{p}\right), \tag{7.26}$$

where $\mathbf{p}$ denotes a set of model-specific parameters, which can be estimated from the training data[4] and are used to configure the structure of the underlying model, and $\mathbf{H}$ is the vector of model hyperparameters that are external to the model, and whose values control the training process. The PdM policies presented in Section 7.2 in this paper rely on the availability of a probabilistic output $\mathbf{y}$ from prognostics.

The selection of hyperparameters $\mathbf{H}$ for each type of model is typically carried out through an optimization step that minimizes the prediction error evaluated on a set of test or validation data points that are not seen during training. In this work, we instead propose a decision-oriented optimization of hyperparameters:

$$\mathbf{H}^* = \arg\min_{\mathbf{H}} M\left(\mathbf{Y}_k\right), \tag{7.27}$$

which aims at extracting the optimal hyperparameter configuration that minimizes the proposed metric M, which is defined in Eq. (7.5), and depends on the model output sequence $\mathbf{Y}_k = [y_1 \;\; y_2 \;\; \ldots y_k]$ as well as the corresponding decision setting and adopted PdM policy.

[3] The output QoI $\mathbf{y}$ is typically either some health indicator, which is used for inference of the RUL, or the RUL itself.

[4] In this work, we choose the mean squared error as the loss function for training regression models, and the log loss function for classification models [43].

For the current case study, four different data-driven models are implemented for delivering RUL predictions. Firstly, a Long Short-Term Memory (LSTM) network classifier is constructed in the Keras Python library with the adopted architecture identical to the one proposed in [46]. The network outputs the class label of the estimated RUL with an associated probability. The second model is a Gaussian naive Bayesian (GNB) classifier, whereby the RUL prediction is again treated as a classification problem [17]. In this case, a parent node is used to model the RUL, which can have a healthy or close-to-failure label that is determined on the basis of the conditional probabilities of each sensor signal. The third adopted model is a Decision Trees (DTs) classifier [6], which is estimated using a maximum depth of four so as to prevent overfitting. Finally, the fourth model implements Bayesian filtering of an exponential degradation (EXP) model for performing regression tasks. The EXP regression model relies on the fitting of an exponential model to the first principal component of the sensor data [33]. The EXP model parameters are initially extracted by fitting the model to each of the training run-to-failure data sequences, and the sample-based statistical properties of the parameters are used as priors in the prediction phase. Thereafter, the model parameters are sequentially updated upon availability of new sensor measurements, using a Bayesian filtering algorithm [56], which delivers the particle-based RUL distribution at each step.

It should be mentioned that the scope of this case study is not the comparison of predictive capabilities of the specific modeling approaches, but the investigation of the metric M and the associated decision policies as a means to compare/evaluate different prognostic algorithms. For the sake of brevity, the reader is referred to the corresponding sources [46, 67, 17, 6, 55] for further information on the mathematical background and the theoretical assumptions of each model.

The adopted steps for PdM planning using all four models are highlighted in Fig. 7.6. Concretely, the available data from all sensing channels are initially passed through a preprocessing layer, which essentially consists of i) a normalization step, so that all variables are scaled to a standardized range, ii) the labeling of RUL values for the case of classification models, and iii) a smoothing step, which is equivalent to filtering. Thereafter, the features of data to be used as inputs for each model are selected and the training phase is carried out using the training dataset. The remaining data are then used to evaluate the algorithms through the proposed metric M. As such, the data-driven prognostic models are trained using an 80% partition of the FD001 dataset, which contains run-to-failure monitoring data from 100 units, i.e., from 100 different degrading engine modules. For the purpose of our investigations, as explained above, this training set is split into data from 80 units that we use for the training, and data from the remaining 20 units that we employ for the evaluation of the different PdM policies and the metric M.

7.4.2 First decision setting: PdM planning for replacement

For the first decision setting, it is assumed that preventive replacement actions can only be performed at discrete points in time $t_k = k \cdot \Delta T$, for $\Delta T = 10$ flight cycles. The heuristic PdM policy 1 requires the probability $\Pr(RUL_{\text{pred},k} \leq \Delta T)$ as input from the prognostics (see Eq. (7.10)). During the training process of the LSTM, GNB and DT prognostic classifiers, the output RUL data are labeled into two distinct classes, one corresponding to $RUL > \Delta T$ and the other to $RUL \leq \Delta T$. In this way, the trained classifiers directly output $\Pr(RUL_{\text{pred},k} \leq \Delta T)$ as the associated class probability. With the EXP model, at each time step t_k, the $RUL_{\text{pred},k}$ is directly given as output in the form of a vector $\mathbf{y}$ of n_{p} weighted samples with a corresponding vector of weights $\mathbf{w}$, obtained via particle

filtering [61, 27]. The required probability is then queried as

$$\Pr(RUL_{\text{pred},k} \leq \Delta T) = \sum_{i=1}^{n_{\text{p}}} \mathcal{L}_{0/1}\left(y^{(i)} \leq \Delta T\right) \cdot w^{(i)}, \tag{7.28}$$

where $\mathcal{L}_{0/1}$ denotes the 0-1 loss function [43].

On the other hand, the PdM policies 2 and 3 require prognostic input in the form of the full PDF $f_{RUL_{\text{pred},k}}(t)$. To this end, for all considered prognostic models, some additional post-processing is required. In the case of the EXP model, one simply has to fit the parameters of an appropriately chosen distribution type to the weighted samples $\mathbf{y}$. In the case of the LSTM, GNB, DT prognostic classifiers, given the training routine that we describe in the previous paragraph, the sole prognostic output is the $\Pr(RUL_{\text{pred},k} \leq \Delta T)$, i.e., a single evaluation of the cumulative distribution function (CDF) of $RUL_{\text{pred},k}$. Fitting the CDF of a chosen distribution type to a single available CDF value is challenging. To tackle this problem, for each classifier type, we choose to simultaneously train two classifiers. Let us, for illustration purposes, consider the LSTM model. We train one LSTM model which outputs the $\Pr(RUL_{\text{pred},k} \leq \Delta T)$, and a second LSTM model which outputs another probability, e.g., the $\Pr(RUL_{\text{pred},k} \leq 2 \cdot \Delta T)$. In such a manner, two values of the CDF are obtained, which enables fitting a chosen distribution type with two parameters. In all models, the lognormal distribution is chosen to model $f_{RUL_{\text{pred},k}}(t)$.

Fig. 7.7 plots the results for the metric M computed via the four employed prognostic models for different assumed $c_{\text{p}}/c_{\text{c}}$ cost ratios. Specifically, Fig. 7.7a plots the results obtained with each model when employing the heuristic PdM policy 1, whereas Fig. 7.7b corresponds to the results obtained when employing the here proposed PdM policy 3, which we found to perform better on this dataset compared to the PdM policy 2, which also operates on the basis of the full RUL distribution as input. We thus choose not to include the results obtained with PdM policy 2 in the plot. An initial observation is that, for this specific case study, and for the specific prognostic models, the PdM policy 1 leads to better decisions than the PdM policy 3 for all prognostic models, with the exception of the DT classifier, for which the results are comparable. This result might appear inconsistent with the results obtained in the theoretical investigations of Section 7.3.

Due to the large uncertainty involved in estimation of M with limited data, a general statement should be made with care. In the current case study, we are limited to 80 available units for training and 20 units for evaluation, which implies presence of significant variability in the results. In particular, evaluation of M on 20 units via Eq. (7.6) is subject to significant statistical uncertainty. Even though the results in Fig. 7.7b appear rather worse than the results in Fig. 7.7a, this difference occurs even if the decisions triggered by the two distinct policies are in effect not so different. As an example, let us consider the LSTM model, and the cost ratio $c_{\text{p}}/c_{\text{c}} = 0.1$. With PdM policy 1 we find $\hat{M} = 1.62\%$. This corresponds to preventive replacements informed at $\mathbf{T}_{\text{R}}$=[230, 200, 290, 260, 180, 260, 170, 200, 210, 150, 130, 330, 150, 250, 280, 330, 190, 150, 180, 190] cycles for the 20 evaluation units and no corrective replacement. Correspondingly, with PdM policy 3 we obtain $\hat{M} = 4.76\%$, which corresponds to preventive replacements informed at $\mathbf{T}_{\text{R}}$=[220, 200, 280, 250, 170, 250, 160, 200, 200, 140, 130, 330, 150, 240, 270, 320, 190, 150, 170, 180] cycles. Comparing the two vectors shows that the difference in $\hat{M}$ originates from the fact that PdM policy 3 informs preventive replacement one decision time step earlier than the PdM policy 1 for some components.

The results in Fig. 7.7a reveal that the LSTM prognostic classifier delivers the best performance among all four prognostic models with respect to PdM planning for replacement. The other three

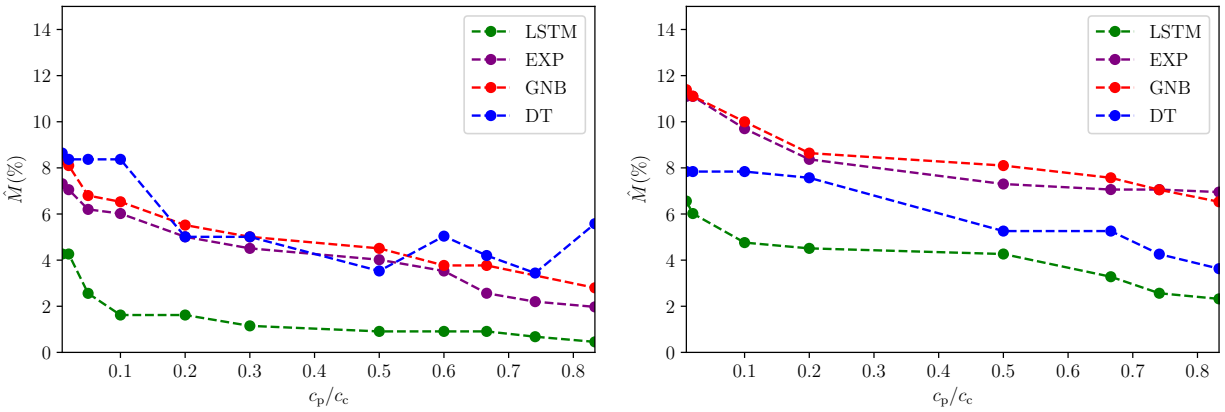

(a) Heuristic PdM policy 1

(b) PdM policy 3

Figure 7.7: Evaluation of the metric M in conjunction with a prognostic model and a PdM policy for planning replacement, as a function of different c_p/c_c cost ratios. The LSTM prognostic classifier gives the best performance with respect to M.

models seem to deliver comparable performance. A practitioner could interpret the difference in the results obtained via the different prognostic models in Fig. 7.7 as the percentage of cost savings that using algorithm x for PdM planning could provide compared to using algorithm y. This straightforward interpretation is a good feature for the use of the metric in practice. Naturally, the metric M entirely depends on the choices related to the decision problem, such as, e.g., the values assigned to the costs c_p, c_c.

Using M as a performance metric has various advantages. Typically, most widely used performance metrics, such as the ones in [58, 45], or standard metrics such as the MSE of predictions, rely upon a regression type of prognostic outcome. They can therefore not easily compare, e.g., the performance of prognostic regression models directly against prognostic classifiers. This is not the case when using metric M, with which any two models can be compared, as long as their prognostic output can be provided as input in the fixed PdM policy. Furthermore, ideally the performance of a prognostic algorithm should be appraised at later prediction stages, when the decisions for preventive replacements actually become relevant, which is what metric M does. Testing a prognostic algorithm with respect to how well it can predict the exact RUL value at an early point in time might provide impractical conclusions.

In Section 7.2.3.2 we discussed optimizing the heuristic threshold in PdM policy 1, and in Section 7.3.2 we showed that this can lead to a significant improvement in the PdM decision-making, quantified with respect to metric M. This process is also performed in the context of the current case study within the training phase. Specifically, we employ the heuristic decision rule of Eq. (7.10) and we search for the optimal value p^*_{thres} that leads to minimization of $\hat{M}$ when evaluating the PdM policy 1 on the 80 training set units. We then employ the heuristic decision rule of Eq. (7.10) with the optimal value p^*_{thres} for evaluating $\hat{M}$ on the remaining 20 test set units. The values that the metric $\hat{M}$ assumes for each prognostic model with the corresponding optimized heuristic PdM policy 1 are plotted in Fig. 7.8a, demonstrating the non-negligible improvement in the decision-making.

The optimal values of p^*_{thres} found for different c_p/c_c ratios are plotted in Fig. 7.8b. It may appear

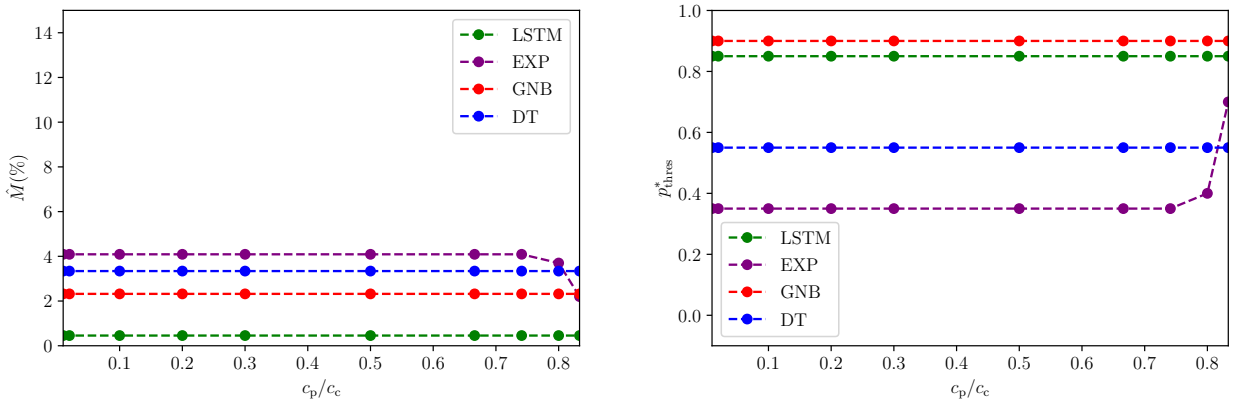

(a) Value for metric M when employing the PdM policy 1 with optimized p^*_{thres}.

(b) Optimal heuristic decision thresholds along varying c_p/c_c ratios.

Figure 7.8: Optimizing the heuristic decision threshold for the heuristic PdM policy 1 within the training process.

surprising that p^*_{thres} assumes a large and constant value along the whole c_p/c_c axis for most of the models. The reason is that the specific models considered here seem to deliver an overestimation of the classification or regression probabilities. p^*_{thres} assumes a large value in order to correct for this bias. Furthermore, the fact that the optimization of p_{thres} is performed on a limited number of units is the reason for which p^*_{thres} assumes constant values over the c_p/c_c axis for most models.

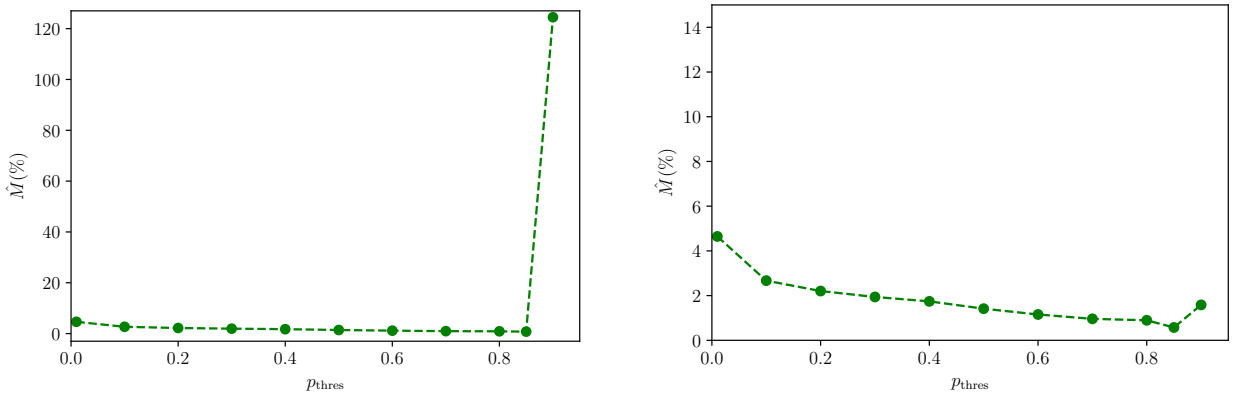

(a) LSTM model with $c_p/c_c = 0.01$. For large c_c values, the risk associated with optimizing p_{thres} is large.

(b) LSTM model with $c_p/c_c = 0.5$. For small c_c values, the risk associated with optimizing p_{thres} is small.

Figure 7.9: Risk associated with optimizing p_{thres} in the heuristic PdM policy 1.

It should be noted that despite the improvement in the decision-making performance upon optimizing p_{thres}, a risk always exists in terms of introducing an over-relaxation in the probability space, which can lead to corrective replacements. This might be acceptable for large c_p/c_c cost ratio values (e.g., see Fig. 7.9b), however, it can lead to significantly poor performance at small cost ratios, where a single corrective replacement is strongly weighted. An illustrative example of such a case is shown in Fig. 7.9a. For this studied case, the optimal threshold $p^*_{\text{thres}} = 0.85$ is found, which is the value that best accounts for the probability bias that is present in the employed LSTM model. This value

results in no triggering of corrective replacements when employing this PdM policy on the 80 training units, and is also the value for which early preventive replacements are minimized. However, a small increase in p_{thres} (changing its value to 0.9) leads to a very large increase in the value of M. This occurs as 2/80 components fail, inducing the very large c_{c} cost.

7.4.3 Second decision setting: PdM planning for component ordering and replacement

In this section, along with the considerations of Section 7.4.2, we further consider that a component is readily available for replacement only if it was ordered on time. A component should be ordered at a time informed by the heuristic PdM policy of Section 7.2.4.2. A deterministic lead time $L = 2 \cdot \Delta T = 20$ cycles is assumed, which is the time from component ordering to delivery. The heuristic PdM policy requires the probabilities $\Pr(RUL_{\text{pred},k} \leq w + \Delta T)$ (see Eq. (7.19)) and $\Pr(RUL_{\text{pred},k} \leq \Delta T)$ (see Eq. (7.20)) as input from the prognostics. To this end, during the training process, the output RUL data are labelled into three distinct classes, and the considered prognostic classifiers are trained as multiclass classifiers.

Fig. 7.10a plots the results for the metric M computed via the four employed prognostic models for varying c_{c} cost, fixed costs $c_{\text{p}} = 100$, $c_{\text{unav}} = 10$, $c_{\text{inv}} = 1$ and heuristic threshold values $p_{\text{thres}}^{\text{rep}} = p_{\text{thres}}^{\text{order}} = c_{\text{p}}/c_{\text{c}}$. The LSTM prognostic classifier delivers the best performance with respect to PdM planning for component ordering and replacement, with the other three models delivering comparable performance. For all four models, the metric M assumes significantly higher values than those of Fig. 7.7a, owing to the additional costs related to late ordering and holding inventory of a component. Naturally, the magnitude of M strongly depends on the chosen $c_{\text{p}}, c_{\text{c}}, c_{\text{unav}}, c_{\text{inv}}$ costs.

The heuristic decision rule of Eq. (7.20) determines the PR versus DN action without taking into account whether or not a new component is in stock. This proves to be a suboptimal choice, especially when the c_{unav} value is non-negligible. Let us take the LSTM model and the engine unit with ID=100 (with true failure time at 200 cycles) as an example, for $c_{\text{c}} = 1000$. The heuristic PdM policy informs component ordering at $T_{\text{order}}^{(i)} = 170$ cycles, and a preventive replacement already at the next decision time step, i.e., at $T_{\text{R}}^{(i)} = 180$ cycles with component unavailability, which based on Eq. (7.15) induces $C_{\text{delay}}^{(i)} = 100$. Hence, this simple heuristic PdM policy should be improved in the future.

For the LSTM model, we additionally perform an optimization of the two heuristic thresholds on the training data. We then employ the heuristic PdM policy with the optimal values $p_{\text{thres}}^{\text{order}^*} = 0.11$ and $p_{\text{thres}}^{\text{rep}^*} = 0.5$ for evaluating $\hat{M}$ on the test set units. The results plotted in Fig. 7.10b demonstrate that this threshold optimization leads to a significant improvement of the policy.

7.5 Concluding remarks

In this paper, we introduce a decision-oriented metric M for assessing and optimizing data-driven prognostic algorithms. The proposed metric assesses and optimizes algorithms by accounting for

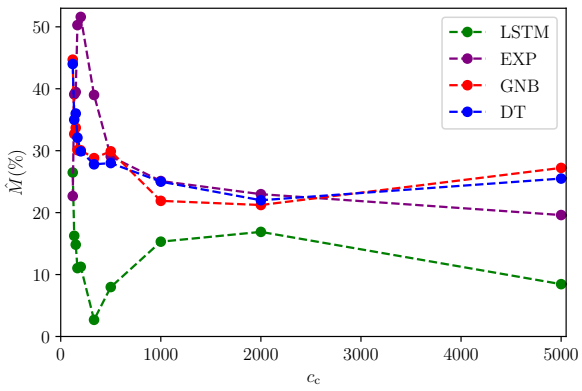

(a) Choice of threshold values $p_{\text{thres}}^{\text{rep}} = p_{\text{thres}}^{\text{order}} = c_p/c_c$ for the heuristic PdM policy. The LSTM prognostic classifier gives the best performance with respect to M.

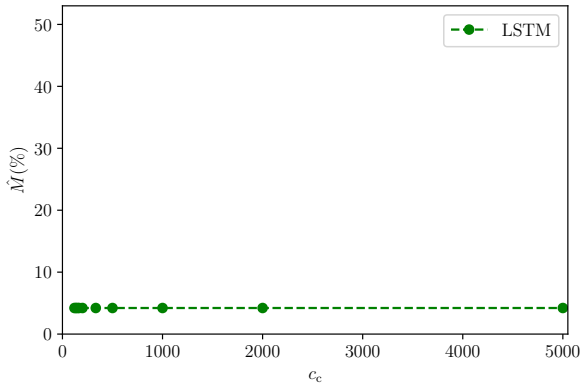

(b) Heuristic PdM policy with optimal $p_{\text{thres}}^{\text{rep}^*} = 0.5$ and $p_{\text{thres}}^{\text{order}^*} = 0.11$ for the LSTM prognostic classifier.

Figure 7.10: Evaluation of the metric M in conjunction with a prognostic model and the heuristic PdM policy of Section 7.2.4.2 for planning component ordering and replacement. $\hat{M}$ is plotted as a function of c_c values varying in the range $[120, 5000]$. The remaining costs are fixed: $c_p = 100$, $c_{\text{unav}} = 10$, $c_{\text{inv}} = 1$.

their effect on downstream predictive maintenance (PdM) decisions that are to be triggered by their predictions (outputs). Hence, it is defined in association with a specific decision context and a corresponding PdM policy, which informs the maintenance actions based on input uncertain Remaining Useful Life (RUL) predictions. Here, we specifically define and discuss the metric within two common PdM decision settings: i) component replacement planning and ii) component ordering-replacement planning. We numerically investigate the metric with the aid of: 1) a hypothetical virtual RUL simulator and 2) an application case study related to turbofan engine degradation, for which a run-to-failure dataset is readily available (the CMAPSS dataset). For the latter case study, four data-driven prognostic models for classification and regression are employed. We tune the hyperparameters of these algorithms and assess their performance on the basis of the decision-oriented metric M.

For component replacement planning, we discuss two PdM policies of varying complexity that are most commonly used in the PHM literature. The first policy is a simple heuristic policy, which informs replacement via imposing a heuristic threshold on the probability of RUL exceedance at the next decision time step. A significant improvement to this policy occurs when optimizing the value of the heuristic threshold. The optimal value is found as the argument that minimizes the metric M estimated on n run-to-failure experiments contained in the training dataset. The second policy operates on the basis of the availability of the full RUL distribution, and searches for the optimal future time to replacement. This is done with the aid of a renewal-theory-based objective function. This objective function, which is derived from an assumption adopted in state-of-the-art literature, incorrectly assumes that the predicted distribution of the time to failure of the component corresponds to the underlying distribution of the time to failure of the whole population of components. We here clarify this, and propose an alternative objective function based on an alternative assumption, which is shown to lead to an enhanced performance.

For component ordering-replacement planning, we restrict ourselves to one simple heuristic PdM policy, which informs ordering and replacement via heuristic thresholds on the probability of RUL exceedance in future decision time steps. We show that optimizing the value of the heuristic thresholds leads to a considerable improvement of this PdM policy.

For the CMAPSS case study, the Long Short-Term Memory (LSTM) network classifier is shown to deliver the best performance among the implemented prognostic models with respect to both PdM for replacement planning and PdM for component ordering-replacement planning.

The proposed decision-oriented performance assessment of prognostic algorithms through the metric M has multiple advantages over conventional metrics that appraise the quality of a prognostic algorithm. Notably, M can be used to compare the performance of any two algorithms, i.e., it does not require a regression-based prognostic outcome like most prediction-based metrics. Besides, M automatically appraises the efficacy of prognostic algorithms at later prediction stages, which are crucial for decision-making. Finally, the metric M can be interpreted as the percentage cost savings for maintenance associated with the use of each algorithm relative to the perfect policy.

The availability of monitoring datasets from run-to-failure experiments is essential to a data-driven evaluation of the proposed metric. This could potentially free the analyst altogether from the need of *a-priori* defining a stochastic model describing the deterioration process. Availability of only a limited amount of such data, however, poses a bottleneck for this evaluation, as it leads to an estimate with fairly large variability. For instance, in the CMAPSS case study, we see that 20 run-to-failure samples are not sufficient for obtaining a reliable estimate of the metric M. Furthermore, the metric depends on the initial choice of different cost values associated with a decision setting, e.g., the preventive/corrective replacement cost, the unavailability cost. In order to perform and optimize maintenance planning, one cannot escape quantifying these costs. While an exact estimate of these uncertain costs is often difficult to obtain in practice, a rough estimate can typically be made be experienced engineers. For the purpose of defining the metric, such rough estimates should be sufficient for practical applications (see Figs. 7.7 and 7.10), considering that alternative metrics do not consider and account for these costs at all.

A promising avenue of future research relates to training of prognostic algorithms to receive monitoring data as input and directly output a decision within a certain decision setting, whereby the PdM policy can be learnt during the training process, e.g., via deep reinforcement learning [1, 34]. Such advanced policies will typically need to be calibrated to the specifics of the cost model, deterioration processes and monitoring data, and would require the availability of a large amount of training data.

Acknowledgments

The work of A. Kamariotis and E. Chatzi has been carried out with the support of the Technical University of Munich - Institute for Advanced Study, Germany, funded by the German Excellence Initiative and the TÜV SÜD Foundation.

References

[1] C. P. Andriotis, K. G. Papakonstantinou, and E. N. Chatzi. "Deep reinforcement learning driven inspection and maintenance planning under incomplete information and constraints". In: *Reliability Engineering & System Safety* 212 (2021), p. 107551.

[2] G. Arcieri, C. Hoelzl, O. Schwery, D. Straub, K. G. Papakonstantinou, and E. Chatzi. "Bridging POMDPs and Bayesian decision making for robust maintenance planning under model uncertainty: An application to railway systems". In: *Reliability Engineering & System Safety* 239 (2023), p. 109496.

[3] M. Arias Chao, C. Kulkarni, K. Goebel, and O. Fink. "Fusing physics-based and deep learning models for prognostics". In: *Reliability Engineering & System Safety* 217 (2022), p. 107961.

[4] V. Atamuradov, K. Medjaher, P. Dersin, B. Lamoureux, and N. Zerhouni. "Prognostics and Health Management for Maintenance Practitioners-Review, Implementation and Tools Evaluation". In: *International Journal of Prognostics and Health Management* 8 (Dec. 2017), p. 31.

[5] K. Benaggoune, S. Meraghni, J. Ma, L. Mouss, and N. Zerhouni. "Post Prognostic Decision for Predictive Maintenance Planning with Remaining Useful Life Uncertainty". In: *2020 Prognostics and Health Management Conference (PHM-Besançon)*. 2020, pp. 194–199.

[6] L. Breiman. *Classification and regression trees*. Chapman & Hall/CRC, 1984.

[7] C. Chen, J. Shi, N. Lu, Z. H. Zhu, and B. Jiang. "Data-driven Predictive Maintenance Strategy Considering the Uncertainty in Remaining Useful Life Prediction". In: *Neurocomputing* (2022).

[8] M. Compare, P. Baraldi, and E. Zio. "Challenges to IoT-Enabled Predictive Maintenance for Industry 4.0". In: *IEEE Internet of Things Journal* 7.5 (2020), pp. 4585–4597.

[9] I. de Pater and M. Mitici. "Predictive maintenance for multi-component systems of repairables with Remaining-Useful-Life prognostics and a limited stock of spare components". In: *Reliability Engineering & System Safety* 214 (2021), p. 107761.

[10] I. de Pater, A. Reijns, and M. Mitici. "Alarm-based predictive maintenance scheduling for aircraft engines with imperfect Remaining Useful Life prognostics". In: *Reliability Engineering & System Safety* 221 (2022), p. 108341.

[11] P. Do, A. Voisin, E. Levrat, and B. Iung. "A proactive condition-based maintenance strategy with both perfect and imperfect maintenance actions". In: *Reliability Engineering & System Safety* 133 (2015), pp. 22–32.

[12] W. Fauriat and E. Zio. "Estimation of the value of prognostic information for condition-based and predictive maintenance". In: *European Safety and Reliability Conference*. Hanover, Germany, Sept. 2019.

[13] W. Fauriat and E. Zio. "Optimization of an aperiodic sequential inspection and condition-based maintenance policy driven by value of information". In: *Reliability Engineering & System Safety* 204 (2020), p. 107133.

[14] O. Fink. "Data-Driven Intelligent Predictive Maintenance of Industrial Assets". In: *Women in Industrial and Systems Engineering: Key Advances and Perspectives on Emerging Topics*. Springer International Publishing, 2020, pp. 589–605.

[15] O. Fink, Q. Wang, M. Svensén, P. Dersin, W.-J. Lee, and M. Ducoffe. "Potential, challenges and future directions for deep learning in prognostics and health management applications". In: *Engineering Applications of Artificial Intelligence* 92 (2020), p. 103678.

[16] E. Frederick, J. DeCastro, and J. Litt. *User's Guide for the Commercial Modular Aero-Propulsion System Simulation (C-MAPSS)*. Tech. rep. NASA/ARL, 2007.

[17] N. Friedman, D. Geiger, and M. Goldszmidt. "Bayesian network classifiers". In: *Machine Learning* 29 (1997), pp. 131–163.

[18] D. Galar, K. Goebel, P. Sandborn, and U. Kumar. *Prognostics and Remaining Useful Life (RUL) Estimation: Predicting with Confidence (1st ed.)* CRC Press, 2021.

[19] K. Goebel and R. Rajamani. "Policy, regulations and standards in prognostics and health management". In: *International Journal of Prognostics and Health Management* 12.1 (2021).

[20] Y. Hu, P. Baraldi, F. Di Maio, and E. Zio. "Online Performance Assessment Method for a Model-Based Prognostic Approach". In: *IEEE Transactions on Reliability* 65.2 (2016), pp. 718–735.

[21] K. T. Huynh, A. Grall, and C. Bérenguer. "A Parametric Predictive Maintenance Decision-Making Framework Considering Improved System Health Prognosis Precision". In: *IEEE Transactions on Reliability* 68.1 (2019), pp. 375–396.

[22] K. Javed, R. Gouriveau, and N. Zerhouni. "A New Multivariate Approach for Prognostics Based on Extreme Learning Machine and Fuzzy Clustering". In: *IEEE Transactions on Cybernetics* 45.12 (2015), pp. 2626–2639.

[23] K. Javed, R. Gouriveau, and N. Zerhouni. "State of the art and taxonomy of prognostics approaches, trends of prognostics applications and open issues towards maturity at different technology readiness levels". In: *Mechanical Systems and Signal Processing* 94 (2017), pp. 214–236.

[24] F. Jensen and T. Nielsen. *Bayesian Networks and Decision Graphs, 2nd Edition*. New York: Springer, 2007.

[25] A. Kamariotis, E. Chatzi, and D. Straub. "A framework for quantifying the value of vibration-based structural health monitoring". In: *Mechanical Systems and Signal Processing* 184 (2023), p. 109708.

[26] A. Kamariotis, E. Chatzi, and D. Straub. "Value of information from vibration-based structural health monitoring extracted via Bayesian model updating". In: *Mechanical Systems and Signal Processing* 166 (2022), p. 108465.

[27] A. Kamariotis, L. Sardi, I. Papaioannou, E. Chatzi, and D. Straub. "On off-line and on-line Bayesian filtering for uncertainty quantification of structural deterioration". In: *Data-Centric Engineering* 4 (2023), e17.

[28] A. Kamariotis, K. Tatsis, E. Chatzi, K. Goebel, and D. Straub. "A metric for assessing and optimizing data-driven prognostic algorithms for predictive maintenance". In: *Reliability Engineering & System Safety* 242 (2024), p. 109723.

[29] G. van Kempen and L. van Vliet. "Mean and variance of ratio estimators used in fluorescence ratio imaging". In: *Cytometry* 39.4 (2000), pp. 300–305.

[30] N.-H. Kim, D. An, and J.-H. Choi. *Prognostics and Health Management of Engineering Systems. An introduction*. Springer, 2017.

[31] S. Kim, J.-H. Choi, and N. H. Kim. "Inspection schedule for prognostics with uncertainty management". In: *Reliability Engineering & System Safety* 222 (2022), p. 108391.

[32] M. J. Kochenderfer. *Decision making under uncertainty: Theory and application*. English. MIT Lincoln Laboratory Series. The MIT Press, 2015.

[33] K. Le Son, M. Fouladirad, A. Barros, E. Levrat, and B. Iung. "Remaining useful life estimation based on stochastic deterioration models: A comparative study". In: *Reliability Engineering & System Safety* 112 (2013), pp. 165–175.

[34] J. Lee and M. Mitici. "Deep reinforcement learning for predictive aircraft maintenance using probabilistic Remaining-Useful-Life prognostics". In: *Reliability Engineering & System Safety* 230 (2023), p. 108908.

[35] Y. Lei, N. Li, L. Guo, N. Li, T. Yan, and J. Lin. "Machinery health prognostics: A systematic review from data acquisition to RUL prediction". In: *Mechanical Systems and Signal Processing* 104 (2018), pp. 799–834.

[36] A. D. Lewis and K. M. Groth. "Metrics for evaluating the performance of complex engineering system health monitoring models". In: *Reliability Engineering & System Safety* 223 (2022), p. 108473.

[37] X. Li, Q. Ding, and J.-Q. Sun. "Remaining useful life estimation in prognostics using deep convolution neural networks". In: *Reliability Engineering & System Safety* 172 (2018), pp. 1–11.

[38] X. Li, W. Zhang, and Q. Ding. "Deep learning-based remaining useful life estimation of bearings using multi-scale feature extraction". In: *Reliability Engineering & System Safety* 182 (2019), pp. 208–218.

[39] J. Luque and D. Straub. "Risk-based optimal inspection strategies for structural systems using dynamic Bayesian Networks". In: *Structural Safety* 76 (2019), pp. 68–80.

[40] A. Mancuso, M. Compare, A. Salo, and E. Zio. "Optimal Prognostics and Health Management-driven inspection and maintenance strategies for industrial systems". In: *Reliability Engineering & System Safety* 210 (2021), p. 107536.

[41] M. Memarzadeh and M. Pozzi. "Value of information in sequential decision making: Component inspection, permanent monitoring and system-level scheduling". In: *Reliability Engineering & System Safety* 154 (2016), pp. 137–151.

[42] M. Mitici, I. de Pater, A. Barros, and Z. Zeng. "Dynamic predictive maintenance for multiple components using data-driven probabilistic RUL prognostics: The case of turbofan engines". In: *Reliability Engineering & System Safety* 234 (2023), p. 109199.

[43] K. P. Murphy. *Machine Learning: A Probabilistic Perspective*. The MIT Press, 2012.

[44] *NASA Ames Prognostics Data Repository, NASA Ames Research Center*. https://www.nasa.gov/content/prognostics-center-of-excellence-data-set-repository.

[45] P. Nectoux, R. Gouriveau, K. Medjaher, E. Ramasso, B. Chebel-Morello, N. Zerhouni, and C. Varnier. "PRONOSTIA : An experimental platform for bearings accelerated degradation tests." In: *IEEE International Conference on Prognostics and Health Management, PHM'12*. Vol. sur CD ROM. Denver, Colorado, United States: IEEE Catalog Number : CPF12PHM-CDR, June 2012, pp. 1–8.

[46] K. T. Nguyen and K. Medjaher. "A new dynamic predictive maintenance framework using deep learning for failure prognostics". In: *Reliability Engineering & System Safety* 188 (2019), pp. 251–262.

[47] K. T. Nguyen, K. Medjaher, and C. Gogu. "Probabilistic deep learning methodology for uncertainty quantification of remaining useful lifetime of multi-component systems". In: *Reliability Engineering & System Safety* 222 (2022), p. 108383.

[48] M. D. Pandey and J. van der Weide. "Stochastic renewal process models for estimation of damage cost over the life-cycle of a structure". In: *Structural Safety* 67 (2017), pp. 27–38.

[49] K. Papakonstantinou and M. Shinozuka. "Planning structural inspection and maintenance policies via dynamic programming and Markov processes. Part I: Theory". In: *Reliability Engineering & System Safety* 130 (2014), pp. 202–213.

[50] P. Paris and F. Erdogan. "A Critical Analysis of Crack Propagation Laws". In: *Journal of Basic Engineering* 85.4 (1963), pp. 528–533.

[51] I. de Pater and M. Mitici. "Novel metrics to evaluate probabilistic remaining useful life prognostics with applications to turbofan engines". In: *PHM Society European Conference*. Vol. 7(1). 2022, pp. 96–109.

[52] H. Purohit, R. Tanabe, K. Ichige, T. Endo, Y. Nikaido, K. Suefusa, and Y. Kawaguchi. "MIMII Dataset: Sound Dataset for Malfunctioning Industrial Machine Investigation and Inspection". In: *arXiv:1909.09347* (2019).

[53] H. Raiffa and R. Schlaifer. *Applied statistical decision theory*. Harvard University, Boston: Division of Research, Graduate School of Business Administration, 1961.

[54] B. Saha and K. Goebel. "Battery Data Set". In: *NASA Prognostics Data Repository* (2007).

[55] B. Saha, K. Goebel, S. Poll, and J. Christophersen. "Prognostics Methods for Battery Health Monitoring Using a Bayesian Framework". In: *IEEE Transactions on Instrumentation and Measurement* 58.2 (2009), pp. 291–296.

[56] S. Särkkä. *Bayesian Filtering and Smoothing*. English. United Kingdom: Cambridge University Press, 2013.

[57] A. Saxena, J. Celaya, E. Balaban, K. Goebel, B. Saha, S. Saha, and M. Schwabacher. "Metrics for evaluating performance of prognostic techniques". In: *2008 International Conference on Prognostics and Health Management*. 2008, pp. 1–17.

[58] A. Saxena, J. Celaya, B. Saha, S. Saha, and K. Goebel. "Metrics for Offline Evaluation of Prognostic Performance". In: *International Journal of Prognostics and Health Management* 1 (Jan. 2010), pp. 2153–2648.

[59] A. Saxena, K. Goebel, D. Simon, and N. Eklund. "Damage propagation modeling for aircraft engine run-to-failure simulation". In: *2008 International Conference on Prognostics and Health Management*. 2008, pp. 1–9.

[60] X.-S. Si, W. Wang, C.-H. Hu, and D.-H. Zhou. "Remaining useful life estimation – A review on the statistical data driven approaches". In: *European Journal of Operational Research* 213.1 (2011), pp. 1–14.

[61] K. E. Tatsis, V. K. Dertimanis, and E. N. Chatzi. "Sequential Bayesian Inference for Uncertain Nonlinear Dynamic Systems: A Tutorial". In: *Journal of Structural Dynamics* (2022), pp. 236–262.

[62] H. C. Tijms. "Renewal-Reward Processes". In: *A First Course in Stochastic Models*. John Wiley & Sons, Ltd, 2003. Chap. 2, pp. 33–79.

[63] J. van Noortwijk. "A survey of the application of gamma processes in maintenance". In: *Reliability Engineering and System Safety* 94.1 (2009), pp. 2–21.

[64] Y. Wu, M. Yuan, S. Dong, L. Lin, and Y. Liu. "Remaining useful life estimation of engineered systems using vanilla LSTM neural networks". In: *Neurocomputing* 275 (2018), pp. 167–179.

[65] T. Yan, Y. Lei, N. Li, X. Si, L. Pintelon, and R. Dewil. "Online joint replacement-order optimization driven by a nonlinear ensemble remaining useful life prediction method". In: *Mechanical Systems and Signal Processing* 173 (2022), p. 109053.

[66] J. Zeng and Z. Liang. "A Deep Gaussian Process Approach for Predictive Maintenance". In: *IEEE Transactions on Reliability* (2022), pp. 1–18.

[67] J. Zhang, P. Wang, R. Yan, and R. X. Gao. "Long short-term memory for machine remaining life prediction". In: *Journal of Manufacturing Systems* 48 (2018), pp. 78–86.

[68] Z. Zhang, X. Si, C. Hu, and Y. Lei. "Degradation data analysis and remaining useful life estimation: A review on Wiener-process-based methods". In: *European Journal of Operational Research* 271.3 (2018), pp. 775–796.

[69] L. Zhuang, A. Xu, and X.-L. Wang. "A prognostic driven predictive maintenance framework based on Bayesian deep learning". In: *Reliability Engineering & System Safety* 234 (2023), p. 109181.

[70] E. Zio. "Prognostics and Health Management (PHM): Where are we and where do we (need to) go in theory and practice". In: *Reliability Engineering & System Safety* 218 (2022), p. 108119.